Contents

Contents i

List of Tables iii

List of Figures iv

7 Mean Field Theory of Phase Transitions 1

7.1 References . . . 1

7.2 Phases of matter . . . 2

7.2.1 Spontaneous symmetry breaking . . . 2

7.2.2 Beyond the Landau paradigm . . . 4

7.3 The van der Waals system . . . 5

7.3.1 Equation of state . . . 5

7.3.2 Analytic form of the coexistence curve near the critical point . . . 10

7.3.3 History of the van der Waals equation . . . 14

7.4 Fluids, Magnets, and the Ising Model . . . 15

7.4.1 Lattice gas description of a fluid . . . 15

7.4.2 Phase diagrams and critical exponents . . . 16

7.4.3 Gibbs-Duhem relation for magnetic systems . . . 19

7.4.4 Order-disorder transitions . . . 19

7.5 Mean Field Theory . . . 21

7.5.1 The mean field *Ansatz* . . . 21

7.5.2 Zero external field . . . 22
7.5.3 Finite external field . . . 25
7.5.4 Magnetization dynamics . . . 28
7.5.5 Beyond nearest neighbors . . . 31
7.5.6 Ising model with long-ranged forces . . . 31
7.6 Landau Theory of Phase Transitions . . . 33
7.6.1 Quartic free energy with Ising symmetry . . . 33
7.6.2 Cubic terms in Landau theory : first order transitions . . . 35
7.6.3 Order parameter dynamics . . . 37
7.6.4 Sixth order Landau theory : tricritical point . . . 38
7.6.5 Hysteresis for the sextic potential . . . 41
7.6.6 Weak crystallization . . . 43
7.7 Variational Density Matrix Method . . . 44
7.7.1 The variational principle . . . 44
7.7.2 Variational density matrix for the Ising model . . . 45
7.7.3 q-state Potts model . . . 48
7.7.4 XY Model . . . 52
7.8 Mean Field Theory of Fluctuations . . . 55
7.8.1 Correlation and response in mean field theory . . . 55
7.8.2 Calculation of the response functions . . . 56
7.8.3 Beyond the two-state Ising model . . . 59
7.8.4 Magnetic ordering . . . 62
7.9 Global Symmetries . . . 65
7.9.1 Symmetries and symmetry groups . . . 65
7.9.2 Domain walls and lower critical dimension . . . 66
7.9.3 Continuous symmetries . . . 68
7.9.4 Random systems : Imry-Ma argument . . . 69
7.9.5 Hohenberg-Mermin-Wagner theorem . . . 71

7.9.6 Goldstone's theorem . . . 76
7.10 Ginzburg-Landau Theory . . . 80
7.10.1 Ginzburg-Landau free energy . . . 80
7.10.2 Domain wall profile . . . 81
7.10.3 Ginzburg criterion . . . 82
7.11 Appendix I: Bifurcations . . . 83
7.11.1 $N = 1$ dynamical systems . . . 83
7.11.2 Saddle-node bifurcation . . . 84
7.11.3 Transcritical bifurcation . . . 85
7.11.4 Pitchfork bifurcation . . . 86
7.11.5 Imperfect bifurcation . . . 86
7.12 Appendix II: Equivalence of the Mean Field Descriptions . . . 89
7.12.1 Variational density matrix . . . 90
7.12.2 Mean field approximation . . . 91
7.13 Appendix III: Additional Examples of Mean Field Theory . . . 93
7.13.1 Blume-Capel model . . . 93
7.13.2 Ising antiferromagnet in an external field . . . 94
7.13.3 Canted quantum antiferromagnet . . . 98
7.13.4 Coupled order parameters . . . 100
7.14 Appendix IV: Derivation of Ginzburg-Landau Free Energy . . . 104

List of Tables

7.1 van der Waals parameters for some common gases . . . 8

7.2 Critical exponents 27

List of Figures

7.1 Phase diagrams for H_2O and the quantum Hall effect. 3
7.2 Pressure *versus* volume for the van der Waals gas 7
7.3 Molar free energy $f(T, v)$ of the van der Waals system 9
7.4 Pressure-volume isotherms for the van der Waals system, with Maxwell construction . . 10
7.5 Maxwell construction in the (v, p) plane 11
7.6 Universality of the liquid-gas transition 13
7.7 The lattice gas model 16
7.8 Comparison of liquid-gas and Ising ferromagnet phase diagrams 17
7.9 Order-disorder transition on the square lattice 20
7.10 Ising mean field theory at $h = 0$ 23
7.11 Ising mean field theory at $h = 0.1$ 25
7.12 Dissipative magnetization dynamics $\dot{m} = -f'(m)$ 29
7.13 Magnetization hysteresis 30
7.14 Phase diagram for the quartic Landau free energy 34
7.15 Behavior of the quartic free energy $f(m) = \frac{1}{2}am^2 - \frac{1}{3}ym^3 + \frac{1}{4}bm^4$ 36
7.16 Fixed points for $\varphi(u) = \frac{1}{2}ru^2 - \frac{1}{3}u^3 + \frac{1}{4}u^4$ and flow $\dot{u} = -\varphi'(u)$ 38
7.17 Behavior of the sextic free energy $f(m) = \frac{1}{2}am^2 + \frac{1}{4}bm^4 + \frac{1}{6}cm^6$ 39
7.18 High temperature cubic perovskite crystal structure of $BaTiO_3$. 40
7.19 Sextic free energy $\varphi(u) = \frac{1}{2}ru^2 - \frac{1}{4}u^4 + \frac{1}{6}u^6$ for different values of r 42
7.20 Fixed point branches $\varphi'(u^*) = 0$ under the flow $\dot{u} = -\varphi'(u)$ for the sextic potential 43
7.21 Variational field free energy *versus* magnetization 47

7.22 Variational mean field theory of the $q = 7$ state Potts model 51
7.23 Domain walls in the one, two and three dimensional Ising model 67
7.24 A domain wall in an XY ferromagnet 69
7.25 Imry-Ma domains and free energy *versus* domain size 71
7.26 The double well and Mexican hat potentials. 79
7.27 Evolution of $G(x, \alpha)$ as a function of the control parameter α 84
7.28 Flow diagrams for $\dot{u} = r + u^2$ and $\dot{u} = ru - u^2$ 85
7.29 Extended phase space flow for the saddle-node and transcritical bifurcations 86
7.30 Supercritical and subcritical pitchfork bifurcations 87
7.31 Extended phase space flow for supercritical and subcritical pitchfork bifurcations 87
7.32 Scaled free energy and phase diagram 88
7.33 Imperfect pitchfork bifurcation 89
7.34 Mean field phase diagram for the Blume-Capel model 95
7.35 Mean field solution for an Ising antiferromagnet in an external field 96
7.36 Mean field phase diagram for an Ising antiferromagnet in an external field 97
7.37 Mean field phase diagram for the model of eqn. 7.420 100
7.38 Phase diagram for the model of eqn. 7.432 104

Chapter 7

Mean Field Theory of Phase Transitions

7.1 References

- M. Kardar, *Statistical Physics of Particles* (Cambridge, 2007)
  A superb modern text, with many insightful presentations of key concepts.
- M. Plischke and B. Bergersen, *Equilibrium Statistical Physics* ($3^{\rm rd}$ edition, World Scientific, 2006)
  An excellent graduate level text. Good discussion of mean field theory.
- G. Parisi, *Statistical Field Theory* (Addison-Wesley, 1988)
  An advanced text focusing on field theoretic approaches, covering mean field and Landau-Ginzburg theories before moving on to renormalization group and beyond.
- J. P. Sethna, *Entropy, Order Parameters, and Complexity* (Oxford, 2006)
  An excellent introductory text with a very modern set of topics and exercises. Available online at
  http://www.physics.cornell.edu/sethna/StatMech

7.2 Phases of matter

Condensed matter physicists are not interested in electrons, nuclei, and photons in isolation. Rather it is the collective properties of these interacting constituents which lead to the remarkably rich phenomenology of condensed matter. This richness is manifested by the bewildering array of *phases of matter* that can be conjured. Until relatively recently, phases of matter were described based on the *Landau paradigm*, in which an ordered phase is described by one or more nonzero *order parameters*, each of which describes a *broken global symmetry*.

7.2.1 Spontaneous symmetry breaking

In quantum mechanics, the eigenstates of a Hamiltonian H_0 which commutes with all the *generators* of a symmetry group G may be classified according to the *representations* of that group. Typically this entails the appearance of degeneracies in the eigenspectrum, with degenerate states transforming into each other under the group operations. Adding a perturbation V to the Hamiltonian which breaks G down to a subgroup H will accordingly split these degeneracies, and the new multiplets of $H = H_0 + V$ are characterized by representations of the lower symmetry group H.

In quantum field theory, or in the thermodynamic limit of a classical system, as a consequence of the infinite number of degrees of freedom, symmetries may be *spontaneously broken*. This means that even if the Hamiltonian H (or action S) for the field theory is invariant under a group G of symmetry transformations, the ground state or thermodynamic density matrix may not be invariant under the full symmetry group G. The presence or absence of spontaneous symmetry breaking (SSB), and its detailed manifestations, will in general depend on the couplings, or the temperature in the case of quantum statistical mechanics. SSB is usually associated with the presence of a local *order parameter* which transforms nontrivially under some group operations, and whose quantum statistical average vanishes in a fully symmetric phase, but takes nonzero values in a symmetry-broken phase[1]. The parade example is the Ising model, $H = -\sum_{i<j} J_{ij}\,\sigma_i\,\sigma_j$, where each $\sigma_i = \pm 1$ and the subscript i indexes a physical location in space, such as a site $\boldsymbol{R}_i$ on a particular lattice. We further assume that the interactions are all ferromagnetic: $J_{ij} > 0$. The model is explicitly $\mathbb{Z}_2$ symmetric under $\sigma_i \to \varepsilon\sigma_i$ for all i, where $\varepsilon \in \{+1, -1\}$, yet if the interaction matrix $J_{ij} = J(\boldsymbol{R}_i - \boldsymbol{R}_j)$ is short-ranged and the space dimension d is greater than one, there is a *critical temperature* $T_{\rm c}$ below which SSB sets in, and the system develops a spontaneous magnetization $\phi = \langle\sigma_i\rangle$. You know how in quantum mechanics, the eigenstates of a particle moving in one-dimensional double-well potential $V(x) = V(-x)$ can be classified by their parity eigenvalues P, and the lowest two energy states are respectively symmetric ($\mathsf{P} = +1$) and antisymmetric ($\mathsf{P} = -1$) , and are delocalized among both wells. For a quantum field theory, however, with (Euclidean) Lagrangian density $\mathcal{L}_{\rm E} = \frac{1}{2}(\boldsymbol{\nabla}\phi)^2 + V(\phi)$, for $d > 1$ and $T < T_{\rm c}$, the system actually picks the left or the right well, so that $\langle\phi(\boldsymbol{r})\rangle \neq 0$. Another example is the spontaneously broken $\mathsf{O}(2)$ invariance of superfluids, where the boson annihilation operator $\psi(\boldsymbol{r})$ develops a spontaneous average $\big\langle\psi(\boldsymbol{r})\big\rangle = \sqrt{n_0}\,e^{i\theta}$, where n_0 is the condensate density and θ the condensate phase[2]

[1] While SSB is generally associated with the existence of a phase transition, not all phase transitions involve SSB. Exceptions include the Berezinskii-Kosterlitz-Thouless (BKT) transition, and also those topological phases which have no local order parameter.

[2] In two-dimensional superfluids, there order parameter vanishes at any finite temperature as a consequence

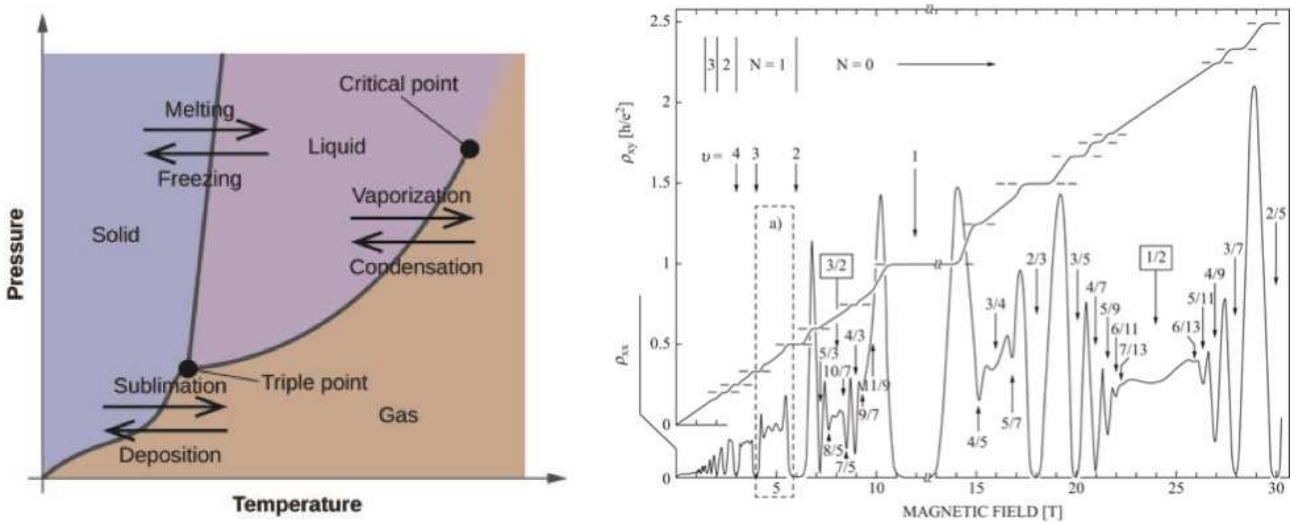


Figure 7.1: Left: Phase diagram of H_2O in the (T, p) plane. Right: Low temperature ($T \approx 150\,\text{mK}$) longitudinal resistivity ρ_{xx} and Hall resistivity ρ_{xy} as a function of applied magnetic field in a two-dimensional electron gas system (GaAs/AlGaAs heterostructure), from R. Willett *et al.*, *Phys. Rev. Lett.* **59**, 1776 (1987). Each dip in ρ_{xx} and concomitant plateau in ρ_{xy} corresponds to a distinct phase of matter.

Truth be told, the above description is a bit of a swindle. In the ferromagnetic ($J_{ij} > 0$) Ising model, for example, at $T = 0$, there are still two ground states, $|\Uparrow\rangle \equiv |\uparrow\uparrow\uparrow\cdots\rangle$ and $|\Downarrow\rangle \equiv |\downarrow\downarrow\downarrow\cdots\rangle$. The (ergodic) zero temperature density matrix is $\rho_0 = \frac{1}{2}|\Uparrow\rangle\langle\Uparrow| + \frac{1}{2}|\Downarrow\rangle\langle\Downarrow|$, and therefore $\langle\sigma_i\rangle = \text{Tr}\,(\rho_0\,\sigma_i) = 0$. The order parameter apparently has vanished. WTF?! There are at least two compelling ways to resolve this seeming conundrum:

(i) First, rather than defining the order parameter of the Ising model, for example, to be the expected value $m = \langle\sigma_i\rangle$ of the local spin[3], consider instead the behavior of the *correlation function* $C_{ij} = \langle\sigma_i\,\sigma_j\rangle$ in the limit $d_{ij} = |\boldsymbol{R}_i - \boldsymbol{R}_j| \to \infty$. In a disordered phase, there is no correlation between infinitely far separated spins, hence $\lim_{d_{ij}\to\infty} C_{ij} = 0$. In the ordered phase, this is no longer true, and we define the *spontaneous magnetization* m from the long distance correlator: $m^2 \equiv \lim_{d_{ij}\to\infty}\langle\sigma_i\,\sigma_j\rangle$. In this formulation, SSB is associated with the emergence of *long-ranged order* in the correlators of operators which transform nontrivially under the symmetry group.

(ii) Second, we could impose an external field which *explicitly* breaks the symmetry, such as a Zeeman term $H' = -h\sum_i \sigma_i$ in the Ising model. We now compute the magnetization (per site) $m(T, V, h) = \langle\sigma_i\rangle$ as a function of temperature T, the external field h, *and* the volume V of our system. The order parameter $m(T)$ in zero field is then defined as

$$m(T) = \lim_{h\to 0}\lim_{V\to\infty} m(T, V, h) \quad . \tag{7.1}$$

The order of limits here is crucially important. The thermodynamic limit $V \to \infty$ is taken first,

of the Hohenberg-Mermin-Wagner theorem (see §7.9.5). Yet the system still possesses a nonzero *superfluid stiffness* ρ_s and zero viscosity for temperatures below the BKT transition temperature T_{BKT}.

[3]We assume translational invariance, which means $\langle\sigma_i\rangle$ is independent of the site index i.

which means that the energy difference between $|\Uparrow\rangle$ and $|\Downarrow\rangle$, being proportional to hV, diverges, thus infinitely suppressing the $|\Downarrow\rangle$ state if $h > 0$ (and the $|\Uparrow\rangle$ state if $h < 0$). The magnitude of the order parameter will be independent of the way in which we take $h \to 0$, but its sign will depend on whether $h \to 0^+$ or $h \to 0^-$, with $\mathsf{sgn}(m) = \mathsf{sgn}(h)$. Physically, the direction in which a system orders can be decided by the presence of small stray fields or impurities.

Note that in both formulations, SSB is necessarily associated with the existence of a local operator $\mathcal{O}_i$ which is identified as the order parameter field. In (i) the correlations $\langle \mathcal{O}_i \, \mathcal{O}_j \rangle$ exhibit long-ranged order in the symmetry-broken phase. In (ii) $\mathcal{O}_i$ is the operator to which the external field h_i couples.

For a ferromagnet, the order parameter is the magnetization density, $\boldsymbol{m}$, and the broken symmetry is the group of rotations $\mathsf{O}(3)$ or $\mathsf{SU}(2)$, or possibly $\mathbb{Z}_2$. Under a group operation $g \in \mathsf{G}$, the order parameter transforms as $\boldsymbol{m} \to g\boldsymbol{m}$. For a crystal or charge density wave, the order parameters are the Fourier components $\varrho_{\boldsymbol{G}}$ of the density at a series of wavevectors which comprise the reciprocal lattice of the structure. The broken symmetry is that of continuous translation, *i.e.* the group $\mathbb{R}^d$ under addition, and under the group operation $t_{\boldsymbol{a}}$ corresponding to translation by $\boldsymbol{a} \in \mathbb{R}^d$, we have $\varrho_{\boldsymbol{G}} \to t_{\boldsymbol{a}} \, \varrho_{\boldsymbol{G}} = \varrho_{\boldsymbol{G}} \, e^{i\boldsymbol{G}\cdot\boldsymbol{a}}$. A given order parameter ϕ will in general depend on temperature T, pressure p, applied magnetic field $\boldsymbol{H}$, various coupling parameters which enter the Hamiltonian $\{g_i\}$, *etc.* A multidimensional plot which labels the various phases of a system as a function of all these parameters is known as a *phase diagram*. Points, lines, or surfaces separating different phases are the loci of *phase transitions*, where the free energy and the order parameters of the system exhibit singularities. At a *first order transition*, certain properties change discontinuously. The canonical example of a first order transition is the freezing or boiling of liquid water to solid ice or gaseous vapor. These transitions involve a discontinuous change in the density as T or p is varied so as to cross a phase boundary[4]. At a *second order transition*, one or more order parameters vanish as a phase boundary is approached. Within the Landau paradigm, a nonzero order parameter is associated with the spontaneous breaking of a symmetry, such as spin rotation (in a magnet), space translation (in a crystal), *etc.* Furthermore, a second order transition between phases A and B is possible only if the symmetry groups $\mathsf{G}_{\rm A}$ of the A phase and $\mathsf{G}_{\rm B}$ of the B phase, both of which must be subgroups of the symmetry group G of the Hamiltonian, satisfy $\mathsf{G}_{\rm A} \subset \mathsf{G}_{\rm B}$ or $\mathsf{G}_{\rm B} \subset \mathsf{G}_{\rm A}$. A phase transition which takes place at $T = 0$ as a function of other parameters (p, H, *etc.*) is called a *quantum phase transition*. A modern, more accurate classification is between *first order* and *continuous* phase transitions. The latter term allows for transitions where there is no order symmetry-breaking order parameter yet there are thermodynamic singularities in certain derivatives of the free energy or correlation functions.

7.2.2 Beyond the Landau paradigm

The classical $\mathsf{O}(2)$ model in $d = 2$ is precluded from achieving long-ranged order and spontaneous $\mathsf{O}(2)$ symmetry breaking at any finite temperature by the Hohenberg-Mermin-Wagner theorem, which we shall discuss below in §7.9.5. Nevertheless, the model does exhibit a second order phase transition,

[4]The phase boundary between liquid and vapor terminates in a *critical point*, and it is therefore possible to continuously evolve from liquid to vapor without ever encountering a singularity. Thus, from the point of view of order parameters and broken symmetry, there is no essential distinction between liquid and vapor phases.

known as the Berezinskii-Kosterlitz-Thouless (BKT) transition[5]. The energy density in the continuum model is written as $\varepsilon(\boldsymbol{r}) = \frac{1}{2}\rho_{\rm s}(\boldsymbol{\nabla}\Theta)^2$, where $\rho_{\rm s}$ is the *stiffness parameter* and $\Theta(\boldsymbol{r})$ is a planar angle, with Θ and $\Theta + 2\pi n$ identified for all integers n. The model features point defects which are known as vortices, about which the winding number $q = \frac{1}{2\pi}\oint_{\mathcal{C}} d\boldsymbol{r}\cdot\boldsymbol{\nabla}\Theta$ along a small loop $\mathcal{C}$ enclosing the vortex is its integer *vorticity* $q \in \mathbb{Z}$. Integrating the energy density for a single $q = 1$ vortex with $\Theta(\boldsymbol{r}) = \tan^{-1}(y/x)$ yields $E = \pi\rho_{\rm s}\ln(R/a)$, where R is the system radius and a an ultraviolet cutoff, which is naturally imposed in any lattice-based model. Since a vortex can be in any location, its entropy is $S = k_{\rm B}\ln(R^2/a^2)$, and we see that free vortices should proliferate when $F = E - TS = (\pi\rho_{\rm s} - 2k_{\rm B}T)\ln(R/a) < 0$, *i.e.* $T > T_{\rm c} = \pi\rho_{\rm s}/2k_{\rm B}$. This very crude derivation, which neglects interactions between the vortices, is essentially correct[6]. The phase transition is associated with an *unbinding* of vortex-antivortex pairs. In the confined phase, where $T < T_{\rm c}$, the correlation function $C(\boldsymbol{r}, T) = \langle e^{i\Theta(\boldsymbol{r})}\, e^{-i\Theta(\boldsymbol{0})}\rangle$ decays as a power law, and there is no long-ranged order associated with a spontaneous breaking of $\mathsf{O}(2)$. In the plasma phase, where $T > T_{\rm c}$, free vortices and antivortices (*i.e.* defects with $q_i < 0$) are present, and $C(\boldsymbol{r}, T)$ decays exponentially with a finite correlation length ξ. We will discuss the BKT transition and its analysis via the renormalization group later in this course.

Over the past 25 years or so, a new paradigm has emerged for certain phases of matter which have no order parameter in the conventional sense. These are called *topological phases*, and are exemplified by the phases of the quantum Hall effect. Typically topological phases exhibit a *bulk excitation gap*, meaning it requires a finite amount of energy in order to excite these systems in their bulk, and in this respect, they are akin to insulators. However, at the edges of finite systems, there exist *gapless edge states* which may carry current. The structure of the edge states is intimately related to the nature of the bulk phase, which despite being a condensate of sorts, has no local order parameter. Topological phases are of intense current interest, both theoretically and experimentally, but they remain somewhat exotic, as compared with, say, metals. Yet the metallic phase, which is an example of a *Landau Fermi liquid*, is difficult to characterize in terms of a conventional order parameter[7]. Another violation of the Landau paradigm which has been revealed in recent years is the (at this point purely theoretical) notion of *deconfined quantum criticality*. A deconfined quantum critical point violates the Landau requirement that the symmetry groups on either side of the transition have a subgroup relation.

7.3 The van der Waals system

7.3.1 Equation of state

Recall the van der Waals equation of state,

$$\left(p + \frac{a}{v^2}\right)(v - b) = RT \quad , \tag{7.2}$$

[5]V. L. Berezinskii, *Sov. Phys. JETP* **32**, 493 (1971); J. M. Kosterlitz and D. J. Thouless, *J. Phys. C: Solid State Phys.* **6**, 1181 (1973).

[6]More precisely, since the superfluid density $\rho_{\rm s}(T)$ temperature-dependent, the jump condition is given by $\rho_{\rm s}(T_{\mathsf{BKT}}) = 2k_{\rm B}T_{\mathsf{BKT}}/\pi$.

[7]The order parameter of a Fermi liquid is sometimes taken to be the *quasiparticle weight* Z, which, in isotropic systems, characterizes the discontinuous drop in the momentum occupation function $n(k)$ as one crosses the Fermi surface at $k = k_{\rm F}$.

where $v = N_{\rm A}V/N$ is the molar volume. Solving for $p(v,T)$, we have

$$p = \frac{RT}{v-b} - \frac{a}{v^2} \quad . \tag{7.3}$$

Let us fix the temperature T and examine the function $p(v)$. Clearly $p(v)$ is a decreasing function of volume for v just above the minimum allowed value $v = b$, as well as for $v \to \infty$. But is $p(v)$ a monotonic function for all $v \in [b, \infty]$?

We can answer this by computing the derivative,

$$\left(\frac{\partial p}{\partial v}\right)_T = \frac{2a}{v^3} - \frac{RT}{(v-b)^2} \quad . \tag{7.4}$$

Setting this expression to zero for finite v, we obtain the equation[8]

$$\frac{2a}{bRT} = \frac{u^3}{(u-1)^2} \quad , \tag{7.5}$$

where $u \equiv v/b$ is dimensionless. It is easy to see that the function $f(u) = u^3/(u-1)^2$ has a unique minimum for $u > 1$. Setting $f'(u^*) = 0$ yields $u^* = 3$, and so $f_{\rm min} = f(3) = \frac{27}{4}$. Thus, for $T > T_{\rm c} = 8a/27bR$, the LHS of eqn. 7.5 lies below the minimum value of the RHS, and there is no solution. This means that $p(v, T > T_{\rm c})$ is a monotonically decreasing function of v.

At $T = T_{\rm c}$ there is a saddle-node bifurcation[9]. Setting $v_{\rm c} = bu^* = 3b$ and evaluating $p_{\rm c} = p(v_{\rm c}, T_{\rm c})$, we have that the location of the *critical point* for the van der Waals system is[10]

$$p_{\rm c} = \frac{a}{27\,b^2} \quad , \quad v_{\rm c} = 3b \quad , \quad T_{\rm c} = \frac{8a}{27\,bR} \quad . \tag{7.6}$$

For $T < T_{\rm c}$, there are two solutions to eqn. 7.5, corresponding to a local minimum and a local maximum of the function $p(v)$. The locus of points in the (v,p) plane for which $(\partial p/\partial v)_T = 0$ is obtained by setting eqn. 7.4 to zero and solving for T, then substituting this into eqn. 7.3. The result is

$$p^*(v) = \frac{a}{v^2} - \frac{2ab}{v^3} \quad . \tag{7.7}$$

Expressed in terms of dimensionless quantities $\bar{p} = p/p_{\rm c}$ and $\bar{v} = v/v_{\rm c}$, this equation becomes

$$\bar{p}^*(\bar{v}) = \frac{3}{\bar{v}^2} - \frac{2}{\bar{v}^3} \quad . \tag{7.8}$$

[8] There is always a solution to $(\partial p/\partial v)_T = 0$ at $v = \infty$.

[9] See the appendix in §7.11

[10] Equivalently, one can obtain the location of the saddle-node bifurcation in the local extrema of $p(T,v)$ by setting $(\partial p/\partial v)_T = 0$ and $(\partial^2 p/\partial v^2)_T = 0$. This yields two equations for the two unknowns $(T_{\rm c}, v_{\rm c})$. Invoking the van der Waals equation of state then yields $p_{\rm c} = p(T_{\rm c}, v_{\rm c})$.

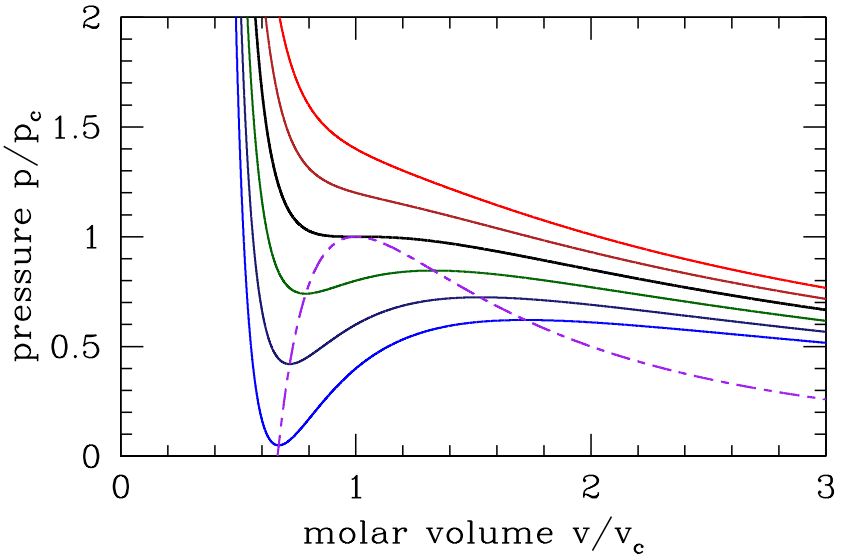


Figure 7.2: Pressure *versus* molar volume for the van der Waals gas at temperatures in equal intervals from $T = 1.10\,T_{\rm c}$ (red) to $T = 0.85\,T_{\rm c}$ (blue). The purple curve is $\bar{p}^*(\bar{v})$.

Along the curve $p = p^*(v)$, the isothermal compressibility, $\kappa_T = -v^{-1}\big(\partial v/\partial p\big)_T$ diverges, heralding a *thermodynamic instability*. To understand better, let us compute the free energy of the van der Waals system, $F = E - TS$. Regarding the energy E, we showed back in chapter 2 that

$$\left(\frac{\partial \varepsilon}{\partial v}\right)_T = T\left(\frac{\partial p}{\partial T}\right)_v - p = \frac{a}{v^2} \quad , \tag{7.9}$$

which entails

$$\varepsilon(T,v) = \tfrac{1}{2}\mathfrak{f}RT - \frac{a}{v} \quad , \tag{7.10}$$

where $\varepsilon = E/\nu$ is the molar internal energy. The first term is the molar energy of an ideal gas, where $\mathfrak{f}$ is the number of molecular degrees of freedom, which is the appropriate low density limit. The molar specific heat is then $c_V = \big(\partial\varepsilon/\partial T\big)_v = \frac{1}{2}\mathfrak{f}R$, which means that the molar entropy is

$$s(T,v) = \int^T\!\! dT'\,\frac{c_V}{T'} = \tfrac{1}{2}\mathfrak{f}R\log(T/T_{\rm c}) + s_1(v) \quad . \tag{7.11}$$

We then write $f = \varepsilon - Ts$, and we fix the function $s_1(v)$ by demanding that $p = -\big(\partial f/\partial v\big)_T$. This yields $s_1(v) = R\log(v-b) + s_0$, where s_0 is a constant. Thus[11],

$$f(T,v) = \tfrac{1}{2}\mathfrak{f}RT\left(1 - \log\big(T/T_{\rm c}\big)\right) - \frac{a}{v} - RT\log(v-b) - Ts_0 \quad . \tag{7.12}$$

We know that under equilibrium conditions, f is driven to a minimum by spontaneous processes. Now suppose that $\big(\partial^2 f/\partial v^2\big)_T < 0$ over some range of v at a given temperature T. This would mean that

[11] Don't confuse the molar free energy (f) with the number of molecular degrees of freedom ($\mathfrak{f}$)!

gas	$a\ \left(\frac{\mathrm{L}^2\cdot\mathrm{bar}}{\mathrm{mol}^2}\right)$	$b\ \left(\frac{\mathrm{L}}{\mathrm{mol}}\right)$	p_c (bar)	T_c (K)	v_c (L/mol)
Acetone	14.09	0.0994	52.82	505.1	0.2982
Argon	1.363	0.03219	48.72	150.9	0.0966
Carbon dioxide	3.640	0.04267	74.04	304.0	0.1280
Ethanol	12.18	0.08407	63.83	516.3	0.2522
Freon	10.78	0.0998	40.09	384.9	0.2994
Helium	0.03457	0.0237	2.279	5.198	0.0711
Hydrogen	0.2476	0.02661	12.95	33.16	0.0798
Mercury	8.200	0.01696	1055	1723	0.0509
Methane	2.283	0.04278	46.20	190.2	0.1283
Nitrogen	1.408	0.03913	34.06	128.2	0.1174
Oxygen	1.378	0.03183	50.37	154.3	0.0955
Water	5.536	0.03049	220.6	647.0	0.0915

Table 7.1: van der Waals parameters for some common gases. (Source: *Wikipedia*)

one mole of the system at volume v and temperature T could lower its free energy by rearranging into two half-moles, with respective molar volumes $v \pm \delta v$, each at temperature T, where δv is a positive infinitesimal. The total volume and temperature thus remain fixed, but the free energy changes by an amount $\Delta f = \frac{1}{2}\big(\partial^2 f/\partial v^2\big)_T (\delta v)^2 < 0$. This means that the system is unstable – it can lower its free energy by dividing up into two subsystems each with different densities (*i.e.* molar volumes). Note that the onset of stability occurs when

$$\left.\frac{\partial^2 f}{\partial v^2}\right|_T = -\left.\frac{\partial p}{\partial v}\right|_T = \frac{1}{v\kappa_T} = 0 \quad , \tag{7.13}$$

which is to say when $\kappa_T = \infty$. As we saw, this occurs at $p = p^*(v)$, given in eqn. 7.7.

However, this condition, $\big(\partial^2 f/\partial v^2\big)_T < 0$, is in fact too strong. We need not limit our analysis to cases where δv is infinitesimal, in which case the system can be unstable even at molar volumes where $\big(\partial^2 f/\partial v^2\big)_T > 0$. The reason is shown graphically in fig. 7.3. At the fixed temperature T, for any molar volume v between $v_{\rm liquid} \equiv v_1$ and $v_{\rm gas} \equiv v_2$, the system can lower its free energy by *phase separating* into regions of different molar volumes. In general we can write

$$v = (1-x)\,v_1 + x\,v_2 \quad , \tag{7.14}$$

so $v = v_1$ when $x = 0$ and $v = v_2$ when $x = 1$. The free energy upon phase separation is simply

$$f = (1-x)\,f_1 + x\,f_2 \quad , \tag{7.15}$$

where $f_j = f(v_j, T)$. This function is given by the straight black line connecting the points at volumes v_1 and v_2 in fig. 7.3.

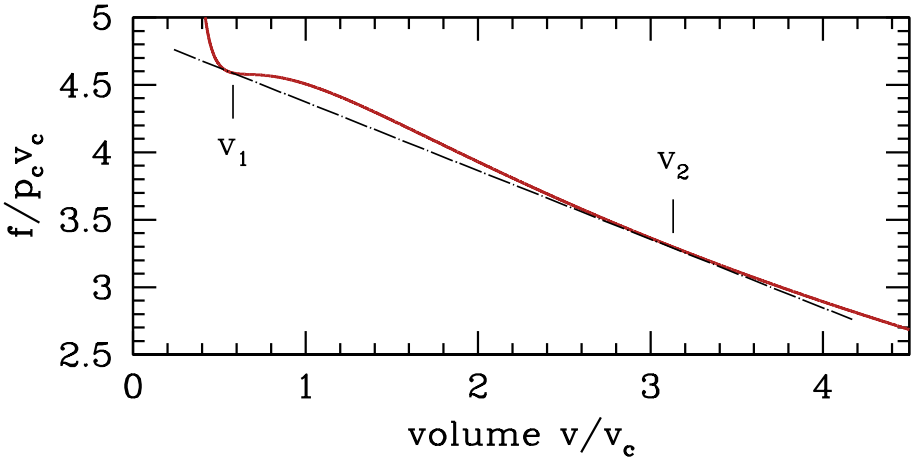


Figure 7.3: The molar free energy $f(T,v)$ of the van der Waals system at $T = 0.85\,T_{\rm c}$. The dot-dashed black line shows the Maxwell construction connecting molar volumes $v_{1,2}$ on opposite sides of the coexistence curve.

The two equations which give us v_1 and v_2 are

$$\left.\frac{\partial f}{\partial v}\right|_{v_1,T} = \left.\frac{\partial f}{\partial v}\right|_{v_2,T} = \frac{f(T,v_2)-f(T,v_1)}{(v_2-v_1)} \quad . \tag{7.16}$$

Equivalently, in terms of the pressure, $p = -\big(\partial f/\partial v\big)_T$, these equations are equivalent to

$$p(T,v_1) = p(T,v_2) = \frac{1}{v_2-v_1}\int\limits_{v_1}^{v_2} dv\, p(T,v) \quad . \tag{7.17}$$

This procedure is known as the *Maxwell construction*, and is depicted graphically in fig. 7.5. When the Maxwell construction is enforced, the isotherms resemble the curves in fig. 7.4. In this figure, all points within the purple shaded region have $\partial^2 f/\partial v^2 < 0$, hence this region is unstable to infinitesimal fluctuations. The boundary of this region is called the *spinodal*, and the spontaneous phase separation into two phases is a process known as *spinodal decomposition*. The dot-dashed orange curve is the coexistence (*binodal*) curve. Between the coexistence curve and the spinodal, the homogeneous phase is metastable and transformation to the stable phase requires *nucleation*. In a nucleation process, an energy barrier must be overcome in order to achieve the lower free energy state. There is no energy barrier for spinodal decomposition – it is a spontaneous process.

Suppose we follow along an isotherm starting from the high molar volume (gas) phase. If $T > T_{\rm c}$, the volume v decreases continuously as the pressure p increases. If $T < T_{\rm c}$, then at the instant the isotherm first intersects the orange boundary curve in fig. 7.4, there is a discontinuous change in the molar volume from high (gas) to low (liquid) at fixed p. This discontinuous change is the hallmark of a *first order phase transition*. The volume discontinuity is $\Delta v \propto (T_{\rm c}-T)^{1/2}$. This is an example of a *critical behavior* in which the *order parameter* ϕ, which in this case may be taken to be the difference $\phi = v_{\rm G} - v_{\rm L}$, behaves as a power law in $\big|T-T_{\rm c}\big|$, where $T_{\rm c}$ is the *critical temperature*. In this case, we have $\phi(T) \propto (T_{\rm c}-T)_+^{\beta}$, where

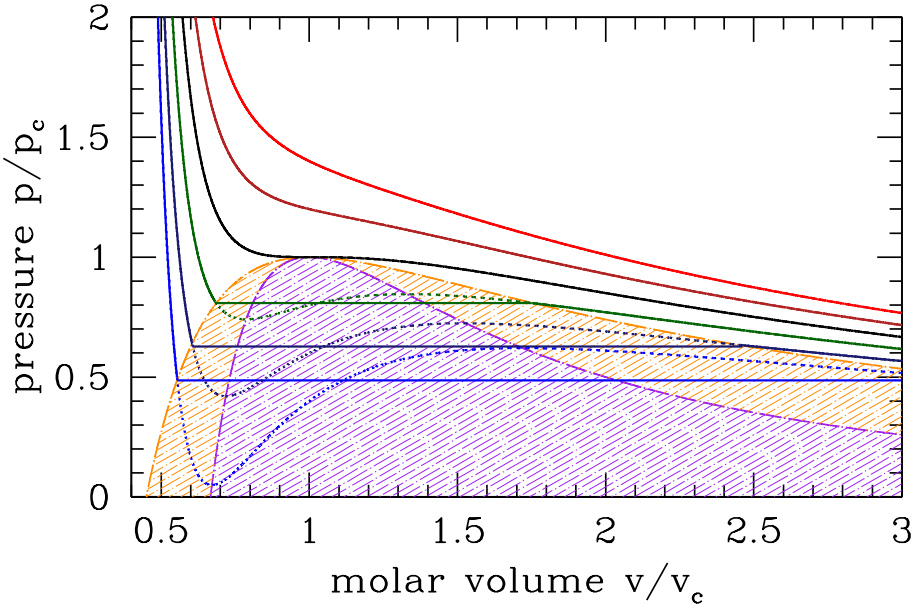


Figure 7.4: Pressure-volume isotherms for the van der Waals system, as in fig. 7.2, but corrected to account for the Maxwell construction. The boundary of the purple shaded region is the spinodal line $\bar{p}^*(\bar{v})$. The boundary of the orange shaded region is the stability boundary with respect to phase separation, and is called the *coexistence curve*.

$\beta = \frac{1}{2}$ is the exponent, and where $(T_c - T)_+$ is defined to be $T_c - T$ if $T < T_c$ and 0 otherwise. Recall the isothermal compressibility is $\kappa_T = -v^{-1}\big(\partial v/\partial p\big)_T$. This is finite along the coexistence curve – it diverges only along the spinodal. It therefore diverges at the critical point, which lies at the intersection of the spinodal and the coexistence curve.

It is convenient to express the equation of state and the coexistence curve in terms of dimensionless variables. Writing

$$\bar{p} = \frac{p}{p_c} \quad , \quad \bar{v} = \frac{v}{v_c} \quad , \quad \bar{T} = \frac{T}{T_c} \quad , \tag{7.18}$$

the dimensionless van der Waals equation of state takes the form

$$\bar{p} = \frac{8\bar{T}}{3\bar{v} - 1} - \frac{3}{\bar{v}^2} \quad . \tag{7.19}$$

7.3.2 Analytic form of the coexistence curve near the critical point

We write $v_L = v_c + w_L$ and $v_G = v_c + w_G$. One of our equations is $p(v_c + w_L, T) = p(v_c + w_G, T)$. Taylor expanding in powers of w_L and w_G, we have

$$0 = p_v(v_c, T)\,(w_G - w_L) + \tfrac{1}{2}\,p_{vv}(v_c, T)\,\big(w_G^2 - w_L^2\big) + \tfrac{1}{6}\,p_{vvv}(v_c, T)\,\big(w_G^3 - w_L^3\big) + \ldots \quad , \tag{7.20}$$

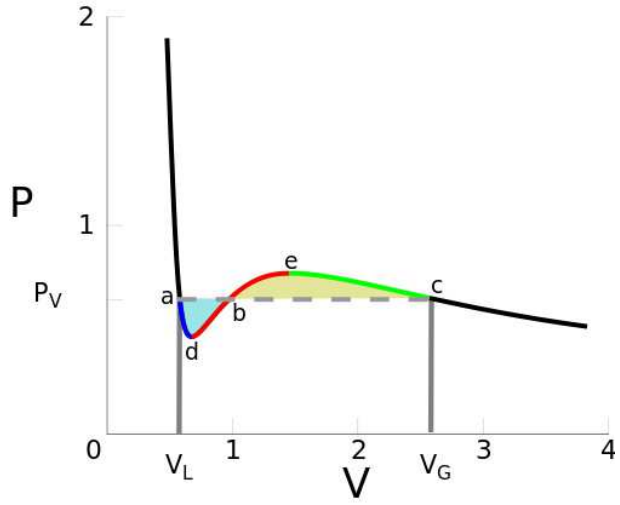


Figure 7.5: Maxwell construction in the (v, p) plane. The system is absolutely unstable between volumes $v_{\rm d}$ and $v_{\rm e}$. For $v \in [v_{\rm a}, v_{\rm d}]$ or $v \in [v_{\rm e}, v_{\rm c}]$, the solution is unstable with respect to phase separation. Source: *Wikipedia*.

where

$$p_v \equiv \frac{\partial p}{\partial v} \quad , \quad p_{vv} \equiv \frac{\partial^2 p}{\partial v^2} \quad , \quad p_{vvv} \equiv \frac{\partial^3 p}{\partial v^3} \quad , \quad p_{vT} \equiv \frac{\partial^2 p}{\partial v\, \partial T} \quad , \quad \text{etc.} \tag{7.21}$$

The second equation we write as

$$\int\limits_{w_{\rm L}}^{w_{\rm G}} dw\, p(v_{\rm c}+w,T) = \tfrac{1}{2}(w_{\rm G}-w_{\rm L})\Big(p(v_{\rm c}+w_{\rm L},T)+p(v_{\rm c}+w_{\rm G},T)\Big) \quad . \tag{7.22}$$

Expanding in powers of $w_{\rm L}$ and $w_{\rm G}$, this becomes

$$\begin{aligned} &p(v_{\rm c},T)\,(w_{\rm G}-w_{\rm L}) + \tfrac{1}{2}\,p_v(v_{\rm c},T)\,\big(w_{\rm G}^2-w_{\rm L}^2\big) + \tfrac{1}{6}\,p_{vv}(v_{\rm c},T)\,\big(w_{\rm G}^3-w_{\rm L}^3\big) \\ &\qquad\qquad + \tfrac{1}{24}\,p_{vvv}(v_{\rm c},T)\,\big(w_{\rm G}^4-w_{\rm L}^4\big) + \tfrac{1}{120}\,p_{vvvv}(v_{\rm c},T)\,\big(w_{\rm G}^5-w_{\rm L}^5\big) + \ldots \\ &= \tfrac{1}{2}(w_{\rm G}-w_{\rm L})\Big\{2\,p(v_{\rm c},T) + p_v(v_{\rm c},T)\,(w_{\rm G}+w_{\rm L}) + \tfrac{1}{2}\,p_{vv}(v_{\rm c},T)\,\big(w_{\rm G}^2+w_{\rm L}^2\big) \\ &\qquad\qquad + \tfrac{1}{6}\,p_{vvv}(v_{\rm c},T)\,\big(w_{\rm G}^3+w_{\rm L}^3\big) + \tfrac{1}{24}\,p_{vvvv}(v_{\rm c},T)\,\big(w_{\rm G}^4+w_{\rm L}^4\big) + \ldots\Big\} \end{aligned} \tag{7.23}$$

Subtracting the LHS from the RHS, we find that we can then divide by $\frac{1}{12}(w_{\rm G}-w_{\rm L})^3$, resulting in

$$0 = p_{vv}(v_{\rm c},T) + \tfrac{1}{2}\,p_{vvv}(v_{\rm c},T)\,(w_{\rm G}+w_{\rm L}) + \tfrac{1}{20}\,p_{vvvv}(v_{\rm c},T)\,\big(3w_{\rm G}^2+4w_{\rm G}w_{\rm L}+3w_{\rm L}^2\big) + \mathcal{O}\big(w_{\rm G,L}^3\big) \quad . \tag{7.24}$$

We now define $w_\pm \equiv w_{\rm G} \pm w_{\rm L}$. In terms of these variables, eqns. 7.20 and 7.24 become

$$\begin{aligned} 0 &= p_v(v_{\rm c},T) + \tfrac{1}{2}\,p_{vv}(v_{\rm c},T)\,w_+ + \tfrac{1}{8}\,p_{vvv}(v_{\rm c},T)\,\big(w_+^2+\tfrac{1}{3}\,w_-^2\big) + \mathcal{O}\big(w_\pm^3\big) \\ 0 &= p_{vv}(v_{\rm c},T) + \tfrac{1}{2}\,p_{vvv}(v_{\rm c},T)\,w_+ + \tfrac{1}{8}\,p_{vvvv}(v_{\rm c},T)\,\big(w_+^2+\tfrac{1}{5}\,w_-^2\big) + \mathcal{O}\big(w_\pm^3\big) \quad . \end{aligned} \tag{7.25}$$

We now write $T = T_{\rm c} + \Theta$ and evaluate $w_\pm$ as expansions in Θ. Note that $p_v(v_{\rm c}, T_{\rm c}) = p_{vv}(v_{\rm c}, T_{\rm c}) = 0$, since the critical point is an inflection point in the (v, p) plane. Thus, we have $p_v(v_{\rm c}, T) = p^0_{vT}\,\Theta + \mathcal{O}(\Theta^2)$, where $p^0_{vT} = p_{vT}(v_{\rm c}, T_{\rm c})$. We can then see that $w_- \propto \sqrt{-\Theta}$, while $w_+ \propto \Theta$ as $\Theta \to 0^-$, and we have

$$\begin{aligned} 0 &= p^0_{vT}\,\Theta + \tfrac{1}{24}\,p^0_{vvv}\,w_-^2 + \mathcal{O}(\Theta^2) \\ 0 &= p^0_{vvT}\,\Theta + \tfrac{1}{2}\,p^0_{vvv}\,w_+ + \tfrac{1}{40}\,p^0_{vvvv}\,w_-^2 + \mathcal{O}(\Theta^2) \quad . \end{aligned} \tag{7.26}$$

Thus,

$$\begin{aligned} w_- &= \left(\frac{24\,p^0_{vT}}{p^0_{vvv}}\right)^{1/2}\sqrt{-\Theta} + \ldots \\ w_+ &= \left(\frac{6\,p^0_{vT}\,p^0_{vvvv} - 10\,p^0_{vvv}\,p^0_{vvT}}{5\,(p^0_{vvv})^2}\right)\Theta + \ldots \quad . \end{aligned} \tag{7.27}$$

We then have

$$\begin{aligned} w_{\rm L} &= -\left(\frac{6\,p^0_{vT}}{p^0_{vvv}}\right)^{1/2}\sqrt{-\Theta} + \left(\frac{3\,p^0_{vT}\,p^0_{vvvv} - 5\,p^0_{vvv}\,p^0_{vvT}}{5\,(p^0_{vvv})^2}\right)\Theta + \mathcal{O}\big(\Theta^{3/2}\big) \\ w_{\rm G} &= \left(\frac{6\,p^0_{vT}}{p^0_{vvv}}\right)^{1/2}\sqrt{-\Theta} + \left(\frac{3\,p^0_{vT}\,p^0_{vvvv} - 5\,p^0_{vvv}\,p^0_{vvT}}{5\,(p^0_{vvv})^2}\right)\Theta + \mathcal{O}\big(\Theta^{3/2}\big) \quad . \end{aligned} \tag{7.28}$$

Close to the critical point, the dimensionless equation of state may be written as $\pi = \pi(\epsilon, t)$, where

$$\bar p = 1 + \pi \quad , \quad \bar v = 1 + \epsilon \quad , \quad \bar T = 1 + t \quad , \tag{7.29}$$

where $\pi(0,0) = 0$. Equivalently,

$$\pi = \frac{p - p_{\rm c}}{p_{\rm c}} \quad , \quad \epsilon = \frac{v - v_{\rm c}}{v_{\rm c}} \quad , \quad t = \frac{T - T_{\rm c}}{T_{\rm c}} = \frac{\Theta}{T_{\rm c}} \quad . \tag{7.30}$$

Here π, ϵ, and t are, respectively, the dimensionless deviations of pressure, molar volume, and temperature from their critical point values. For the van der Waals equation of state in eqn. 7.19, we have

$$\begin{aligned} \pi(\epsilon, t) &= \frac{8(1+t)}{2+3\epsilon} - \frac{3}{(1+\epsilon)^2} - 1 \\ &= 4t - 6t\epsilon + 9\epsilon^2 t - \tfrac{3}{2}\epsilon^3 - \tfrac{27}{2}\epsilon^3 t + \tfrac{21}{4}\epsilon^4 + \tfrac{81}{4}\epsilon^4 t - \tfrac{99}{8}\epsilon^5 + \ldots \quad . \end{aligned} \tag{7.31}$$

Expressed in these dimensionless quantities, eqns. 7.28 take the form

$$\epsilon_{\rm L,G} = \mp\left(\frac{6\,\pi^0_{\epsilon t}}{\pi^0_{\epsilon\epsilon\epsilon}}\right)^{1/2}(-t)^{1/2} + \left(\frac{3\,\pi^0_{\epsilon t}\,\pi^0_{\epsilon\epsilon\epsilon\epsilon} - 5\,\pi^0_{\epsilon\epsilon\epsilon}\,\pi^0_{\epsilon\epsilon t}}{5\,(\pi^0_{\epsilon\epsilon\epsilon})^2}\right)t + \mathcal{O}\big((-t)^{3/2}\big) \quad . \tag{7.32}$$

For the van der Waals system , we have

$$\pi^0_{\epsilon t} = -6 \quad , \quad \pi^0_{\epsilon\epsilon t} = 18 \quad , \quad \pi^0_{\epsilon\epsilon\epsilon} = -9 \quad , \quad \pi^0_{\epsilon\epsilon\epsilon\epsilon} = 126 \quad , \tag{7.33}$$

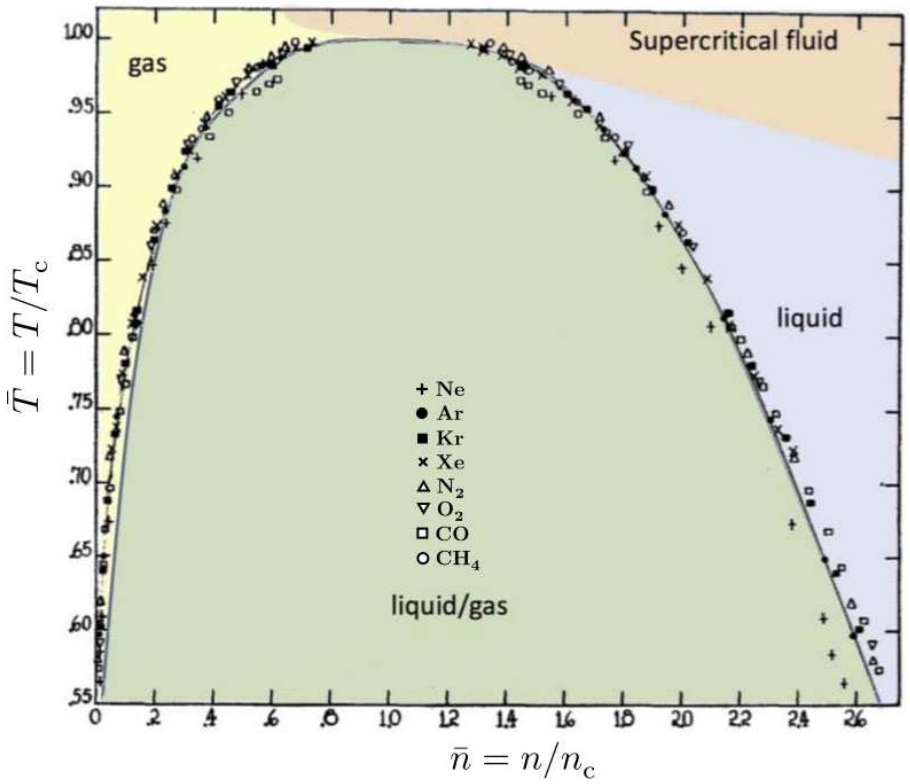


Figure 7.6: Universality of the liquid-gas transition for eight different atomic and molecular fluids, from E. A. Guggenheim, *J. Chem. Phys.* **13**, 253 (1945). Dimensionless temperature $\bar{T} = T/T_c$ *versus* dimensionless number density $\bar{n} = n/n_c = v_c/v$ is shown. The van der Waals / mean field theory gives $\Delta n = n_{\rm liquid} - n_{\rm gas} \propto (-t)^{1/2}$, while experiments show a result closer to $\Delta n \propto (-t)^{1/3}$. Here $t \equiv \bar{T} - 1 = (T - T_c)/T_c$ is the dimensionless temperature deviation with respect to the critical point. (Image adapted from Matthew Schwartz's Harvard lecture notes, adapted from Guggenheim 1945.)

where the derivatives are evaluated at critical point, where $\epsilon = t = \pi = 0$. Thus, for van der Waals,

$$\epsilon_{\rm L,G} = \mp 2\sqrt{-t} - \tfrac{18}{5}\,t + \ldots \quad . \tag{7.34}$$

We identify the difference $\Delta v \equiv v_{\rm G} - v_{\rm L}$ as the *order parameter* for the transition which occurs at $T = T_c$. We see that the order parameter behaves as a power law for T just below the critical point, with $\Delta v \propto (-t)^\beta$ and $\beta = \frac{1}{2}$, which is the *order parameter critical exponent*.

The spinodal boundary for the vdW system is then given by the solution to

$$0 = \frac{\partial \pi}{\partial \epsilon} = -6t + 18\epsilon t - \tfrac{9}{2}\epsilon^2 - \tfrac{81}{2}\epsilon^2 t + 21\epsilon^3 + \ldots \quad . \tag{7.35}$$

For the spinodal, it is easy to see that the lowest order nontrivial solution is $\epsilon = \mp\frac{2}{\sqrt{3}}\sqrt{-t}$. For the coexistence curve, we found $\epsilon_{\rm L,G} = \mp 2\sqrt{-t}$.

Fig. 7.6 shows the universality of the liquid-gas transition for eight different fluids: Ne, Ar, Kr, Xe, N_2, O_2, CO, and CH_4. The experimental coexistence curve expressed in dimensionless variables $\bar{n} = 1/\bar{v}$

and $\bar{T} = T/T_{\rm c}$ is fairly well-fit to the curve[12]

$$\bar{n}_{\rm L,G}(t) = 1 \pm \tfrac{7}{4}(1-\bar{T})^{1/3} + \tfrac{3}{4}(1-\bar{T}) \tag{7.36}$$

which shows that the critical exponent β is much closer to $\beta = \frac{1}{3}$ than to the vdW value $\beta^{\rm vdW} = \frac{1}{2}$. The van der Waals equation is in essence a *mean field theory* of the liquid-gas transition.

7.3.3 History of the van der Waals equation

The van der Waals equation of state first appears in van der Waals' 1873 PhD thesis[13], *"Over de Continuïteit van den Gas - en Vloeistoftoestand"* ("On the continuity of the gas and liquid state"). In his Nobel lecture[14], van der Waals writes of how he was inspired by Rudolf Clausius' 1857 treatise on the nature of heat, where it is posited that a gas in fact consists of microscopic particles whizzing around at high velocities. van der Waals reasoned that liquids, which result when gases are compressed, also consist of 'small moving particles': *"Thus I conceived the idea that there is no essential difference between the gaseous and the liquid state of matter..."*

Clausius' treatise showed how his kinetic theory of heat was consistent with Boyle's law for gases ($pV = \text{constant}$ at fixed temperature). van der Waals pondered why this might fail for the non-dilute liquid phase, and he reasoned that there were two principal differences: inter-particle attraction and excluded volume. These considerations prompted him to posit his famous equation,

$$p = \frac{RT}{v-b} - \frac{a}{v^2} \quad . \tag{7.37}$$

The first term on the RHS accounts for excluded volume effects, and the second for mutual attractions.

In the limiting case of $p \to \infty$, the molar volume approaches $v = b$. On physical grounds, one might expect $b = v_0/\zeta$, where $v_0 = N_{\rm A}\,\omega_0$ is $N_{\rm A}$ times the volume ω_0 of a single molecule, and the *packing fraction* is $\zeta = N\omega_0/V = v_0/v$, which is the ratio of the total molecular volume to the total system volume. In three dimensions, the maximum possible packing fraction is for fcc and hcp lattices, each of which have coordination number 12, with $\zeta_{\rm max} = \frac{\pi}{3\sqrt{2}} = 0.74048$. Dense random packing results in $\zeta_{\rm drp} = 0.634$. Expanding the vdW equation of state in inverse powers of v yields

$$p = \frac{RT}{v} + \left(b - \frac{a}{RT}\right)\cdot\frac{RT}{v^2} + \mathcal{O}\big(v^{-3}\big) \quad , \tag{7.38}$$

and we read off the second virial coefficient $B_2 = \big(b - \frac{a}{RT}\big)/N_{\rm A}$. For hard spheres, $a = 0$, and the result $B_2 = 4\omega_0$ from the Mayer cluster expansion corresponds to $b_{\rm Mayer} = 4v_0$, which is larger than the result from even the loosest regular sphere packing, *i.e.* that for a cubic lattice, with $\zeta_{\rm cub} = \frac{\pi}{6}$.

[12] See M. Schwartz, https://scholar.harvard.edu/files/schwartz/files/9-phases.pdf.

[13] Johannes Diderik van der Waals, the eldest of ten children, was the son of a carpenter. As a child he received only a primary school education. He worked for a living until age 25, and was able to enroll in a three-year industrial evening school for working class youth. Afterward he continued his studies independently, in his spare time, working as a teacher. By the time he obtained his PhD, he was 36 years old. He received the Nobel Prize for Physics in 1910.

[14] See http://www.nobelprize.org/nobel_prizes/physics/laureates/1910/waals-lecture.pdf

The law of corresponding states

Another of van der Waals' great achievements was his articulation of the *law of corresponding states*. Recall that the van der Waals equation of state, when written in terms of dimensionless quantities $\bar{p} = p/p_{\rm c}$, $\bar{v} = v/v_{\rm c}$, and $\bar{T} = T/T_{\rm c}$, takes the form of eqn. 7.19. Thus, while the a and b parameters are specific to each fluid – see Tab. 7.1 – when written in terms of these scaled dimensionless variables, the equation of state and all its consequent properties (*i.e.* the liquid-gas phase transition) are *universal*.

The van der Waals equation is best viewed as semi-phenomenological. Interaction and excluded volume effects surely are present, but the van der Waals equation itself only captures them in a very approximate way. It is applicable to gases, where it successfully predicts features that are not present in ideal systems (*e.g.* throttling). It is of only qualitative and pedagogical use in the study of fluids, the essential physics of which lies in the behavior of quantities like the pair distribution function $g(r)$. As we saw in chapter 6, any adequate first principles derivation of $g(r)$ - a function which can be measured in scattering experiments - involves rather complicated approximation schemes to close the BBGKY hierarchy. Else one must resort to numerical simulations such as the Monte Carlo method. Nevertheless, the lessons learned from the van der Waals system are invaluable and they provide us with a first glimpse of what is going on in the vicinity of a phase transition, and how nonanalytic behavior, such as $v_{\rm G} - v_{\rm L} \propto (T_{\rm c} - T)^\beta$ with noninteger exponent β may result due to singularities in the free energy at the critical point.

7.4 Fluids, Magnets, and the Ising Model

7.4.1 Lattice gas description of a fluid

The usual description of a fluid follows from a continuum Hamiltonian of the form

$$\hat{H}(\boldsymbol{p}, \boldsymbol{x}) = \sum_{i=1}^{N} \frac{\boldsymbol{p}_i^2}{2m} + \sum_{i<j} u(\boldsymbol{x}_i - \boldsymbol{x}_j) \quad . \tag{7.39}$$

The potential $u(\boldsymbol{r})$ is typically central, depending only on the magnitude $|\boldsymbol{r}|$, and short-ranged. Now consider a discretized version of the fluid, in which we divide up space into cells (cubes, say), each of which can accommodate at most one fluid particle (due to excluded volume effects). That is, each cube has a volume on the order of a^3, where a is the diameter of the fluid particles. In a given cube i we set the occupancy $n_i = 1$ if a fluid particle is present and $n_i = 0$ if there is no fluid particle present. We then have that the potential energy is

$$U = \sum_{i<j} u(\boldsymbol{x}_i - \boldsymbol{x}_j) = \tfrac{1}{2} \sum_{\boldsymbol{R} \neq \boldsymbol{R}'} V_{\boldsymbol{R},\boldsymbol{R}'}\, n_{\boldsymbol{R}}\, n_{\boldsymbol{R}'} \quad , \tag{7.40}$$

where $V_{\boldsymbol{R},\boldsymbol{R}'} \approx u(\boldsymbol{R} - \boldsymbol{R}')$, where R_k is the position at the center of cube k. The grand partition function is then approximated as

$$\Xi(T, V, \mu) \approx \sum_{\{n_{\boldsymbol{R}}\}} \left(\prod_{\boldsymbol{R}} \xi^{n_{\boldsymbol{R}}} \right) \exp\left(-\frac{1}{2k_{\rm B}T} \sum_{\boldsymbol{R} \neq \boldsymbol{R}'} V_{\boldsymbol{R},\boldsymbol{R}'}\, n_{\boldsymbol{R}}\, n_{\boldsymbol{R}'} \right) \quad , \tag{7.41}$$

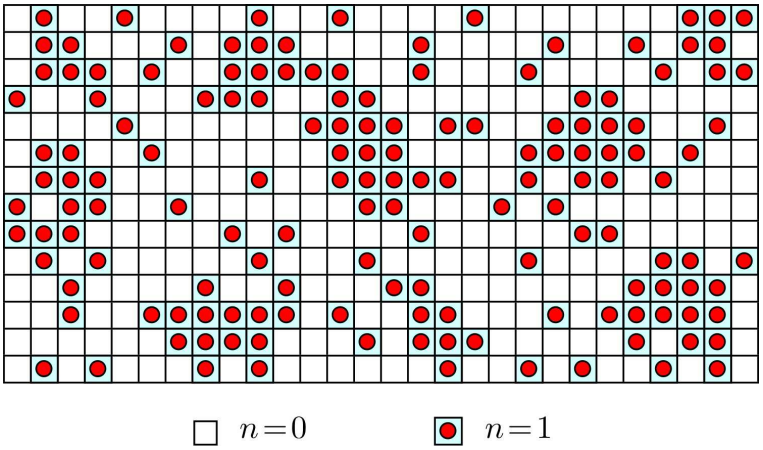


Figure 7.7: The lattice gas model. An occupied cell corresponds to $n = 1$ ($\sigma = +1$), and a vacant cell to $n = 0$ ($\sigma = -1$).

where $\xi = e^{\beta\mu}\,\lambda_T^{-d}\,a^d$, and where a is the side length of each cube (chosen to be on the order of the hard sphere diameter). The λ_T^{-d} factor arises from the integration over the momenta. Note $N = \sum_{\boldsymbol{R}} n_{\boldsymbol{R}}$ is the total number of fluid particles, so $\prod_{\boldsymbol{R}} \xi^{n_{\boldsymbol{R}}} = \xi^N$ where $\xi = e^{\beta\mu}(a/\lambda_T)^d$.

Thus, we arrive at $\Xi = \mathsf{Tr}\,\exp(-\beta\hat{H}_{\mathsf{LG}})$ where $\hat{H}_{\mathsf{LG}}$ is the *lattice gas Hamiltonian*,

$$\begin{aligned}\hat{H}_{\mathsf{LG}} &= \tfrac{1}{2}\sum_{\boldsymbol{R}\neq\boldsymbol{R}'} V_{\boldsymbol{R},\boldsymbol{R}'}\,n_{\boldsymbol{R}}\,n_{\boldsymbol{R}'} - k_{\mathrm{B}}T\log\xi\sum_{\boldsymbol{R}} n_{\boldsymbol{R}} \\ &= -\tfrac{1}{2}\sum_{\boldsymbol{R}\neq\boldsymbol{R}'} J_{\boldsymbol{R},\boldsymbol{R}'}\,\sigma_{\boldsymbol{R}}\,\sigma_{\boldsymbol{R}'} - H\sum_{\boldsymbol{R}}\sigma_{\boldsymbol{R}} + E_0 \quad ,\end{aligned} \tag{7.42}$$

where $\sigma_{\boldsymbol{R}} \equiv 2n_{\boldsymbol{R}} - 1$ is a spin variable taking the possible values $\{-1, +1\}$, and

$$J_{\boldsymbol{R},\boldsymbol{R}'} = -\tfrac{1}{4}u(\boldsymbol{R}-\boldsymbol{R}') \qquad , \qquad H = \tfrac{1}{2}\mu + \tfrac{1}{2}dk_{\mathrm{B}}T\log(a/\lambda_T) - \tfrac{1}{4}{\sum_{\boldsymbol{R}}}'u(\boldsymbol{R}) \tag{7.43}$$

and $E_0 = \frac{1}{8}N_{\mathrm{c}}\,{\sum_{\boldsymbol{R}}}'u(\boldsymbol{R}) - \frac{1}{2}N_{\mathrm{c}}k_{\mathrm{B}}T\log\xi$, where $N_{\mathrm{c}} = V/a^d$ is the number of unit cells, and where the prime on the sum indicates that $\boldsymbol{R} = 0$ is to be excluded. For the Lennard-Jones system, $u(\boldsymbol{R}-\boldsymbol{R}') < 0$ is due to the attractive tail of the potential, hence $J_{\boldsymbol{R},\boldsymbol{R}'} > 0$, which prefers alignment of the spins $\sigma_{\boldsymbol{R}}$ and $\sigma_{\boldsymbol{R}'}$. This interaction is therefore *ferromagnetic*. The spin Hamiltonian in eqn. 7.42 is recognized as the Ising model.

7.4.2 Phase diagrams and critical exponents

The physics of the liquid-gas transition in fact has a great deal in common with that of the transition between a magnetized and unmagnetized state of a magnetic system. The correspondences are[15] $p \leftrightarrow H$

[15] H is more properly analogous to μ. However, since $\mu = \mu(p,T)$, H can also be regarded as analogous to p. Note also that $\beta p = z\lambda_T^{-d}$ for the ideal gas, in which case $\xi = z\,(a/\lambda_T)^d$ is proportional to $p/k_{\mathrm{B}}T$.

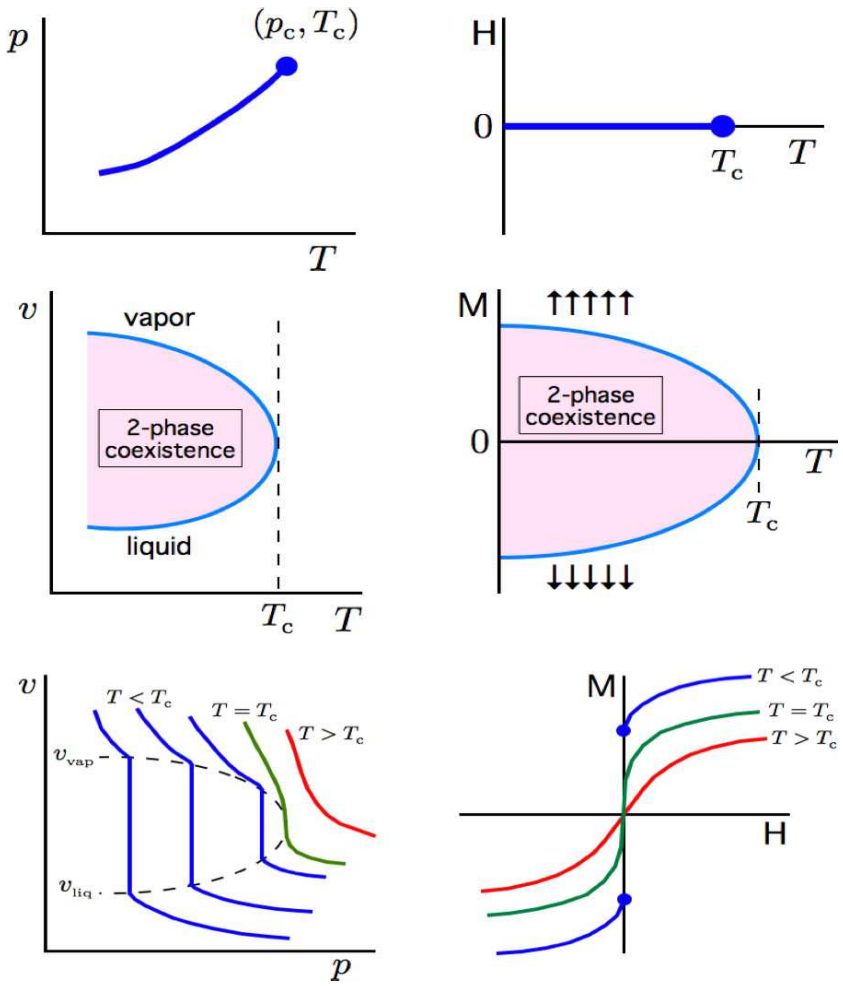


Figure 7.8: Comparison of the liquid-gas phase diagram with that of the Ising ferromagnet.

and $v \leftrightarrow m$, where m is the magnetization density, defined here to be the total magnetization M divided by the number of lattice sites[16] N_c, *viz.*

$$m = \frac{M}{N_c} = \frac{1}{N_c} \sum_{\boldsymbol{R}} \langle \sigma_{\boldsymbol{R}} \rangle \quad . \tag{7.44}$$

Sketches of the phase diagrams are reproduced in fig. 7.8. Of particular interest is the *critical point*, which occurs at (T_c, p_c) in the fluid system and (T_c, H_c) in the magnetic system, with $H_c = 0$ by symmetry.

In the fluid, the coexistence curve in the (p, T) plane separates high density (liquid) and low density (vapor) phases. The specific volume v (or the density $n = v^{-1}$) jumps discontinuously across the coexistence curve. In the magnet, the coexistence curve in the (H, T) plane separates positive magnetization and negative magnetization phases. The magnetization density m jumps discontinuously across the

[16]Note the distinction between the number of lattice sites N_c and the number of occupied cells N. According to our definitions, $N = \frac{1}{2}(M + N_c)$.

coexistence curve. For $T > T_{\rm c}$, the latter system is a *paramagnet*, in which the magnetization varies smoothly as a function of H. This behavior is most apparent in the bottom panel of the figure, where $v(p)$ and $m(H)$ curves are shown.

For $T < T_{\rm c}$, the fluid exists in a *two phase region*, which is spatially inhomogeneous, supporting local regions of high and low density. There is no stable homogeneous thermodynamic phase for (T, v) within the two phase region shown in the middle left panel. Similarly, for the magnet, there is no stable homogeneous thermodynamic phase at fixed temperature T and magnetization m if (T, m) lies within the coexistence region. Rather, the system consists of blobs where the spin is predominantly up, and blobs where the spin is predominantly down.

Note also the analogy between the isothermal compressibility κ_T and the isothermal susceptibility χ_T:

$$\kappa_T = -\frac{1}{v}\left(\frac{\partial v}{\partial p}\right)_T \quad , \quad \chi_T = \left(\frac{\partial m}{\partial H}\right)_T \quad , \tag{7.45}$$

with $\kappa_T(T_{\rm c}, p_{\rm c}) = \infty$ and $\chi_T(T_{\rm c}, H_{\rm c}) = \infty$.

The *order parameter* for a second order phase transition is a quantity which vanishes in the disordered phase and is finite in the ordered phase. For the fluid, the order parameter can be chosen to be $\Psi \propto (v_{\rm vap} - v_{\rm liq})$, the difference in the specific volumes of the vapor and liquid phases. In the vicinity of the critical point, the system exhibits power law behavior in many physical quantities, *viz.*

$$m(T, H_{\rm c}) \sim \big(T_{\rm c} - T\big)_+^{\beta} \quad , \quad \chi(T, H_{\rm c}) \sim |T - T_{\rm c}|^{-\gamma} \quad , \quad C(T, H_{\rm c}) \sim |T - T_{\rm c}|^{-\alpha} \quad , \quad m(T_{\rm c}, H) \sim \pm |H|^{1/\delta} \quad . \tag{7.46}$$

The quantities α, β, γ, and δ are the *critical exponents* associated with the transition. These exponents satisfy certain equalities, such as the Rushbrooke and Griffiths relations:

$$\alpha + 2\beta + \gamma = 2 \quad \text{(Rushbrooke)} \qquad , \qquad \beta + \gamma = \beta\delta \quad \text{(Griffiths)} \quad . \tag{7.47}$$

Originally such relations were derived as inequalities, and only after the advent of scaling and renormalization group theories it was realized that they held as equalities.

In addition to the exponents α, β, γ, and δ, one defines the *correlation length exponent* ν from the behavior of the two-point connected correlation function

$$G(\boldsymbol{r}, T) = \langle \psi(0)\, \psi(\boldsymbol{r}) \rangle - \langle \psi(0) \rangle \langle \psi(\boldsymbol{r}) \rangle \quad , \tag{7.48}$$

where $\psi(\boldsymbol{r})$ is a local operator, such as the local density in a fluid or the local spin polarization in a magnet[17]. In the limits $T \to T_{\rm c}$ and $H \to H_{\rm c} = 0$, one has

$$G(\boldsymbol{r}, T, H) = r^{-(d-2+\eta)}\, \phi\big(r/\xi(T), H/\xi_H(T)\big) \quad , \tag{7.49}$$

where η is the *anomalous exponent*, $\phi(r/\xi, H/\xi_H)$ is a *scaling function*, $\xi(T) \propto |T - T_{\rm c}|^{-\nu}$ is the *correlation length*, and $\xi_H(T) \propto |T - T_{\rm c}|^{\Delta}$, with $\Delta = \beta\delta$, is a field scale. As we have seen, for the lattice gas system

[17] The local 'order parameter field' $\psi(\boldsymbol{r})$ may carry vector or tensor indices. In general, it transforms as a non-trivial representation of the system's global symmetry group G.

the effective magnetic field H is a proxy for the pressure or the chemical potential. Along with the new exponents η and ν come additional exponent relations,

$$(2-\eta)\nu = \gamma \qquad , \qquad d\,\nu = 2-\alpha \quad \text{(hyperscaling)} \quad . \tag{7.50}$$

Thus there are three relations among the six critical exponents α, β, γ, δ, η, and ν, which entails that there are three independent values among the six[18].

7.4.3 Gibbs-Duhem relation for magnetic systems

Homogeneity of $E(S,M,N)$ means $E = TS + HM + \mu N$, by Euler's theorem. After invoking the First Law $dE = T\,dS + H\,dM + \mu\,dN$, we have

$$S\,dT + M\,dH + N\,d\mu = 0 \quad . \tag{7.51}$$

Now consider two magnetic phases in coexistence. We must have $d\mu_1 = d\mu_2$, hence

$$d\mu_1 = -s_1\,dT - m_1\,dH = -s_2\,dT - m_2\,dH = d\mu_2 \quad , \tag{7.52}$$

where $m = M/N$ is the magnetization per site and $s = S/N$ is the specific entropy. Thus, we obtain the Clapeyron equation for magnetic systems,

$$\left(\frac{dH}{dT}\right)_{\rm coex} = -\frac{s_1 - s_2}{m_1 - m_2} \quad . \tag{7.53}$$

Thus, if $m_1 \neq m_2$ and $\big(dH/dT\big)_{\rm coex} = 0$, then we must have $s_1 = s_2$, which says that there is *no latent heat associated with the transition*. This absence of latent heat is a consequence of the *symmetry* which guarantees that $G(T,H,N) = G(T,-H,N)$.

Recall our discussion in §2.11.2 of the Clausius-Clapeyron relation for liquid-gas systems. From $G = E - TS + pV = G(T,p,N)$, the differential of the Gibbs free energy per particle, $\mu = G/N$, is given by $d\mu = -s\,dT + v\,dp$, where $v = V/N$ is the volume per particle[19]. This leads to the Clapeyron relation,

$$\left(\frac{dp}{dT}\right)_{\rm coex} = \frac{s_2 - s_1}{v_2 - v_1} = \frac{\ell}{T\,\Delta v} \quad , \tag{7.54}$$

which determines the slope of the coexistence curve in the (T,p) plane.

7.4.4 Order-disorder transitions

Another application of the Ising model lies in the theory of order-disorder transitions in alloys. Examples include Cu_3Au, CuZn, and other compounds. In CuZn, the Cu and Zn atoms occupy sites of a body centered cubic (BCC) lattice, forming an alloy known as β-brass. Below $T_{\rm c} \simeq 740\,{\rm K}$, the atoms

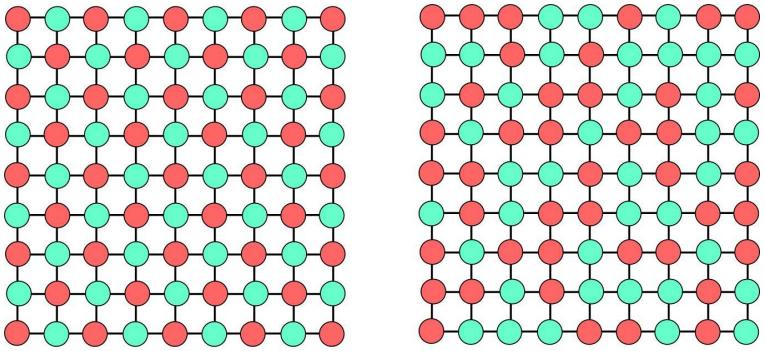


Figure 7.9: Order-disorder transition on the square lattice. Below $T = T_{\rm c}$, order develops spontaneously on the two $\sqrt{2} \times \sqrt{2}$ sublattices. There is perfect sublattice order at $T = 0$ (left panel).

are ordered, with the Cu preferentially occupying one simple cubic sublattice and the Zn preferentially occupying the other.

The energy is a sum of pairwise interactions, with a given link contributing $\varepsilon_{\rm AA}$, $\varepsilon_{\rm BB}$, or $\varepsilon_{\rm AB}$, depending on whether it is an A-A, B-B, or A-B/B-A link. Here A and B represent Cu and Zn, respectively. Thus, we can write the energy of the link $\langle ij \rangle$ as

$$E_{ij} = \varepsilon_{\rm AA}\, P_i^{\rm A}\, P_j^{\rm A} + \varepsilon_{\rm BB}\, P_i^{\rm B}\, P_j^{\rm B} + \varepsilon_{\rm AB}\left(P_i^{\rm A}\, P_j^{\rm B} + P_i^{\rm B}\, P_j^{\rm A}\right) \quad , \tag{7.55}$$

where

$$P_i^{\rm A} = \tfrac{1}{2}(1+\sigma_i) = \begin{cases} 1 & \text{if site } i \text{ contains Cu} \\ 0 & \text{if site } i \text{ contains Zn} \end{cases} \quad , \quad P_i^{\rm B} = \tfrac{1}{2}(1-\sigma_i) = \begin{cases} 1 & \text{if site } i \text{ contains Zn} \\ 0 & \text{if site } i \text{ contains Cu} \end{cases} .$$

The Hamiltonian is then

$$\begin{aligned} \hat{H} = \sum_{\langle ij \rangle} E_{ij} &= \sum_{\langle ij \rangle} \left\{ \tfrac{1}{4}\big(\varepsilon_{\rm AA} + \varepsilon_{\rm BB} - 2\varepsilon_{\rm AB}\big)\,\sigma_i\,\sigma_j + \tfrac{1}{4}\big(\varepsilon_{\rm AA} - \varepsilon_{\rm BB}\big)\,(\sigma_i + \sigma_j) + \tfrac{1}{4}\big(\varepsilon_{\rm AA} + \varepsilon_{\rm BB} + 2\varepsilon_{\rm AB}\big) \right\} \\ &= -J \sum_{\langle ij \rangle} \sigma_i\,\sigma_j - H \sum_{i=1}^{N} \sigma_i + E_0 \quad , \end{aligned} \tag{7.56}$$

where the exchange constant J and the magnetic field H are given by

$$J = \tfrac{1}{4}\big(2\varepsilon_{\rm AB} - \varepsilon_{\rm AA} - \varepsilon_{\rm BB}\big) \qquad , \qquad H = \tfrac{1}{4} z \big(\varepsilon_{\rm BB} - \varepsilon_{\rm AA}\big) \quad , \tag{7.57}$$

and $E_0 = \frac{1}{8} N z \big(\varepsilon_{\rm AA} + \varepsilon_{\rm BB} + 2\varepsilon_{\rm AB}\big)$, where N is the total number of lattice sites and $z = 8$ is the *lattice coordination number*, which is the number of nearest neighbors of any given site.

[18] Hyperscaling is generally valid only at or below the system's *upper critical dimension* $d_{\rm u}$, which is the dimension above which the critical exponents given by *mean field theory* (see below) are exact.

[19] In §2.11.2 we considered, equivalently, the differential of the molar free energy $g = N_{\rm A}\mu$, with v the molar volume.

Note that

$$\begin{aligned} 2\varepsilon_{\rm AB} > \varepsilon_{\rm AA} + \varepsilon_{\rm BB} \quad &\Longrightarrow \quad J > 0 \quad \text{(ferromagnetic)} \\ 2\varepsilon_{\rm AB} < \varepsilon_{\rm AA} + \varepsilon_{\rm BB} \quad &\Longrightarrow \quad J < 0 \quad \text{(antiferromagnetic)} \quad . \end{aligned} \tag{7.58}$$

The antiferromagnetic case is depicted in fig. 7.9.

7.5 Mean Field Theory

7.5.1 The mean field *Ansatz*

Consider the Ising model Hamiltonian,

$$\hat{H} = -J \sum_{\langle ij \rangle} \sigma_i \, \sigma_j - H \sum_{i=1}^{N} \sigma_i \quad , \tag{7.59}$$

where the first sum on the RHS is over all links of the lattice. Each spin can be either 'up' ($\sigma = +1$) or 'down' ($\sigma = -1$). We further assume that the spins are located on a Bravais lattice[20] and that the coupling between sites i and j is $J_{ij} = J\big(|\boldsymbol{R}_i - \boldsymbol{R}_j|\big)$, where $\boldsymbol{R}_i$ is the position of the $i^{\rm th}$ spin. Here we assume $J_{ij} = 0$ beyond nearest neighbors; later we will assume a more general set of couplings. We also set the self-interaction terms to zero: $J_{ii} = 0$ for all i.

On each site i we decompose σ_i into a contribution from its thermodynamic average and a fluctuation:

$$\sigma_i = \langle \sigma_i \rangle + \delta\sigma_i \quad . \tag{7.60}$$

We will write $\langle \sigma_i \rangle \equiv m$, the local magnetization (dimensionless), and assume that m is independent of position i. Then

$$\begin{aligned} \sigma_i \, \sigma_j &= (m + \delta\sigma_i)\,(m + \delta\sigma_j) \\ &= m^2 + m\,(\delta\sigma_i + \delta\sigma_j) + \delta\sigma_i \, \delta\sigma_j \\ &= -m^2 + m\,(\sigma_i + \sigma_j) + \delta\sigma_i \, \delta\sigma_j \quad . \end{aligned} \tag{7.61}$$

The last term on the RHS of the second equation above is quadratic in the fluctuations, and we assume this to be negligibly small. This neglect of the fluctuations is the *mean field Ansatz*, and results in the *mean field Hamiltonian*

$$\hat{H}_{\rm MF} = \tfrac{1}{2} N z J \, m^2 - \big(H + zJm\big) \sum_{i=1}^{N} \sigma_i \quad , \tag{7.62}$$

where N is the total number of lattice sites. Note that the number of nearest-neighbor links is given by $N_{\rm links} = \frac{1}{2} z N$, where z is the lattice coordination number, *i.e.* the number of nearest neighbors for any

[20] A Bravais lattice is one in which any site is equivalent to any other site through an appropriate discrete translation. Examples of Bravais lattices include the linear chain, square, triangular, simple cubic, face-centered cubic, *etc.* lattices. The honeycomb lattice is not a Bravais lattice, because there are two sets of inequivalent sites – those in the center of a Y and those in the center of an upside down Y.

given site, and N is the number of lattice sites[21]. The first term is a constant, although the value of m is yet to be determined. The Boltzmann weights are then completely determined by the second term, which is just what we would write down for a Hamiltonian of *noninteracting* spins in an effective 'mean field'

$$H_{\rm eff} = H + zJm \quad . \tag{7.63}$$

In other words, $H_{\rm eff} = H_{\rm ext} + H_{\rm int}$, where the external field is applied field $H_{\rm ext} = H$, and the 'internal field' is $H_{\rm int} = zJm$. The internal field accounts for the interaction with the *average* values of all other spins coupled to a spin at a given site, hence it is often called the 'mean field'. Since the spins are noninteracting, we have

$$m = \frac{e^{\beta H_{\rm eff}} - e^{-\beta H_{\rm eff}}}{e^{\beta H_{\rm eff}} + e^{-\beta H_{\rm eff}}} = \tanh\left(\frac{H + zJm}{k_{\rm B}T}\right) \quad . \tag{7.64}$$

It is a simple matter to solve for the free energy, given the noninteracting Hamiltonian $\hat{H}_{\rm MF}$. The partition function is

$$Z = {\rm Tr}\ e^{-\beta \hat{H}_{\rm MF}} = e^{-\frac{1}{2}\beta N z J\, m^2} \left(\sum_\sigma e^{\beta(H + zJm)\sigma} \right)^N = e^{-\beta F} \quad . \tag{7.65}$$

We now define dimensionless variables:

$$f \equiv \frac{F}{NzJ} \qquad , \qquad \theta \equiv \frac{k_{\rm B}T}{zJ} \qquad , \qquad h \equiv \frac{H}{zJ} \quad , \tag{7.66}$$

and obtain the dimensionless free energy

$$f(m, \theta, h) = \tfrac{1}{2}m^2 - \theta\, \log\cosh\left(\frac{m+h}{\theta}\right) - \theta \log 2 \quad . \tag{7.67}$$

Differentiating with respect to m gives the mean field equation,

$$m = \tanh\left(\frac{m+h}{\theta}\right) \quad , \tag{7.68}$$

which is equivalent to the self-consistency requirement, $m = \langle \sigma_i \rangle$. In terms of the dimensionless variables θ and h, the physics is universal, and independent of details such as the magnitude of J, the value of z, and Boltzmann's constant.

7.5.2 Zero external field

When $h = 0$ the mean field equation becomes $m = \tanh(m/\theta)$. This nonlinear equation can be solved graphically, as in the top panel of fig. 7.10. The RHS is a tanh function which gets steeper with decreasing dimensionless temperature θ. If, at $m = 0$, the slope of $\tanh(m/\theta)$ is smaller than unity, then the curve $y = \tanh(m/\theta)$ will intersect $y = m$ only at $m = 0$. However, if the slope is larger than unity, there will be three such intersections. Since the slope is $1/\theta$, we identify $\theta_{\rm c} = 1$ as the *mean field transition temperature*.

[21] Here we consider a finite lattice in a periodic geometry. Note that if we count each link twice, then each site is counted z times because there are z links which connect to any given site. Thus $2N_{\rm links} = zN$, which is to say $N_{\rm links} = \frac{1}{2}zN$.

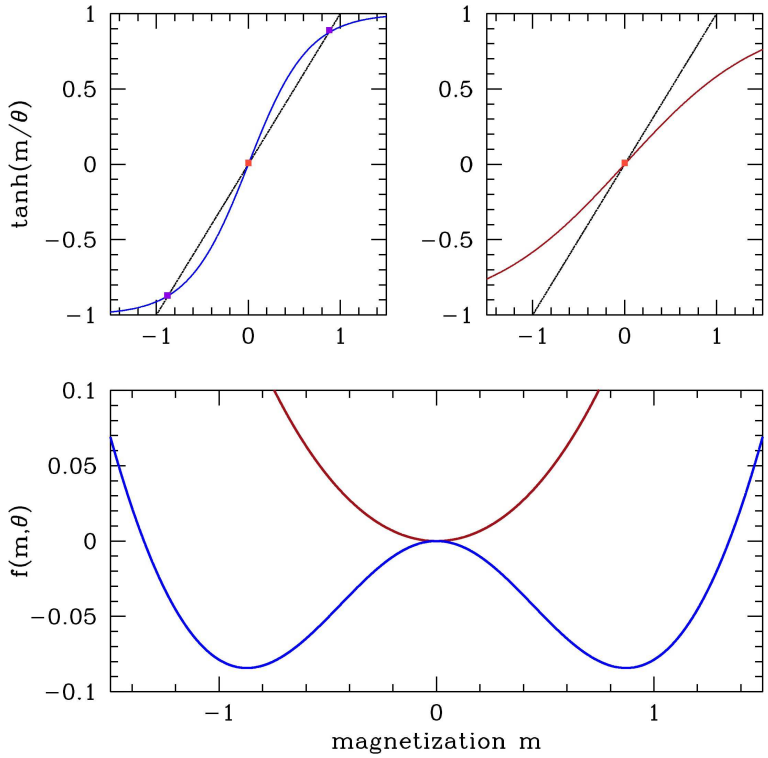


Figure 7.10: Results for $h = 0$. Upper panels: graphical solution to self-consistency equation $m = \tanh(m/\theta)$ at temperatures $\theta = 0.65$ (blue) and $\theta = 1.5$ (dark red). Lower panel: mean field free energy, with energy shifted by $\theta \log 2$ so that $f(m = 0, \theta) = 0$.

The mean field free energies are plotted in the bottom panel of fig. 7.10. It is possible to make analytical progress by assuming m is small and Taylor expanding the free energy $f(m, \theta)$ in powers of m when we are very close to the critical point, *i.e.* when $|\theta - \theta_{\rm c}| \ll 1$. Then we have[22]

$$f(m,\theta) = -\theta \log 2 + \tfrac{1}{2} m^2 - \theta \, \log\cosh\Big(\frac{m}{\theta}\Big) = f_0 + \tfrac{1}{2}(\theta - \theta_{\rm c})\, m^2 + \frac{m^4}{12} + \ldots \quad , \tag{7.69}$$

with $f_0 = -\theta \log 2$. Note that the sign of the quadratic term is positive for $\theta > \theta_{\rm c}$ and negative for $\theta < \theta_{\rm c}$. Thus, the shape of the free energy $f(m, \theta)$ as a function of m qualitatively changes at $\theta = \theta_{\rm c} = 1$, the mean field transition temperature, also known as the (dimensionless) *critical temperature*. Within our mean field theory, the predicted critical temperature is $T_{\rm c} = zJ\theta_{\rm c}/k_{\rm B} = zJ/k_{\rm B}$.

In the high temperature phase, $\theta > \theta_{\rm c}$, and there is a unique minimum to $f(\theta, m)$ lying at $m = 0$. This is the disordered phase, where the *order parameter* m vanishes. By contrast, in the low temperature phase $\theta < \theta_{\rm c}$, there are three solutions to the mean field equations. One solution is always at $m = 0$. The other two solutions must be related by the $\mathbb{Z}_2$ symmetry of the free energy ($m \to -m$ with $h = 0$). For $\theta > \theta_{\rm c}$, the free energy $f(m, \theta)$ has a single minimum at $m = 0$. Below $\theta_{\rm c}$, the curvature at $m = 0$ reverses, and

[22] We invoke the Taylor series expansion $\log\cosh x = \frac{1}{2}x^2 - \frac{1}{12}x^4 + \frac{1}{45}x^6 - \frac{17}{2520}x^8 + \ldots$. With $\varepsilon \equiv \theta - \theta_{\rm c}$, we drop terms which are $\mathcal{O}(\varepsilon^2 m^2, \varepsilon m^4, m^6)$. As we shall see, for $\varepsilon < 0$ we have $m^2 \propto -\varepsilon$, in which case the singular part of the free energy (*i.e.* neglecting f_0) is proportional to ε^2, while the terms we are dropping are $\mathcal{O}(\varepsilon^3)$ and smaller.

$m = 0$ becomes a local maximum. There are then two equivalent minima symmetrically displaced on either side of $m = 0$. Differentiating with respect to m, we find these additional local minima to lie at $m^2 = 3(\theta_{\rm c} - \theta) + \mathcal{O}\big((\Delta\theta)^2\big)$. Thus, we find for $|\theta - \theta_{\rm c}| \ll 1$,

$$m(\theta, h = 0) = \pm\sqrt{3}\,\big(\theta_{\rm c} - \theta\big)_+^{1/2} \quad , \tag{7.70}$$

where the $+$ subscript indicates that this solution is only for $\theta_{\rm c} - \theta > 0$. As the blue curve in fig. 7.10 shows, these nonzero solutions for m in the low temperature phase lie at a lower value of the free energy f than $m = 0$.

Again, for $\theta > \theta_{\rm c}$ the only solution is $m = 0$. The high temperature phase is thus one where the $\mathbb{Z}_2$ (*i.e.* $m \to -m$) symmetry is *unbroken*. In the low temperature phase, the magnetization m is nonzero, and takes on one of two possible values which are degenerate in free energy. The degeneracy is guaranteed by the $\mathbb{Z}_2$ symmetry present when $h = 0$. But the system must somehow choose! This is the phenomenon of *spontaneous symmetry breaking* (SSB). The exponent with which $m(\theta)$ vanishes as $\theta \to \theta_{\rm c}^-$ is denoted as β. That is, $m(\theta, h = 0) \propto (\theta_{\rm c} - \theta)_+^{\beta}$ with $\beta = \frac{1}{2}$ for our mean field theory.

Specific heat

We can now expand the free energy $f(\theta, h = 0)$. We find

$$f(\theta, h = 0) = \begin{cases} -\theta \log 2 & \text{if } \theta > \theta_{\rm c} \\ -\theta \log 2 - \frac{3}{4}(\theta_{\rm c} - \theta)^2 + \mathcal{O}\big((\theta_{\rm c} - \theta)^3\big) & \text{if } \theta < \theta_{\rm c} \end{cases} \quad . \tag{7.71}$$

Thus, if we compute the heat capacity, we find in the vicinity of $\theta = \theta_{\rm c}$

$$c_V = -\theta\,\frac{\partial^2 f}{\partial \theta^2} = \begin{cases} 0 & \text{if } \theta > \theta_{\rm c} \\ \frac{3}{2} & \text{if } \theta < \theta_{\rm c} \end{cases} \quad . \tag{7.72}$$

Thus, the specific heat is *discontinuous* at $\theta = \theta_{\rm c}$. We emphasize that our results here are only valid for $|\theta - \theta_{\rm c}| \ll 1$. The general result valid for all θ (within our mean field theory) is[23]

$$c_V(\theta) = \frac{1}{\theta} \cdot \frac{m^2(\theta) - m^4(\theta)}{\theta - 1 + m^2(\theta)} \quad , \tag{7.73}$$

With this expression one can check both limits $\theta \to 0$ and $\theta \to \theta_{\rm c}$. As $\theta \to 0$ the magnetization saturates and one has $m^2(\theta) \simeq 1 - 4\,e^{-2/\theta}$. The numerator then vanishes as $e^{-2/\theta}$, which overwhelms the denominator that itself vanishes as θ^2. As a result, $c_V(\theta \to 0) = 0$, as expected. As $\theta \to \theta_{\rm c}^-$, we have $m^2 = 3(\theta_{\rm c} - \theta) + \ldots$ and we recover $c_V(\theta_{\rm c}^-) = \frac{3}{2}$. In the theory of critical phenomena, $c_V(\theta) \propto |\theta - \theta_{\rm c}|^{-\alpha}$ as $\theta \to \theta_{\rm c}$. We see that mean field theory yields $\alpha = 0$.

[23] To obtain this result, one writes $f = f\big(\theta, m(\theta)\big)$ and then differentiates twice with respect to θ, using the chain rule. Along the way, any naked (*i.e.* undifferentiated) term proportional to $\partial f/\partial m$ may be dropped, since this vanishes at any θ by the mean field equation.

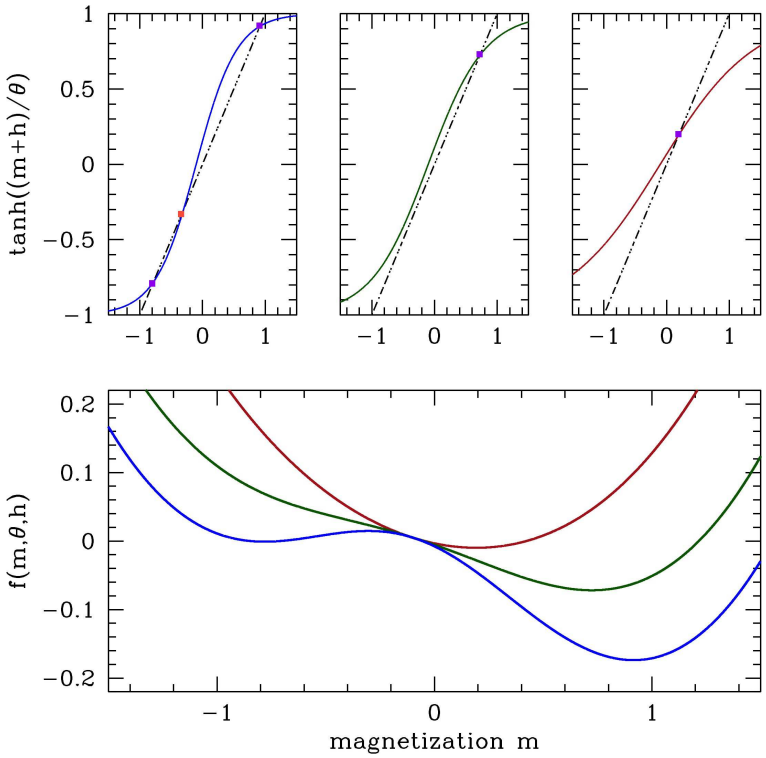


Figure 7.11: $f(m,\theta,h)$ for $h = 0.1$. Upper panels: graphical solution to the self-consistency equation $m = \tanh\big((m+h)/\theta\big)$ at temperatures $\theta = 0.65$ (blue), $\theta = 0.9$ (dark green), and $\theta = 1.5$ (dark red). Lower panel: mean field free energy, with energy shifted by $f(m=0,\theta,h) = -\theta\log 2 - \theta\log\cosh(h/\theta)$.

7.5.3 Finite external field

Let us first assume $|h| \ll |\theta - 1| \ll 1$, *i.e.* that we are very close to the critical point $(\theta_{\rm c}, h_{\rm c}) = (1,0)$. The mean field solution for $m(\theta,h)$ will then be small, and we may expand the free energy from eqn. 7.67 in m and h, *viz.*

$$\begin{aligned} f(m,\theta,h) &= -\theta\,\log 2 + \tfrac{1}{2}(1-\theta^{-1})\,m^2 + \frac{m^4}{12\,\theta^3} - \frac{hm}{\theta} \\ &= f_0 + \tfrac{1}{2}\,(\theta-\theta_{\rm c})\,m^2 + \tfrac{1}{12}m^4 - hm + \ldots \quad . \end{aligned} \tag{7.74}$$

Note that we have only gone to linear order in h. Setting $\partial f/\partial m = 0$, we obtain

$$\tfrac{1}{3}m^3 + (\theta-\theta_{\rm c})\cdot m - h = 0 \quad . \tag{7.75}$$

If $\theta > \theta_{\rm c}$ then we have a solution $m = h/(\theta-\theta_{\rm c})$. The m^3 term can be ignored because it is higher order in h, provided $|h| \ll |\theta-\theta_{\rm c}|^{3/2} \ll 1$. This is known as the *Curie-Weiss law*[24]. The zero field magnetic

[24]Pierre Curie was a pioneer in the fields of crystallography, magnetism, and radiation physics. In 1880, Pierre and his older brother Jacques discovered piezoelectricity. He was 21 years old at the time. It was in 1895 that Pierre made the first systematic studies of the effects of temperature on magnetic materials, and he formulated

susceptibility is then given by

$$\chi(\theta > \theta_{\rm c}) = \left.\frac{\partial m}{\partial h}\right|_{h=0} = \frac{1}{\theta - \theta_{\rm c}} \quad , \tag{7.76}$$

where the susceptibility critical exponent γ is $\gamma = 1$. If $\theta < \theta_{\rm c}$ then while there is still a solution at $m = h/(\theta - \theta_{\rm c})$, it lies at a local maximum of the free energy, as shown in fig. 7.11. The minimum of the free energy occurs close to the $h = 0$ solution $m = m_0(\theta) \equiv \pm\sqrt{3}\,(\theta_{\rm c} - \theta)$, and writing $m = m_0 + \delta m$ we find δm to linear order in h as $\delta m(\theta, h) = h/2(\theta_{\rm c} - \theta)$. Thus,

$$m(\theta < \theta_{\rm c}, h) = \pm\sqrt{3}\,(\theta_{\rm c} - \theta)^{1/2} + \frac{h}{2(\theta_{\rm c} - \theta)} \quad \Rightarrow \quad \chi(\theta < \theta_{\rm c}) = \frac{1}{2(\theta_{\rm c} - \theta)} \quad . \tag{7.77}$$

Both above and below the critical temperature we find that $\chi(\theta)$ diverges as $A_\pm|\theta - \theta_{\rm c}|^{-\gamma}$ where the exponent on either side of the transition is $\gamma = 1$, but the *critical amplitudes* differ: $A_+ = 1$ and $A_- = \frac{1}{2}$.

Finally, we can set $\theta = \theta_{\rm c}$ and examine $m(h)$. We find, from eqn. 7.75,

$$m(\theta = \theta_{\rm c}, h) = (3h)^{1/3} \propto h^{1/\delta} \quad , \tag{7.78}$$

where δ is a new critical exponent. Mean field theory gives $\delta = 3$. Note that at $\theta = \theta_{\rm c} = 1$ we have $m = \tanh(m + h)$, and inverting we find

$$h(m, \theta = \theta_{\rm c}) = \tfrac{1}{2}\log\left(\frac{1+m}{1-m}\right) - m = \frac{m^3}{3} + \frac{m^5}{5} + \ldots \quad , \tag{7.79}$$

which is consistent with what we just found for $m(h, \theta = \theta_{\rm c})$.

How well does mean field theory do in describing the phase transition of the Ising model? In table 7.2 we compare our mean field results for the exponents α, β, γ, and δ with exact values for the two-dimensional Ising model, numerical work on the three-dimensional Ising model, and experiments on the liquid-gas transition in CO_2. The first thing to note is that the exponents are dependent on the dimension of space, and this is something that mean field theory completely misses. In fact, it turns out that the mean field exponents are *exact* provided $d > d_{\rm u}$, where $d_{\rm u}$ is the *upper critical dimension* of the theory. For the Ising model, $d_{\rm u} = 4$, and above four dimensions (which is of course unphysical) the mean field exponents are in fact exact. We see that all in all the MFT results compare better with the three dimensional exponent values than with the two-dimensional ones – this makes sense since MFT does better in higher dimensions. The reason for this is that higher dimensions means more nearest neighbors, which effectively reduces the relative importance of the fluctuations we neglected to include.

what is known as *Curie's Law*, $\chi = C/T$, where C is a constant. Curie married Marie Sklodowska in the same year. Their research turned toward radiation, recently discovered by Becquerel and Röntgen. In 1898, Pierre and Marie Curie discovered radium. They shared the 1903 Nobel Prize in Physics with Becquerel. Marie went on to win the 1911 Nobel Prize in Chemistry and was the first person ever awarded two Nobel Prizes. Their daughter Irène Joliot Curie shared the 1935 Prize in Chemistry (with her husband), also for work on radioactivity. Pierre Curie met an untimely and unfortunate end in the Spring of 1906. Walking across the Place Dauphine, he slipped and fell under a heavy horse-drawn wagon carrying military uniforms. His skull was crushed by one of the wagon wheels, killing him instantly. Later on that year, Pierre-Ernest Weiss proposed a modification of Curie's Law to account for ferromagnetism. This became known as the Curie-Weiss law, $\chi = C/(T - T_{\rm c})$.

Exponent	MFT	2D Ising (exact)	3D Ising (numerical)	binary liquid (3D)
α	0	0	0.11008(1)	0.113(5)
β	1/2	1/8	0.326419(3)	0.316(8)
γ	1	7/4	1.237075(10)	1.240(7)
δ	3	15	4.78984(1)	–
η	0	1/4	0.036298(2)	0.016(7)
ν	1/2	1	0.629971(4)	0.625(5)

Table 7.2: Critical exponents from mean field theory, exact results for the two-dimensional Ising model, numerical results for the three-dimensional Ising model, and experiments near liquid–liquid demixing critical points in three-dimensional binary mixtures: triethylamine and water (α : D. Beysens and A. Bourgou, *Phys. Rev. A* **19**, 2407 (1979)), isobutyric acid and water (β : S. C. Greer, *Phys. Rev. A* **14**, 1770 (1976)), and 3-methylpentane-nitroethane (γ, η, ν : R. F. Chang *et al.*, *Phys. Rev. Lett.* **37**, 1481 (1976)).

Metastable states at $h \neq 0$

Consider the free energy $f(m, \theta, h)$ in eqn. 7.67, now for general θ not restricted to the immediate vicinity of θ_c. When $\theta < \theta_c$ and h is sufficiently small – just how small we are about to find out – the free energy as a function of m has one local maximum and two local minima, one of which is the thermodynamically stable state (*i.e.* the one for which $mh > 0$), and the other (with $mh < 0$) is metastable. Consider the case $h > 0$. As the temperature is raised, the metastable local minimum at $m < 0$ eventually vanishes, annihilating with the local maximum in a saddle-node bifurcation. To find where this happens, one sets $\partial f/\partial m = 0$ and $\partial^2 f/\partial m^2 = 0$ simultaneously. From eqn. 7.67, we have

$$\frac{\partial f}{\partial m} = m - \tanh\Big(\frac{m+h}{\theta}\Big) \quad , \quad \frac{\partial^2 f}{\partial m^2} = 1 - \theta^{-1}\mathrm{sech}^2\Big(\frac{m+h}{\theta}\Big) \quad . \tag{7.80}$$

Thus $h = \theta\,\tanh^{-1}(m) - m$, and using $\mathrm{sech}^2 x = 1 - \tanh^2 x$, we have $m^2 = 1 - \theta$ and

$$h^*(\theta) = \sqrt{1-\theta} - \frac{\theta}{2}\log\left(\frac{1+\sqrt{1-\theta}}{1-\sqrt{1-\theta}}\right). \tag{7.81}$$

The solutions lie at $h = \pm h^*(\theta)$. For $\theta < \theta_c = 1$ and $h \in \big[-h^*(\theta)\,,\,+h^*(\theta)\big]$, there are three solutions to the mean field equation. Equivalently we could in principle invert the above expression to obtain $\theta^*(h)$. For $\theta > \theta^*(h)$, there is only a single global minimum in the free energy $f(m)$ and there is no additional local minimum. Note $\theta^*(h=0) = 1$. Note that we could in principle invert the above relation to obtain $\theta^*(h)$, but alas this is not analytically possible.

7.5.4 Magnetization dynamics

Dissipative processes drive physical systems to minimum energy states. We can crudely model the dissipative dynamics of a magnet by writing the phenomenological equation

$$\frac{1}{\Gamma}\frac{dm}{dt} = -\frac{\partial f}{\partial m} = \tanh\left(\frac{m+h}{\theta}\right) - m \quad , \tag{7.82}$$

where Γ has the dimensions of frequency. We may define $s = \Gamma t$ to be a dimensionless rescaled time. Under these dynamics, the free energy is never increasing:

$$\frac{df}{ds} = \frac{\partial f}{\partial m}\frac{dm}{ds} = -\left(\frac{\partial f}{\partial m}\right)^2 \leq 0 \quad . \tag{7.83}$$

Clearly the *fixed point* of these dynamics, where $\dot{m} = 0$, is a solution to the mean field equation $\frac{\partial f}{\partial m} = 0$. The time dependent $m(s)$ thus evolves until it reaches the first fixed point encountered, which is to say the first local extremum of the function $f(m)$. This extremum could be a global minimum, but it could also be a local minimum or even an inflection point.

A first order (generally nonlinear) ordinary differential equation of the form $\dot{u} = g(u)$ is called an $N = 1$ component *dynamical system*. For a general N-component dynamical system, $\boldsymbol{u} = (u_1, \ldots, u_N)$ is an N-component vector and $\boldsymbol{V}(\boldsymbol{u})$ is an N-component *vector field*, *i.e.* a set of N functions $V_j(u_1, \ldots, u_N)$ which specify the velocity vector at each point in $\boldsymbol{u}$ space, which is $\mathbb{R}^N$ (or some other N-dimensional manifold, on which we might have to define an *atlas* of coordinate patches). We then have $\dot{\boldsymbol{u}} = \boldsymbol{V}(\boldsymbol{u})$, which is a set of N coupled first-order ODEs. The $N = 1$ case is particularly simple to understand: $u(t)$ flows to the right in regions where $g(u) > 0$ and to the left where $g(u) < 0$. The case $g(u^*) = 0$ corresponds to a *fixed point*. Linearizing about u^*, *i.e.* writing $u(t) = u^* + \eta(t)$, the linearized dynamics are $\dot{\eta} = g'(u^*)\eta$, with $\eta(t) = \eta(0)\exp\big[g'(u^*)t\big]$. Thus for $g'(u^*) > 0$, corresponding to an *unstable fixed point* (UFP), the linearized dynamics take us further and further from u^*, and the linearization soon fails. When $g'(u^*) < 0$, corresponding to a *stable fixed point* (SFP), $u(t)$ approaches u^* and the linearization gets better and better. Generically the approach to a SFP is exponential in time, *i.e.* $t = \log\big[\eta(0)/\eta(t)\big]/|g'(u^*)|$. Given the initial condition $u(0)$, the fate of an $N = 1$ dynamical system is to flow to the closest accessible stable fixed point[25].

Our phenomenological magnetization dynamics is described by $\dot{m} = -f'(m)$, and is thus an $N = 1$ dynamical system with $g(m) = -f'(m)$. Fixed points satisfy $f'(m^*) = 0$. Thus, local minima of the free energy as a function of m, where $f''(m^*) > 0$, correspond to stable fixed points, while local maxima, where $f''(m^*) < 0$, correspond to unstable fixed points. This phase flow is sketched in fig. 7.12. As we have seen, for any value of h there is a temperature θ^* below which the free energy $f(m)$ has two local minima and one local maximum. When $h = 0$ the minima are degenerate, but at finite h one of the minima is a global minimum. Thus, for $\theta < \theta^*(h)$ there are three solutions to the mean field equations. In the language of dynamical systems, under the dynamics of eqn. 7.82, minima of $f(m)$ correspond

[25] For the nongeneric case where $g(u^*) = 0$ and $g'(u^*) = 0$ vanish concomitantly, u^* is a *half-stable* fixed point when $g(u) = Au^2 + \mathcal{O}(u^3)$ with $A > 0$. In this case, for initial conditions $u(0) < 0$ the velocity $\dot{u}(t)$ is positive and the flow asymptotically approaches $u(\infty) = 0$, while for $u(0) > 0$ the velocity is also positive and the flow is to infinity, which is reached at a finite time $t_\infty = 1/Au(0)$. If $g(u) = Bu^3 + \mathcal{O}(u^4)$, then $u^* = 0$ is nonlinearly stable ($B < 0$) or unstable ($B > 0$).

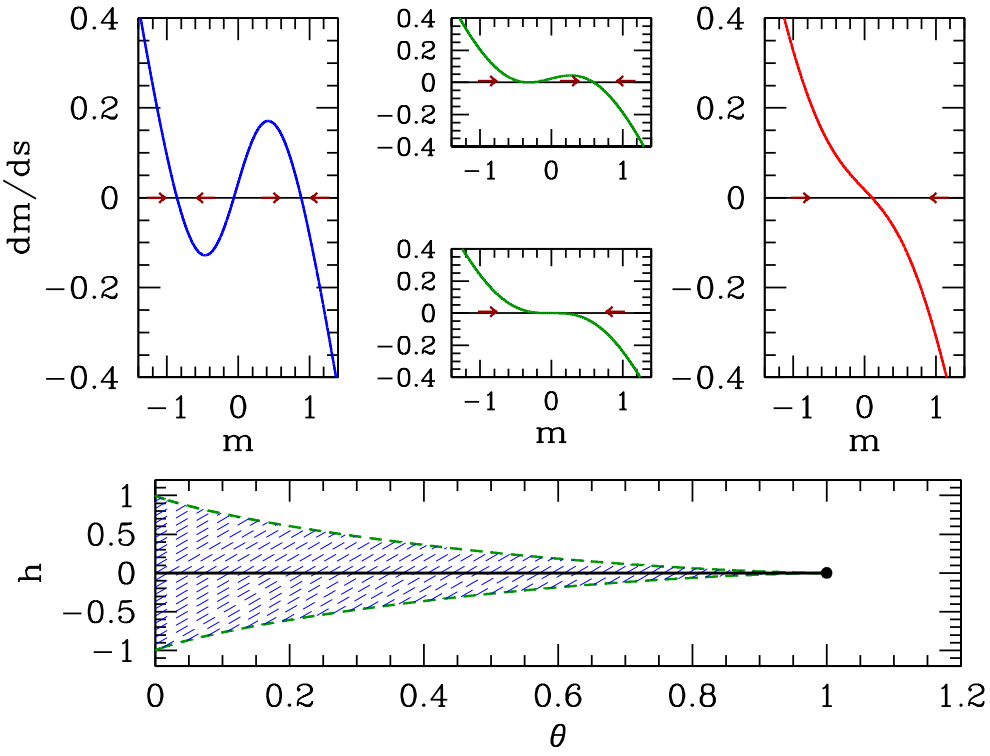


Figure 7.12: Dissipative magnetization dynamics $\dot{m} = -f'(m)$. Bottom panel shows $h^*(\theta)$ from eqn. 7.81. For (θ, h) within the blue shaded region, the free energy $f(m)$ has a global minimum plus a local minimum and a local maximum. Otherwise $f(m)$ has only a single global minimum. Top panels show an imperfect bifurcation in the magnetization dynamics at $h = 0.0215$, for which $\theta^* = 0.90$. Temperatures shown: $\theta = 0.65$ (blue), $\theta = \theta^*(h) = 0.90$ (green), and $\theta = 1.2$. The rightmost stable fixed point corresponds to the global minimum of the free energy. The bottom of the middle two upper panels shows $h = 0$, where both of the attractive fixed points and the repulsive fixed point coalesce into a single attractive fixed point (supercritical pitchfork bifurcation).

to attractive fixed points and maxima to repulsive fixed points. If $h > 0$, the rightmost of these fixed points corresponds to the global minimum of the free energy. As θ is increased, this fixed point evolves smoothly. At $\theta = \theta^*$, the (metastable) local minimum and the local maximum coalesce and annihilate in a saddle-node bifurcation. However at $h = 0$ all three fixed points coalesce at $\theta = \theta_c$ and the bifurcation is a supercritical pitchfork. As a function of θ at finite h, the dynamics are said to exhibit an *imperfect bifurcation*, which is a deformed supercritical pitchfork.

The solution set for the mean field equation is simply expressed by inverting the tanh function to obtain $h(\theta, m)$. One readily finds

$$h(\theta, m) = \frac{\theta}{2} \log\left(\frac{1+m}{1-m}\right) - m \quad . \tag{7.84}$$

As we see in the bottom panel of fig. 7.13, $m(h)$ becomes multivalued for $h \in \big[-h^*(\theta) \, , \, +h^*(\theta) \big]$, where $h^*(\theta)$ is given in eqn. 7.81. Now imagine that $\theta < \theta_c$ and we slowly ramp the field h from a large negative value to a large positive value, and then slowly back down to its original value. On the time

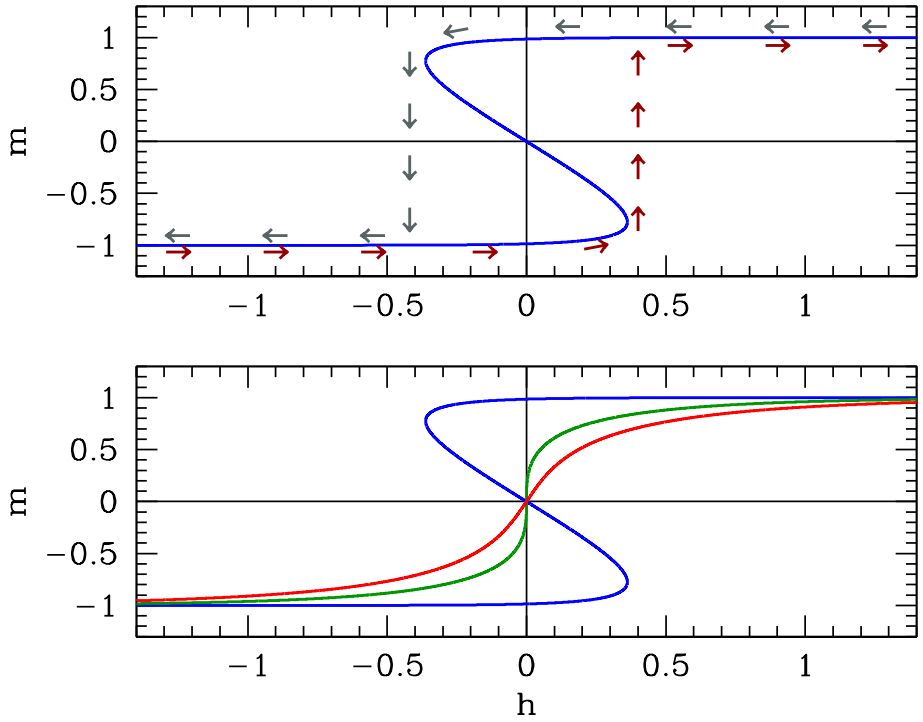


Figure 7.13: Top panel: hysteresis as a function of ramping the dimensionless magnetic field h at $\theta = 0.40$. Dark red arrows below the curve track the evolution of m upon a slow increase of h. Dark grey arrows above the curve track a slow decrease of h. Bottom panel : solution set for $m(\theta, h)$ as a function of h at temperatures $\theta = 0.40$ (blue), $\theta = \theta_c = 1.0$ (dark green), and $\theta = 1.25$ (red).

scale of the magnetization dynamics, we can regard $h(s)$ as a constant. (Remember the time variable is s here.) Thus, $m(s)$ will flow to the nearest stable fixed point. Initially the system starts with $m = -1$ and h large and negative, and there is only one fixed point, at $m^* \approx -1$. As h slowly increases, the fixed point value m^* also slowly increases. As h exceeds $-h^*(\theta)$, a saddle-node bifurcation occurs, and two new fixed points are created at positive m, one stable and one unstable. The global minimum of the free energy still lies at the fixed point with $m^* < 0$. However, when h crosses $h = 0$, the global minimum of the free energy lies at the most positive fixed point m^*. The dynamics, however, keep the system stuck in what is a metastable phase. This persists until $h = +h^*(\theta)$, at which point another saddle-node bifurcation occurs, and the attractive fixed point at $m^* < 0$ annihilates with the repulsive fixed point. The dynamics then act quickly to drive m to the only remaining fixed point. This process is depicted in the top panel of fig. 7.13. As one can see from the figure, the system follows a stable fixed point until the fixed point disappears, even though that fixed point may not always correspond to a global minimum of the free energy. The resulting $m(h)$ curve is then not reversible as a function of time, and it possesses a characteristic shape known as a *hysteresis loop*. Etymologically, the word *hysteresis* derives from the Greek $\upsilon\sigma\tau\varepsilon\rho\eta\sigma\iota\varsigma$, which means 'lagging behind' (and not from $\iota\sigma\tau o\rho\iota\alpha$, which means 'inquiry'). Systems which are hysteretic exhibit a *history-dependence* to their status, which is not uniquely determined by external conditions. Hysteresis may be exhibited with respect to changes in applied magnetic field, changes in temperature, or changes in other externally determined parameters.

7.5.5 Beyond nearest neighbors

Up to this point we have assumed nearest-neighbor interactions on a lattice of coordination number z. Suppose, instead, that we had started with the more general model,

$$\hat{H} = -\tfrac{1}{2}\sum_{i\neq j} J_{ij}\,\sigma_i\,\sigma_j - H\sum_i \sigma_i \quad , \tag{7.85}$$

where $J_{ij} = J\big(|\boldsymbol{R}_i - \boldsymbol{R}_j|\big)$ is the coupling between spins on sites i and j[26]. We may set $J_{ii} = J(0) = 0$ for all i since the diagonal elements of J_{ij} each contribute a constant to the energy. Each pair (ij) with $i \neq j$ is thus counted once in the interaction term; this may be replaced by a sum over all i and j if we include a factor of $\frac{1}{2}$.[27] The resulting mean field Hamiltonian is then

$$\hat{H}_{\rm MF} = \tfrac{1}{2}N\hat{J}(0)\,m^2 - \big(H + \hat{J}(0)\,m\big)\sum_{i=1}^{N}\sigma_i \quad . \tag{7.86}$$

Here, $\hat{J}(\boldsymbol{q})$ is the lattice Fourier transform of the interaction function $J(\boldsymbol{R})$:[28]

$$\hat{J}(\boldsymbol{q}) = \sum_{\boldsymbol{R}} J(\boldsymbol{R})\,e^{-i\boldsymbol{q}\cdot\boldsymbol{R}} \quad . \tag{7.87}$$

For nearest neighbor interactions only, one has $\hat{J}(0) = zJ$, where z is the *lattice coordination number*, *i.e.* the number of nearest neighbors of any given site. The scaled free energy is as in eqn. 7.67, with $f = F/N\hat{J}(0)$, $\theta = k_{\rm B}T/\hat{J}(0)$, and $h = H/\hat{J}(0)$. The analysis proceeds precisely as before, and we conclude $\theta_{\rm c} = 1$, *i.e.* $k_{\rm B}T_{\rm c}^{\rm MF} = \hat{J}(0)$. For example, on the simple cubic lattice there are six nearest neighbors and twelve next-nearest neighbors. Thus, if J is the nearest neighbor coupling and J' the next-nearest neighbor coupling, we have $\hat{J}(0) = 6J + 12J'$.

7.5.6 Ising model with long-ranged forces

Consider an Ising model where $J_{ij} = J/N$ for all i and j, so that there is a very weak interaction between every pair of spins. The Hamiltonian is then

$$\hat{H} = -\frac{J}{2N}\left(\sum_{i=1}^{N}\sigma_i\right)^2 - H\sum_{i=1}^{N}\sigma_i \quad . \tag{7.88}$$

[26]Note that we may write $\frac{1}{2}\sum_{i\neq j}A_{ij}$ as $\sum_{i<j}A_{ij}$ provided $A = A^{\rm T}$ is symmetric. Clearly $A_{ij} = \sigma_i\,\sigma_j$ is symmetric under interchange of indices i and j. Each version of the sum counts all unique *pairs* $(i,j) = (j,i)$ exactly once.

[27]The self-interaction terms with $i = j$ contribute a constant to $\hat{H}$ and may be either included or excluded. However, this property only pertains to the $\sigma_i = \pm 1$ model. For higher spin versions of the Ising model, say where $S_i \in \{-1, 0, +1\}$, then S_i^2 is not constant and we should explicitly exclude the self-interaction terms.

[28]The sum in the discrete Fourier transform is over all 'direct Bravais lattice vectors' and the wavevector $\boldsymbol{q}$ may be restricted to the 'first Brillouin zone'. These terms are familiar from elementary solid state physics.

The partition function is

$$Z = \operatorname*{Tr}_{\{\sigma_i\}} \exp\left[\frac{\beta J}{2N}\left(\sum_{i=1}^{N}\sigma_i\right)^2 + \beta H \sum_{i=1}^{N}\sigma_i\right] \quad . \tag{7.89}$$

We now invoke the Gaussian integral,

$$\int_{-\infty}^{\infty} dx\, e^{-\alpha x^2 - \beta x} = \sqrt{\frac{\pi}{\alpha}}\, e^{\beta^2/4\alpha} \quad . \tag{7.90}$$

Thus,

$$\exp\left[\frac{\beta J}{2N}\left(\sum_{i=1}^{N}\sigma_i\right)^2\right] = \left(\frac{N\beta J}{2\pi}\right)^{1/2}\int_{-\infty}^{\infty} dm\, e^{-\frac{1}{2}N\beta J m^2 + \beta J m \sum_{i=1}^{N}\sigma_i} \quad , \tag{7.91}$$

and we can write the partition function as

$$Z = \left(\frac{N\beta J}{2\pi}\right)^{1/2}\int_{-\infty}^{\infty} dm\, e^{-\frac{1}{2}N\beta J m^2}\left(\sum_{\sigma} e^{\beta(H+Jm)\sigma}\right)^N = \left(\frac{N}{2\pi\theta}\right)^{1/2}\int_{-\infty}^{\infty} dm\, e^{-NA(m)/\theta} \quad , \tag{7.92}$$

where $\theta = k_{\rm B}T/J$, $h = H/J$, and

$$A(m) = \tfrac{1}{2}m^2 - \theta \log\left[2\cosh\left(\frac{h+m}{\theta}\right)\right] \quad . \tag{7.93}$$

Since $N \to \infty$, we can perform the integral using the method of steepest descents. Thus, we must set

$$\left.\frac{dA}{dm}\right|_{m^*} = 0 \quad \Longrightarrow \quad m^* = \tanh\left(\frac{m^*+h}{\theta}\right) \quad . \tag{7.94}$$

Expanding about $m = m^*$, we write[29]

$$A(m) = A(m^*) + \tfrac{1}{2}A''(m^*)\,(m-m^*)^2 + \tfrac{1}{6}\,A'''(m^*)\,(m-m^*)^3 + \ldots \quad . \tag{7.95}$$

Writing $\nu = m - m^*$ and performing the integration, we obtain

$$\begin{aligned} Z &= \left(\frac{N}{2\pi\theta}\right)^{1/2} e^{-NA(m^*)/\theta}\int_{-\infty}^{\infty} d\nu\, \exp\left[-\frac{NA''(m^*)}{2\theta}\,\nu^2 - \frac{NA'''(m^*)}{6\theta}\,\nu^3 + \ldots\right] \\ &= \frac{1}{\sqrt{A''(m^*)}}\, e^{-NA(m^*)/\theta}\cdot\left\{1 + \mathcal{O}(N^{-1})\right\} \quad . \end{aligned} \tag{7.96}$$

The corresponding free energy per site

$$f = \frac{F}{NJ} = A(m^*) + \frac{\theta}{2N}\,\log A''(m^*) + \mathcal{O}(N^{-2}) \quad , \tag{7.97}$$

where m^* is the solution to the mean field equation which minimizes $A(m)$. Mean field theory is *exact* for this model!

[29] Here we assume a single nondegenerate minimum with $A''(m^*) > 0$. If $h = 0$ and $\theta < 1$ there are two degenerate minims, contributing an additional $-\theta\log 2$ to the free energy/ In addition, precisely at the critical point we have $A''(m^*) = 0$ and the expansion fails. Nevertheless, the conclusion that mean field thermodynamics is exact in the $N \to \infty$ limit remains correct.

7.6 Landau Theory of Phase Transitions

Landau's theory of phase transitions is based on an expansion of the free energy of a thermodynamic system in terms of an *order parameter*, which is nonzero in an ordered phase and zero in a disordered phase. For example, the magnetization density m of a ferromagnet in zero external field but at finite temperature typically vanishes for temperatures $T > T_{\rm c}$, where $T_{\rm c}$ is the *critical temperature*, also called the *Curie temperature* in a ferromagnet. A low order expansion in powers of the order parameter is appropriate sufficiently close to the phase transition, *i.e.* at temperatures such that the order parameter, if nonzero, is still small.

The order parameter m might be a scalar or a vector or even a matrix. In many cases the free energy $f(m)$ is invariant under the operations of a *symmetry group* G, such that $f(m) = f(\mathsf{g}m)$ for all $\mathsf{g} \in \mathsf{G}$, where $\mathsf{g}m$ is the action of the group element g on m. For example, we might have $\mathsf{G} = \mathbb{Z}_2$ with elements $\mathsf{g} \in \{+1, -1\}$ and $m \in \mathbb{R}$. As we saw previously, in the high temperature phase $f(m)$ has a global minimum at $m = 0$. But in the low temperature phase, $f(m)$ is minimized at $m = \pm m_0 \neq 0$, with $m = 0$ a local maximum. The free energy is symmetric under the action of $\mathbb{Z}_2$, but the system has to choose one from among the two degenerate 'vacua' $m = \pm m_0$. This is the phenomenon of *spontaneous symmetry breaking* (SSB) described in §7.2.1. The order parameter or one of its derivatives exhibits a singularity or discontinuity as a function of thermodynamic parameters, such as the temperature T. This singular behavior occurs along a subset of parameter space, identified as a *critical point* or *critical surface*. The imposition of a finite external field h *explicitly breaks* the G-symmetry, hence SSB can occur only at $h = 0$.

7.6.1 Quartic free energy with Ising symmetry

The simplest example is the quartic free energy,

$$f(m, \theta, h = 0) = f_0 + \tfrac{1}{2}am^2 + \tfrac{1}{4}bm^4 \quad , \tag{7.98}$$

where $f_0 = f_0(\theta)$, $a = a(\theta)$, and $b = b(\theta)$. Here, θ is a dimensionless measure of the temperature[30]. We assume $b > 0$, which is necessary if the free energy is to be bounded from below[31].

The equation of state, which relates the intensive quantities m and θ at $h = 0$, is then

$$\frac{\partial f}{\partial m} = 0 = am + bm^3 \quad , \tag{7.99}$$

has three solutions in the complex m plane: (i) $m = 0$, (ii) $m = \sqrt{-a/b}$, and (iii) $m = -\sqrt{-a/b}$. The latter two solutions lie along the (physical) real axis provided $a < 0$. We assume that there exists a unique temperature $\theta_{\rm c}$ where $a(\theta_{\rm c}) = 0$. Minimizing f, we find

$$\begin{aligned} a < 0 \quad (\theta < \theta_{\rm c}) \quad &: \quad f(\theta) = f_0 - \frac{a^2}{4b} \\ a > 0 \quad (\theta > \theta_{\rm c}) \quad &: \quad f(\theta) = f_0 \quad . \end{aligned} \tag{7.100}$$

[30] For example in an Ising ferromagnet we might define $\theta = k_{\rm B}T/\hat{J}(0)$, as before.

[31] It is always the case that f is bounded from below, on physical grounds. Were b negative, we'd have to consider higher order terms in the Landau expansion.

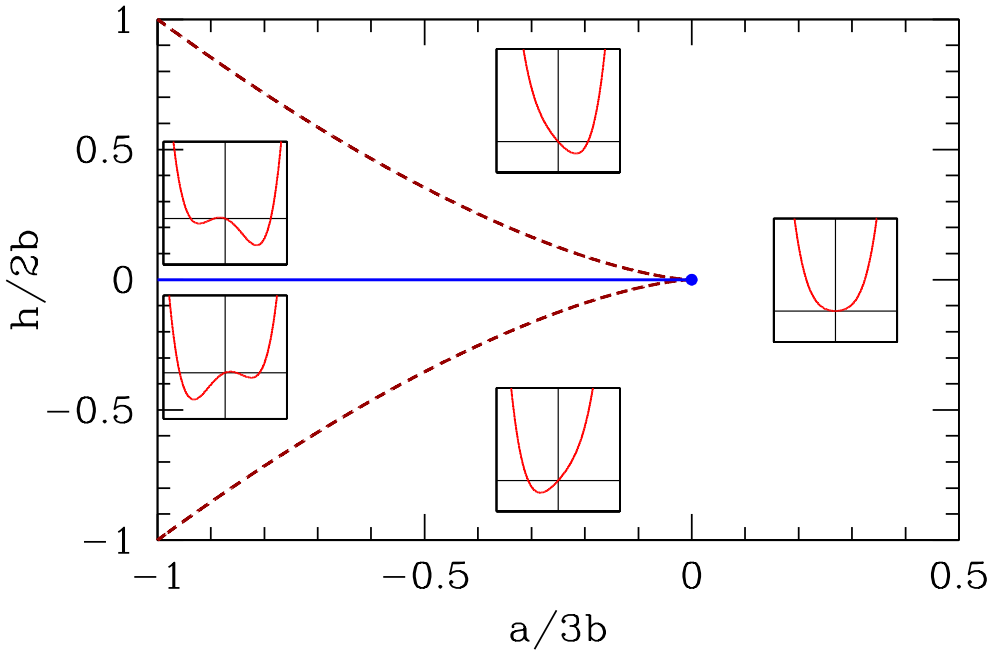


Figure 7.14: Phase diagram for the quartic Landau free energy $f = f_0 + \frac{1}{2}am^2 + \frac{1}{4}bm^4 - hm$, with $b > 0$. There is a first order line at $h = 0$ extending from $a = -\infty$ and terminating in a critical point at $a = 0$. For $|h| < h^*(a)$ (dashed red line) there are three solutions to the mean field equation, corresponding to one global minimum, one local minimum, and one local maximum. Insets show behavior of the free energy $f(m)$.

Thus $a(\theta)$ changes sign at $\theta = \theta_c$, where the free energy is continuous, since $a(\theta_c) = 0$. The specific heat, however, is discontinuous across the transition, with

$$c(\theta_c^+) - c(\theta_c^-) = -\theta_c \left.\frac{\partial^2}{\partial\theta^2}\right|_{\theta=\theta_c} \left(\frac{a^2}{4b}\right) = -\frac{\theta_c \left[a'(\theta_c)\right]^2}{2b(\theta_c)} \quad . \tag{7.101}$$

The presence of a magnetic field h breaks the $\mathbb{Z}_2$ symmetry of $m \to -m$. The free energy becomes

$$f(m, \theta, h) = f_0 + \tfrac{1}{2}am^2 + \tfrac{1}{4}bm^4 - hm \quad , \tag{7.102}$$

and the mean field equation is

$$bm^3 + am - h = 0 \quad . \tag{7.103}$$

This is a cubic equation for m with real coefficients, and as such it can either have three real solutions or one real solution and two complex solutions related by complex conjugation. Clearly we must have $a < 0$ in order to have three real roots, since $bm^3 + am$ is monotonically increasing otherwise. The boundary between these two classes of solution sets occurs when two roots coincide, which means $f''(m) = 0$ as well as $f'(m) = 0$. Simultaneously solving these two equations, we find

$$h^*(a) = \pm\frac{2}{3^{3/2}} \frac{(-a)^{3/2}}{b^{1/2}} \quad , \tag{7.104}$$

or, equivalently,

$$a^*(h) = -\frac{3}{2^{2/3}}\, b^{1/3}\, |h|^{2/3}. \tag{7.105}$$

If, for fixed h, we have $a < a^*(h)$, then there will be three real solutions to the mean field equation $f'(m) = 0$, one of which is a global minimum (the one for which $m \cdot h > 0$). For $a > a^*(h)$ there is only a single global minimum, at which m also has the same sign as h. If we solve the mean field equation perturbatively in h/a, we find

$$\begin{aligned} m(a,h) &= \frac{h}{a} - \frac{b}{a^4}\, h^3 + \mathcal{O}(h^5) \qquad\qquad (a > 0) \\ &= \pm\frac{|a|^{1/2}}{b^{1/2}} + \frac{h}{2\,|a|} \mp \frac{3\,b^{1/2}}{8\,|a|^{5/2}}\, h^2 + \mathcal{O}(h^3) \qquad (a < 0) \quad . \end{aligned} \tag{7.106}$$

7.6.2 Cubic terms in Landau theory : first order transitions

Next, consider a free energy with a cubic term,

$$f = f_0 + \tfrac{1}{2}am^2 - \tfrac{1}{3}ym^3 + \tfrac{1}{4}bm^4 \quad , \tag{7.107}$$

with $b > 0$ for stability. Without loss of generality, we may assume $y > 0$ (else send $m \to -m$). Note that we no longer have $m \to -m$ (*i.e.* $\mathbb{Z}_2$) symmetry. The cubic term favors positive m. What is the phase diagram in the (a, y) plane?

Extremizing the free energy with respect to m, we obtain

$$\frac{\partial f}{\partial m} = 0 = am - ym^2 + bm^3 \quad . \tag{7.108}$$

This cubic equation factorizes into a linear and quadratic piece, and hence may be solved simply. The three solutions are $m = 0$ and

$$m = m_\pm \equiv \frac{y}{2b} \pm \sqrt{\Big(\frac{y}{2b}\Big)^2 - \frac{a}{b}} \quad . \tag{7.109}$$

We now see that for $y^2 < 4ab$ there is only one real solution, at $m = 0$, while for $y^2 > 4ab$ there are three real solutions. Which solution has lowest free energy? To find out, we compare the energy $f(0)$ with $f(m_+)$[32]. Thus, we set

$$f(m) = f(0) \quad \Longrightarrow \quad \tfrac{1}{2}am^2 - \tfrac{1}{3}ym^3 + \tfrac{1}{4}bm^4 = 0 \quad , \tag{7.110}$$

and we now have two quadratic equations to solve simultaneously:

$$0 = a - ym + bm^2 \qquad , \qquad 0 = \tfrac{1}{2}a - \tfrac{1}{3}ym + \tfrac{1}{4}bm^2 = 0 \quad . \tag{7.111}$$

Eliminating the quadratic term gives $m = 3a/y$. Finally, substituting $m = m_+$ gives us a relation between a, b, and y:

$$y^2 = \tfrac{9}{2}\, ab \quad . \tag{7.112}$$

[32]We needn't waste our time considering the $m = m_-$ solution, since the cubic term prefers positive m.

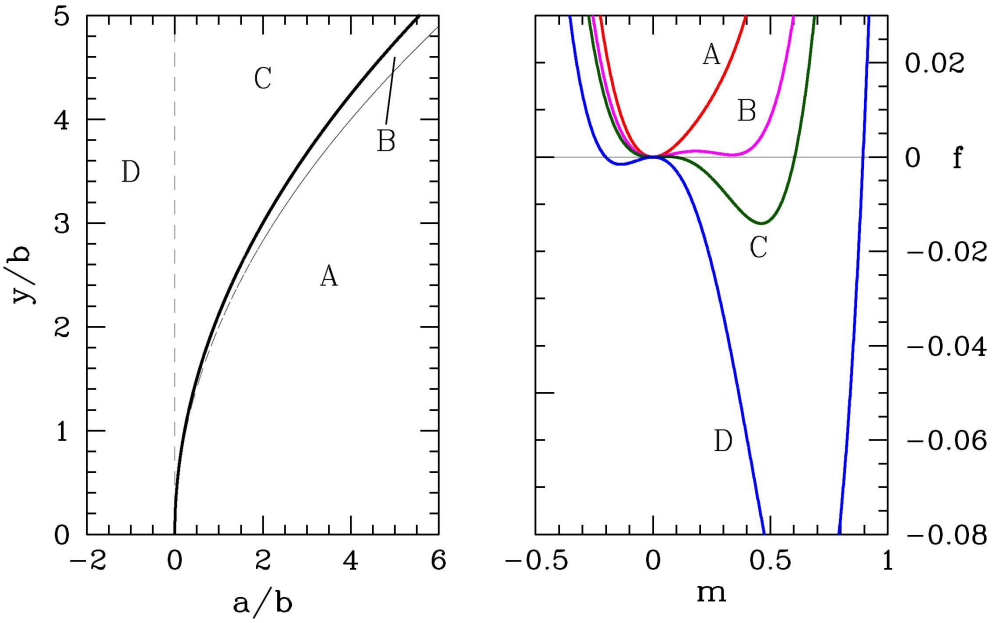


Figure 7.15: Behavior of the quartic free energy $f(m) = \frac{1}{2}am^2 - \frac{1}{3}ym^3 + \frac{1}{4}bm^4$. A: $y^2 < 4ab$; B: $4ab < y^2 < \frac{9}{2}ab$; C and D: $y^2 > \frac{9}{2}ab$. The thick black line denotes a line of first order transitions, where the order parameter is discontinuous across the transition.

Thus, we have the following:

$$\begin{aligned} a > \frac{y^2}{4b} \quad &: \quad \text{1 real root } m = 0 \\ \frac{y^2}{4b} > a > \frac{2y^2}{9b} \quad &: \quad \text{3 real roots; minimum at } m = 0 \\ \frac{2y^2}{9b} > a \quad &: \quad \text{3 real roots; minimum at } m = \frac{y}{2b} + \sqrt{\left(\frac{y}{2b}\right)^2 - \frac{a}{b}} \end{aligned} \tag{7.113}$$

The solution $m = 0$ lies at a local minimum of the free energy for $a > 0$ and at a local maximum for $a < 0$. Over the range $y^2/4b > a > 2y^2/9b$, then, there is a global minimum at $m = 0$, a local minimum at $m = m_+$, and a local maximum at $m = m_-$, with $m_+ > m_- > 0$. For $2y^2/9b > a > 0$, there is a local minimum at $m = 0$, a global minimum at $m = m_+$, and a local maximum at $m = m_-$, again with $m_+ > m_- > 0$. For $a < 0$, there is a local maximum at $m = 0$, a local minimum at $m = m_-$, and a global minimum at $m = m_+$, with $m_+ > 0 > m_-$. See fig. 7.15.

With $y = 0$, we have a second order transition at $a = 0$. With $y \neq 0$, there is a discontinuous (first order) transition at $a_c = 2y^2/9b > 0$ and $m_c = 2y/3b$. This occurs before a reaches the value $a = 0$ where the curvature at $m = 0$ turns negative. If we write $a = \alpha(T - T_0)$, then the expected second order transition at $T = T_0$ is *preempted* by a first order transition at $T_c = T_0 + 2y^2/9\alpha b$.

7.6.3 Order parameter dynamics

Suppose we now impose some dynamics on the system, of the simple relaxational type

$$\frac{dm}{dt} = -\Gamma \frac{\partial f}{\partial m} \quad , \tag{7.114}$$

where Γ is a phenomenological kinetic coefficient. Assuming $y > 0$ and $b > 0$, it is convenient to adimensionalize by writing

$$m \equiv \frac{y}{b} \cdot u \qquad , \qquad a \equiv \frac{y^2}{b} \cdot r \qquad , \qquad t \equiv \frac{b}{\Gamma y^2} \cdot s \quad . \tag{7.115}$$

Then we obtain

$$\frac{du}{ds} = -\frac{\partial \varphi}{\partial u} \quad , \tag{7.116}$$

where the dimensionless free energy function is

$$\varphi(u) = \tfrac{1}{2} r u^2 - \tfrac{1}{3} u^3 + \tfrac{1}{4} u^4 \quad . \tag{7.117}$$

We see that there is a single control parameter, $r = ab/y^2$. The fixed points of the dynamics are then the stationary points of $\varphi(u)$, where $\varphi'(u) = 0$, with $\varphi'(u) = u\,(r - u + u^2)$. The solutions to $\varphi'(u) = 0$ are then given by

$$u^* = 0 \qquad , \qquad u^* = \tfrac{1}{2} \pm \big(\tfrac{1}{4} - r\big)^{1/2} \quad . \tag{7.118}$$

The second of these is a parabola $r = u(1-u)$ opening to the left in the (r, u) plane. For $r > \frac{1}{4}$ there is one fixed point at $u = 0$, which is attractive under the dynamics $\dot{u} = -\varphi'(u)$ since $\varphi''(0) = r$. At $r = \frac{1}{4}$ there occurs a saddle-node bifurcation and a pair of fixed points is generated, one stable and one unstable. As we see from fig. 7.14, the interior fixed point is always unstable and the two exterior fixed points are always stable. At $r = 0$ there is a transcritical bifurcation where two fixed points of opposite stability collide and bounce off one another (metaphorically speaking).

At the saddle-node bifurcation, $r = \frac{1}{4}$ and $u = \frac{1}{2}$, and we find $\varphi(u = \frac{1}{2}; r = \frac{1}{4}) = \frac{1}{192}$, which is positive. Thus, the thermodynamic state of the system remains at $u = 0$ until the value of $\varphi(u_+)$ crosses zero. This occurs when $\varphi(u) = 0$ and $\varphi'(u) = 0$, the simultaneous solution of which yields $r = \frac{2}{9}$ and $u = \frac{2}{3}$.

Suppose we slowly ramp the control parameter r up and down as a function of the dimensionless time s. Under the dynamics of eqn. 7.116, $u(s)$ flows to the first stable fixed point encountered – this is always the case for a dynamical system with a one-dimensional phase space. Then as r is further varied, u follows the position of whatever locally stable fixed point it initially encountered. Thus, $u\big(r(s)\big)$ evolves smoothly until a bifurcation is encountered. The situation is depicted by the arrows in fig. 7.16. The equilibrium thermodynamic value for $u(r)$ is discontinuous; there is a first order phase transition at $r = \frac{2}{9}$, as we've already seen. As r is increased, $u(r)$ follows a trajectory indicated by the magenta arrows. For a negative initial value of u, the evolution as a function of r will be *reversible*. However, if $u(0)$ is initially positive, then the system exhibits *hysteresis*, as shown. Starting with a large positive value of r, $u(s)$ quickly evolves to $u = 0^+$, which means a positive infinitesimal value. Then as r is decreased, the system remains at $u = 0^+$ even through the first order transition, because $u = 0$ is an attractive fixed point. However, once r begins to go negative, the $u = 0$ fixed point becomes repulsive,

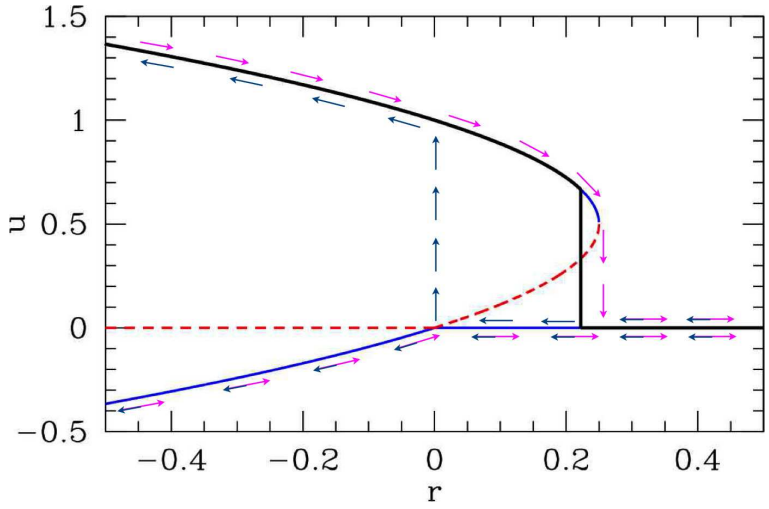


Figure 7.16: Fixed points for $\varphi(u) = \frac{1}{2}ru^2 - \frac{1}{3}u^3 + \frac{1}{4}u^4$ and flow under the dynamics $\dot{u} = -\varphi'(u)$. Solid curves represent stable fixed points and dashed curves unstable fixed points. Magenta arrows show behavior under slowly increasing control parameter r and dark blue arrows show behavior under slowly decreasing r. For $u > 0$ there is a hysteresis loop. The thick black curve shows the equilibrium thermodynamic value of $u(r)$, *i.e.* that value which minimizes the free energy $\varphi(u)$. There is a first order phase transition at $r = \frac{2}{9}$, where the thermodynamic value of u jumps from $u = 0$ to $u = \frac{2}{3}$.

and $u(s)$ quickly flows to the stable fixed point $u_+ = \frac{1}{2} + \left(\frac{1}{4} - r\right)^{1/2}$. Further decreasing r, the system remains on this branch. If r is later increased, then $u(s)$ remains on the upper branch past $r = 0$, until the u_+ fixed point annihilates with the unstable fixed point at $u_- = \frac{1}{2} - \left(\frac{1}{4} - r\right)^{1/2}$, at which time $u(s)$ quickly flows down to $u = 0^+$ again.

7.6.4 Sixth order Landau theory : tricritical point

Finally, consider a model with $\mathbb{Z}_2$ symmetry, with the Landau free energy

$$f = f_0 + \tfrac{1}{2}am^2 + \tfrac{1}{4}bm^4 + \tfrac{1}{6}cm^6 \quad , \tag{7.119}$$

with $c > 0$ for stability. We seek the phase diagram in the (a, b) plane. Extremizing f with respect to m,

$$\frac{\partial f}{\partial m} = 0 = m\left(a + bm^2 + cm^4\right) \quad , \tag{7.120}$$

which is a quintic with five solutions over the complex m plane. One solution is obviously $m = 0$. The other four are

$$m = \pm\sqrt{-\frac{b}{2c} \pm \sqrt{\left(\frac{b}{2c}\right)^2 - \frac{a}{c}}} \quad . \tag{7.121}$$

For each $\pm$ symbol in the above equation, there are two options, hence four roots in all.

If $a > 0$ and $b > 0$, then four of the roots are complex and there is a unique minimum at $m = 0$.

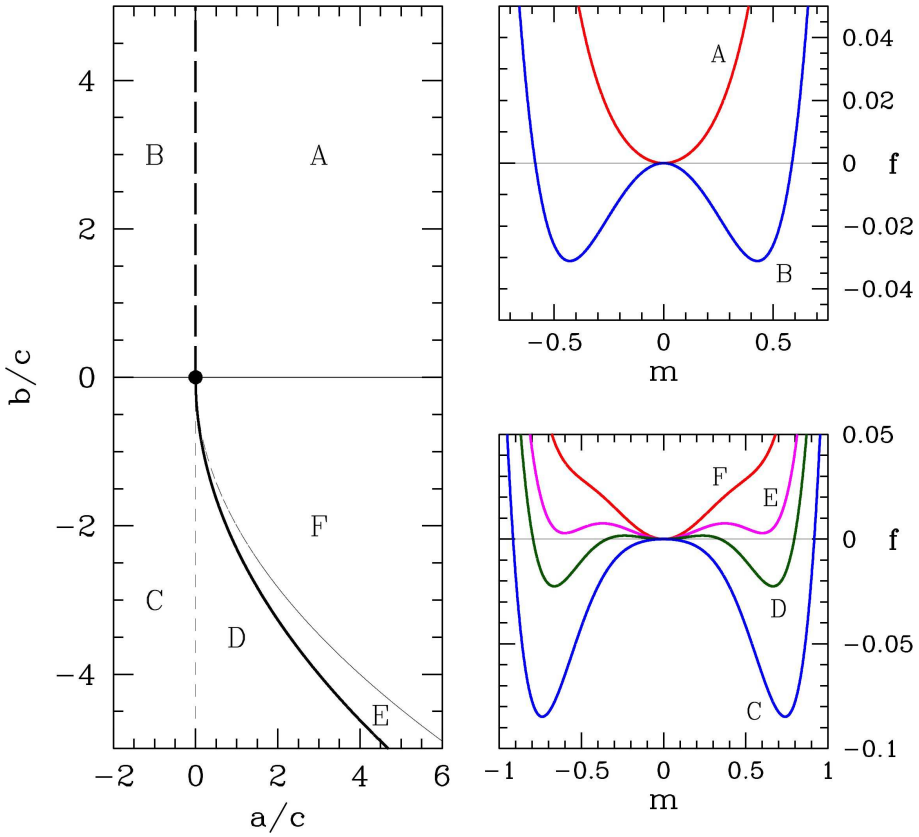


Figure 7.17: Behavior of the sextic free energy $f(m) = \frac{1}{2}am^2 + \frac{1}{4}bm^4 + \frac{1}{6}cm^6$. A: $a > 0$ and $b > 0$; B: $a < 0$ and $b > 0$; C: $a < 0$ and $b < 0$; D: $a > 0$ and $b < -\frac{4}{\sqrt{3}}\sqrt{ac}$; E: $a > 0$ and $-\frac{4}{\sqrt{3}}\sqrt{ac} < b < -2\sqrt{ac}$; F: $a > 0$ and $-2\sqrt{ac} < b < 0$. The thick dashed line is a line of second order transitions, which meets the thick solid line of first order transitions at the tricritical point, $(a, b) = (0, 0)$.

For $a < 0$, there are only three solutions to $f'(m) = 0$ for real m, regardless of the sign of b, since the minus choice for the $\pm$ sign under the radical leads to imaginary roots. One of the solutions is $m = 0$, which is a local maximum of $f(m)$. The other two are degenerate minima at

$$m = \pm\sqrt{-\frac{b}{2c} + \sqrt{\left(\frac{b}{2c}\right)^2 - \frac{a}{c}}} \quad . \tag{7.122}$$

The most interesting situation is $a > 0$ and $b < 0$. If $a > 0$ and $b < -2\sqrt{ac}$, all five roots are real. There must be three minima, separated by two local maxima. Clearly if m^* is a solution, then so is $-m^*$. Thus, the only question is whether the outer minima are of lower energy than the minimum at $m = 0$. We assess this by demanding $f(m^*) = f(0)$, where m^* is the position of the largest root (*i.e.* the rightmost minimum). This gives a second quadratic equation,

$$0 = \tfrac{1}{2}a + \tfrac{1}{4}bm^2 + \tfrac{1}{6}cm^4 \quad , \tag{7.123}$$

which together with equation 7.120 gives $b = -\frac{4}{\sqrt{3}}\sqrt{ac}$. Thus, we have the following, for fixed $a > 0$:

$$\begin{aligned} b > -2\sqrt{ac} \quad &: \quad \text{1 real root } m = 0 \\ -2\sqrt{ac} > b > -\tfrac{4}{\sqrt{3}}\sqrt{ac} \quad &: \quad \text{5 real roots; minimum at } m = 0 \\ -\tfrac{4}{\sqrt{3}}\sqrt{ac} > b \quad &: \quad \text{5 real roots; minima at } m = \pm\sqrt{-\frac{b}{2c} + \sqrt{\left(\frac{b}{2c}\right)^2 - \frac{a}{c}}} \end{aligned} \tag{7.124}$$

The point $(a, b) = (0, 0)$, which lies at the confluence of a first order line and a second order line, is known as a *tricritical point*.

The case of barium titanate

The compound $BaTiO_3$ is a *ferroelectric* in which, at sufficiently low temperatures, a spontaneous electric polarization density P develops. The Landau free energy density may be written as

$$f(P, \varepsilon) = f_0 + \tfrac{1}{2}aP^2 + \tfrac{1}{4}bP^4 + \tfrac{1}{6}cP^6 - EP + d\varepsilon P^2 + \frac{\varepsilon^2}{2k} \quad , \tag{7.125}$$

where E is the electric field and ε is a component of the strain field[33]. Note that the coupling between strain and polarization is linear in the former and quadratic in the latter, which is a consequence of symmetry associated with the displacive transition. In other materials such as KH_2PO_4, where the symmetry is lower, the coupling is of the form εP.

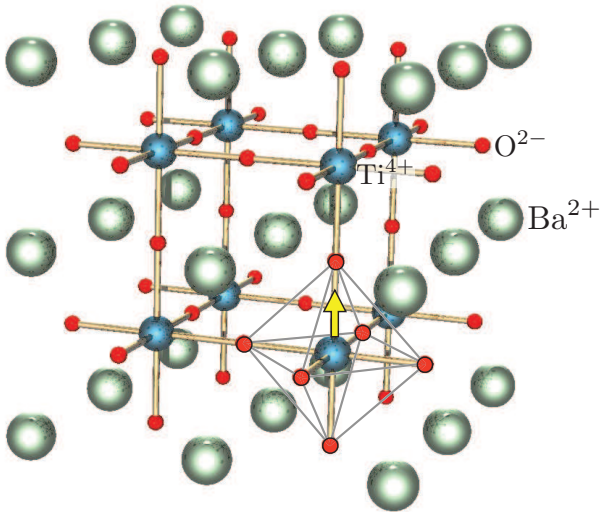


Figure 7.18: High temperature cubic perovskite crystal structure of $BaTiO_3$. Ba^{2+} sites are in green, Ti^{4+} in blue, and O^{2-} in red. The yellow arrow shows the direction in which the Ti^{4+} ion moves as the material is cooled below T_c within the displacive model. Image credit: Wikipedia.

[33] Recall the strain tensor in a solid is given by $\varepsilon_{ij} = \frac{1}{2}\left(\frac{\partial u_i}{\partial x^j} + \frac{\partial u_j}{\partial x^i}\right)$, where $\boldsymbol{u}(\boldsymbol{r})$ is the local displacement field.

Setting $\partial f/\partial\varepsilon = 0$ we obtain $\varepsilon = -kdP^2$, resulting in the effective free energy density

$$f_{\text{eff}}(P) = f_0 + \tfrac{1}{2}aP^2 + (\tfrac{1}{4}b - \tfrac{1}{2}kd^2)P^4 + \tfrac{1}{6}cP^6 - EP \quad . \tag{7.126}$$

If $b > 0$, and $kd^2 > \frac{1}{2}b$, the second order transition is driven to become first order due to the coupling to strain. However, it is oftentimes possible under experimental conditions to ensure that the strain is always zero, for example in the case of a thin epitaxial film whose lattice constants are perfectly matched to a substrate. In this case, stresses develop which constrain the strain to be $\varepsilon = 0$, and in the absence of an electric field E the transition is second order.

7.6.5 Hysteresis for the sextic potential

Once again, we consider the dissipative dynamics $\dot{m} = -\Gamma f'(m)$. We adimensionalize by writing

$$m \equiv \sqrt{\frac{|b|}{c}} \cdot u \qquad , \qquad a \equiv \frac{b^2}{c} \cdot r \qquad , \qquad t \equiv \frac{c}{\Gamma b^2} \cdot s \quad . \tag{7.127}$$

Then we obtain once again the dimensionless equation $du/ds = -\partial\varphi/\partial u$, where

$$\varphi(u) = \tfrac{1}{2}ru^2 \pm \tfrac{1}{4}u^4 + \tfrac{1}{6}u^6 \quad . \tag{7.128}$$

Once again, as in the case of the cubic Landau theory examined in §7.6.2, there is a single control parameter, which here is given by $r = ac/b^2$, but there are two distinct sub-cases to consider. In eqn. 7.128, the coefficient of the quartic term is positive if $b > 0$ and negative if $b < 0$. That is, the coefficient is $\text{sgn}(b)$. When $b > 0$ we can ignore the sextic term for sufficiently small u, and we recover the quartic free energy studied earlier. There is then a second order transition at $r = 0$. The free energy curves for various values of r are plotted in fig. 7.19.

New and interesting behavior occurs for $b < 0$. The fixed points of the dynamics are obtained by setting $\varphi'(u) = 0$. We have

$$\varphi(u) = \tfrac{1}{2}ru^2 - \tfrac{1}{4}u^4 + \tfrac{1}{6}u^6 \qquad , \qquad \varphi'(u) = u\,(r - u^2 + u^4) \quad . \tag{7.129}$$

Thus, the equation $\varphi'(u) = 0$ factorizes into a linear factor u and a quartic factor $u^4 - u^2 + r$ which is quadratic in u^2. Thus, we can easily obtain the roots:

$$\begin{aligned} r < 0 \quad &: \quad u^* = 0 \quad , \; u^* = \pm\sqrt{\tfrac{1}{2} + \sqrt{\tfrac{1}{4} - r}} \\ 0 < r < \tfrac{1}{4} \quad &: \quad u^* = 0 \quad , \; u^* = \pm\sqrt{\tfrac{1}{2} + \sqrt{\tfrac{1}{4} - r}} \quad , \; u^* = \pm\sqrt{\tfrac{1}{2} - \sqrt{\tfrac{1}{4} - r}} \\ r > \tfrac{1}{4} \quad &: \quad u^* = 0 \quad . \end{aligned} \tag{7.130}$$

In fig. 7.20, we plot the fixed points and the hysteresis loops for this system. At $r = \frac{1}{4}$, there are two symmetrically located saddle-node bifurcations at $u = \pm\frac{1}{\sqrt{2}}$. We find $\varphi(u = \pm\frac{1}{\sqrt{2}}, r = \frac{1}{4}) = \frac{1}{48}$, which is positive, indicating that the stable fixed point $u^* = 0$ remains the thermodynamic minimum for the free

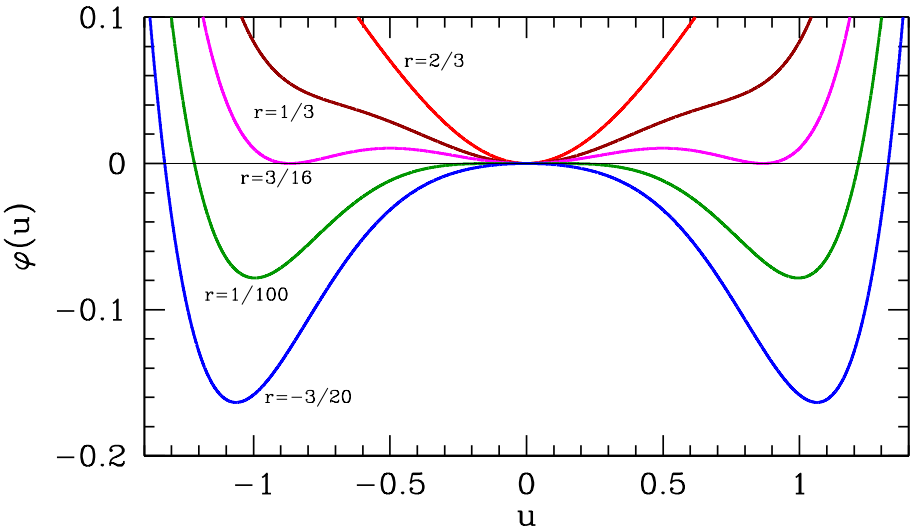


Figure 7.19: Free energy $\varphi(u) = \frac{1}{2}ru^2 - \frac{1}{4}u^4 + \frac{1}{6}u^6$ for different values of the control parameter r.

energy $\varphi(u)$ as r is decreased through $r = \frac{1}{4}$. Setting $\varphi(u) = 0$ and $\varphi'(u) = 0$ simultaneously, we obtain $r = \frac{3}{16}$ and $u = \pm\frac{\sqrt{3}}{2}$. The thermodynamic value for u therefore jumps discontinuously from $u = 0$ to $u = \pm\frac{\sqrt{3}}{2}$ (either branch) at $r = \frac{3}{16}$; this is a first order transition.

Under the dissipative dynamics considered here, the system exhibits hysteresis, as indicated in the figure, where the arrows show the evolution of $u(s)$ for very slowly varying $r(s)$. When the control parameter r is large and positive, the flow is toward the sole fixed point at $u^* = 0$. At $r = \frac{1}{4}$, two simultaneous saddle-node bifurcations take place at $u^* = \pm\frac{1}{\sqrt{2}}$; the outer branch is stable and the inner branch unstable in both cases. At $r = 0$ there is a subcritical pitchfork bifurcation, and the fixed point at $u^* = 0$ becomes unstable.

Suppose one starts off with $r \gg \frac{1}{4}$ with some value $u > 0$. The flow $\dot{u} = -\varphi'(u)$ then rapidly results in $u \to 0^+$. This is the 'high temperature phase' in which there is no magnetization. Now let r decrease slowly, using s as the dimensionless time variable. The scaled magnetization $u(s) = u^*\big(r(s)\big)$ will remain pinned at the fixed point $u^* = 0^+$. As r passes through $r = \frac{1}{4}$, two new stable values of u^* appear, but our system remains at $u = 0^+$, since $u^* = 0$ is a stable fixed point. But after the subcritical pitchfork, $u^* = 0$ becomes unstable. The magnetization $u(s)$ then flows rapidly to the stable fixed point at $u^* = \frac{1}{\sqrt{2}}$, and follows the curve $u^*(r) = \sqrt{\frac{1}{2} + (\frac{1}{4} - r)^{1/2}}$ for all $r < 0$.

Now suppose we start increasing r (*i.e.* increasing temperature). The magnetization follows the stable fixed point $u^*(r) = \sqrt{\frac{1}{2} + (\frac{1}{4} - r)^{1/2}}$ past $r = 0$, beyond the first order phase transition point at $r = \frac{3}{16}$, and all the way up to $r = \frac{1}{4}$, at which point this fixed point is annihilated at a saddle-node bifurcation. The flow then rapidly takes $u \to u^* = 0^+$, where it remains as r continues to be increased further. Within the region $r \in \big[0, \frac{1}{4}\big]$ of control parameter space, the dynamics are said to be *irreversible* and the behavior of $u(s)$ is said to be *hysteretic*.

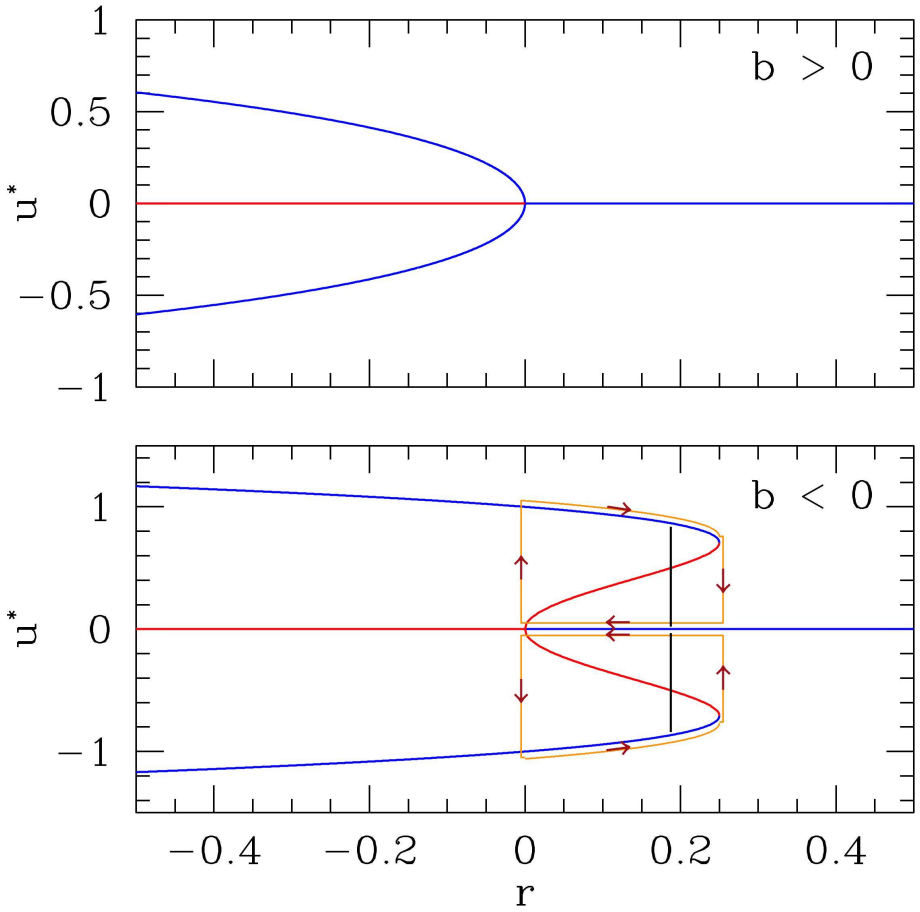


Figure 7.20: Fixed points branches $\varphi'(u^*) = 0$ for the sextic potential $\varphi(u) = \frac{1}{2}ru^2 + \frac{\sigma}{4}u^4 + \frac{1}{6}u^6$ with $\sigma = \mathrm{sgn}(b)$ (top for $\sigma = +1$, bottom for $\sigma = -1$). Blue curves indicate stable branches and red unstable branches under the dynamics $\dot{u} = -\varphi'(u)$. For $b > 0$ there is a supercritical pitchfork bifurcation at $(0, 0)$ and no hysteresis. For $b < 0$ there is a subcritical pitchfork bifurcation at $(0, 0)$ and two saddle-node bifurcations at $(\frac{1}{4}, \pm\frac{1}{\sqrt{2}})$. Solid curves show stable fixed points and dashed curves show unstable fixed points. The thick solid black segment indicates the order parameter discontinuity in u at the thermodynamic first order phase transition. Note the overall $u \to -u$ symmetry. Within the region $r \in [0, \frac{1}{4}]$ the dynamics are irreversible and the system exhibits the phenomenon of hysteresis. There is a first order phase transition at $r = \frac{3}{16}$, indicated by the thick black line segment which shows the discontinuous jump of the order parameter u at the transition.

7.6.6 Weak crystallization

That *weak crystallization*, meaning crystallization in a weakly first-order transition, should result in a triangular lattice in $d = 2$ was argued by Alexander and McTague[34] based on a Landau theory of the transition. The argument is as follows. Let $\varrho_{\boldsymbol{G}}$ be the amplitude of the Fourier component of the density

[34] S. Alexander and J. McTague, *Phys. Rev. Lett.* **41**, 702 (1978). See also E. I. Kats, V. V. Lebedev, and A. R. Muranov, *Phys. Rep.* **228**, 1 (1993).

$\varrho(\boldsymbol{r})$ with wavevector $\boldsymbol{G}$, which is a reciprocal lattice vector of the incipient crystalline phase. Then construct the free energy

$$F\big[\{\varrho_{\boldsymbol{G}}\}\big] = \frac{1}{2}\sum_{\boldsymbol{G}} \chi^{-1}(\boldsymbol{G})\,|\varrho_{\boldsymbol{G}}|^2 - \frac{1}{3}\,B\sum_{\boldsymbol{G}_1}\sum_{\boldsymbol{G}_2}\sum_{\boldsymbol{G}_3} \varrho_{\boldsymbol{G}_1}\,\varrho_{\boldsymbol{G}_2}\,\varrho_{\boldsymbol{G}_3}\,\delta_{\boldsymbol{G}_1+\boldsymbol{G}_2+\boldsymbol{G}_3,\boldsymbol{0}} + \frac{1}{4}\,C\sum_{\boldsymbol{G}_1}\sum_{\boldsymbol{G}_2}\sum_{\boldsymbol{G}_3}\sum_{\boldsymbol{G}_4} \varrho_{\boldsymbol{G}_1}\,\varrho_{\boldsymbol{G}_2}\,\varrho_{\boldsymbol{G}_3}\,\varrho_{\boldsymbol{G}_4}\,\delta_{\boldsymbol{G}_1+\boldsymbol{G}_2+\boldsymbol{G}_3+\boldsymbol{G}_4,\boldsymbol{0}} + \cdots \quad , \tag{7.131}$$

where

$$\chi^{-1}(\boldsymbol{k}) = r + b\,(\boldsymbol{k}^2 - G^2)^2 \tag{7.132}$$

is the inverse static susceptibility at wavevector $\boldsymbol{k}$, which for fixed r is minimized for $|\boldsymbol{k}| = G$. The quadratic term determines the magnitude of the preferred wavevectors at which condensation takes place at $r = r_{\rm c} > 0$, but this energy is degenerate over the circle (or sphere in $d = 3$) of radius G. For weak crystallization, then, the cubic term determines the crystal structure, and evidently prefers structures whose reciprocal lattices contain the maximum number of triangles, in order to satisfy the $\boldsymbol{G}_1 + \boldsymbol{G}_2 + \boldsymbol{G}_3 = 0$ condition. In $d = 2$ this prefers a reciprocal lattice which is triangular, hence the underlying direct Bravais lattice is also triangular. The real space structure may be triangular or honeycomb. In $d = 3$, this condition prefers the fcc structure among all regular lattices, and the corresponding direct lattice is thus bcc. It should be emphasized that the Alexander-McTague theory applies to the weak crystallization of a fluid, and really describes the formation of a charge density wave structure, rather than a Wigner crystal of point particles.

7.7 Variational Density Matrix Method

7.7.1 The variational principle

Suppose we are given a Hamiltonian $\hat{H}$. From this we construct the free energy, F:

$$F = E - TS = \mathrm{Tr}\,(\varrho\,\hat{H}) + k_{\rm B}T\,\mathrm{Tr}\,(\varrho\,\log\varrho) \quad . \tag{7.133}$$

Here, ϱ is the *density matrix*[35]. A physical density matrix must be (i) normalized (*i.e.* $\mathrm{Tr}\,\varrho = 1$), (ii) Hermitian, and (iii) non-negative definite (*i.e.* all the eigenvalues of ϱ must be non-negative).

Our goal is to extremize the free energy subject to the various constraints on ϱ. Let us assume that ϱ is diagonal in the basis of eigenstates of $\hat{H}$, *i.e.*

$$\varrho = \sum_\gamma P_\gamma\,|\,\gamma\,\rangle\langle\,\gamma\,| \quad , \tag{7.134}$$

where P_γ is the probability that the system is in state $|\,\gamma\,\rangle$. Then

$$F = \sum_\gamma E_\gamma\,P_\gamma + k_{\rm B}T\sum_\gamma P_\gamma\log P_\gamma \quad . \tag{7.135}$$

[35] How do we take the logarithm of a matrix? The rule is this: $A = \log B$ if $B = \exp(A)$. The exponential of a matrix may be evaluated via its Taylor expansion.

Thus, the free energy is a function of the set $\{P_\gamma\}$. We now extremize F subject to the normalization constraint. This means we form the extended function

$$F^*\big(\{P_\gamma\},\lambda\big) = F\big(\{P_\gamma\}\big) + \lambda\Big(\sum_\gamma P_\gamma - 1\Big) \quad , \tag{7.136}$$

and then freely extremize over both the probabilities $\{P_\gamma\}$ as well as the Lagrange multiplier λ. This yields the Boltzmann distribution,

$$P_\gamma^{\rm eq} = \frac{1}{Z}\,\exp(-E_\gamma/k_{\rm B}T) \quad , \tag{7.137}$$

where $Z = \sum_\gamma e^{-E_\gamma/k_{\rm B}T} = {\rm Tr}\, e^{-\hat{H}/k_{\rm B}T}$ is the canonical partition function, which is related to λ through

$$\lambda = k_{\rm B}T\,(\log Z - 1) \quad . \tag{7.138}$$

Note that the Boltzmann weights are, appropriately, all positive.

If the spectrum of $\hat{H}$ is bounded from below, our extremum should in fact yield a minimum for the free energy F. Furthermore, since we have freely minimized over all the probabilities, subject to the single normalization constraint, *any distribution $\{P_\gamma\}$ other than the equilibrium one must yield a greater value of F.*

Alas, the Boltzmann distribution, while exact, is often intractable to evaluate. For one-dimensional systems, there are general methods such as the transfer matrix approach which do permit an exact evaluation of the free energy. However, beyond one dimension the situation is in general hopeless. A family of solvable ("integrable") models exists in two dimensions, but their solutions require specialized techniques and are extremely difficult. The idea behind the variational density matrix approximation is to construct a tractable *trial* density matrix ϱ which depends on a set of variational parameters $\{x_\alpha\}$, and to minimize F with respect to this set.

7.7.2 Variational density matrix for the Ising model

Consider once again the Ising model Hamiltonian,

$$\hat{H} = -\frac{1}{2}\sum_{i,j=1}^N J_{ij}\,\sigma_i\,\sigma_j - H\sum_{i=1}^N \sigma_i \quad . \tag{7.139}$$

The states of the system $|\boldsymbol{\sigma}\rangle$ may be labeled by the values of the spin variables: $|\boldsymbol{\sigma}\rangle = |\sigma_1,\sigma_2,\ldots,\sigma_N\rangle$. We assume the density matrix is diagonal in this basis, *i.e.*

$$\varrho_N(\boldsymbol{\sigma}\,|\,\boldsymbol{\sigma}') \equiv \varrho_N(\boldsymbol{\sigma})\,\delta_{\boldsymbol{\sigma},\boldsymbol{\sigma}'} \quad , \tag{7.140}$$

where $\delta_{\boldsymbol{\sigma},\boldsymbol{\sigma}'} = \prod_{i=1}^N \delta_{\sigma_i,\sigma_i'}$ and where N is the number of sites. Indeed, this is the case for the exact density matrix, which is to say the Boltzmann weight, $\varrho_N(\boldsymbol{\sigma}) = Z_N^{-1} e^{-\beta\hat{H}(\boldsymbol{\sigma})}$.

We now write a *trial density matrix* which is a product over contributions from independent single sites:

$$\varrho_N(\boldsymbol{\sigma}) = \prod_{i=1}^N \varrho(\sigma_i) \quad , \tag{7.141}$$

where

$$\varrho(\sigma) = \left(\frac{1+m}{2}\right)\delta_{\sigma,1} + \left(\frac{1-m}{2}\right)\delta_{\sigma,-1} \quad . \tag{7.142}$$

Note that we've changed our notation slightly. We are denoting by $\varrho(\sigma)$ the corresponding diagonal element of the matrix

$$\varrho = \frac{1}{2}\begin{pmatrix} 1+m & 0 \\ 0 & 1-m \end{pmatrix} \quad , \tag{7.143}$$

and the full density matrix is a tensor product over the single site matrices: $\varrho_N = \varrho \otimes \varrho \otimes \cdots \otimes \varrho$. Note also that ϱ and ϱ_N are normalized with unit trace.

Note that ϱ and hence ϱ_N are appropriately normalized. The variational parameter here is m, which, if ρ is to be non-negative definite, must satisfy $-1 \le m \le 1$. The quantity m has the physical interpretation of the average spin on any given site, since

$$\langle \sigma_i \rangle = \sum_\sigma \varrho(\sigma)\,\sigma = m. \tag{7.144}$$

We may now evaluate the average energy:

$$\begin{aligned} E = \mathsf{Tr}\,(\varrho_N \hat{H}) &= -\sum_{i<j} J_{ij}\, m^2 - H\sum_i m \\ &= -\tfrac{1}{2} N \hat{J}(0)\, m^2 - NHm \quad , \end{aligned} \tag{7.145}$$

where once again $\hat{J}(0)$ is the discrete Fourier transform of $J(\boldsymbol{R})$ at wavevector $\boldsymbol{q} = 0$. The entropy is given by

$$\begin{aligned} S &= -k_{\rm B}\,\mathsf{Tr}\,(\varrho_N \log \varrho_N) = -Nk_{\rm B}\,\mathsf{Tr}\,(\varrho \log \varrho) \\ &= -Nk_{\rm B}\left\{\left(\frac{1+m}{2}\right)\log\left(\frac{1+m}{2}\right) + \left(\frac{1-m}{2}\right)\log\left(\frac{1-m}{2}\right)\right\} \quad . \end{aligned} \tag{7.146}$$

We now define the dimensionless free energy per site: $f \equiv F/N\hat{J}(0)$. We have

$$f(m,\theta,h) = -\tfrac{1}{2}\,m^2 - hm + \theta\left\{\left(\frac{1+m}{2}\right)\log\left(\frac{1+m}{2}\right) + \left(\frac{1-m}{2}\right)\log\left(\frac{1-m}{2}\right)\right\} \quad , \tag{7.147}$$

where $\theta \equiv k_{\rm B}T/\hat{J}(0)$ is the dimensionless temperature, and $h \equiv H/\hat{J}(0)$ the dimensionless magnetic field, as before. We extremize $f(m)$ by setting

$$\frac{\partial f}{\partial m} = 0 = -m - h + \frac{\theta}{2}\log\left(\frac{1+m}{1-m}\right) \quad . \tag{7.148}$$

Solving for m, we obtain

$$m = \tanh\left(\frac{m+h}{\theta}\right) \quad , \tag{7.149}$$

which is precisely what we found in eqn. 7.68. There is a second order phase transition at a critical temperature $\theta_{\rm c} = 1$.

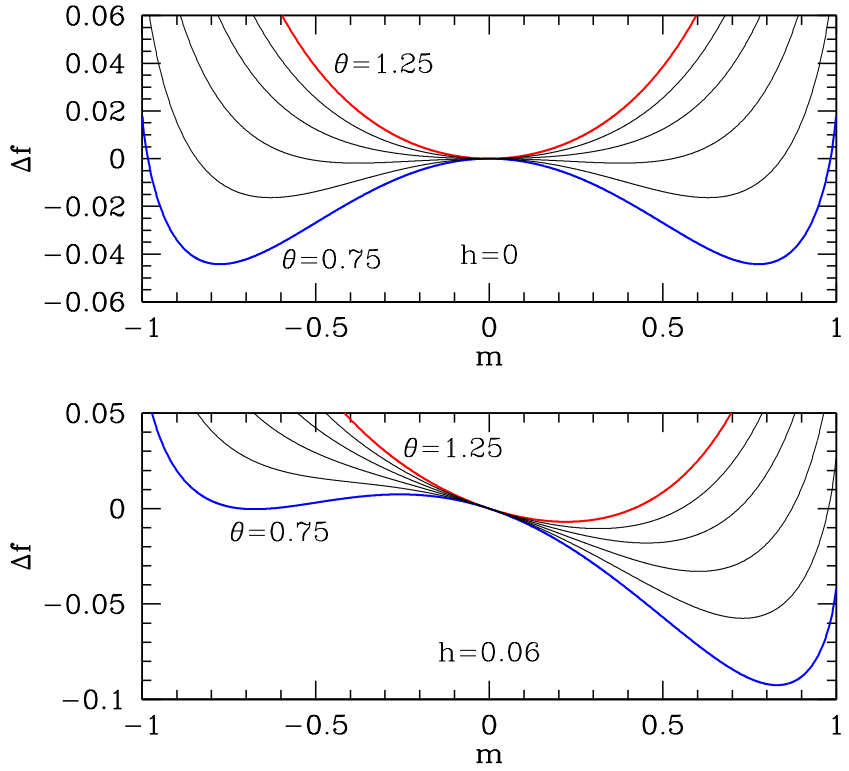


Figure 7.21: Variational field free energy $\Delta f = f(m,\theta,h) + \theta\,\log 2$ *versus* magnetization m at six equally spaced temperatures interpolating between 'high' ($\theta = 1.25$, red) and 'low' ($\theta = 0.75$, blue) values. Top panel: $h = 0$. Bottom panel: $h = 0.06$.

Note that the optimal value of m indeed satisfies the requirement $|m| \le 1$ of non-negative probability. This nonlinear equation may be solved graphically. For $h = 0$, the unmagnetized solution $m = 0$ always applies. However, for $\theta < 1$ there are two additional solutions at $m = \pm m_{\rm A}(\theta)$, with $m_{\rm A}(\theta) = \sqrt{3(1-\theta)} + \mathcal{O}\big((1-\theta)^{3/2}\big)$ for θ close to (but less than) one. These solutions, which are related by the $\mathbb{Z}_2$ symmetry of the $h = 0$ model, are in fact the low (free) energy solutions. This is shown clearly in figure 7.21, where the variational free energy $f(m,\theta)$ is plotted as a function of m for a range of temperatures interpolating between 'high' and 'low' values. At the *critical temperature* $\theta_{\rm c} = 1$, the lowest energy state changes from being unmagnetized (high temperature) to magnetized (low temperature).

For $h > 0$, there is no longer a $\mathbb{Z}_2$ symmetry (*i.e.* $\sigma_i \to -\sigma_i\ \forall\ i$). The high temperature solution now has $m > 0$ (or $m < 0$ if $h < 0$), and this smoothly varies as t is lowered, approaching the completely polarized limit $m = 1$ as $\theta \to 0$. At very high temperatures, the argument of the $\tanh$ function is small, and we may approximate $\tanh(x) \simeq x$, in which case

$$m(h,\theta) = \frac{h}{\theta - \theta_{\rm c}} \quad . \tag{7.150}$$

This is called the *Curie-Weiss law*. One can infer $\theta_{\rm c}$ from the high temperature susceptibility $\chi(\theta) = (\partial m/\partial h)_{h=0}$ by plotting χ^{-1} *versus* θ and extrapolating to obtain the θ-intercept. In our case, $\chi(\theta) = (\theta - \theta_{\rm c})^{-1}$. For low θ and weak h, there are two inequivalent minima in the free energy.

When m is small, it is appropriate to expand $f(m,\theta,h)$, obtaining

$$f(m,\theta,h) = -\theta\,\log 2 - hm + \tfrac{1}{2}\,(\theta-1)\,m^2 + \tfrac{\theta}{12}\,m^4 + \tfrac{\theta}{30}\,m^6 + \tfrac{\theta}{56}\,m^8 + \ldots \quad . \tag{7.151}$$

This is known as the *Landau expansion* of the free energy in terms of the *order parameter* m. An order parameter is a thermodynamic variable ϕ which distinguishes ordered and disordered phases. Typically $\phi = 0$ in the disordered (high temperature) phase, and $\phi \neq 0$ in the ordered (low temperature) phase. When the order sets in continuously, *i.e.* when ϕ is continuous across $\theta_{\rm c}$, the phase transition is said to be *second order*. When ϕ changes abruptly, the transition is *first order*. It is also quite commonplace to observe phase transitions between two ordered states. For example, a crystal, which is an ordered state, may change its lattice structure, say from a high temperature tetragonal phase to a low temperature orthorhombic phase. When the symmetry group of the low-temperature phase is a subgroup of that of the high-temperature phase, as can occur in a tetragonal-to-orthorhombic transition, the transition may be second order. When the two symmetries are completely unrelated, for example in a hexagonal-to-tetragonal transition, or in a transition between a ferromagnet and an antiferromagnet, the transition is in general first order.

Throughout this discussion, we have assumed that the interactions J_{ij} are predominantly *ferromagnetic*, *i.e.* $J_{ij} > 0$, so that all the spins prefer to align. When $J_{ij} < 0$, the interaction is said to be *antiferromagnetic* and prefers anti-alignment of the spins (*i.e.* $\sigma_i\,\sigma_j = -1$). Clearly not every pair of spins can be anti-aligned – there are two possible spin states and a thermodynamically extensive number of spins. But on the square lattice, for example, if the only interactions J_{ij} are between nearest neighbors and the interactions are antiferromagnetic, then the lowest energy configuration ($T = 0$ ground state) will be one in which spins on opposite sublattices are anti-aligned. The square lattice is *bipartite* – it breaks up into two interpenetrating sublattices A and B (which are themselves square lattices, rotated by 45° with respect to the original, and with a larger lattice constant by a factor of $\sqrt{2}$), such that any site in A has nearest neighbors in B, and *vice versa*. The honeycomb lattice is another example of a bipartite lattice. So is the simple cubic lattice. The triangular lattice, however, is not bipartite (it is *tripartite*). Consequently, with nearest neighbor antiferromagnetic interactions, the triangular lattice Ising model is highly *frustrated*. The moral of the story is this: antiferromagnetic interactions can give rise to complicated magnetic ordering, and, when frustrated by the lattice geometry, may have finite specific entropy even at $T = 0$.

7.7.3 q-state Potts model

The Hamiltonian for the Potts model is

$$\hat{H} = -\frac{1}{2}\sum_{i,j=1}^{N} J_{ij}\,\delta_{\sigma_i,\sigma_j} - H\sum_{i=1}^{N}\delta_{\sigma_i,1} \quad . \tag{7.152}$$

Here, $\sigma_i \in \{1,\ldots,q\}$, with integer q. This is the so-called 'q-state Potts model'. The quantity H is analogous to an external magnetic field, and preferentially aligns (for $H > 0$) the local spins in the $\sigma = 1$ direction. We will assume $H \geq 0$.

The q-component set is conveniently taken to be the set $\{1,\ldots,q\}$, but it could be anything, such as

$$\sigma_i \in \{\text{tomato, penny, ostrich, Grateful Dead ticket from 1987, } \ldots\} \quad . \tag{7.153}$$

The interaction energy is $-J_{ij}$ if sites i and j contain the same object (q possibilities), and 0 if i and j contain different objects ($q^2 - q$ possibilities).

The two-state Potts model is equivalent to the Ising model. Let the allowed values of σ be ± 1. Then the quantity

$$\delta_{\sigma,\sigma'} = \tfrac{1}{2} + \tfrac{1}{2}\,\sigma\sigma' \tag{7.154}$$

equals 1 if $\sigma = \sigma'$, and is zero otherwise. The three-state Potts model cannot be written as a simple three-state Ising model, *i.e.* one with a bilinear interaction $\sigma\,\sigma'$ where $\sigma \in \{-1, 0, +1\}$. However, it is straightforward to verify the identity

$$\delta_{\sigma,\sigma'} = 1 + \tfrac{1}{2}\,\sigma\sigma' + \tfrac{3}{2}\,\sigma^2\sigma'^2 - (\sigma^2 + \sigma'^2) \quad . \tag{7.155}$$

Thus, the $q = 3$-state Potts model is equivalent to a $S = 1$ (three-state) Ising model which includes both bilinear ($\sigma\sigma'$) and biquadratic ($\sigma^2\sigma'^2$) interactions, as well as a local field term which couples to the square of the spin, σ^2. In general one can find such correspondences for higher q Potts models, but, as should be expected, the interactions become increasingly complex, with bi-cubic, bi-quartic, bi-quintic, *etc.* terms. Such a formulation, however, obscures the beautiful S_q symmetry inherent in the model, where S_q is the permutation group on q symbols, which has $q!$ elements.

Getting back to the mean field theory, we write the single site variational density matrix ϱ as a diagonal matrix with entries

$$\varrho(\sigma) = x\,\delta_{\sigma,1} + \left(\frac{1-x}{q-1}\right)\left(1 - \delta_{\sigma,1}\right) \quad , \tag{7.156}$$

with $\varrho_N(\sigma_1, \ldots, \sigma_N) = \varrho(\sigma_1) \cdots \varrho(\sigma_N)$. Note that $\mathsf{Tr}\,(\varrho) = 1$. The variational parameter is x. When $x = q^{-1}$, all states are equally probable. But for $x > q^{-1}$, the state $\sigma = 1$ is preferred, and the other $(q-1)$ states have identical but smaller probabilities. It is a simple matter to compute the energy and entropy:

$$\begin{aligned} E &= \mathsf{Tr}\,(\varrho_N \hat{H}) = -\tfrac{1}{2} N \hat{J}(0) \left\{ x^2 + \frac{(1-x)^2}{q-1} \right\} - NHx \\ S &= -k_{\rm B}\,\mathsf{Tr}\,(\varrho_N \log \varrho_N) = -N k_{\rm B} \left\{ x \log x + (1-x) \log\left(\frac{1-x}{q-1}\right) \right\} \quad . \end{aligned} \tag{7.157}$$

The dimensionless free energy per site is then

$$f(x, \theta, h) = -\tfrac{1}{2} \left\{ x^2 + \frac{(1-x)^2}{q-1} \right\} + \theta \left\{ x \log x + (1-x) \log\left(\frac{1-x}{q-1}\right) \right\} - hx \quad , \tag{7.158}$$

where $\theta = k_{\rm B}T/\hat{J}(0)$ and $h = H/\hat{J}(0)$. We now extremize with respect to x to obtain the mean field equation,

$$\frac{\partial f}{\partial x} = 0 = -x + \frac{1-x}{q-1} + \theta\,\log x - \theta\,\log\left(\frac{1-x}{q-1}\right) - h \quad . \tag{7.159}$$

For reference, the second derivative of f with respect to x is given by

$$\frac{\partial^2 f}{\partial x^2} = -\frac{q}{q-1} + \frac{\theta}{x(1-x)} \quad , \tag{7.160}$$

and solving for $f''(x) = 0$, we obtain

$$x_\pm = \frac{1}{2} \pm \frac{1}{2}\sqrt{1 - \frac{\theta}{\theta_0}} \quad , \qquad \theta_0 = \frac{q}{4(q-1)} \quad . \tag{7.161}$$

Note that when $h = 0$, $x = q^{-1}$ is a solution to $f'(x) = 0$, corresponding to a S_q-symmetric disordered state in which all states are equally probable. At high temperatures, for small h, we expect $x - q^{-1} \propto h$. Using `Mathematica`, one can set $x \equiv q^{-1} + u$ and expand the mean field equation in powers of u. One obtains

$$h = \frac{q\,(q\theta - 1)}{q-1}\,u - \frac{q^3\,(q-2)\,\theta}{2\,(q-1)^2}\,u^2 + \mathcal{O}(u^3) \quad . \tag{7.162}$$

For weak fields, $|h| \ll 1$, and in the high temperature phase we have

$$u(\theta) = \frac{(q-1)\,h}{q\,(q\theta - 1)} + \mathcal{O}(h^2) \quad , \tag{7.163}$$

which again is of the Curie-Weiss form, with a Curie temperature $\theta_{\rm C} = q^{-1}$. The difference $u = x - q^{-1}$ is the order parameter for the transition. However, for $q > 2$ we expect the transition to be first order, which we can see by expanding the free energy in powers of u, obtaining the Landau expansion. Expressed in terms of the order parameter u (rather than $x = q^{-1} + u$), the free energy $f(u, \theta, h)$ is

$$f(u,\theta,h) = f_0 - \frac{qu^2}{2(q-1)} - hu + \theta\,(q^{-1} + u)\log(1 + qu) + \theta\,(1 - q^{-1} - u)\log\left(1 - \frac{qu}{q-1}\right) \quad , \tag{7.164}$$

with $f_0 = -\theta \log q - (h + \frac{1}{2})\,q^{-1}$; note that $f(u = 0, \theta, h) = f_0$. Expanding in powers of u, we find

$$\begin{aligned} f(u,\theta,h) = f_0 - hu + \frac{q^2\,(\theta - q^{-1})}{2\,(q-1)}\,u^2 - \frac{(q-2)\,q^3\,\theta}{6\,(q-1)^2}\,u^3 \\ + \frac{q^3\theta}{12}\Big[1 + (q-1)^{-3}\Big]u^4 - \frac{q^4\theta}{20}\Big[1 - (q-1)^{-4}\Big]u^5 + \frac{q^5\theta}{30}\Big[1 + (q-1)^{-5}\Big]u^6 + \ldots \quad . \end{aligned} \tag{7.165}$$

Note that, for $q = 2$, the coefficients of u^3, u^5, and higher order odd powers of u vanish in the Landau expansion. This is consistent with what we found for the Ising model, and is related to the $\mathbb{Z}_2$ symmetry of that model. For $q \geq 3$, there is a cubic term in the mean field free energy, and thus we generically expect a first order transition, as we found in §7.6.2. It is important to understand that while the mean field theory which yields the free energy function $f(u, \theta, h)$ is an approximation to a full interacting theory for which no analytic solutions may exist, truncating the MF free energy to yield a low-order polynomial in u and h, *i.e.* a Landau free energy, constitutes a further approximation to the mean field theory itself. In particular, if at $h = 0$ we include only terms in $f(u, \theta)$ up to fourth order in u, we will obtain a free energy of the form $f(u) = \frac{1}{2}au^2 - \frac{1}{3}yu^3 + \frac{1}{4}bu^4$, where $\{a, y, b\}$ may be read off from eqn. 7.165. We found earlier that such a free energy results in a first order transition at $a = 2y^2/9b$. One can thus compute expressions for the critical temperature $\theta_{\rm c}^{\rm L}$ and order parameter discontinuity $u(\theta_{\rm c}^{\rm L-})$ as functions of q, but these will not be the same as what one obtains by working with the untruncated mean field free energy. For $q = 2$ there is a $\mathbb{Z}_2$ symmetry and our Potts model mean field theory predicts a

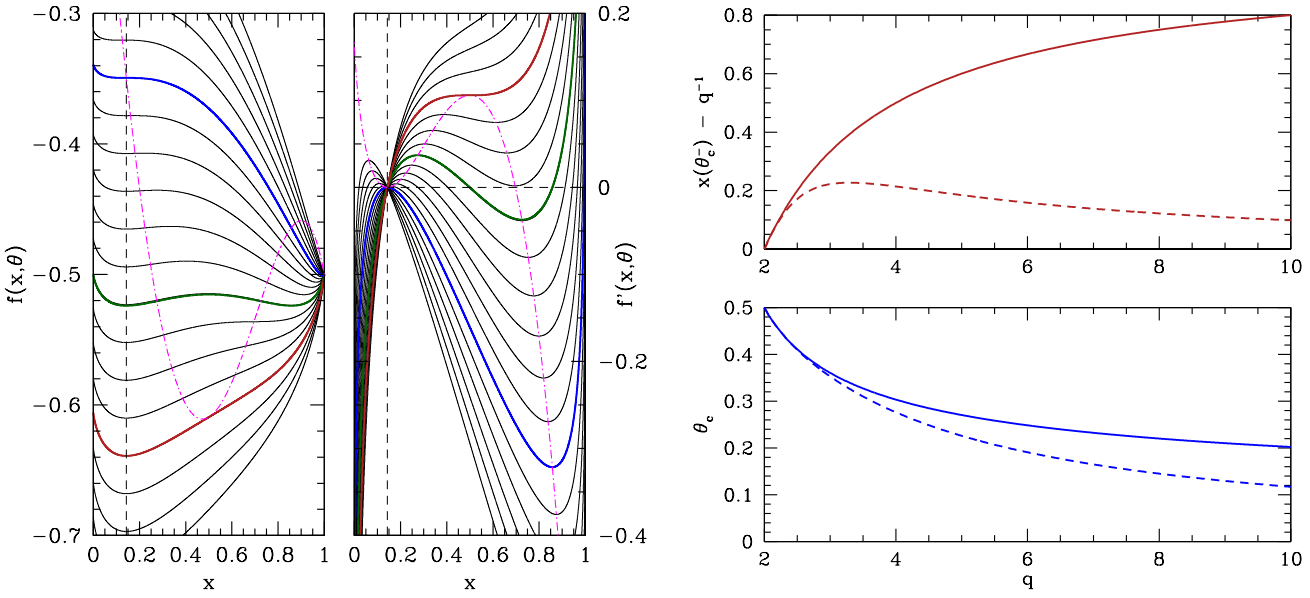


Figure 7.22: The left panels show the variational free energy $f(x,\theta)$ of the $q = 7$ state Potts model and its x-derivative $f'(x,\theta)$ *versus* the variational parameter x, for a set of equally spaced temperatures. The vertical dashed black line is at $x = q^{-1} = \frac{1}{7}$. The dot-dash magenta curve in both cases is the locus of points for which the second derivative $f''(x,\theta)$ with respect to x vanishes. Three characteristic temperatures are marked: (i) $\theta = q^{-1}$ (blue), where the coefficient of the quadratic term in the Landau expansion changes sign, (ii) $\theta = \theta_0$ (red), the temperature above which which the free energy is everywhere convex and has only one minimum at $x = q^{-1}$ (symmetric phase), and (iii) $\theta = \theta_c$ (green), where the first order transition occurs. The right panels show comparisons of the order parameter jump at θ_c (top) and critical temperature θ_c (bottom) *versus* q for untruncated (solid lines) and truncated (dashed lines) expansions of the mean field free energy. Note the agreement as $q \to 2$, where the jump is small and a truncated expansion is then valid.

second order transition at $\theta_c = \frac{1}{2}$.[36] For $q > 2$, the mean field critical point is obtained by simultaneously solving the equations $f'(u) = 0$ and $f(0) = f(u)$, both at $h = 0$. These are two equations for the two unknowns u_c and θ_c, with $u_c > 0$ the value of the order parameter just inside the ordered phase. This can be done numerically, but there is an analytic solution (see fig. 7.22):

$$\theta_c = \frac{q-2}{2(q-1)\log(q-1)} \quad , \qquad u_c = u(\theta_c^-) = 1 - \frac{2}{q} \quad . \tag{7.166}$$

In fig. 7.22 we plot the mean field free energy $f(x,\theta)$ and its x-derivative $f'(x,\theta)$ *versus* x for an equally spaced set of temperatures. Also plotted are the critical temperature θ_c and the order parameter discontinuity $u(\theta_c^-)$ *versus* q for the q-state Potts model MFT. For comparison, θ_c and $u(\theta_c^-)$ are also plotted for the truncated quartic free energy Landau theory.

[36] In §7.7.2 we found $\theta_c = 1$ for the Ising model. So why do we find $\theta_c = \frac{1}{2}$ for the $q = 2$ Potts model?

7.7.4 XY Model

Variational density matrix

Consider the so-called XY model, in which each site contains a continuous planar spin, represented by an angular variable $\phi_i \in [-\pi, \pi]$:

$$\hat{H} = -\frac{1}{2}\sum_{i\neq j}^{N} J_{ij}\cos\big(\phi_i - \phi_j\big) - H\sum_{i=1}^{N}\cos\phi_i \quad . \tag{7.167}$$

We write the (diagonal elements of the) full density matrix once again as a product:

$$\varrho_N(\boldsymbol{\phi}) = \prod_{i=1}^{N}\varrho(\phi_i) \quad . \tag{7.168}$$

Our goal will be to extremize the free energy with respect to the *function* $\varrho(\phi)$. To this end, we compute

$$E = \mathsf{Tr}\,(\varrho_N\,\hat{H}) = -\tfrac{1}{2}N\hat{J}(0)\,\Big|\mathsf{Tr}\,\big(\varrho\,e^{i\phi}\big)\Big|^2 - NH\,\mathsf{Tr}\,\big(\varrho\,\cos\phi\big) \quad . \tag{7.169}$$

The entropy is $S = -Nk_{\rm B}\,\mathsf{Tr}\,(\varrho\,\log\varrho)$. Note that for any function $A(\phi)$, we have[37]

$$\mathsf{Tr}\,(\varrho\,A) \equiv \int_{-\pi}^{\pi}\frac{d\phi}{2\pi}\,\varrho(\phi)\,A(\phi) \quad . \tag{7.170}$$

We now extremize the *functional* $F\big[\varrho(\phi)\big] = E - TS$ with respect to $\varrho(\phi)$, under the condition that $\mathsf{Tr}\;\varrho = 1$. We therefore use Lagrange's method of undetermined multipliers, writing

$$F^* = F - Nk_{\rm B}T\,\lambda\,\Big(\mathsf{Tr}\,\varrho - 1\Big) \quad . \tag{7.171}$$

Note that F^* is a *function* of the Lagrange multiplier λ and a *functional* of the density matrix $\varrho(\phi)$. The prefactor $Nk_{\rm B}T$ which multiplies λ is of no mathematical consequence – we could always redefine the multiplier to be $\lambda' \equiv Nk_{\rm B}T\lambda$. It is present only to maintain homogeneity and proper dimensionality of F^* with λ itself dimensionless and of order N^0. We now have

$$\begin{aligned}\frac{\delta F^*}{\delta\varrho(\phi)} = \frac{\delta}{\delta\varrho(\phi)}\Bigg\{&-\tfrac{1}{2}N\hat{J}(0)\,\Big|\mathsf{Tr}\big(\varrho\,e^{i\phi}\big)\Big|^2 - NH\,\mathsf{Tr}\big(\varrho\,\cos\phi\big)\\ &+ Nk_{\rm B}T\;\mathsf{Tr}\,(\varrho\,\log\varrho) - Nk_{\rm B}T\,\lambda\,\Big(\mathsf{Tr}\,\varrho - 1\Big)\Bigg\} \quad .\end{aligned} \tag{7.172}$$

[37] The denominator of 2π in the measure is not necessary, and in fact it is even slightly cumbersome. It divides out whenever we take a ratio to compute a thermodynamic average. I introduce this factor to preserve the relation $\mathsf{Tr}\;1 = 1$. I personally find unnormalized traces to be profoundly unsettling on purely aesthetic grounds.

To this end, we note that

$$\frac{\delta}{\delta\varrho(\phi)}\,\mathsf{Tr}\,(\varrho\,A) = \frac{\delta}{\delta\varrho(\phi)}\int\limits_{-\pi}^{\pi}\frac{d\phi}{2\pi}\,\varrho(\phi)\,A(\phi) = \frac{1}{2\pi}\,A(\phi) \quad . \tag{7.173}$$

Thus, we have

$$\frac{\delta F^*}{\delta\varrho(\phi)} = -\frac{N\hat{J}(0)}{4\pi}\left[\mathop{\mathsf{Tr}}_{\phi'}\big(\varrho\,e^{i\phi'}\big)\,e^{-i\phi} + \mathop{\mathsf{Tr}}_{\phi'}\big(\varrho\,e^{-i\phi'}\big)\,e^{i\phi}\right] - \frac{NH}{2\pi}\cos\phi + \frac{Nk_{\rm B}T}{2\pi}\Big[\log\varrho(\phi) + 1 - \lambda\Big] \quad . \tag{7.174}$$

Now let us define

$$\mathop{\mathsf{Tr}}_{\phi}\big(\varrho\,e^{i\phi}\big) = \int\limits_{-\pi}^{\pi}\frac{d\phi}{2\pi}\,\varrho(\phi)\,e^{i\phi} \equiv m\,e^{i\phi_0} \quad . \tag{7.175}$$

We then have

$$\log\varrho(\phi) = \frac{\hat{J}(0)}{k_{\rm B}T}\,m\,\cos(\phi-\phi_0) + \frac{H}{k_{\rm B}T}\,\cos\phi + \lambda - 1. \tag{7.176}$$

Clearly the free energy will be reduced if $\phi_0 = 0$ so that the mean field is maximal and aligns with the external field, which prefers $\phi = 0$. Thus, we conclude

$$\varrho(\phi) = \mathcal{C}\,\exp\!\left(\frac{H_{\rm eff}}{k_{\rm B}T}\,\cos\phi\right) \quad , \tag{7.177}$$

where $H_{\rm eff} = \hat{J}(0)\,m + H$ and $\mathcal{C} = e^{\lambda-1}$. The value of λ is then determined by invoking the constraint,

$$\mathsf{Tr}\,\varrho = 1 = \mathcal{C}\int\limits_{-\pi}^{\pi}\frac{d\phi}{2\pi}\,\exp\!\left(\frac{H_{\rm eff}}{k_{\rm B}T}\,\cos\phi\right) = \mathcal{C}\,I_0(H_{\rm eff}/k_{\rm B}T) \quad , \tag{7.178}$$

where $I_0(z)$ is the modified Bessel function of the first kind. We are free to define $\varepsilon \equiv H_{\rm eff}/k_{\rm B}T$, and treat ε as our single variational parameter. We then have the normalized single site density matrix

$$\varrho(\phi) = \frac{\exp(\varepsilon\cos\phi)}{\int\limits_{-\pi}^{\pi}\frac{d\phi'}{2\pi}\,\exp(\varepsilon\cos\phi')} = \frac{\exp(\varepsilon\cos\phi)}{I_0(\varepsilon)} \quad . \tag{7.179}$$

We next compute the following averages:

$$\big\langle\,e^{\pm i\phi}\,\big\rangle = \int\limits_{-\pi}^{\pi}\frac{d\phi}{2\pi}\,\varrho(\phi)\,e^{\pm i\phi} = \frac{I_1(\varepsilon)}{I_0(\varepsilon)} \tag{7.180}$$

$$\big\langle\cos(\phi-\phi')\big\rangle = \mathsf{Re}\,\big\langle e^{i\phi}\,e^{-i\phi'}\big\rangle = \left(\frac{I_1(\varepsilon)}{I_0(\varepsilon)}\right)^2 \quad , \tag{7.181}$$

as well as

$$\mathsf{Tr}\,(\varrho\,\log\varrho) = \int\limits_{-\pi}^{\pi}\frac{d\phi}{2\pi}\,\frac{e^{\varepsilon\cos\phi}}{I_0(\varepsilon)}\Big\{\varepsilon\cos\phi - \log I_0(\varepsilon)\Big\} = \varepsilon\,\frac{I_1(\varepsilon)}{I_0(\varepsilon)} - \log I_0(\varepsilon) \quad . \tag{7.182}$$

The dimensionless free energy per site is therefore

$$f(\varepsilon,\theta,h) = -\frac{1}{2}\left(\frac{I_1(\varepsilon)}{I_0(\varepsilon)}\right)^2 + (\theta\varepsilon - h)\,\frac{I_1(\varepsilon)}{I_0(\varepsilon)} - \theta\,\log I_0(\varepsilon) \quad , \tag{7.183}$$

with $\theta = k_{\rm B}T/\hat{J}(0)$ and $h = H/\hat{J}(0)$ and $f = F/N\hat{J}(0)$ as before. Note that the mean field equation is $m = \theta\varepsilon - h = \langle\, e^{i\phi}\,\rangle$, *i.e.*

$$\theta\varepsilon - h = \frac{I_1(\varepsilon)}{I_0(\varepsilon)} \quad . \tag{7.184}$$

For small ε, we may expand the Bessel functions, using

$$I_\nu(z) = (\tfrac{1}{2}z)^\nu \sum_{k=0}^{\infty} \frac{(\frac{1}{4}z^2)^k}{k!\,\Gamma(k+\nu+1)} \quad , \tag{7.185}$$

to obtain

$$f(\varepsilon,\theta,h) = \tfrac{1}{4}\left(\theta - \tfrac{1}{2}\right)\varepsilon^2 + \tfrac{1}{64}\left(2 - 3\theta\right)\varepsilon^4 - \tfrac{1}{2}h\varepsilon + \tfrac{1}{16}h\varepsilon^3 + \ldots \quad . \tag{7.186}$$

This predicts a second order phase transition at $\theta_{\rm c} = \frac{1}{2}$.[38] Note also the Curie-Weiss form of the susceptibility at high θ:

$$\frac{\partial f}{\partial \varepsilon} = 0 \quad \Longrightarrow \quad \varepsilon = \frac{h}{\theta - \theta_{\rm c}} + \ldots \quad . \tag{7.187}$$

Neglect of fluctuations method

Consider again the Hamiltonian of eqn. 7.167. Define $z_i \equiv \exp(i\phi_i)$ and write $z_i = w + \delta z_i$, where $w \equiv \langle z_i\rangle$ and $\delta z_i \equiv z_i - w$. Of course we also have the complex conjugate relations $z_i^* = w^* + \delta z_i^*$ and $w^* = \langle z_i^*\rangle$. Writing $\cos(\phi_i - \phi_j) = \mathsf{Re}\,(z_i^* z_j)$, by neglecting the terms proportional to $\delta z_i^*\,\delta z_j$ in $\hat{H}$ we arrive at the mean field Hamiltonian,

$$\hat{H}^{\rm MF} = \tfrac{1}{2}N\hat{J}(0)\,|w|^2 - \tfrac{1}{2}\hat{J}(0)\sum_{i=1}^{N}\left(w^* z_i + w z_i^*\right) - \tfrac{1}{2}H\sum_{i=1}^{N}\left(z_i^* + z_i\right) \tag{7.188}$$

It is clear that the free energy will be minimized if the mean field w breaks the $\mathsf{O}(2)$ symmetry in the same direction as the external field H, which means $w \in \mathbb{R}$ and

$$\hat{H}^{\rm MF} = \tfrac{1}{2}N\hat{J}(0)\,|w|^2 - \left(H + \hat{J}(0)\,|w|\right)\sum_{i=1}^{N}\cos\phi_i \quad . \tag{7.189}$$

The dimensionless free energy per site is then

$$f = \tfrac{1}{2}|w|^2 - \theta\log I_0\!\left(\frac{h+|w|}{\theta}\right) \quad . \tag{7.190}$$

[38] Note that the coefficient of the quartic term in ε is negative for $\theta > \frac{2}{3}$. At $\theta = \theta_{\rm c} = \frac{1}{2}$, the coefficient is positive, but for larger θ one must include higher order terms in the Landau expansion.

Differentiating with respect to $|w|$, one obtains

$$|w| \equiv m = I_1\left(\frac{h+m}{\theta}\right) \Big/ I_0\left(\frac{h+m}{\theta}\right) \quad , \tag{7.191}$$

which is the same equation as eqn. 7.184. The two mean field theories yield the same results in every detail (see §7.12).

7.8 Mean Field Theory of Fluctuations

7.8.1 Correlation and response in mean field theory

We now consider the matter of correlation and response functions within mean field theory. A correlation function is a thermodynamic average of fields at various sites, such as $\langle \sigma_i \sigma_j \rangle$ (two-point correlation function), $\langle \sigma_i \sigma_j \sigma_k \sigma_l \rangle$ (four-point correlation function), *etc.* A response function describes the influence of external fields on thermodynamic averages, such as $\partial m_i / \partial H_j$, the variation of the local magnetization $m_i = \langle \sigma_i \rangle$ at site i due to the presence of a local field H_j at site j. We shall see that there is a direct relation between correlation and response functions.

Consider the Ising model,

$$\hat{H} = -\tfrac{1}{2} \sum_{i,j=1}^{N} J_{ij}\, \sigma_i\, \sigma_j - \sum_{i=1}^{N} H_i\, \sigma_i \quad , \tag{7.192}$$

where the local magnetic field on site k is now H_k. We assume without loss of generality that the diagonal terms vanish: $J_{ii} = 0$. Now consider the partition function $Z = \mathrm{Tr}\; e^{-\beta \hat{H}}$ as a function of the temperature T and the local field values $\{H_i\}$. We have

$$\begin{aligned} \frac{\partial Z}{\partial H_i} &= \beta\, \mathrm{Tr}\left[\sigma_i\, e^{-\beta \hat{H}}\right] = \beta Z \langle \sigma_i \rangle \\ \frac{\partial^2 Z}{\partial H_i\, \partial H_j} &= \beta^2\, \mathrm{Tr}\left[\sigma_i\, \sigma_j\, e^{-\beta \hat{H}}\right] = \beta^2 Z \langle \sigma_i\, \sigma_j \rangle \quad . \end{aligned} \tag{7.193}$$

Thus,

$$\begin{aligned} m_i &= -\frac{\partial F}{\partial H_i} = \langle \sigma_i \rangle \\ \chi_{ij} &= \frac{\partial m_i}{\partial H_j} = -\frac{\partial^2 F}{\partial H_i\, \partial H_j} = \frac{1}{k_{\mathrm{B}} T} \cdot \Big\{ \langle \sigma_i\, \sigma_j \rangle - \langle \sigma_i \rangle \langle \sigma_j \rangle \Big\} \quad . \end{aligned} \tag{7.194}$$

Expressions such as $\langle \sigma_i \rangle$, $\langle \sigma_i\, \sigma_j \rangle$, *etc.* are in general called *correlation functions*. For example, we define the *spin-spin correlation function* C_{ij} as

$$C_{ij} \equiv \langle \sigma_i\, \sigma_j \rangle - \langle \sigma_i \rangle \langle \sigma_j \rangle \quad . \tag{7.195}$$

Expressions such as $\partial F/\partial H_i$ and $\partial^2 F/\partial H_i\,\partial H_j$ are called *response functions*. The above relation between correlation functions and response functions, $C_{ij} = k_{\rm B}T\,\chi_{ij}$, is valid *only for the equilibrium distribution*. In particular, this relationship is *invalid* if one uses an approximate distribution, such as the variational density matrix formalism of mean field theory.

The question then arises: within mean field theory, which is more accurate – correlation functions or response functions? A simple argument suggests that the *response functions* are more accurate representations of the real physics. To see this, let's write the variational density matrix $\varrho^{\rm var}$ as the sum of the exact equilibrium (Boltzmann) distribution $\varrho^{\rm eq} = Z^{-1}\exp(-\beta\hat{H})$ plus a deviation $\delta\varrho$:

$$\varrho^{\rm var} = \varrho^{\rm eq} + \delta\varrho \quad . \tag{7.196}$$

Then if we calculate a correlator using the variational distribution, we have

$$\langle\sigma_i\,\sigma_j\rangle_{\rm var} = {\rm Tr}\left[\varrho^{\rm var}\,\sigma_i\,\sigma_j\right] = {\rm Tr}\left[\varrho^{\rm eq}\,\sigma_i\,\sigma_j\right] + {\rm Tr}\left[\delta\varrho\,\sigma_i\,\sigma_j\right] \quad . \tag{7.197}$$

On the other hand, the free energy is given by

$$F^{\rm var} = F^{\rm eq} + \sum_{\boldsymbol{\sigma}} \frac{\partial F}{\partial\varrho_{\boldsymbol{\sigma}}}\bigg|_{\varrho^{\rm eq}} \delta\varrho_{\boldsymbol{\sigma}} + \frac{1}{2}\sum_{\boldsymbol{\sigma},\boldsymbol{\sigma}'} \frac{\partial^2 F}{\partial\varrho_{\boldsymbol{\sigma}}\partial\varrho_{\boldsymbol{\sigma}'}}\bigg|_{\varrho^{\rm eq}} \delta\varrho_{\boldsymbol{\sigma}}\,\delta\varrho_{\boldsymbol{\sigma}'} + \ldots \quad . \tag{7.198}$$

Here $\boldsymbol{\sigma}$ denotes a state of the system, *i.e.* $|\,\boldsymbol{\sigma}\,\rangle = |\,\sigma_1,\ldots,\sigma_N\,\rangle$, where every spin polarization is specified. Since the free energy is an extremum (and in fact an absolute minimum) with respect to the distribution, the second term on the RHS vanishes. Thus for the correlation functions $C^{\rm var} - C^{\rm eq} = \mathcal{O}(\delta\varrho)$ while for the free energy $F^{\rm var} - F^{\rm eq} = \mathcal{O}(\delta\varrho^2)$.

7.8.2 Calculation of the response functions

Consider the variational density matrix $\varrho(\boldsymbol{\sigma}) = \prod_{i=1}^N \varrho_i(\sigma_i)$, where

$$\varrho_i(\sigma_i) = \left(\frac{1+m_i}{2}\right)\delta_{\sigma_i,1} + \left(\frac{1-m_i}{2}\right)\delta_{\sigma_i,-1} \quad . \tag{7.199}$$

The variational energy $E = {\rm Tr}\,(\varrho\,\hat{H})$ is

$$E = -\frac{1}{2}\sum_{i,j=1}^N J_{ij}\,m_i\,m_j - \sum_{i=1}^N H_i\,m_i \tag{7.200}$$

and the entropy $S = -k_{\rm B}\,{\rm Tr}\,(\varrho\log\varrho)$ is

$$S = -k_{\rm B}\sum_{i=1}^N \left\{\left(\frac{1+m_i}{2}\right)\log\left(\frac{1+m_i}{2}\right) + \left(\frac{1-m_i}{2}\right)\log\left(\frac{1-m_i}{2}\right)\right\} \quad . \tag{7.201}$$

Setting the variation $\partial F/\partial m_i = 0$, with $F = E - TS$, we obtain the mean field equations,

$$m_i = \tanh\left(\beta J_{ij}\,m_j + \beta H_i\right) \quad , \tag{7.202}$$

where we use the summation convention: $J_{ij}\,m_j \equiv \sum_j J_{ij}\,m_j$. Suppose $T > T_{\rm c}$ and m_i is small. Then we can expand the RHS of the above mean field equations, obtaining

$$\big(\delta_{ij} - \beta J_{ij}\big)\,m_j = \beta H_i \quad . \tag{7.203}$$

Thus, the susceptibility tensor χ is the inverse of the matrix $(k_{\rm B}T\,\mathbb{1} - \mathbb{J})$:

$$\chi_{ij} = \frac{\partial m_i}{\partial H_j} = \big(k_{\rm B}T\,\mathbb{1} - \mathbb{J}\big)^{-1}_{ij} \quad , \tag{7.204}$$

where $\mathbb{1}$ is the identity. Note also that so-called *connected averages* of the kind in eqn. 7.195 vanish identically if we compute them using our variational density matrix, since all the sites are independent, hence for $i \neq j$ we have

$$\langle \sigma_i\,\sigma_j\rangle = \mathsf{Tr}\,\big(\varrho^{\rm var}\,\sigma_i\,\sigma_j\big) = \mathsf{Tr}\,\big(\varrho_i^{\rm var}\,\sigma_i\big)\,\mathsf{Tr}\,\big(\varrho_j^{\rm var}\,\sigma_j\big) = \langle\sigma_i\rangle\langle\sigma_j\rangle \quad , \tag{7.205}$$

and therefore $\chi_{ij} = 0$ if we compute the correlation functions themselves from the variational density matrix, rather than from the free energy F. As we have argued above, the latter approximation is more accurate.

Assuming $J_{ij} = J(\boldsymbol{R}_i - \boldsymbol{R}_j)$, where $\boldsymbol{R}_i$ is a Bravais lattice site, we can Fourier transform the above equation, resulting in

$$\hat{m}(\boldsymbol{q}) = \frac{\hat{H}(\boldsymbol{q})}{k_{\rm B}T - \hat{J}(\boldsymbol{q})} \equiv \hat{\chi}(\boldsymbol{q})\,\hat{H}(\boldsymbol{q}) \quad . \tag{7.206}$$

Once again, our definition of lattice Fourier transform of a function $\phi(\boldsymbol{R})$ is

$$\hat{\phi}(\boldsymbol{q}) \equiv \sum_{\boldsymbol{R}} \phi(\boldsymbol{R})\,e^{-i\boldsymbol{q}\cdot\boldsymbol{R}} \qquad , \qquad \phi(\boldsymbol{R}) = \Omega\int\limits_{\hat{\Omega}} \frac{d^dq}{(2\pi)^d}\,\hat{\phi}(\boldsymbol{q})\,e^{i\boldsymbol{q}\cdot\boldsymbol{R}} \quad , \tag{7.207}$$

where Ω is the unit cell in real space, called the *Wigner-Seitz cell*, and $\hat{\Omega}$ is the first Brillouin zone, which is the unit cell in *reciprocal space*. Similarly, we have

$$\begin{aligned}\hat{J}(\boldsymbol{q}) &= \sum_{\boldsymbol{R}} J(\boldsymbol{R})\Big(1 - i\boldsymbol{q}\cdot\boldsymbol{R} - \tfrac{1}{2}(\boldsymbol{q}\cdot\boldsymbol{R})^2 + \ldots\Big) \\ &= \hat{J}(0)\cdot\Big\{1 - q^2R_*^2 + \mathcal{O}(q^4)\Big\} \quad ,\end{aligned} \tag{7.208}$$

where

$$R_*^2 = \frac{\sum_{\boldsymbol{R}} \boldsymbol{R}^2 J(\boldsymbol{R})}{2d\sum_{\boldsymbol{R}} J(\boldsymbol{R})} \quad . \tag{7.209}$$

Here we have assumed rotational symmetry for the lattice, in which case

$$\sum_{\boldsymbol{R}} R^\mu R^\nu J(\boldsymbol{R}) = \frac{1}{d}\cdot\delta^{\mu\nu}\sum_{\boldsymbol{R}} \boldsymbol{R}^2 J(\boldsymbol{R}) \quad . \tag{7.210}$$

On cubic lattices with nearest neighbor interactions only, one has $R_* = a/\sqrt{2d}$, where a is the lattice constant and d is the dimension of space.

Thus, with the identification $k_{\rm B}T_{\rm c} = \hat{J}(0)$, we have

$$\hat{\chi}(\boldsymbol{q}) = \frac{1}{k_{\rm B}(T-T_{\rm c}) + k_{\rm B}T_{\rm c}\,R_*^2\,\boldsymbol{q}^2 + \mathcal{O}(q^4)} = \frac{1}{k_{\rm B}T_{\rm c}\,R_*^2}\cdot\frac{1}{\xi^{-2}+q^2+\mathcal{O}(q^4)} \quad , \tag{7.211}$$

where

$$\xi(T) = R_*\cdot\left(\frac{T-T_{\rm c}}{T_{\rm c}}\right)^{-1/2} \tag{7.212}$$

is the *correlation length*. With the definition $\xi(T) \propto |T-T_{\rm c}|^{-\nu}$ as $T \to T_{\rm c}$, we obtain the mean field correlation length exponent $\nu = \frac{1}{2}$. The exact result for the two-dimensional Ising model is $\nu = 1$, whereas $\nu \approx 0.6$ for the $d = 3$ Ising model. Note that $\hat{\chi}(\boldsymbol{q}=0,T)$ diverges as $(T-T_{\rm c})^{-1}$ for $T > T_{\rm c}$.

In real space, we have

$$m_i = \sum_j \chi_{ij}\,H_j \qquad , \qquad \chi_{ij} = \Omega\int\limits_{\hat{\Omega}}\frac{d^dq}{(2\pi)^d}\,\hat{\chi}(\boldsymbol{q})\,e^{i\boldsymbol{q}\cdot(\boldsymbol{R}_i-\boldsymbol{R}_j)} \quad . \tag{7.213}$$

Note that $\hat{\chi}(\boldsymbol{q})$ is properly periodic under $\boldsymbol{q} \to \boldsymbol{q}+\boldsymbol{G}$, where $\boldsymbol{G}$ is a reciprocal lattice vector, which satisfies $e^{i\boldsymbol{G}\cdot\boldsymbol{R}} = 1$ for any direct Bravais lattice vector $\boldsymbol{R}$. Indeed, we have

$$\begin{aligned}\hat{\chi}^{-1}(\boldsymbol{q}) &= k_{\rm B}T - \hat{J}(\boldsymbol{q}) \\ &= k_{\rm B}T - J\sum_{\boldsymbol{\delta}} e^{i\boldsymbol{q}\cdot\boldsymbol{\delta}} \quad ,\end{aligned} \tag{7.214}$$

where $\boldsymbol{\delta}$ is a nearest neighbor separation vector, and where in the second line we have assumed nearest neighbor interactions only. On cubic lattices in d dimensions, there are $2d$ nearest neighbor separation vectors, $\boldsymbol{\delta} = \pm a\,\hat{\mathbf{e}}_\mu$, where $\mu \in \{1,\ldots,d\}$. The real space susceptibility is then

$$\chi(\boldsymbol{R}, H=0) = \int\limits_{-\pi}^{\pi}\frac{d\theta_1}{2\pi}\cdots\int\limits_{-\pi}^{\pi}\frac{d\theta_d}{2\pi}\,\frac{e^{in_1\theta_1}\cdots e^{in_d\theta_d}}{k_{\rm B}T - (2J\cos\theta_1+\ldots+2J\cos\theta_d)} \quad , \tag{7.215}$$

where $\boldsymbol{R} = a\sum_{\mu=1}^d n_\mu\,\hat{\mathbf{e}}_\mu$ is a general direct lattice vector for the cubic Bravais lattice in d dimensions, and the $\{n_\mu\}$ are integers.

The long distance behavior was discussed in chapter 6 (see §6.4.7 on Ornstein-Zernike theory[39]). For convenience we reiterate those results:

- In $d = 1$ dimension,

$$\chi_{d=1}(x) = \left(\frac{\xi}{2k_{\rm B}T_{\rm c}R_*^2}\right)e^{-|x|/\xi} \quad . \tag{7.216}$$

[39]There is a sign difference between the particle susceptibility defined in chapter 6 and the spin susceptibility defined here. The origin of the difference is that the single particle potential v as defined was repulsive for $v > 0$, meaning the local density response δn should be negative, while in the current discussion a positive magnetic field H prefers $m > 0$.

- In $d = 2$ dimensions,

$$\chi_{d=2}(\boldsymbol{x}) = \left(\frac{1}{2\pi k_{\rm B} T_{\rm c} R_*^2}\right) K_0(|\boldsymbol{x}|/\xi) \quad . \tag{7.217}$$

- In $d > 2$, with $r \to \infty$ and ξ fixed,

$$\chi_d^{\rm OZ}(\boldsymbol{r}) \simeq C_d \cdot \frac{\xi^{(3-d)/2}}{k_{\rm B} T_{\rm c}\, R_*^2} \cdot \frac{e^{-r/\xi}}{r^{(d-1)/2}} \cdot \left\{1 + \mathcal{O}\left(\frac{d-3}{r/\xi}\right)\right\} \quad , \tag{7.218}$$

  where the C_d are dimensionless constants.

- In $d > 2$, with $\xi \to \infty$ and r fixed (*i.e.* $T \to T_{\rm c}$ at fixed separation $\boldsymbol{r}$),

$$\chi_d(\boldsymbol{r}) \simeq \frac{C_d'}{k_{\rm B} T_{\rm c} R_*^2} \cdot \frac{e^{-r/\xi}}{r^{d-2}} \cdot \left\{1 + \mathcal{O}\left(\frac{d-3}{r/\xi}\right)\right\} \quad . \tag{7.219}$$

Close to the critical point the spatial dependence of the two-point correlation $C(\boldsymbol{r}, T) = k_{\rm B} T\, \chi(\boldsymbol{r}, T)$ is given by

$$C(\boldsymbol{r}, T) = r^{-(d-2+\eta)}\, \phi\big(r/\xi(T)\big) \quad , \tag{7.220}$$

where η is the *anomalous critical exponent* and $\phi(r/\xi)$ is a *scaling function*. The condition $T \approx T_{\rm c}$ means that $\xi(T) \gg a$, where a is a microscopic length, such as a lattice constant[40]. Thus, we've encountered in this section two additional critical exponents, the anomalous exponent η and the correlation length exponent ν, which we first met in §7.4.2, whose mean field values are $\eta = 0$ and $\nu = \frac{1}{2}$.

7.8.3 Beyond the two-state Ising model

Consider a general spin model, and a variational density matrix $\varrho^{\rm var}$ which is a product of single site density matrices:

$$\varrho^{\rm var}\big[\{\boldsymbol{S}_i\}\big] = \prod_{i=1}^N \varrho_i(\boldsymbol{S}_i) \quad , \tag{7.221}$$

where $\boldsymbol{m}_i = {\rm Tr}\left(\varrho^{\rm var} \boldsymbol{S}_i\right)$ is the local magnetization and $\boldsymbol{S}_i$, which may be a scalar (*e.g.*, σ_i in the Ising model previously discussed), is the local spin operator. Note that $\varrho_i(\boldsymbol{S}_i)$ depends parametrically on the variational parameter(s) $\boldsymbol{m}_i$ (*e.g.*, as in eqn. 7.143). Let the Hamiltonian be

$$\hat{H} = -\frac{1}{2} \sum_{i,j=1}^N J_{i,j}^{\mu\nu}\, S_i^\mu\, S_j^\nu + \sum_{i=1}^N \hat{h}_i(\boldsymbol{S}_i) - \sum_{i=1}^N \boldsymbol{H}_i \cdot \boldsymbol{S}_i \quad , \tag{7.222}$$

with an implied sum over repeated Greek indices μ and ν. Here we separate the external applied fields $\boldsymbol{H}_i$ from the local Hamiltonians $\hat{h}_i(\boldsymbol{S}_i)$, which are presumed time-reversal symmetric, *i.e.*

$${\rm Tr}\left[\boldsymbol{S} \exp(-\beta \hat{h}(\boldsymbol{S})\right] = 0 \quad . \tag{7.223}$$

[40] The scaling functions on the high and low temperature sides of the transition may be different, and are denoted as $\phi_\pm(r/\xi)$, respectively.

The variational free energy is

$$F^{\rm var} = -\frac{1}{2}\sum_{i,j=1}^{N} J_{ij}^{\mu\nu}\, m_i^\mu\, m_j^\nu + \sum_{i=1}^{N}\varphi(\boldsymbol{m}_i, T) - \sum_{i=1}^{N} H_i^\mu\, m_i^\mu \quad , \tag{7.224}$$

where the single site free energy $\varphi(\boldsymbol{m}_i, T)$ in the absence of an external field is given by

$$\varphi(\boldsymbol{m}_i, T) = \mathsf{Tr}\Big[\varrho_i(\boldsymbol{S})\,\hat{h}(\boldsymbol{S})\Big] + k_{\rm B}T\,\mathsf{Tr}\Big[\varrho_i(\boldsymbol{S})\log\varrho_i(\boldsymbol{S})\Big] \quad , \tag{7.225}$$

where $\hat{h}(\boldsymbol{S})$ is the single site Hamiltonian. We then have

$$\frac{\partial F^{\rm var}}{\partial m_i^\mu} = -\sum_j J_{ij}^{\mu\nu}\, m_j^\nu - H_i^\mu + \frac{\partial\varphi(\boldsymbol{m}_i, T)}{\partial m_i^\mu} \quad . \tag{7.226}$$

For the noninteracting system, we have $J_{ij}^{\mu\nu} = 0$, and the weak field response must be linear. In this limit we may write $m_i^\mu = \chi^0_{\mu\nu}(T)\, H_i^\nu + \mathcal{O}(\boldsymbol{H}_i^3)$, and we conclude

$$\frac{\partial\varphi(\boldsymbol{m}_i, T)}{\partial m_i^\mu} = \big[\chi^0(T)\big]^{-1}_{\mu\nu}\, m_i^\nu + \mathcal{O}\big(m_i^3\big) \quad . \tag{7.227}$$

Note that this entails the following expansion for the single site free energy:

$$\varphi(\boldsymbol{m}_i, T) = \varphi(\boldsymbol{0}, T) + \tfrac{1}{2}\big[\chi^0(T)\big]^{-1}_{\mu\nu} m_i^\mu\, m_i^\nu + \mathcal{O}(m^4) \quad . \tag{7.228}$$

Finally, we restore the interaction term and extremize $F^{\rm var}$ by setting $\partial F^{\rm var}/\partial m_i^\mu = 0$. To linear order, then,

$$m_i^\mu = \chi^0_{\mu\nu}(T)\left(H_i^\nu + \sum_j J_{ij}^{\nu\lambda}\, m_j^\lambda\right) \quad . \tag{7.229}$$

Typically the local susceptibility is a scalar in the internal spin space, *i.e.* $\chi^0_{\mu\nu}(T) = \chi^0(T)\,\delta_{\mu\nu}$, in which case we obtain

$$\big(\delta^{\mu\nu}\,\delta_{ij} - \chi^0(T)\, J_{ij}^{\mu\nu}\big)\, m_j^\nu = \chi^0(T)\, H_i^\mu \quad . \tag{7.230}$$

In Fourier space, then,

$$\hat{\chi}_{\mu\nu}(\boldsymbol{q}, T) = \chi^0(T)\left(\mathbb{1} - \chi^0(T)\,\hat{\mathbb{J}}(\boldsymbol{q})\right)^{-1}_{\mu\nu} \quad , \tag{7.231}$$

where $\hat{\mathbb{J}}(\boldsymbol{q})$ is the matrix whose elements are $\hat{J}^{\mu\nu}(\boldsymbol{q})$. If $\hat{J}^{\mu\nu}(\boldsymbol{q}) = \hat{J}(\boldsymbol{q})\,\delta^{\mu\nu}$, then the susceptibility is isotropic in spin space, with

$$\hat{\chi}(\boldsymbol{q}, T) = \frac{1}{\big[\chi^0(T)\big]^{-1} - \hat{J}(\boldsymbol{q})} \quad . \tag{7.232}$$

Consider now the following examples:

(i) Spin-S with $\mathbb{Z}_2$ symmetry and $\hat{h}(\hat{S}) = 0$: Write $\varrho_i(S_i) = \zeta^{-1}\,\exp(\mathfrak{h}S_i/k_{\rm B}T)$, where $\mathfrak{h}$ acts as a local field. The normalization is[41]

$$\zeta(\mathfrak{h}, T) = \mathsf{Tr}\, e^{\mathfrak{h}\hat{S}/k_{\rm B}T} = \sum_{k=-S}^{S} e^{k\mathfrak{h}/k_{\rm B}T} = \frac{\sinh\big[(S+\frac{1}{2})\,\mathfrak{h}/k_{\rm B}T\big]}{\sinh\big[\mathfrak{h}/2k_{\rm B}T\big]} \quad . \tag{7.233}$$

[41] Here we distinguish the spin 'operator' $\hat{S}$ from its maximal value S.

The local magnetization m_i is then given by $m_i = m(\mathfrak{h}_i, T) = \mathsf{Tr}(\varrho_i S_i)$. The relation between m, $\mathfrak{h}$, and T is then given by

$$\begin{aligned} m = \langle \hat{S} \rangle &= k_{\rm B} T \, \frac{\partial \log \zeta}{\partial \mathfrak{h}} = (S + \tfrac{1}{2}) \, \mathrm{ctnh}\big[(S + \tfrac{1}{2}) \, \mathfrak{h}/k_{\rm B}T\big] - \tfrac{1}{2} \, \mathrm{ctnh}\big[\mathfrak{h}/2k_{\rm B}T\big] \\ &= \frac{S(S+1)}{3k_{\rm B}T} \, \mathfrak{h} + \mathcal{O}(\mathfrak{h}^3) \end{aligned} \tag{7.234}$$

at each site. We identify the single-site susceptibility as

$$\chi^0(T) = \frac{S(S+1)}{3k_{\rm B}T} \quad , \tag{7.235}$$

which is the Curie result. The free-field single-site free energy (see eqn. 7.225) is then

$$\varphi(m_i, T) = k_{\rm B}T \, \mathsf{Tr} \left(\varrho_i \log \varrho_i \right) = \mathfrak{h}_i \, m_i - k_{\rm B}T \log \zeta_i \quad , \tag{7.236}$$

whence for each i we have

$$\frac{\partial \varphi}{\partial m} = \mathfrak{h} + m \, \frac{\partial \mathfrak{h}}{\partial m} - \overbrace{k_{\rm B}T \, \frac{\partial \log \zeta}{\partial \mathfrak{h}}}^{= m} \, \frac{\partial \mathfrak{h}}{\partial m} = \mathfrak{h} \quad \Rightarrow \quad \varphi(m,T) = -k_{\rm B}T \log(2S+1) \frac{m^2}{2\chi^0(T)} + \mathcal{O}(m^4) \tag{7.237}$$

and $m = \chi^0(T) \, \mathfrak{h}$.

(ii) Spin-S with $\mathbb{Z}_2$ symmetry and $\hat{h}(\hat{S}) = K\hat{S}^2$: We take $\varrho_i(S_i) = \zeta^{-1} \exp(\beta \mathfrak{h} S_i - \beta K S_i^2)$, and one obtains the partition function

$$\zeta(\mathfrak{h}, T) = \sum_{j=-S}^{S} e^{\mathfrak{h} j / k_{\rm B}T} e^{-Kj^2/k_{\rm B}T} \quad . \tag{7.238}$$

The single site susceptibility is then

$$\chi^0(T) = k_{\rm B}T \, \frac{\partial^2 \log \zeta}{\partial \mathfrak{h}^2} \bigg|_{\mathfrak{h}=0} = \frac{1}{k_{\rm B}T} \cdot \frac{\sum_{j=-S}^{S} j^2 \, e^{-Kj^2/k_{\rm B}T}}{\sum_{l=-S}^{S} e^{-Kl^2/k_{\rm B}T}} \quad . \tag{7.239}$$

When $K \to 0$ we recover $\chi^0(T) = S(S+1)/3k_{\rm B}T$. In the large K limit we obtain

$$\chi^0(T) = \begin{cases} \frac{2}{k_{\rm B}T} \, e^{-K/k_{\rm B}T} + \mathcal{O}(e^{-2K/k_{\rm B}T}) & \text{for } S \in \mathbb{Z} \\ \frac{1}{4\,k_{\rm B}T} & \text{for } S \in \mathbb{Z} + \frac{1}{2} \quad . \end{cases} \tag{7.240}$$

Thus for $K \to \infty$ we effectively recover the $S = 0$ and $S = \frac{1}{2}$ cases for $S \in \mathbb{Z}$ and $S \in \mathbb{Z} + \frac{1}{2}$, respectively. *What happens for $K \to -\infty$?*

(iii) Classical spin $\boldsymbol{S} = S\hat{\boldsymbol{n}}$ with $\hat{h}(\boldsymbol{S}) = 0$ and $\hat{\boldsymbol{n}}$ an N-component unit vector: We take the single site density matrix to be $\varrho_i(\boldsymbol{S}_i) = z^{-1}\exp(\boldsymbol{\mathfrak{h}}_i \cdot \boldsymbol{S}_i/k_{\rm B}T)$. The single site field-free partition function is then

$$\zeta(\boldsymbol{\mathfrak{h}}, T) = \int \frac{d\hat{\boldsymbol{n}}}{\Omega_N}\ \exp(\boldsymbol{\mathfrak{h}}\cdot\boldsymbol{S}/k_{\rm B}T) = 1 + \frac{S^2\boldsymbol{\mathfrak{h}}^2}{2N(k_{\rm B}T)^2} + \mathcal{O}(\boldsymbol{\mathfrak{h}}^4) \quad , \tag{7.241}$$

with $\Omega_N = 2\pi^{N/2}/\Gamma(N/2)$ the total solid angle, and therefore

$$\boldsymbol{m} = k_{\rm B}T\,\frac{\partial\log\zeta}{\partial\boldsymbol{\mathfrak{h}}} = \frac{S^2\boldsymbol{\mathfrak{h}}}{Nk_{\rm B}T} + \mathcal{O}(\boldsymbol{\mathfrak{h}}^3) \quad , \tag{7.242}$$

from which we read off $\chi^0(T) = S^2/Nk_{\rm B}T$. Note that this agrees in the classical ($S \to \infty$) limit, for $N = 3$, with our previous result.

7.8.4 Magnetic ordering

Recall our mean field expression for the susceptibility $\hat{\chi}_{\mu\nu}(\boldsymbol{q}, T)$,

$$\hat{\chi}_{\mu\nu}(\boldsymbol{q}, T) = \chi^0(T)\,\Big(\mathbb{1} - \chi^0(T)\,\hat{\mathbb{J}}(\boldsymbol{q})\Big)^{-1}_{\mu\nu} \quad , \tag{7.243}$$

where $\chi^0(T)$ is the local susceptibility for the noninteracting model with all couplings $J_{ij} = 0$. Physically, $\chi^0(T) \to 0$ as $T \to \infty$ and therefore $\hat{\chi}_{\mu\nu}(\boldsymbol{q}, T) \sim \chi^0(T)\,\delta_{\mu\nu}$ at high temperatures.

Consider the case where there is isotropy in spin space. The susceptibility $\chi(\boldsymbol{q}, T)$ then diverges when $\chi^0(T)\hat{J}(\boldsymbol{q}) = 1$, where $\chi^0(T)$ is the local susceptibility. As we know, such a divergence heralds the onset of a *phase transition* where there is a *spontaneous magnetization* in the ordered (*i.e.* low temperature) phase. Typically this happens at a particular wavevector $\boldsymbol{Q}$, or a set of symmetry related wavevectors $\{\boldsymbol{Q}_1, \boldsymbol{Q}_2, \ldots\}$. The ordering wavevector is that value of $\boldsymbol{q}$ which results in a *maximum* of $\hat{J}(\boldsymbol{q})$: $\max_{\boldsymbol{q}}\big\{\hat{J}(\boldsymbol{q})\big\} = \hat{J}(\boldsymbol{Q})$. The susceptibility, for isotropic systems, can be written

$$\hat{\chi}(\boldsymbol{q}) = \frac{\chi^0(T)}{\big[1 - \chi^0(T)\,\hat{J}(\boldsymbol{Q})\big] + \chi^0(T)\big[\hat{J}(\boldsymbol{Q}) - \hat{J}(\boldsymbol{q})\big]} \quad . \tag{7.244}$$

Assuming a continuous phase transition that is not pre-empted by a first-order one, the critical temperature $T_{\rm c}$ is determined by the relation

$$\chi^0(T_{\rm c})\,\hat{J}(\boldsymbol{Q}) = 1. \tag{7.245}$$

Expanding about $T = T_{\rm c}$ and about $\boldsymbol{q} = \boldsymbol{Q}$, where

$$\hat{J}(\boldsymbol{q}) = \hat{J}(\boldsymbol{Q})\Big\{1 - (\boldsymbol{q}-\boldsymbol{Q})^2 R_*^2 + \ldots\Big\} \quad , \tag{7.246}$$

we have

$$\hat{\chi}(\boldsymbol{q}) \approx \frac{\chi^0(T_{\rm c})/R_*^2}{\xi^{-2}(T) + (\boldsymbol{q}-\boldsymbol{Q})^2} \quad , \tag{7.247}$$

where

$$\xi^{-2}(T) = -\frac{\chi^{0\prime}(T_{\rm c})}{\chi^0(T_{\rm c})}\cdot R_*^{-2}\cdot(T - T_{\rm c}) \quad . \tag{7.248}$$

Thus, $\xi(T) \propto (T - T_{\rm c})^{-1/2}$. The real space susceptibility $\chi(\boldsymbol{R}, T)$ oscillates with wavevector $\boldsymbol{Q}$ and decays on the scale of the correlation length $\xi(T)$.

- *Ferromagnet:* $J_{ij} = +J > 0$ if i and j are nearest neighbors; otherwise $J_{ij} = 0$. On a hypercubic lattice (d dimensions, $2d$ nearest neighbor vectors $\boldsymbol{\delta} = \pm a\,\hat{\mathbf{e}}_\nu$), we then have

$$\hat{J}(\boldsymbol{q}) = J \sum_{\boldsymbol{\delta}} e^{-i\boldsymbol{q}\cdot\boldsymbol{\delta}} = 2J\big\{\cos(q_1 a) + \cos(q_2 a) + \ldots + \cos(q_d a)\big\} \quad . \tag{7.249}$$

  The ordering wavevector is $\boldsymbol{Q} = 0$, and $\hat{J}(\boldsymbol{Q}) = 2dJ$. For the spin-$S$ Heisenberg model, then, $k_{\rm B}T_{\rm C} = \frac{2}{3} d\, S(S+1)\, J$, and the susceptibility is

$$\hat{\chi}(\boldsymbol{q}, T) = \frac{\frac{1}{3}S(S+1)/k_{\rm B}}{(T - T_{\rm C}) + T_{\rm C}\, d^{-1} \sum_{\nu=1}^{d} \big[1 - \cos(q_\nu a)\big]} \quad . \tag{7.250}$$

  The uniform susceptibility $\chi = \hat{\chi}(\boldsymbol{q} = 0)$ is then

$$\chi(T) = \frac{S(S+1)}{3k_{\rm B}(T - T_{\rm C})} \quad , \tag{7.251}$$

  where $T_{\rm C}$ is the *Curie temperature*.

  Ferromagnetic insulators: ferrites, EuO, TDAE-C_{60}.

- *Antiferromagnet:* $J_{ij} = -J < 0$ if i and j are nearest neighbors; otherwise $J_{ij} = 0$. On a hypercubic lattice (d dimensions, $2d$ nearest neighbors), we then have

$$\hat{J}(\boldsymbol{q}) = -J \sum_{\boldsymbol{\delta}} e^{-i\boldsymbol{q}\cdot\boldsymbol{\delta}} = -2J\big\{\cos(q_1 a) + \cos(q_2 a) + \ldots + \cos(q_d a)\big\} \quad . \tag{7.252}$$

  The ordering wavevector is $\boldsymbol{Q} = (\pi/a, \ldots, \pi/a)$, at the zone corner, where $\hat{J}(\boldsymbol{Q}) = 2dJ$. For the spin-$S$ Heisenberg model, then, $k_{\rm B}T_{\rm N} = \frac{2}{3} d\, S(S+1) J$, and the susceptibility is

$$\hat{\chi}(\boldsymbol{q}, T) = \frac{S(S+1)/3k_{\rm B}}{(T - T_{\rm N}) + T_{\rm N}\, d^{-1} \sum_{\nu=1}^{d} \big[1 + \cos(q_\nu a)\big]} \quad . \tag{7.253}$$

  The uniform susceptibility $\chi_{\rm unif}(T) \equiv \hat{\chi}(\boldsymbol{q} = 0, T)$ is then

$$\chi(\boldsymbol{q} = 0, T) = \frac{S(S+1)}{3k_{\rm B}(T + T_{\rm N})} \quad , \tag{7.254}$$

  where $T_{\rm N}$ is the *Néel temperature*. Note that $\chi(\boldsymbol{q} = 0, T)$ *does not diverge*. Indeed, plotting the inverse uniform susceptibility $\chi^{-1}(\boldsymbol{q} = 0, T)$ *versus* T, one obtains an intercept along the T-axis at $T = -T_{\rm N}$. This is one crude way of estimating the Néel temperature. What *does* diverge is the *staggered susceptibility* $\chi_{\rm stag}(T) \equiv \hat{\chi}(\boldsymbol{Q}, T)$, *i.e.* the susceptibility at the ordering wavevector:

$$\chi(\boldsymbol{Q}, T) = \frac{S(S+1)}{3k_{\rm B}(T - T_{\rm N})} \quad . \tag{7.255}$$

  Antiferromagnetic insulators: MnO, CoO, FeO, NiO, La_2CuO_4.

- *Frustrated Antiferromagnet:* On the triangular lattice, the antiferromagnetic state is frustrated. What does mean field theory predict? We begin by writing primitive direct lattice vectors $\{\boldsymbol{a}_1, \boldsymbol{a}_2\}$ and primitive reciprocal lattice vectors $\{\boldsymbol{b}_1, \boldsymbol{b}_2\}$, *viz.*

$$\begin{aligned} \boldsymbol{a}_1 &= a\,(1,0) & \boldsymbol{b}_1 &= \frac{4\pi}{a\sqrt{3}}\,\big(\tfrac{\sqrt{3}}{2}, -\tfrac{1}{2}\big) \\ \boldsymbol{a}_2 &= a\,\big(\tfrac{1}{2}, \tfrac{\sqrt{3}}{2}\big) & \boldsymbol{b}_2 &= \frac{4\pi}{a\sqrt{3}}\,(0,1) \quad , \end{aligned} \tag{7.256}$$

where a is the lattice constant. Note that $\boldsymbol{a}_i \cdot \boldsymbol{b}_j = 2\pi\,\delta_{ij}$: The six nearest neighbor vectors are then

$$\boldsymbol{\delta} \in \Big\{ \boldsymbol{a}_1, \boldsymbol{a}_2, \boldsymbol{a}_2 - \boldsymbol{a}_1, -\boldsymbol{a}_1, -\boldsymbol{a}_2, \boldsymbol{a}_1 - \boldsymbol{a}_2 \Big\} \quad , \tag{7.257}$$

and writing $\boldsymbol{q} \equiv \theta_1 \boldsymbol{b}_1/2\pi + \theta_2\,\boldsymbol{b}_2/2\pi$, we find

$$\hat{J}(\boldsymbol{q}) = -2J\big\{\cos(\theta_1) + \cos(\theta_2) + \cos(\theta_1 - \theta_2)\big\} \quad . \tag{7.258}$$

We suspect that this should be maximized somewhere along the perimeter of the Brillouin zone. The face center lies at $(\theta_1, \theta_2) = 2\pi(\frac{1}{2}, \frac{1}{2})$, where $\hat{J}(\boldsymbol{q}) = +2J$. However, an even greater value is obtained at either of the two inequivalent zone corners, $(\theta_1, \theta_2) = 2\pi(\frac{2}{3}, \frac{1}{3})$ and $(\theta_1, \theta_2) = 2\pi(\frac{1}{3}, \frac{2}{3})$, where $\hat{J}(\boldsymbol{q}) = +3J$. Each of these corresponds to a *tripartite* division of the triangular lattice into three $\sqrt{3} \times \sqrt{3}$ triangular sublattices.

- *Helimagnet:* Consider a cubic lattice system with mixed ferromagnetic and antiferromagnetic interactions:

$$J_{ij} = \begin{cases} +J_1 > 0 & \text{6 nearest neighbors} \\ -J_2 < 0 & \text{12 next-nearest neighbors} \\ 0 & \text{otherwise} \quad . \end{cases} \tag{7.259}$$

Then

$$\begin{aligned} \hat{J}(\boldsymbol{q}) = 2J_1\big[\,&\cos(q_x a) + \cos(q_y a) + \cos(q_z a)\big] \\ &- 4J_2\big[\,\cos(q_x a)\cos(q_y a) + \cos(q_x a)\cos(q_z a) + \cos(q_y a)\cos(q_z a)\big] \quad . \end{aligned} \tag{7.260}$$

The ordering wavevector is then

$$\boldsymbol{Q} = \begin{cases} a^{-1}\cos^{-1}(J_1/4J_2)\,(\pm\hat{\boldsymbol{x}} \pm \hat{\boldsymbol{y}} \pm \hat{\boldsymbol{z}}) & \text{if } J_1 < 4J_2 \\ 0 & \text{if } J_1 \geq 4J_2 \quad . \end{cases} \tag{7.261}$$

Thus, for $J_1 < 4J_2$ the order is *incommensurate* with the lattice. Note also that in this incommensurate regime there are eight symmetry-related ordering wavevectors $\boldsymbol{Q} = Q_0\,(\pm\hat{\boldsymbol{x}} \pm \hat{\boldsymbol{y}} \pm \hat{\boldsymbol{z}})/\sqrt{3}$, with $Q_0 = \sqrt{3}\,a^{-1}\cos^{-1}(J_1/4J_2)$, which point from the center of a cube toward each of its eight vertices. The maximum value of $\hat{J}(\boldsymbol{q})$ is

$$\hat{J}(\boldsymbol{Q}) = \begin{cases} 3J_1^2/4J_2 & \text{if } J_1 < 4J_2 \\ 6(J_1 - 2J_2) & \text{if } J_1 \geq 4J_2 \quad , \end{cases} \tag{7.262}$$

hence incommensurate order sets in at $T_{\rm I} = S(S+1)J_1^2/4k_{\rm B}J_2$. The uniform susceptibility is

$$\hat{\chi}(\boldsymbol{q}=0,T) = \frac{S(S+1)/3k_{\rm B}}{T - 8\,T_{\rm I}\,\frac{J_2}{J_1}\Big(1-\frac{2J_2}{J_1}\Big)} \quad . \tag{7.263}$$

Thus,

$$\chi(\boldsymbol{q}=0,T) \simeq \begin{cases} \mathcal{C}/(T+T^*) \quad , \qquad 0 < J_1 < 2J_2 \text{ (AFM-like)} \\ \\ \mathcal{C}/(T-T^*) \quad , \quad 2J_2 < J_1 < 4J_2 \text{ (FM-like)} \quad . \end{cases} \tag{7.264}$$

7.9 Global Symmetries

7.9.1 Symmetries and symmetry groups

Interacting systems can be broadly classified according to their *global symmetry group*. Consider the following five examples:

$$\hat{H}_{\rm Ising} = -\frac{1}{2}\sum_{i,j=1}^{N} J_{ij}\,\sigma_i\,\sigma_j \quad , \quad \sigma_i \in \{-1,+1\} \quad , \tag{7.265}$$

which is the Ising model,

$$\hat{H}_{p-{\rm clock}} = -\frac{1}{2}\sum_{i,j=1}^{N} J_{ij}\,\cos\left(\frac{2\pi(l_i-l_j)}{p}\right) \quad , \quad l_i \in \{1,2,\ldots,p\} \quad , \tag{7.266}$$

which is the p-state clock model,

$$\hat{H}_{q-{\rm Potts}} = -\frac{1}{2}\sum_{i,j=1}^{N} J_{ij}\,\delta_{\sigma_i,\sigma_j} \quad , \quad \sigma_i \in \{1,2,\ldots,q\} \quad , \tag{7.267}$$

which is the q-state Potts model,

$$\hat{H}_{XY} = -\frac{1}{2}\sum_{i,j=1}^{N} J_{ij}\,\cos(\phi_i-\phi_j) \quad , \quad \phi_i \in \big[0,2\pi\big] \quad , \tag{7.268}$$

which is the XY model (also called the $\mathsf{O}(2)$ model), and

$$\hat{H}_{\mathsf{O}(p)} = -\frac{1}{2}\sum_{i,j=1}^{N} J_{ij}\,\hat{\boldsymbol{n}}_i\cdot\hat{\boldsymbol{n}}_j \quad , \quad \hat{\boldsymbol{n}}_i \in S^{p-1} \quad , \tag{7.269}$$

which is the $\mathsf{O}(p)$ model.

The Ising Hamiltonian is left invariant by the global symmetry group $\mathbb{Z}_2$. This group has two elements, which we write as E and r. E is the identity operation, *i.e.* $E\,\sigma_i = \sigma_i$ for all i. The r operation reverses the

spins: $r\,\sigma_i = -\sigma_i$. By simultaneously reversing *all* the spins $\sigma_i \to -\sigma_i$, the interactions remain invariant. Note that $r^2 = E$.

The degrees of freedom of the *p-state clock model* are integer variables l_i each of which ranges from 1 to p. The Hamiltonian is invariant under the discrete group D_p which is the *dihedral group* of symmetry operations of a p-gon. D_p has $2p$ elements which include p rotations r^j where r is a counterclockwise rotation through an angle $2\pi/p$ and $j \in \{0, \ldots, p-1\}$ as well as the products of each rotation with the reflection σ with respect to any fixed symmetry axis of the p-gon.

We've already met up with the q-state Potts model, where each site supports a 'spin' σ_i which can be in any of q possible states, which we may label by integers $\{1\,,\,\ldots\,,\,q\}$. The energy of two interacting sites i and j is $-J_{ij}$ if $\sigma_i = \sigma_j$ and zero otherwise. This energy function is invariant under global operations of the *symmetric group on q characters*, S_q , which is the group of permutations of the sequence $\{1\,,\,2\,,\,3\,,\,\ldots\,,\,q\}$. The group S_q has $q!$ elements. Note the difference between a $\mathbb{Z}_q$ symmetry and an S_q symmetry. In the former case, the Hamiltonian is invariant only under the q-element cyclic permutations, *e.g.*

$$r \equiv \begin{pmatrix} 1\,2\,\cdots\,q-1\,q \\ 2\,3\,\cdots\quad q\quad 1 \end{pmatrix} \tag{7.270}$$

and its powers r^l with $l = 0, \ldots, q-1$.

All these models – the Ising, p-state clock, and q-state Potts models – possess a global symmetry group which is *discrete*. That is, each of the symmetry groups $\mathbb{Z}_2$, $\mathbb{Z}_p$, and S_q is a discrete group, with a finite number of elements. The XY Hamiltonian $\hat{H}_{XY}$ on the other hand is invariant under a *continuous* group of transformations $\phi_i \to \phi_i + \alpha$, where ϕ_i is the angle variable on site i. More to the point, we could write the interaction term $\cos(\phi_i - \phi_j)$ as $\frac{1}{2}\big(z_i^* z_j + z_i z_j^*\big)$, where $z_i = e^{i\phi_i}$ is a phase which lives on the unit circle, and z_i^* is the complex conjugate of z_i. The model is then invariant under the global transformation $z_i \to e^{i\alpha} z_i$. The phases $e^{i\alpha}$ form a group under multiplication, called $\mathsf{U}(1)$, which is the same as $\mathsf{SO}(2)$. Equivalently, we could write the interaction as $\hat{\boldsymbol{n}}_i \cdot \hat{\boldsymbol{n}}_j$, where $\hat{\boldsymbol{n}}_i = (\cos\phi_i\,,\,\sin\phi_i)$, which explains the $\mathsf{O}(2) = \mathsf{SO}(2) \rtimes \mathbb{Z}_2$ symmetry, since the symmetry operations are global rotations in the plane plus reflections, which is to say the two-dimensional orthogonal group. This last representation generalizes nicely to unit vectors in p dimensions, where $\hat{\boldsymbol{n}} = (n^1\,,\,n^2\,,\,\ldots\,,\,n^p)$. with $\hat{\boldsymbol{n}}^2 = 1$. The dot product $\hat{\boldsymbol{n}}_i \cdot \hat{\boldsymbol{n}}_j$ is then invariant under global rotations in this n-dimensional space, which is the group $\mathsf{O}(p)$.

7.9.2 Domain walls and lower critical dimension

Depending on whether the global symmetry group G of a model is discrete or continuous, there exists a *lower critical dimension* d_ℓ at or below which no G-breaking phase transition may take place at finite temperature. That is, for $d \le d_\ell$, the critical temperature is $T_{\rm c} = 0$. Owing to its neglect of fluctuations, mean field theory generally *overestimates* the value of $T_{\rm c}$ because it overestimates the stability of the ordered phase[42]. Indeed, there are many examples where mean field theory predicts a finite $T_{\rm c}$ when the actual critical temperature is $T_{\rm c} = 0$. This happens whenever $d \le d_\ell$.

[42]It is a simple matter to concoct models for which the mean field transition temperature *underestimates* the actual critical temperature. Consider for example an Ising model with interaction $u(\sigma, \sigma') = -\epsilon^{-1}\log(1 + \epsilon\sigma\sigma')$, where the spins take values $\sigma, \sigma' = \pm 1$, and where $0 < \epsilon < 1$. If we write $\sigma = \langle\sigma\rangle + \delta\sigma$ at each site and neglect terms quadratic in fluctuations, the resulting mean field Hamiltonian is equivalent to a set of decoupled spins in

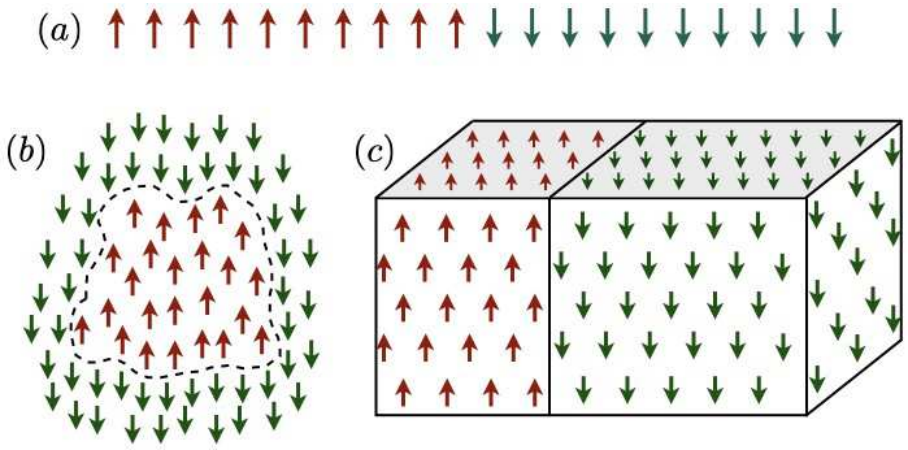


Figure 7.23: Domain walls in the (a) $d = 1$, (b) $d = 2$, and (c) $d = 3$ Ising model.

Let's test the stability of the ordered (ferromagnetic) state of the one-dimensional Ising model at low temperatures. We consider order-destroying *domain wall* excitations which interpolate between regions of degenerate, symmetry-related ordered phase, *i.e.* $\uparrow\uparrow\uparrow\uparrow\uparrow$ and $\downarrow\downarrow\downarrow\downarrow\downarrow$[43]. For a system with a discrete symmetry at low temperatures, the domain wall is abrupt, on the scale of a single lattice spacing. If the exchange energy is J, then the energy of a single domain wall is $2J$, since a link of energy $-J$ is replaced with one of energy $+J$. However, in a system of length L (with *anti*periodic boundary conditions), there are L possible locations for the domain wall, hence its entropy is $k_{\rm B} \log L$. For a system with M domain walls, the free energy is[44]

$$\begin{aligned} F &= 2MJ - k_{\rm B}T \log \binom{L}{M} \\ &= L \cdot \left\{ 2Jx + k_{\rm B}T \Big[x \log x + (1-x) \log(1-x) \Big] \right\} \quad , \end{aligned} \tag{7.271}$$

where $x = M/L$ is the density of domain walls, and where we have used Stirling's approximation for $k!$ when k is large. Extremizing with respect to x, we find

$$\frac{x}{1-x} = e^{-2J/k_{\rm B}T} \qquad \Longrightarrow \qquad x = \frac{1}{e^{2J/k_{\rm B}T} + 1} \quad . \tag{7.272}$$

The average distance between domain walls is x^{-1}, which is finite for finite T. Thus, the thermodynamic state of the system is *disordered*, with no net average magnetization.

Consider next an Ising domain wall in d dimensions. Let the linear dimension of the system be $L \cdot a$, where L is a real number and a is the lattice constant. Then the energy of a single domain wall which

an external field $h = zm/(1+\epsilon m^2)$. The mean field transition temperature is $T_{\rm c}^{\rm MF} = z$, the lattice coordination number, independent of ϵ. On the other hand, we may also write $u(\sigma,\sigma') = u_\epsilon - J_\epsilon\,\sigma\sigma'$, where $u_\epsilon = -\log(1-\epsilon^2)/2\epsilon$ and $J_\epsilon = \epsilon^{-1}\tanh^{-1}(\epsilon)$. On the square lattice, where $z = 4$, one has the exact result $T_{\rm c}(\epsilon) = 2J_\epsilon/\sinh^{-1}(1)$, which diverges as $\epsilon \to 1$, while $T_{\rm c}^{\rm MF} = 4$ remains finite. For $\epsilon > 0.9265$, one has $T_{\rm c}(\epsilon) > T_{\rm c}^{\rm MF}$.

[43]Here and below we reiterate some material from §6.2.3.

[44]With periodic boundary conditions, M must be even. With antiperiodic boundary conditions, M must be odd. The thermodynamic conclusions are the same, however.

partitions the entire system is $2J \cdot L^{d-1}$. The domain wall entropy is difficult to compute, because the wall can fluctuate significantly, but for a single domain wall we have $S \gtrsim k_{\rm B} \log L$. Thus, the free energy $F = 2JL^{d-1} - k_{\rm B}T \log L$ is dominated by the energy term if $d > 1$, suggesting that the system *may* be ordered. We can do a slightly better job in $d = 2$ by writing

$$Z \approx \exp\left(L^d \sum_P N_P \, e^{-2PJ/k_{\rm B}T} \right) \quad , \tag{7.273}$$

where the sum is over all closed loops of perimeter P, and N_P is the number of such loops. An example of such a loop circumscribing a domain is depicted in the panel (b) of fig. 7.23. It turns out that

$$N_P \simeq \kappa^P P^{-\theta} \cdot \Big\{ 1 + \mathcal{O}(P^{-1}) \Big\} \quad , \tag{7.274}$$

where $\kappa < z - 1$ with z the lattice coordination number, and θ is some exponent. We can understand the κ^P factor in the following way. At each step along the perimeter of the loop, there are $\kappa = z-1$ possible directions to go (since one doesn't backtrack). The fact that the loop must avoid overlapping itself and must return to its original position to be closed leads to a reduced $\kappa < z - 1$ and to the power law term $P^{-\theta}$, which is subleading since $\kappa^P P^{-\theta} = \exp(P \log \kappa - \theta \log P)$ and $P \gg \log P$ for $P \gg 1$. Thus,

$$F \approx -\frac{1}{\beta} L^d \sum_P P^{-\theta} \, e^{(\log \kappa - 2\beta J)P} \quad , \tag{7.275}$$

which diverges if $\log \kappa > 2\beta J$, *i.e.* if $T > 2J/k_{\rm B} \log(z-1)$. We identify this singularity with the phase transition. The high temperature phase involves a proliferation of such loops. The excluded volume effects between the loops, which we have not taken into account, then enter in an essential way so that the sum converges. Thus, we have the following picture:

$$\begin{aligned} &\log \kappa < 2\beta J \;\; : \;\; \text{large loops suppressed ; ordered phase} \\ &\log \kappa > 2\beta J \;\; : \;\; \text{large loops proliferate ; disordered phase} \quad . \end{aligned}$$

On the square lattice, we obtain

$$k_{\rm B} T_{\rm c}^{\rm approx} = \frac{2J}{\log 3} = 1.82\, J \qquad , \qquad k_{\rm B} T_{\rm c}^{\rm exact} = \frac{2J}{\sinh^{-1}(1)} = 2.27\, J \quad .$$

The agreement is better than we should reasonably expect from such a crude argument.

Nota bene : Beware of arguments which allegedly prove the existence of an ordered phase. Generally speaking, any approximation will *underestimate* the entropy, and thus will overestimate the stability of the putative ordered phase.

7.9.3 Continuous symmetries

When the global symmetry group is continuous, the domain walls interpolate smoothly between ordered phases. The energy generally involves a stiffness term,

$$E = \tfrac{1}{2} \rho_{\rm s} \int d^d r \, (\boldsymbol{\nabla} \theta)^2 \quad , \tag{7.276}$$

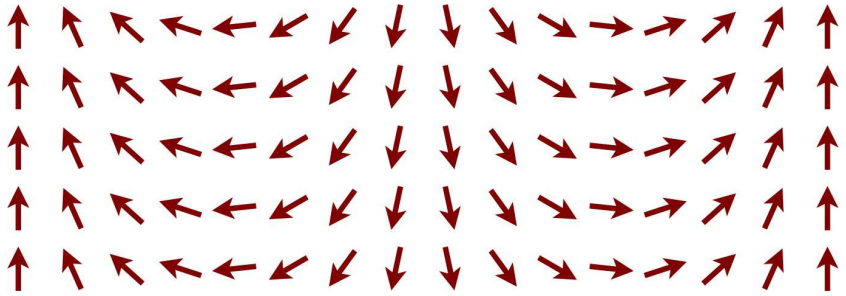


Figure 7.24: A domain wall in an XY ferromagnet.

where $\theta(\boldsymbol{r})$ is the angle of a local rotation about a single axis and where $\rho_{\rm s}$ is the *spin stiffness*. Of course, in O(n) models, the rotations can be with respect to several different axes simultaneously.

In the ordered phase, we have $\theta(\boldsymbol{r}) = \theta_0$, a constant. Now imagine a domain wall in which $\theta(\boldsymbol{r})$ rotates by 2π across the width of the sample. We write $\theta(\boldsymbol{r}) = 2\pi n x/L$, where L is the linear size of the sample (here with dimensions of length) and n is an integer telling us how many complete twists the order parameter field makes. The domain wall then resembles that in fig. 7.24. The gradient energy is

$$E = \tfrac{1}{2}\rho_{\rm s}\, L^{d-1} \int_0^L dx \left(\frac{2\pi n}{L}\right)^2 = 2\pi^2 n^2 \rho_{\rm s}\, L^{d-2} \quad . \tag{7.277}$$

Recall that in the case of discrete symmetry, the domain wall energy scaled as $E \propto L^{d-1}$. Thus, with $S \gtrsim k_{\rm B} \log L$ for a single wall, we see that the entropy term dominates if $d \leq 2$, in which case there is no finite temperature phase transition. Thus, the lower critical dimension d_ℓ depends on whether the global symmetry is discrete or continuous, with

$$\begin{aligned} \text{discrete global symmetry} \quad &\Longrightarrow \quad d_\ell = 1 \\ \text{continuous global symmetry} \quad &\Longrightarrow \quad d_\ell = 2 \quad . \end{aligned} \tag{7.278}$$

Note that all along we have assumed local, *short-ranged* interactions. Long-ranged interactions can enhance order and thereby suppress d_ℓ.

Thus, we expect that for models with discrete symmetries, $d_\ell = 1$ and there is no finite temperature phase transition for $d \leq 1$. For models with continuous symmetries, $d_\ell = 2$, and we expect $T_{\rm c} = 0$ for $d \leq 2$. In this context we should emphasize that the two-dimensional XY model *does* exhibit a phase transition at finite temperature, called the *Kosterlitz-Thouless* transition. However, this phase transition is *not* associated with the breaking of the continuous global O(2) symmetry and rather has to do with the unbinding of vortices and antivortices. So there is still no true long-ranged order below the critical temperature $T_{\rm KT}$, even though there is a phase transition!

7.9.4 Random systems : Imry-Ma argument

Oftentimes, particularly in condensed matter systems, intrinsic randomness exists due to quenched impurities, grain boundaries, immobile vacancies, *etc.* How does this quenched randomness affect a

system's attempt to order at $T = 0$? This question was taken up in a beautiful and brief paper by J. Imry and S.-K. Ma, *Phys. Rev. Lett.* **35**, 1399 (1975). Imry and Ma considered models in which there are short-ranged interactions and a random local field coupling to the local order parameter:

$$\hat{H}_{\rm RFI} = -J \sum_{\langle ij \rangle} \sigma_i \, \sigma_j - \sum_{i=1}^{N} H_i \, \sigma_i \tag{7.279}$$

$$\hat{H}_{{\rm RFO}(N)} = -J \sum_{\langle ij \rangle} \hat{\boldsymbol{n}}_i \cdot \hat{\boldsymbol{n}}_j - \sum_{i=1}^{N} H_i^\alpha \, n_i^\alpha \quad , \tag{7.280}$$

where

$$\langle\!\langle \, H_i^\alpha \, \rangle\!\rangle = 0 \qquad , \qquad \langle\!\langle \, H_i^\alpha \, H_j^\beta \, \rangle\!\rangle = \Gamma \, \delta^{\alpha\beta} \, \delta_{ij} \quad , \tag{7.281}$$

where $\langle\!\langle \, \bullet \, \rangle\!\rangle$ denotes a configurational average over the disorder. Imry and Ma reasoned that a system could try to lower its free energy by forming *domains* in which the order parameter takes advantage of local fluctuations in the random field. The size of these domains is assumed to be $L_{\rm d}$, a length scale to be determined. See the sketch in the left panel of fig. 7.25.

There are two contributions to the energy of a given domain: bulk and surface terms. The bulk energy is given by

$$E_{\rm bulk} = -H_{\rm rms} \, (L_{\rm d}/a)^{d/2} \quad , \tag{7.282}$$

where a is the lattice spacing. This is because when we add together $(L_{\rm d}/a)^d$ random fields, the magnitude of the result is proportional to the square root of the number of terms, *i.e.* to $(L_{\rm d}/a)^{d/2}$. The quantity $H_{\rm rms} = \sqrt{\Gamma}$ is the root-mean-square fluctuation in the random field at a given site. The surface energy is

$$E_{\rm surface} \propto \begin{cases} J \, (L_{\rm d}/a)^{d-1} & \text{(discrete symmetry)} \\ J \, (L_{\rm d}/a)^{d-2} & \text{(continuous symmetry)} \quad . \end{cases} \tag{7.283}$$

We compute the critical dimension $d_{\rm c}$ by balancing the bulk and surface energies,

$$\begin{aligned} d - 1 = \tfrac{1}{2} d \qquad &\Longrightarrow \qquad d_{\rm c} = 2 \qquad \text{(discrete)} \\ d - 2 = \tfrac{1}{2} d \qquad &\Longrightarrow \qquad d_{\rm c} = 4 \qquad \text{(continuous)} \quad . \end{aligned}$$

A system at its critical dimension is then marginal and requires further analysis to understand its properties. The total free energy is $F = (V/L_{\rm d}^d) \cdot \Delta E$, where $\Delta E = E_{\rm bulk} + E_{\rm surf}$. The free energy per unit cell is

$$f = \frac{F}{V/a^d} \approx J \left(\frac{a}{L_{\rm d}} \right)^{d_{\rm c}/2} - H_{\rm rms} \left(\frac{a}{L_{\rm d}} \right)^{d/2} \quad . \tag{7.284}$$

If $d < d_{\rm c}$, the surface term dominates for small $L_{\rm d}$ and the bulk term dominates for large $L_{\rm d}$. There is a global minimum at

$$\frac{L_{\rm d}}{a} = \left(\frac{d_{\rm c}}{d} \cdot \frac{J}{H_{\rm rms}} \right)^{2/(d_{\rm c} - d)} \quad . \tag{7.285}$$

For $d > d_{\rm c}$, the relative dominance of the bulk and surface terms is reversed, and there is a global maximum at this value of $L_{\rm d}$.

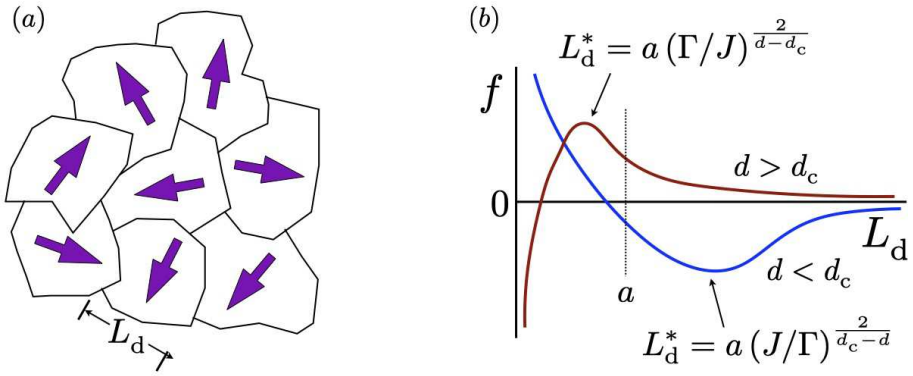


Figure 7.25: (a) Imry-Ma domains for an O(2) model. The arrows point in the direction of the local order parameter field $\langle \hat{\boldsymbol{n}}(\boldsymbol{r}) \rangle$. (b) Free energy density as a function of domain size $L_{\rm d}$. Keep in mind that the minimum possible value for $L_{\rm d}$ is the lattice spacing a.

Sketches of the free energy $f(L_{\rm d})$ in both cases are provided in the right panel of fig. 7.25. We must keep in mind that the domain size $L_{\rm d}$ cannot become smaller than the lattice spacing a. Hence we should draw a vertical line on the graph at $L_d = a$ and discard the portion $L_d < a$ as unphysical. For $d < d_{\rm c}$, we see that the state with $L_d = \infty$, *i.e.* the ordered state, is never the state of lowest free energy. *In dimensions $d < d_{\rm c}$, the ordered state is always unstable to domain formation in the presence of a random field.*

For $d > d_{\rm c}$, there are two possibilities, depending on the relative size of J and $H_{\rm rms}$. We can see this by evaluating $f(L_d = a) = J - H_{\rm rms}$ and $f(L_{\rm d} = \infty) = 0$. Thus, if $J > H_{\rm rms}$, the minimum energy state occurs for $L_{\rm d} = \infty$. In this case, the system has an ordered ground state, and we expect a finite temperature transition to a disordered state at some critical temperature $T_{\rm c} > 0$. If, on the other hand, $J < H_{\rm rms}$, then the fluctuations in H overwhelm the exchange energy at $T = 0$, and the ground state is disordered down to the very smallest length scale (*i.e.* the lattice spacing a).

Please read the essay, Memories of Shang-Keng Ma.

7.9.5 Hohenberg-Mermin-Wagner theorem

The Hohenberg-Mermin-Wagner (HMW) theorem is a powerful result which establishes the absence of broken continuous symmetry for systems at any finite temperature in dimensions $d \leq 2$ under the assumption of sufficiently short-ranged interactions. Extensions o f the theorem have been applied to certain $d = 1$ quantum systems at $T = 0$, such as antiferromagnets, crystals, and Bose superfluids. As we shall see, it is related to Goldstone's theorem, which we shall discuss below in §7.9.6.

Before getting into the details, a plea for proper attribution. Historically, the HMW theorem has often been referred to as the "Mermin-Wagner theorem", but in fact it should rightly be called the "Hohenberg-Mermin-Wagner theorem"[45]. For a latter day perspective, including a brief recounting of the history, see B. I. Halperin, *J. Stat. Phys.* **175**, 521 (2019).

For a poor man's derivation of the HMW theorem, we proffer the following argument. Expanding

[45] P. C. Hohenberg, *Phys. Rev.* **158**, 383 (1967); N. D. Mermin and H. Wagner, *Phys. Rev. Lett.* **17**, 1133 (1966).

in quadratic fluctuations for a translationally invariant quantum system in the thermodynamic limit, consider the model Hamiltonian

$$H = \sum_{\boldsymbol{k}} \overbrace{\left\{ \frac{p_{\boldsymbol{k}}\, p_{-\boldsymbol{k}}}{2m_{\boldsymbol{k}}} + \tfrac{1}{2} m_{\boldsymbol{k}} \omega_{\boldsymbol{k}}^2\, x_{\boldsymbol{k}}\, x_{-\boldsymbol{k}} \right\}}^{H_{\boldsymbol{k}}} = \sum_{\boldsymbol{k}} (a_{\boldsymbol{k}}^\dagger a_{\boldsymbol{k}} + \tfrac{1}{2})\, \hbar\omega_{\boldsymbol{k}} \quad , \tag{7.286}$$

where $\big[p_{\boldsymbol{k}}, x_{\boldsymbol{k}'}\big] = -i\hbar\delta_{\boldsymbol{k}+\boldsymbol{k}',\boldsymbol{0}}$ and $\big[a_{\boldsymbol{k}}, a_{\boldsymbol{k}'}^\dagger\big] = \delta_{\boldsymbol{k},\boldsymbol{k}'}$. The average energy per $\boldsymbol{k}$ mode is given by $\langle H_{\boldsymbol{k}}\rangle = (n_{\boldsymbol{k}} + \frac{1}{2})\hbar\omega_{\boldsymbol{k}}$, with $n_{\boldsymbol{k}} = 1/\big(\exp(\beta\hbar\omega_{\boldsymbol{k}}) - 1\big)$ the mode occupancy. Now let's compute the fluctuations in the local coordinate $x_{\boldsymbol{r}}$:

$$\langle x_{\boldsymbol{r}}^2\rangle = \frac{1}{N}\sum_{\boldsymbol{k}} \langle x_{\boldsymbol{k}} x_{-\boldsymbol{k}}\rangle = \frac{1}{N}\sum_{\boldsymbol{k}} \frac{(n_{\boldsymbol{k}} + \frac{1}{2})\hbar\omega_{\boldsymbol{k}}}{m_{\boldsymbol{k}}\omega_{\boldsymbol{k}}^2} = \mathsf{vol}(\Omega) \int\limits_{\hat{\Omega}} \frac{d^d k}{(2\pi)^d} \left(\frac{1}{\exp(\beta\hbar\omega_{\boldsymbol{k}}) - 1} + \frac{1}{2} \right) \frac{\hbar}{m_{\boldsymbol{k}}\omega_{\boldsymbol{k}}} \quad , \tag{7.287}$$

where N is the number of unit cells in the system, Ω is the unit cell, and $\hat{\Omega}$ is the Brillouin zone.

We presume the dispersion $\omega_{\boldsymbol{k}}$ behaves as $\omega_{\boldsymbol{k}} = c|\boldsymbol{k}|$ as $\boldsymbol{k} \to \boldsymbol{0}$, and further assume that $m_{\boldsymbol{k}\to 0}$ is finite. At finite temperature, the integrand therefore diverges as $T/\omega_{\boldsymbol{k}}^2 \sim T/\boldsymbol{k}^2$ as $\boldsymbol{k} \to \boldsymbol{0}$, and thus the integral is IR-divergent for $d \le 2$. This means that we have *expanded about the wrong vacuum*. Note that the same considerations apply at $T = 0$ in $d = 1$, where $n_{\boldsymbol{k}} = 0$, due to the intrinsic quantum fluctuations.

Formal proof of the HMW theorem

We follow here the original Mermin-Wagner treatment of the HMW theorem. Consider the Heisenberg model,

$$H = -\frac{1}{2}\sum_{\boldsymbol{R},\boldsymbol{R}'} J(\boldsymbol{R} - \boldsymbol{R}')\, \boldsymbol{S}_{\boldsymbol{R}} \cdot \boldsymbol{S}_{\boldsymbol{R}'} - \sum_{\boldsymbol{R}} h_{\boldsymbol{R}}\, S_{\boldsymbol{R}}^z \quad . \tag{7.288}$$

Here the positions $\{\boldsymbol{R}\}$ are sites on some Bravais lattice, the spin operators obey the $\mathsf{SU}(2)$ algebra[46]

$$\big[S_{\boldsymbol{R}}^\alpha, S_{\boldsymbol{R}'}^\beta\big] = i\,\delta_{\boldsymbol{R}\boldsymbol{R}'}\,\epsilon^{\alpha\beta\gamma}\, S_{\boldsymbol{R}}^\gamma \quad , \tag{7.289}$$

and the coupling $J(\boldsymbol{R} - \boldsymbol{R}') = J(\boldsymbol{R}' - \boldsymbol{R})$ is inversion symmetric, and satisfies $J(\boldsymbol{0}) = 0$. The Fourier components $\hat{h}_{\boldsymbol{k}}$ of the magnetic field satisfy $\hat{h}_{-\boldsymbol{k}} = \hat{h}_{\boldsymbol{k}}^*$, since the Hamiltonian must be Hermitian. We will also need to require that the interaction kernel $J(\boldsymbol{R} - \boldsymbol{R}')$ be sufficiently short-ranged, decaying faster than $|\boldsymbol{R} - \boldsymbol{R}'|^{-(d+2)}$, as shall become clear below.

The proof proceeds by finding a bound for the magnitude $|\hat{m}_{\boldsymbol{k}}|$, where $\hat{m}_{\boldsymbol{k}} \equiv \langle S_{\boldsymbol{k}}^z\rangle/N$, with

$$S_{\boldsymbol{k}}^z = \sum_{\boldsymbol{R}} S_{\boldsymbol{R}}^z\, e^{-i\boldsymbol{k}\cdot\boldsymbol{R}} \quad . \tag{7.290}$$

The quantity $m_{\boldsymbol{k}}$ is the order parameter at wavevector $\boldsymbol{k}$. For example, at $\boldsymbol{k} = 0$ we have $\hat{m}_{\boldsymbol{0}} = N^{-1}\sum_{\boldsymbol{R}}\langle S_{\boldsymbol{R}}^z\rangle$, which is the moment per site. The goal is to show that in the limit $\hat{h}_{\boldsymbol{k}} \to 0$ of vanishing external field that the order parameter must vanish if the spatial dimension d is sufficiently small.

[46] We set $\hbar = 1$ for convenience.

Bogoliubov's inequality

The proof utilizes the Bogoliubov inequality,

$$\big|\big\langle [A,C]\big\rangle\big|^2 \le \tfrac{1}{2}\beta\,\big\langle \{A,A^\dagger\}\big\rangle\,\big\langle \big[C^\dagger,[H,C]\big]\big\rangle \quad , \tag{7.291}$$

for any operators A and C, where $\big\langle\mathcal{O}\big\rangle = \mathsf{Tr}\,\big(\mathcal{O}\,e^{-\beta H}\big)/\,\mathsf{Tr}\,e^{-\beta H}$ is the thermodynamic expectation value of the operator $\mathcal{O}$. To prove Eqn. 7.291, we start by defining the operator scalar product,

$$(A,B) \equiv \sum_{m\neq n} \langle\, n\,|\,A^\dagger\,|\,m\,\rangle\langle\, m\,|\,B\,|\,n\,\rangle\left(\frac{W_m - W_n}{E_n - E_m}\right) \quad , \tag{7.292}$$

where $W_m = e^{-\beta E_m}/\,\mathsf{Tr}\,e^{-\beta H}$ is the Boltzmann weight for the state $|m\rangle$.[47] One can check that $(\bullet,\bullet)$ satisfies (i) $(A,B) = (B,A)^*$ (conjugation symmetry), (ii) $(A,\lambda_1 B_1 + \lambda_2 B_2) = \lambda_1(A,B_1) + \lambda_2(A,B_2)$ (linearity), and (iii) $(A,A) \ge 0$ (positive semidefiniteness). Under these conditions, the Schwarz inequality,

$$\big|(A,B)\big|^2 \le (A,A)\,(B,B) \quad , \tag{7.293}$$

holds.

Let's evaluate the Schwarz inequality with $B = [C^\dagger, H]$. We have

$$\begin{aligned}(A,B) = \big(A,[C^\dagger,H]\big) &= \sum_{m\neq n} \langle\, n\,|\,A^\dagger\,|\,m\,\rangle\langle\, m\,|\,(C^\dagger H - HC^\dagger)\,|\,n\,\rangle\left(\frac{W_m - W_n}{E_n - E_m}\right) \\ &= \sum_{m,n} \langle\, n\,|\,A^\dagger\,|\,m\,\rangle\langle\, m\,|\,C^\dagger\,|\,n\,\rangle\,(W_m - W_n) = \big\langle [C^\dagger, A^\dagger]\big\rangle \quad .\end{aligned} \tag{7.294}$$

Substituting $A = B$ in this result, we have

$$(B,B) = \big\langle [C^\dagger, B^\dagger]\big\rangle = \big\langle \big[C^\dagger,[H,C]\big]\big\rangle \quad , \tag{7.295}$$

and thus the Schwarz inequality guarantees

$$\big|\big\langle [C^\dagger, A^\dagger]\big\rangle\big|^2 = \big|\big\langle [A,C]\big\rangle\big|^2 \le (A,A)\,\big\langle \big[C^\dagger,[H,C]\big]\big\rangle \quad . \tag{7.296}$$

Next, note that

$$\begin{aligned}\frac{W_m - W_n}{E_n - E_m} &= \left(\frac{W_m + W_n}{E_n - E_m}\right)\left(\frac{W_m - W_n}{W_m + W_n}\right) \\ &= \left(\frac{W_m + W_n}{E_n - E_m}\right)\tanh\big(\tfrac{1}{2}\beta(E_n - E_m)\big) \le \frac{\beta}{2}\,(W_m + W_n) \quad ,\end{aligned} \tag{7.297}$$

since $0 \le x^{-1}\tanh x \le 1$. Thus we have

$$(A,A) \le \frac{\beta}{2}\sum_{m\neq n} \langle\, n\,|\,A^\dagger\,|\,m\,\rangle\langle\, m\,|\,A\,|\,n\,\rangle\,(W_m + W_n) \le \frac{\beta}{2}\,\big\langle \{A,A^\dagger\}\big\rangle \quad , \tag{7.298}$$

thereby establishing the Bogoliubov inequality of Eqn. 7.291.

[47] When $E_m = E_n$, the ratio in eqn. 7.292 is defined by its $E_m \to E_n$ limit, which is then βW_m.

Application to quantum Heisenberg model

Consider now the quantum Heisenberg model of Eqn. 7.288. Define the Fourier variables

$$S^\alpha_{\boldsymbol{k}} = \sum_{\boldsymbol{R}} S^\alpha_{\boldsymbol{R}}\, e^{-i\boldsymbol{k}\cdot\boldsymbol{R}} \quad , \quad \hat{J}(\boldsymbol{k}) = \sum_{\boldsymbol{R}} J(\boldsymbol{R})\, e^{-i\boldsymbol{k}\cdot\boldsymbol{R}} \quad , \quad \hat{h}_{\boldsymbol{k}} = \frac{1}{N}\sum_{\boldsymbol{R}} h_{\boldsymbol{R}}\, e^{-i\boldsymbol{k}\cdot\boldsymbol{R}} \tag{7.299}$$

and their inverses

$$S^\alpha_{\boldsymbol{R}} = \frac{1}{N}\sum_{\boldsymbol{k}} S^\alpha_{\boldsymbol{k}}\, e^{i\boldsymbol{k}\cdot\boldsymbol{R}} \quad , \quad J(\boldsymbol{R}) = \frac{1}{N}\sum_{\boldsymbol{k}} \hat{J}(\boldsymbol{k})\, e^{i\boldsymbol{k}\cdot\boldsymbol{R}} \qquad h_{\boldsymbol{R}} = \sum_{\boldsymbol{k}} h_{\boldsymbol{k}}\, e^{i\boldsymbol{k}\cdot\boldsymbol{R}} \quad . \tag{7.300}$$

Note the placement of the $1/N$ factors differs in the definitions of $\hat{J}(\boldsymbol{k})$ and $\hat{h}_{\boldsymbol{k}}$. The commutation relations among the Fourier spin components are

$$[S^+_{\boldsymbol{k}}\,,\, S^-_{\boldsymbol{k}'}] = 2S^z_{\boldsymbol{k}+\boldsymbol{k}'} \quad , \quad [S^z_{\boldsymbol{k}}\,,\, S^\pm_{\boldsymbol{k}'}] = \pm S^\pm_{\boldsymbol{k}+\boldsymbol{k}'} \quad . \tag{7.301}$$

We apply the Bogoliubov inequality of Eqn. 7.291 with

$$A = S^-_{-\boldsymbol{k}_1} \quad , \quad A^\dagger = S^+_{\boldsymbol{k}_1} \quad , \quad C = S^+_{\boldsymbol{k}_2} \quad , \quad C^\dagger = S^-_{-\boldsymbol{k}_2} \quad . \tag{7.302}$$

Thus, our version of the inequality may be written

$$\left|\big\langle [S^-_{-\boldsymbol{k}_1}, S^+_{\boldsymbol{k}_2}]\big\rangle\right|^2 \le \tfrac{1}{2}\beta\,\big\langle \{S^-_{-\boldsymbol{k}_1}, S^+_{\boldsymbol{k}_1}\}\big\rangle\,\big\langle \big[S^-_{-\boldsymbol{k}_2}, [H, S^+_{\boldsymbol{k}_2}]\big]\big\rangle \quad , \tag{7.303}$$

Note that we may write $H = H_0 + H_1$ where

$$\begin{aligned} H_0 &= -\frac{1}{2N}\sum_{\boldsymbol{q}} \hat{J}(\boldsymbol{q})\left\{\tfrac{1}{2}S^+_{\boldsymbol{q}}\, S^-_{-\boldsymbol{q}} + \tfrac{1}{2}S^-_{\boldsymbol{q}}\, S^+_{-\boldsymbol{q}} + S^z_{\boldsymbol{q}}\, S^z_{-\boldsymbol{q}}\right\} \\ H_1 &= -\sum_{\boldsymbol{q}} \hat{h}_{-\boldsymbol{q}}\, S^z_{\boldsymbol{q}} \quad . \end{aligned} \tag{7.304}$$

We begin by computing the commutator

$$[H_0, S^+_{\boldsymbol{k}_2}] = \frac{1}{2N}\sum_{\boldsymbol{q}} \hat{J}(\boldsymbol{q})\left\{S^+_{\boldsymbol{q}}\, S^z_{\boldsymbol{k}_2-\boldsymbol{q}} + S^z_{\boldsymbol{k}_2+\boldsymbol{q}}\, S^+_{-\boldsymbol{q}} - S^+_{\boldsymbol{k}_2+\boldsymbol{q}}\, S^z_{-\boldsymbol{q}} - S^z_{\boldsymbol{q}}\, S^+_{\boldsymbol{k}_2-\boldsymbol{q}}\right\} \quad , \tag{7.305}$$

from which we obtain, with a little work,

$$\big[S^-_{-\boldsymbol{k}_2}, [H_0, S^+_{\boldsymbol{k}_2}]\big] = \frac{1}{2N}\sum_{\boldsymbol{q}} \Big(\hat{J}(\boldsymbol{q}) - \hat{J}(\boldsymbol{q}+\boldsymbol{k}_2)\Big)\Big(S^+_{\boldsymbol{q}}\, S^-_{-\boldsymbol{q}} + S^-_{\boldsymbol{q}}\, S^+_{-\boldsymbol{q}} + 4\, S^z_{\boldsymbol{q}}\, S^z_{-\boldsymbol{q}}\Big) \tag{7.306}$$

and where we have invoked $\sum_{\boldsymbol{k}} \hat{J}(\boldsymbol{k}) = 0$, which follows from the condition $J(\boldsymbol{0}) = 0$.

Second we compute $[H_1, S^+_{\boldsymbol{k}_2}] = -\sum_{\boldsymbol{q}} \hat{h}_{-\boldsymbol{q}}\, S^+_{\boldsymbol{q}+\boldsymbol{k}_2}$, and thus

$$\big[S^-_{-\boldsymbol{k}_2}, [H_1, S^+_{\boldsymbol{k}_2}]\big] = 2\sum_{\boldsymbol{q}} \hat{h}_{-\boldsymbol{q}}\, S^z_{\boldsymbol{q}} \quad . \tag{7.307}$$

Third, $[S^-_{-\boldsymbol{k}_1}, S^+_{\boldsymbol{k}_2}] = -S^z_{\boldsymbol{k}_2-\boldsymbol{k}_1}$. Finally, we have $\{S^-_{-\boldsymbol{k}_1}, S^+_{\boldsymbol{k}_1}\} = S^-_{-\boldsymbol{k}_1}S^+_{\boldsymbol{k}_1} + S^+_{\boldsymbol{k}_1}S^-_{-\boldsymbol{k}_1}$. Note that

$$\left|\left\langle [S^-_{-\boldsymbol{k}_1}, S^+_{\boldsymbol{k}_2}]\right\rangle\right|^2 = \left|\langle S^z_{\boldsymbol{k}_2-\boldsymbol{k}_1}\rangle\right|^2 = 4N^2\,|\hat{m}_{\boldsymbol{k}_2-\boldsymbol{k}_1}|^2 \quad . \tag{7.308}$$

We define the quantity $\Gamma(\boldsymbol{k}_2) \equiv \Gamma_0(\boldsymbol{k}_2) + \Gamma_1(\boldsymbol{k}_2)$, where

$$\begin{aligned}\Gamma_0(\boldsymbol{k}_2) &= \left[S^-_{-\boldsymbol{k}_2}, [H_0, S^+_{\boldsymbol{k}_2}]\right] \\ &= \frac{1}{2N}\sum_{\boldsymbol{q}}\Big(\hat{J}(\boldsymbol{q}) - \tfrac{1}{2}\hat{J}(\boldsymbol{q}+\boldsymbol{k}_2) - \tfrac{1}{2}\hat{J}(\boldsymbol{q}-\boldsymbol{k}_2)\Big)\left\langle 4S^z_{\boldsymbol{q}}\,S^z_{-\boldsymbol{q}} + S^+_{\boldsymbol{q}}\,S^-_{-\boldsymbol{q}} + S^-_{\boldsymbol{q}}\,S^+_{-\boldsymbol{q}}\right\rangle \\ &= \sum_{\boldsymbol{R}_1,\boldsymbol{R}_2} J(\boldsymbol{R}_1)\left(1-\cos(\boldsymbol{k}_2\cdot\boldsymbol{R}_1)\right)\left\langle S^x_{\boldsymbol{R}_2}S^x_{\boldsymbol{R}_1+\boldsymbol{R}_2} + S^y_{\boldsymbol{R}_2}S^y_{\boldsymbol{R}_1+\boldsymbol{R}_2} + 2\,S^z_{\boldsymbol{R}_2}S^z_{\boldsymbol{R}_1+\boldsymbol{R}_2}\right\rangle\end{aligned} \tag{7.309}$$

and

$$\Gamma_1(\boldsymbol{k}_2) = \left\langle\left[S^-_{-\boldsymbol{k}_2}, [H_1, S^+_{\boldsymbol{k}_2}]\right]\right\rangle = 2N\sum_{\boldsymbol{q}}\hat{h}_{-\boldsymbol{q}}\,\hat{m}_{\boldsymbol{q}} \quad . \tag{7.310}$$

We may now easily derive the following bounds:

$$\begin{aligned}\Gamma_0(\boldsymbol{k}_2) &\le NS(S+\tfrac{1}{2})\,\boldsymbol{k}_2^2\sum_{\boldsymbol{R}}\boldsymbol{R}^2|J(\boldsymbol{R})| \equiv 4N\mathcal{J}\,\boldsymbol{k}_2^2\,a^2 \\ \Gamma_1(\boldsymbol{k}_2) &\le 2N\sum_{\boldsymbol{q}}|\hat{h}_{-\boldsymbol{q}}|\cdot|\hat{m}_{\boldsymbol{q}}| \quad .\end{aligned} \tag{7.311}$$

with $\mathcal{J} \equiv \frac{1}{4}S(S+\frac{1}{2})\sum_{\boldsymbol{R}}(\boldsymbol{R}/a)^2\,|J(\boldsymbol{R})|$, where we presume a d-dimensional cubic lattice of lattice constant a.

We are almost ready to claim our prize. At this point we have the inequality

$$\left\langle S^-_{\boldsymbol{K}-\boldsymbol{k}_2}S^+_{\boldsymbol{k}_2-\boldsymbol{K}} + S^+_{\boldsymbol{k}_2-\boldsymbol{K}}\,S^-_{\boldsymbol{K}-\boldsymbol{k}_2}\right\rangle \ge \frac{N}{2\beta}\cdot\frac{|\hat{m}_{\boldsymbol{K}}|^2}{\mathcal{J}\boldsymbol{k}_2^2\,a^2 + \frac{1}{2}\sum_{\boldsymbol{q}}|\hat{h}_{-\boldsymbol{q}}|\cdot|\hat{m}_{\boldsymbol{q}}|} \quad , \tag{7.312}$$

with $\boldsymbol{k}_1 \equiv \boldsymbol{k}_2 - \boldsymbol{K}$. We now sum both sides of the equation over $\boldsymbol{k}_2$, which owing to presumed periodic boundary conditions takes a discrete set of values $\boldsymbol{k}_2 = \big(2\pi n_1/N_1a, 2\pi n_2/N_2a, 2\pi n_3/N_3a\big)$, with $N = N_1\,N_2\,N_3$ where $n_j \in \{1,\ldots,N_j\}$. The system is thus a cubic rectangle of dimensions $N_1\times N_2\times N_3$ cells, with each cell of volume a^3. On the LHS, we obtain

$$\sum_{\boldsymbol{k}_2}\left\langle S^-_{\boldsymbol{K}-\boldsymbol{k}_2}S^+_{\boldsymbol{k}_2-\boldsymbol{K}} + S^+_{\boldsymbol{k}_2-\boldsymbol{K}}\,S^-_{\boldsymbol{K}-\boldsymbol{k}_2}\right\rangle = 2N\sum_{\boldsymbol{R}}\left\langle (S^x_{\boldsymbol{R}})^2 + (S^y_{\boldsymbol{R}})^2\right\rangle < 2N^2S(S+1) \quad . \tag{7.313}$$

Thus,

$$|\hat{m}_{\boldsymbol{K}}|^2 < \frac{4S(S+1)}{k_{\rm B}T}\Bigg/\,a^d\int\limits_{\hat{\Omega}}\frac{d^dk}{(2\pi)^d}\,\frac{1}{\mathcal{J}\boldsymbol{k}^2a^2 + \frac{1}{2}\sum_{\boldsymbol{q}}|\hat{h}_{-\boldsymbol{q}}|\cdot|\hat{m}_{\boldsymbol{q}}|} \tag{7.314}$$

Consider the case where $\hat{h}_{\boldsymbol{q}} = \hat{h}_{-\boldsymbol{K}}\,\delta_{\boldsymbol{q},-\boldsymbol{K}} + \hat{h}_{\boldsymbol{K}}\,\delta_{\boldsymbol{q},\boldsymbol{K}}$. The Brillouin zone is a d-dimensional cube of side length $2\pi/a$. We are free to *underestimate* the integral, since this *overestimates* the RHS of the above inequality, and to this end we integrate instead over a d-dimensional sphere of radius $b = \pi/a$, yielding

$$|\hat{m}_{\boldsymbol{K}}|^2 < \frac{4S(S+1)}{k_{\rm B}T}\Bigg/\,\frac{\Omega_d}{(2\pi)^d}\int\limits_0^{\pi}\frac{du\,u^{d-1}}{\mathcal{J}u^2 + |\hat{h}_{\boldsymbol{K}}|\cdot|\hat{m}_{\boldsymbol{K}}|} \quad , \tag{7.315}$$

where $\Omega_d = 2\pi^{d/2}/\Gamma(d/2)$ is the total solid angle in d space dimensions and $u = |\boldsymbol{k}|a$. We simplify notation by defining $h \equiv |\hat{h}_{\boldsymbol{K}}|$ and $m \equiv |\hat{m}_{\boldsymbol{K}}|$. We may now derive the following inequalities.

$$\begin{aligned} d = 1 \ : \quad & m < C_1 \left(\frac{h\mathcal{J}}{(k_{\rm B}T)^2} \right)^{1/3} \\ d = 2 \ : \quad & m < C_2 \, \frac{(\mathcal{J}/k_{\rm B}T)^{1/2}}{\ln^{1/2}(\mathcal{J}/hm)} \\ h = 0, \ d > 2 \ : \quad & m < C_d \, (\mathcal{J}/k_{\rm B}T)^{1/2} \quad , \end{aligned} \tag{7.316}$$

where the $C_{1,2,\ldots}$ are numerical constants. In the limit $h \to 0$, we see that m must vanish for $d = 1$ and $d = 2$. For $d > 2$, there is no such requirement.

7.9.6 Goldstone's theorem

Goldstone's theorem says that whenever the ground state $|\Psi_0\rangle$ of a thermodynamically large quantum system (or QFT) breaks a continuous symmetry of the Hamiltonian H, there is a branch of gapless excitations in the spectrum of H, known as *Goldstone bosons*. Let's illustrate this phenomenon with the explicit example of the spin-S quantum Heisenberg ferromagnet,

$$H = -\sum_{i<j} J_{ij} \, \boldsymbol{S}_i \cdot \boldsymbol{S}_j \quad . \tag{7.317}$$

We assume $J_{ij} = J(\boldsymbol{R}_i - \boldsymbol{R}_j) > 0$, *i.e.* the system is ferromagnetic, preferring all pairs of interacting spins to align. Each component of the total spin operator $\boldsymbol{\mathcal{S}} = \sum_i \boldsymbol{S}_i$ commutes with each term of H, *i.e.*

$$[\mathcal{S}^\alpha, \boldsymbol{S}_i \cdot \boldsymbol{S}_j] = 0 \tag{7.318}$$

because $\boldsymbol{S}_i \cdot \boldsymbol{S}_j$ is rotationally invariant and the $\mathcal{S}^\alpha$ are the generators of rotations. The global symmetry group is $\mathsf{SU}(2)$, which is continuous. It is clear that any state $|\Psi_0\rangle$ for which $\boldsymbol{S}_i \cdot \boldsymbol{S}_j \, |\Psi_0\rangle = S^2 \, |\Psi_0\rangle$ is a ground state of H, since each individual term in the sum is separately minimized. The ground state energy is then $E_0 = -\frac{1}{2} N \hat{J}(\boldsymbol{0}) S^2$, where $\hat{J}(\boldsymbol{k}) = \sum_{\boldsymbol{R}} J(\boldsymbol{R}) \, e^{-i\boldsymbol{k}\cdot\boldsymbol{R}}$.

Consider then the state $|\Uparrow\rangle$ in which $S_i^z \, |\Uparrow\rangle = S \, |\Uparrow\rangle$, *i.e.* all spins maximally polarized in the $\hat{\boldsymbol{z}}$ direction. Clearly $|\Uparrow\rangle$ is a ground state. But so is $|\Downarrow\rangle$. Indeed, so is any state of the form $|\Psi_0(\hat{\boldsymbol{n}})\rangle = \otimes_i |\hat{\boldsymbol{n}}\rangle_i$ in which each spin is in a coherent state maximally polarized along the direction $\hat{\boldsymbol{n}}$, *i.e.* $\hat{\boldsymbol{n}} \cdot \boldsymbol{S}_i \, |\Psi_0(\hat{\boldsymbol{n}})\rangle = S \, |\Psi_0(\hat{\boldsymbol{n}})\rangle$[48]. Thus, we have an entire manifold of states, all with energy E_0, corresponding to total spin $\mathcal{S} = NS$. The degeneracy of this ground state sector is $2N\mathcal{S} + 1$, and states with different values of $\mathcal{S}^z$ are of course orthogonal. In the coherent state basis, we have

$$\left| \langle \, \Psi_0(\hat{\boldsymbol{n}}) \, | \, \Psi_0(\hat{\boldsymbol{n}}') \, \rangle \right|^2 = \left(\frac{1 + \hat{\boldsymbol{n}} \cdot \hat{\boldsymbol{n}}'}{2} \right)^{2N\mathcal{S}} \quad , \tag{7.319}$$

where N is the total number of spins. In the thermodynamic limit, these states are *macroscopically distinct*

$$\left| \langle \, \Psi_0(\hat{\boldsymbol{n}}) \, \big| \, \mathcal{O}_i \, \mathcal{O}_j \, \big| \, \Psi_0(\hat{\boldsymbol{n}}') \, \rangle \right|^2 = \left(\frac{1 + \hat{\boldsymbol{n}} \cdot \hat{\boldsymbol{n}}'}{2} \right)^{2(N-2)\mathcal{S}} \left| \langle \, \hat{\boldsymbol{n}}, \hat{\boldsymbol{n}} \, | \, \mathcal{O}_i \, \mathcal{O}_j \, | \, \hat{\boldsymbol{n}}, \hat{\boldsymbol{n}} \, \rangle \right|^2 \quad , \tag{7.320}$$

[48] In this notation, our previously defined state $|\Psi_0\rangle = |\Uparrow\rangle$ is expressed as $|\Psi_0\rangle = |\Psi_0(\hat{\boldsymbol{z}})\rangle$.

which vanishes in the thermodynamic limit.

Next, consider the operator $S^\alpha(\boldsymbol{k}) = N^{-1}\sum_i S_i^\alpha\, e^{-i\boldsymbol{k}\cdot\boldsymbol{R}_i}$, which we met in Eqn. 7.300. It is straightforward to derive the result

$$[H, \mathcal{S}^-(\boldsymbol{k})] = \frac{1}{N}\sum_{i,j} J(\boldsymbol{R}_i - \boldsymbol{R}_j)\left(1 - e^{i\boldsymbol{k}\cdot(\boldsymbol{R}_j - \boldsymbol{R}_i)}\right) S_j^-\, e^{-i\boldsymbol{k}\cdot\boldsymbol{R}_j}\, S_i^z \quad . \tag{7.321}$$

We assume that the diagonal elements of J_{ij} all vanish, *i.e.* $J(\boldsymbol{0}) = \sum_{\boldsymbol{k}} \hat{J}(\boldsymbol{k}) = 0$. The above identity, acting on the state $|\Uparrow\rangle$, then yields

$$[H, \mathcal{S}^-(\boldsymbol{k})]\,|\Uparrow\rangle = S\big[\hat{J}(\boldsymbol{0}) - \hat{J}(\boldsymbol{k})\big]\,\mathcal{S}^-(\boldsymbol{k})\,|\Uparrow\rangle \quad , \tag{7.322}$$

which establishes that $\mathcal{S}^-_{\boldsymbol{k}}\,|\Uparrow\rangle$ is an *eigenstate* of H, with eigenvalue $E_{\boldsymbol{k}} = E_0 + S\big[\hat{J}(\boldsymbol{0}) - \hat{J}(\boldsymbol{k})\big]$. Thus, the excitation spectrum of this branch, which has one state for each wavevector $\boldsymbol{k}$, is

$$\hbar\omega_{\boldsymbol{k}} = E_{\boldsymbol{k}} - E_0 = S\big[\hat{J}(\boldsymbol{0}) - \hat{J}(\boldsymbol{k})\big] \quad . \tag{7.323}$$

These excitations are called *spin waves*, and they are examples of Goldstone bosons. Note that the $\boldsymbol{k} = \boldsymbol{0}$ spin wave state,

$$\mathcal{S}^-(\boldsymbol{0})\,|\Uparrow\rangle = \sum_i S_i^-\,|\Uparrow\rangle \quad , \tag{7.324}$$

is among the ground state manifold, with total spin $\mathcal{S} = NS$ and polarization $\mathcal{S}^z = NS - 1$.

Note that in systems with a discrete symmetry, such as the Ising model, with symmetry group $\mathbb{Z}_2$, there are in general no Goldstone bosons. For the Ising ferromagnet $H = -\sum_{i<j} J_{ij}\,\sigma_i\,\sigma_j$, where each $\sigma_i = \pm 1$, there are two degenerate ground states, $|\Uparrow\rangle$ and $|\Downarrow\rangle$, each of which has total energy $E_0 = -\frac{1}{2}N\hat{J}(\boldsymbol{0})$. In dimensions $d > 1$, the lowest-lying excitation in either case is a single spin flip, with excitation energy $\Delta E = 2\hat{J}(\boldsymbol{0})$. (In $d = 1$, with nearest-neighbor interactions, the lowest-lying excitation on an open chain is a domain wall, with energy $\hat{J}(\boldsymbol{0}) = 2J$. With periodic boundary conditions, there must be an even number of domain walls present, and hence the lowest-lying energy excitation corresponds to a domain wall pair, with energy $4J$.)

Field theories and Goldstone's theorem

Consider the $|\boldsymbol{\phi}|^4$ field theory for the real n-component field $\boldsymbol{\phi} = (\phi^1, \ldots, \phi^n)$, with relativistic Lagrangian density

$$\mathcal{L} = \tfrac{1}{2}(\partial_\mu\boldsymbol{\phi})(\partial^\mu\boldsymbol{\phi}) - \tfrac{1}{2}\,m^2\,\boldsymbol{\phi}^2 - \tfrac{1}{4}\,\lambda\,(\boldsymbol{\phi}^2)^2 \quad . \tag{7.325}$$

The metric used to raise and lower indices is $g_{\mu\nu} = \mathsf{diag}(+, -, \cdots, -)$. The equations of motion are found to be

$$\partial_\mu\partial^\mu\boldsymbol{\phi} + m^2\boldsymbol{\phi} + \lambda\,\boldsymbol{\phi}^2\,\boldsymbol{\phi} = 0 \quad . \tag{7.326}$$

If $m^2 > 0$, we can obtain solutions when $|\boldsymbol{\phi}| \ll 1$ by dropping the cubic term. The solutions are plane waves: $\boldsymbol{\phi}(\boldsymbol{x}, t) = A\,e^{i(\boldsymbol{k}\cdot\boldsymbol{x} - \omega t)}$ where $\omega^2 = \boldsymbol{k}^2 + m^2$. The spectrum is massive.

What happens when $m^2 < 0$? In this case the potential $V(\boldsymbol{\phi}) = \frac{1}{2}m^2\boldsymbol{\phi}^2 + \frac{1}{4}\lambda(\boldsymbol{\phi}^2)^2$ is minimized when $|\boldsymbol{\phi}| = \phi_0 = \sqrt{-m^2/\lambda}$. Let's write $\boldsymbol{\phi} = \phi_0\,(1+\eta)^{1/2}\,\hat{\boldsymbol{\omega}}$, where $\hat{\boldsymbol{\omega}}$ is a unit vector. One then obtains

$$\mathcal{L} = \tfrac{1}{8}\,\phi_0^2\,\frac{(\partial_\mu\eta)(\partial^\mu\eta)}{1+\eta} + \tfrac{1}{2}\,\phi_0^2\,(1+\eta)\,(\partial_\mu\hat{\boldsymbol{\omega}})(\partial^\mu\hat{\boldsymbol{\omega}}) - \tfrac{1}{4}\,m^2\,\phi_0^2(1-\eta^2) \quad . \tag{7.327}$$

The linearized EL equations are then

$$\begin{aligned} \partial_\mu\partial^\mu\eta &= 2m^2\eta \\ \partial_\mu\partial^\mu\hat{\boldsymbol{\omega}} &= 0 \quad . \end{aligned} \tag{7.328}$$

The first equation results in a massive relativistic dispersion $\omega^2 = \boldsymbol{k}^2 + 2|m^2|$, while the second, as we have seen, yields gapless solutions with $\omega = |\boldsymbol{k}|$, which are the Goldstone bosons. Note that if $\boldsymbol{\phi}$ has $n = 1$ component, then there is no $\hat{\boldsymbol{\omega}}$ field and there are no Goldstone bosons.

Consider next the example of the nonrelativistic complex $|\psi|^4$ theory, otherwise known as the Gross-Pitaevskii model, with

$$\mathcal{L} = i\hbar\,\bar{\psi}\,\partial_t\,\psi - \frac{\hbar^2}{2m}\,|\boldsymbol{\nabla}\psi|^2 - \tfrac{1}{2}g\big(|\psi|^2 - n_0\big)^2 \tag{7.329}$$

We write $\psi = \sqrt{n_0}\,(1+\eta)\,e^{i\xi}$, which yields

$$\mathcal{L} = -\hbar n_0(1+\eta)^2\,\partial_t\xi - \frac{\hbar^2 n_0}{2m}\,(\boldsymbol{\nabla}\eta)^2 - \frac{\hbar^2 n_0}{2m}\,(1+\eta)^2\,(\boldsymbol{\nabla}\xi)^2 - \tfrac{1}{2}\,g n_0^2\,(4\eta^2 + 4\eta^3 + \eta^4) \quad . \tag{7.330}$$

The linearized equations of motion are then found to be

$$\begin{aligned} -2\hbar n_0\,\partial_t\xi &= -\frac{\hbar^2 n_0}{m}\,\nabla^2\eta + 4gn_0^2\,\eta \\ +2\hbar n_0\,\partial_t\eta &= -\frac{\hbar^2 n_0}{m}\,\nabla^2\xi \quad . \end{aligned} \tag{7.331}$$

We now obtain plane wave solutions of the form

$$\begin{pmatrix}\eta(\boldsymbol{x},t)\\ \xi(\boldsymbol{x},t)\end{pmatrix} = \begin{pmatrix}\hat{\eta}\\ \hat{\xi}\end{pmatrix} e^{i(\boldsymbol{k}\cdot\boldsymbol{x}-\omega t)} \quad , \tag{7.332}$$

which, when inserted into the EL equations, yields the pair

$$\begin{aligned} 2i\hbar\omega\,\hat{\xi} &= \left(\frac{\hbar^2\boldsymbol{k}^2}{m} + 4gn_0\right)\hat{\eta} \\ -2i\hbar\omega\,\hat{\eta} &= \frac{\hbar^2\boldsymbol{k}^2}{m}\hat{\xi} \quad . \end{aligned} \tag{7.333}$$

The solutions are

$$\omega = \pm\,c\,|\boldsymbol{k}|\sqrt{1 + \frac{\hbar^2\boldsymbol{k}^2}{4m^2c^2}} \quad . \tag{7.334}$$

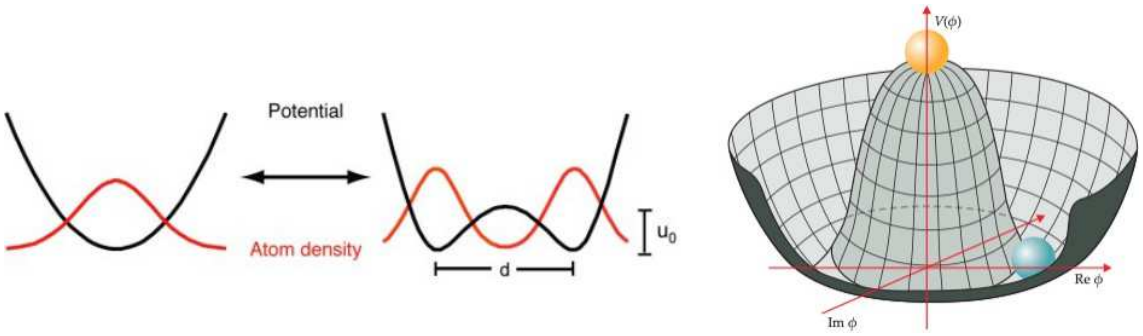


Figure 7.26: Left: double well potential $V(\phi)$ for the scalar field $\phi \in \mathbb{R}$. Right: Mexican hat potential for the complex scalar field $\phi \in \mathbb{C}$ with $V(\phi, \bar{\phi}) = \frac{1}{2}m^2\big(|\phi|^2 - n_0\big)^2$.

with $c = \sqrt{g n_0/m}$. Note that as $\boldsymbol{k} \to 0$ we obtain a massless relativistic dispersion $\omega = \pm c\,|\boldsymbol{k}|$, while for $|\boldsymbol{k}| \to \infty$ we recover the ballistic dispersion $\omega = \hbar \boldsymbol{k}^2/2m$. These massless excitations are Goldstone modes of the broken $\mathsf{U}(1)$ symmetry and correspond to phonons in a superfluid.

Finally, let's get crazy and consider the *gauged*, relativistic $|\psi|^4$ theory, with

$$\mathcal{L} = \frac{1}{2g}\,(\partial_\mu - ieA_\mu)\bar{\psi}\,(\partial^\mu + ieA^\mu)\psi - \frac{m^2}{2gn_0}\,\big(\bar{\psi}\psi - n_0\big)^2 - \tfrac{1}{4}F_{\mu\nu}F^{\mu\nu} \quad , \tag{7.335}$$

where the field strength tensor is written in terms of the gauge field as $F_{\mu\nu} = \partial_\mu A_\nu - \partial_\nu A_\mu$. This theory has a *local gauge symmetry* whereby the combined operations

$$\psi \to \psi\, e^{i\alpha} \qquad , \qquad A_\mu \to A_\mu - e^{-1}\,\partial_\mu \alpha \quad , \tag{7.336}$$

where $\alpha(\boldsymbol{x}, t)$ is a field, leaves $\mathcal{L}$ invariant.

If we drop the gauge field, *i.e.* set $e = 0$, we may again expand about one of the local minima at $|\psi| = n_0^{1/2}$, writing

$$\psi = \sqrt{n_0}\,(1 + \eta)\, e^{i\xi} \quad , \tag{7.337}$$

as above. Then

$$\mathcal{L} = \frac{n_0}{2g}\,(\partial_\mu \eta)(\partial^\mu \eta) + \frac{n_0}{2g}\,(1+\eta)^2\,(\partial_\mu \xi)(\partial^\mu \xi) - \frac{m^2 n_0}{2g}\,\big(4\eta^2 + 4\eta^3 + \eta^4\big) \quad . \tag{7.338}$$

The linearized equations of motion are then

$$\partial_\mu \partial^\mu \eta = -(2m)^2 \eta \qquad , \qquad \partial_\mu \partial^\mu \xi = 0 \quad , \tag{7.339}$$

yielding two modes. The η mode carries a massive relativistic dispersion $\omega^2 = \boldsymbol{k}^2 + (2m)^2$, while the ξ mode is the gapless Goldstone boson with $\omega^2 = \boldsymbol{k}^2$.

When $e \neq 0$, we may take advantage of the gauge invariance to define a shifted gauge field

$$\mathsf{A}_\mu \equiv A_\mu - e^{-1}\partial_\mu \xi \quad . \tag{7.340}$$

The transformed Lagrangian becomes

$$\mathcal{L} = \frac{n_0}{2g}\,(\partial_\mu \eta)(\partial^\mu \eta) + \frac{n_0\,e^2}{2g}\,(1+\eta)^2\,\mathsf{A}_\mu \mathsf{A}^\mu - \frac{m^2 n_0}{2g}\left(4\eta^2 + 4\eta^3 + \eta^4\right) - \tfrac{1}{4}\mathsf{F}_{\mu\nu}\mathsf{F}^{\mu\nu} \quad , \tag{7.341}$$

from which we can read off the following features:

- The photon has become a massive triplet A_μ with $m_{\mathsf{A}} = e\sqrt{n_0/g}$.
- There is no ξ particle! It has been *eaten* by the photon field.
- The Higgs field η has a mass which is independent of e, with $m_\eta = 2m$.

To reiterate what we have learned in this section: Classically, a particle in a double well potential exhibits spontaneous symmetry breaking. It *must* choose which well in which to lie. But quantum mechanically, we know that the ground state is a symmetric superposition of left and right well states. A similar consideration holds in the case of continuous symmetries, for the Mexican hat potential. A classical particle will minimize its energy at any point along the trough of the potential, but the quantum ground state is a rotationally symmetric s-wave state with no nodes. In a field theory setting, there are an *infinite number* of degrees of freedom, and the double well or Mexican hat exists *at every point in space*. This kills tunneling between the different broken symmetry 'pure' states, *viz.* $\langle\, \mathsf{L} \,|\, \mathsf{R} \,\rangle \sim \langle\, \varphi_{\mathsf{L}} \,|\, \varphi_{\mathsf{R}} \,\rangle^V \to 0$ in the $V \to \infty$ limit of infinite system volume. This state of affairs is described in Fig. 7.26.

7.10 Ginzburg-Landau Theory

7.10.1 Ginzburg-Landau free energy

Including gradient terms in the free energy, we write[49]

$$F\big[m(\boldsymbol{x})\,,\,h(\boldsymbol{x})\big] = \int d^d x \left\{ f_0 + \tfrac{1}{2}a\,m^2 + \tfrac{1}{4}b\,m^4 + \tfrac{1}{6}c\,m^6 \;- h\,m + \tfrac{1}{2}\kappa\,(\boldsymbol{\nabla} m)^2 + \ldots \right\} \quad . \tag{7.342}$$

In principle, any term which does not violate the appropriate global symmetry will turn up in such an expansion of the free energy, with some coefficient. Examples include hm^3 (both m and h are odd under time reversal), $m^2(\boldsymbol{\nabla} m)^2$, *etc.* We now ask: what function $m(\boldsymbol{x})$ extremizes the free energy functional $F\big[m(\boldsymbol{x})\,,\,h(\boldsymbol{x})\big]$? The answer is that $m(\boldsymbol{x})$ must satisfy the corresponding Euler-Lagrange equation, which for the above functional is

$$a\,m + b\,m^3 + c\,m^5 - h - \kappa\,\nabla^2 m = 0 \quad . \tag{7.343}$$

If $a > 0$ and h is small (we assume $b > 0$ and $c > 0$), we may neglect the m^3 and m^5 terms. The above equation then simplifies to $\big(a - \kappa\,\nabla^2\big)m = h$. We solve by Fourier transform, obtaining

$$\hat{m}(\boldsymbol{q}) = \frac{\hat{h}(\boldsymbol{q})}{a + \kappa \boldsymbol{q}^2} \qquad \Rightarrow \qquad \hat{\chi}(\boldsymbol{q}) = \frac{\partial \hat{m}(\boldsymbol{q})}{\partial \hat{h}(\boldsymbol{q})} = \frac{1}{a + \kappa \boldsymbol{q}^2} \quad . \tag{7.344}$$

[49] For a systematic derivation of the Ginzburg-Landau free energy, see the appendix in §7.14.

Thus,

$$m(\boldsymbol{x}) = \int d^d x' \, \chi(\boldsymbol{x} - \boldsymbol{x}') \, h(\boldsymbol{x}') \quad , \tag{7.345}$$

where

$$\chi(\boldsymbol{x} - \boldsymbol{x}') = \kappa^{-1} \int \frac{d^d q}{(2\pi)^d} \, \frac{e^{i\boldsymbol{q}\cdot(\boldsymbol{x}-\boldsymbol{x}')}}{\boldsymbol{q}^2 + \xi^{-2}} \quad , \tag{7.346}$$

where the correlation length is $\xi = \sqrt{\kappa/a} \propto (T - T_{\rm c})^{-1/2}$, as before.

If $a < 0$ then there is a spontaneous magnetization, given by the solution to $bm_0^2 + cm_0^4 = |a|$, and we write $m(\boldsymbol{x}) = m_0 + \delta m(\boldsymbol{x})$. Assuming h is weak, we then have two equations

$$\begin{aligned} a + b\, m_0^2 + c\, m_0^4 &= 0 \\ (a + 3b\, m_0^2 + 5c\, m_0^4 - \kappa\, \nabla^2)\, \delta m &= h \quad . \end{aligned} \tag{7.347}$$

Assuming $|a|$ is small, we have $m_0^2 = |a|/b$ and

$$\delta \hat{m}(\boldsymbol{q}) = \frac{\hat{h}(\boldsymbol{q})}{2|a| + \kappa \boldsymbol{q}^2} \quad , \tag{7.348}$$

7.10.2 Domain wall profile

A particularly interesting application of Ginzburg-Landau theory is its application toward modeling the spatial profile of defects such as vortices and domain walls. Consider, for example, the case of Ising ($\mathbb{Z}_2$) symmetry with $h = 0$. We expand the free energy density to order m^4:

$$F\big[m(\boldsymbol{x})\big] = \int d^d x \left\{ f_0 + \tfrac{1}{2} a m^2 + \tfrac{1}{4} b m^4 + \tfrac{1}{2} \kappa \, (\boldsymbol{\nabla} m)^2 \right\} \quad . \tag{7.349}$$

We assume $a < 0$, corresponding to $T < T_{\rm c}$. Consider now a domain wall, where $m(x \to -\infty) = -m_0$ and $m(x \to +\infty) = +m_0$, where m_0 is the equilibrium magnetization, which we obtain from the Euler-Lagrange equation,

$$a\, m + b\, m^3 - \kappa\, \nabla^2 m = 0 \quad , \tag{7.350}$$

assuming a uniform solution where $\boldsymbol{\nabla} m = 0$. This gives $m_0 = \sqrt{|a|/b}$. It is useful to scale $m(\boldsymbol{x})$ by m_0, writing $m(\boldsymbol{x}) = m_0\, \phi(\boldsymbol{x})$. The scaled order parameter function $\phi(\boldsymbol{x})$ interpolates between $\phi(-\infty) = -1$ and $\phi(+\infty) = 1$.

Thus, we have

$$\xi^2\, \boldsymbol{\nabla}^2 \phi = -\phi + \phi^3 \quad , \tag{7.351}$$

where $\xi = \sqrt{\kappa/|a|}$. We assume $\phi(\boldsymbol{x}) = \phi(x_1)$ is only a function of the first coordinate. Then the Euler-Lagrange equation becomes

$$\xi^2 \, \frac{d^2\phi}{dx_1^2} = -\phi + \phi^3 \equiv -\frac{dU}{d\phi} \quad , \tag{7.352}$$

where $U(\phi) = -\frac{1}{4}\big(\phi^2 - 1\big)^2$. The 'potential' $U(\phi)$ is an inverted double well, with maxima at $\phi = \pm 1$. The equation $\ddot{\phi} = -U'(\phi)$, where dot denotes differentiation with respect to ϕ, is simply Newton's second

law with time replaced by space. In order to have a stationary solution at $\phi \to \pm\infty$ where $\phi = \pm 1$, the total energy must be $E = U(\phi = \pm 1) = 0$, where $E = \frac{1}{2}\dot{\phi}^2 + U(\phi)$. This leads to the first order differential equation

$$\sqrt{2}\,\xi\,\frac{d\phi}{dx_1} = 1 - \phi^2 \quad , \tag{7.353}$$

with solution

$$\phi(\boldsymbol{x}) = \tanh\bigl(x_1/\sqrt{2}\,\xi\bigr) \qquad \Rightarrow \qquad m(\boldsymbol{x}) = m_0\,\tanh\bigl(x_1/\sqrt{2}\,\xi\bigr) \quad . \tag{7.354}$$

Note that the domain wall width $\xi = \bigl(\kappa/|a|\bigr)^{1/2}$ diverges at the Ising transition where $a = 0$ and that, per eqn. 7.348, the correlation length in the ordered phase is $\xi_{\rm corr} = 2^{-1/2}\xi$.

7.10.3 Ginzburg criterion

Let us define $A(T, H, V, N)$ to be the usual (*i.e.* thermodynamic) Helmholtz free energy. Then

$$e^{-\beta A} = \int Dm\; e^{-\beta F[m(\boldsymbol{x})]} \quad , \tag{7.355}$$

where the functional $F[m(\boldsymbol{x})]$ is of the Ginzburg-Landau form, given in eqn. 7.349. The integral above is a *functional integral*. We can give it a more precise meaning by defining its measure in the case of periodic functions $m(\boldsymbol{x})$ confined to a rectangular box. Then we can expand

$$m(\boldsymbol{x}) = \frac{1}{\sqrt{V}}\sum_{\boldsymbol{q}} \hat{m}_{\boldsymbol{q}}\, e^{i\boldsymbol{q}\cdot\boldsymbol{x}} \quad , \tag{7.356}$$

and we define the measure

$$Dm \equiv d\hat{m}_0 \prod_{\boldsymbol{q}}{}' d\,\mathsf{Re}\;\hat{m}_{\boldsymbol{q}}\, d\,\mathsf{Im}\;\hat{m}_{\boldsymbol{q}} \quad , \tag{7.357}$$

where the prime on the sum indicates that for each pair $(\boldsymbol{q}, -\boldsymbol{q})$ with $\boldsymbol{q} \neq 0$ only one representative is chosen. Note that the fact that $m(\boldsymbol{x}) \in \mathbb{R}$ means that $\hat{m}_{-\boldsymbol{q}} = \hat{m}^*_{\boldsymbol{q}}$. We'll assume $T > T_{\rm c}$ and $H = 0$ and we'll explore limit $T \to T_{\rm c}^+$ from above to analyze the properties of the critical region close to $T_{\rm c}$. In this limit we can ignore all but the quadratic terms in m, and we have

$$e^{-\beta A} = \int Dm\,\exp\left(-\tfrac{1}{2}\beta\sum_{\boldsymbol{q}}(a + \kappa\,\boldsymbol{q}^2)\,|\hat{m}_{\boldsymbol{q}}|^2\right) = \left(\frac{2\pi k_{\rm B}T}{a}\right)^{1/2}\prod_{\boldsymbol{q}}{}'\left(\frac{\pi k_{\rm B}T}{a + \kappa\,\boldsymbol{q}^2}\right)^{1/2} \quad . \tag{7.358}$$

Thus,

$$A = \tfrac{1}{2}k_{\rm B}T\sum_{\boldsymbol{q}}\log\left(\frac{a + \kappa\,\boldsymbol{q}^2}{\pi k_{\rm B}T}\right) \quad . \tag{7.359}$$

Close to the critical point, we write $a(T) = \alpha t$, where t is the dimensionless quantity $t \equiv (T - T_{\rm c})/T_{\rm c}$, known as the *reduced temperature*.

We now compute the heat capacity $C_V = -T\,\partial^2 A/\partial T^2$. We are really only interested in the singular contributions to C_V, which means that we're only interested in differentiating with respect to T as it appears in $a(T)$. We divide by $Nk_{\rm B}$ where N is the number of unit cells of our system, which we

presume is a lattice-based model. Note $N \sim V/\mathsf{a}^d$ where V is the volume and a the lattice constant. The dimensionless heat capacity per lattice site is then

$$c \equiv \frac{C_V}{N k_{\rm B}} = \frac{\alpha^2 \mathsf{a}^d}{2\kappa^2} \int^{\Lambda} \frac{d^d q}{(2\pi)^d} \, \frac{1}{(\xi^{-2} + \boldsymbol{q}^2)^2} \quad , \tag{7.360}$$

where $\xi = (\kappa/\alpha t)^{1/2} \propto |t|^{-1/2}$ is the correlation length, and where $\Lambda \sim \mathsf{a}^{-1}$ is an ultraviolet cutoff. We define $R_* \equiv (\kappa/\alpha)^{1/2}$, in which case

$$c = \tfrac{1}{2} R_*^{-4} \, \mathsf{a}^d \, \xi^{4-d} \int^{\Lambda\xi} \frac{d^d \bar{q}}{(2\pi)^d} \, \frac{1}{(1+\bar{q}^2)^2} \quad , \tag{7.361}$$

where $\bar{\boldsymbol{q}} \equiv \boldsymbol{q}\xi$. Thus,

$$c(t) \sim \begin{cases} \text{const.} & \text{if } d > 4 \\ -\log t & \text{if } d = 4 \\ t^{\frac{d}{2}-2} & \text{if } d < 4 \quad . \end{cases} \tag{7.362}$$

For $d > 4$, mean field theory is qualitatively accurate, with finite corrections. In dimensions $d \le 4$, the mean field result is overwhelmed by fluctuation contributions as $t \to 0^+$ (*i.e.* as $T \to T_{\rm c}^+$). We see that MFT is sensible provided the fluctuation contributions are small, *i.e.* provided $R_*^{-4} \, \mathsf{a}^d \, \xi^{4-d} \ll 1$, which entails $t \gg t_{\rm G}$, where

$$t_{\rm G} = \left(\frac{\mathsf{a}}{R_*} \right)^{2d/(4-d)} \tag{7.363}$$

is the *Ginzburg reduced temperature*. The criterion for the sufficiency of mean field theory, namely $t \gg t_{\rm G}$, is known as the *Ginzburg criterion*. The region $|t| < t_{\rm G}$ is known as the *critical region*.

In a lattice ferromagnet, as we have seen, $R_* \sim \mathsf{a}$ is on the scale of the lattice spacing itself, hence $t_{\rm G} \sim 1$ and the critical regime is very large. Mean field theory then fails quickly as $T \to T_{\rm c}$. In a (conventional) three-dimensional superconductor, R_* is on the order of the Cooper pair size, and $R_*/\mathsf{a} \sim 10^2 - 10^3$, hence $t_{\rm G} = (a/R_*)^6 \sim 10^{-18} - 10^{-12}$ is negligibly narrow. The mean field theory of the superconducting transition – BCS theory – is then valid essentially all the way to $T = T_{\rm c}$.

7.11 Appendix I: Bifurcations

7.11.1 $N = 1$ dynamical systems

A dynamical system with an $N = 1$ dimensional phase space is a first order ODE $\dot{u} = g(u)$, where $g(u)$ is in general a nonlinear function of u. Thus $\dot{u} > 0$ for values of u where $g(u) > 0$ and $\dot{u} < 0$ for values of u where $g(u) < 0$. For $u = u^*$ where $g(u^*) = 0$ we have a *fixed point*. Linearizing about the fixed point, we write $u = u^* + \eta$, in which case $\dot{\eta} = g'(u^*)\,\eta$. Thus $\eta(t) = \eta(0) \, \exp\big[g'(u^*)t\big]$, which says that $|\eta(t)|$ grows exponentially if $g'(u^*) > 0$ and $|\eta(t)|$ shrinks exponentially if $g'(u^*) < 0$. Thus, for $g'(u^*) > 0$ we say that u^* is an *unstable fixed point* (UFP), while for $g'(u^*) < 0$ we say that u^* is a *stable fixed point* (SFP). The linearization about a UFP rapidly fails due to the exponential increase of the distance from u^*, while the linearization about a SFP gets ever more accurate as $\eta(t) \to 0$.

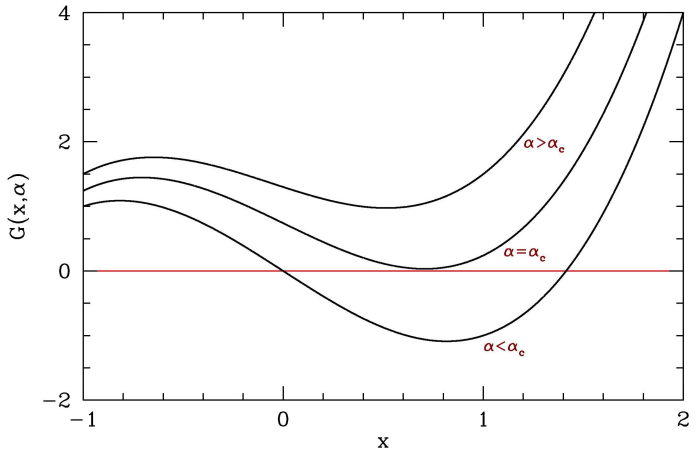


Figure 7.27: Evolution of $G(x,\alpha)$ as a function of the control parameter α.

7.11.2 Saddle-node bifurcation

Generically, $g'(u^*) \neq 0$ at points where $g(u^*) = 0$, since two equations in a single unknown is an overdetermined set. However, consider the function $G(x,\alpha)$, where α is a control parameter. If we demand $G(x,\alpha) = 0$ and $\partial_x G(x,\alpha) = 0$, we have two equations in two unknowns, and in general there will be a zero-dimensional solution set consisting of points $(x_{\rm c},\alpha_{\rm c})$. The situation is depicted in Fig. 7.27.

Let's expand $G(x,\alpha)$ in the vicinity of such a point $(x_{\rm c},\alpha_{\rm c})$:

$$\begin{aligned} G(x,\alpha) &= G(x_{\rm c},\alpha_{\rm c}) + \left.\frac{\partial G}{\partial x}\right|_{(x_{\rm c},\alpha_{\rm c})} (x-x_{\rm c}) + \left.\frac{\partial G}{\partial \alpha}\right|_{(x_{\rm c},\alpha_{\rm c})} (\alpha-\alpha_{\rm c}) + \frac{1}{2}\left.\frac{\partial^2 G}{\partial x^2}\right|_{(x_{\rm c},\alpha_{\rm c})} (x-x_{\rm c})^2 \\ &\qquad + \left.\frac{\partial^2 G}{\partial x\,\partial \alpha}\right|_{(x_{\rm c},\alpha_{\rm c})} (x-x_{\rm c})\,(\alpha-\alpha_{\rm c}) + \frac{1}{2}\left.\frac{\partial^2 G}{\partial \alpha^2}\right|_{(x_{\rm c},\alpha_{\rm c})} (\alpha-\alpha_{\rm c})^2 + \ldots \\ &= A\,(\alpha-\alpha_{\rm c}) + B\,(x-x_{\rm c})^2 + \ldots \quad , \end{aligned} \tag{7.364}$$

where we keep terms of lowest order in the deviations δx and $\delta\alpha$. Note that we can separately change the signs of A and B by redefining $\alpha \to -\alpha$ and/or $x \to -x$, so without loss of generality we may assume both A and B are positive. If we now rescale $u \equiv \sqrt{B/A}\,(x-x_{\rm c})$, $r \equiv \alpha - \alpha_{\rm c}$, and $\tau = \sqrt{AB}\,t$, we have, neglecting the higher order terms, we obtain the 'normal form' of the saddle-node bifurcation,

$$\frac{du}{d\tau} = r + u^2 \quad . \tag{7.365}$$

The evolution of the flow is depicted in Fig. 7.28. For $r < 0$ there are two fixed points – one stable ($u^* = -\sqrt{-r}$) and one unstable ($u = +\sqrt{-r}$). At $r = 0$ these two nodes coalesce and annihilate each other. (The point $u^* = 0$ is half-stable precisely at $r = 0$.) For $r > 0$ there are no longer any fixed points in the vicinity of $u = 0$. In the left panel of Fig. 7.29 we show the flow in the extended (r,u) plane. The unstable and stable nodes annihilate at $r = 0$.

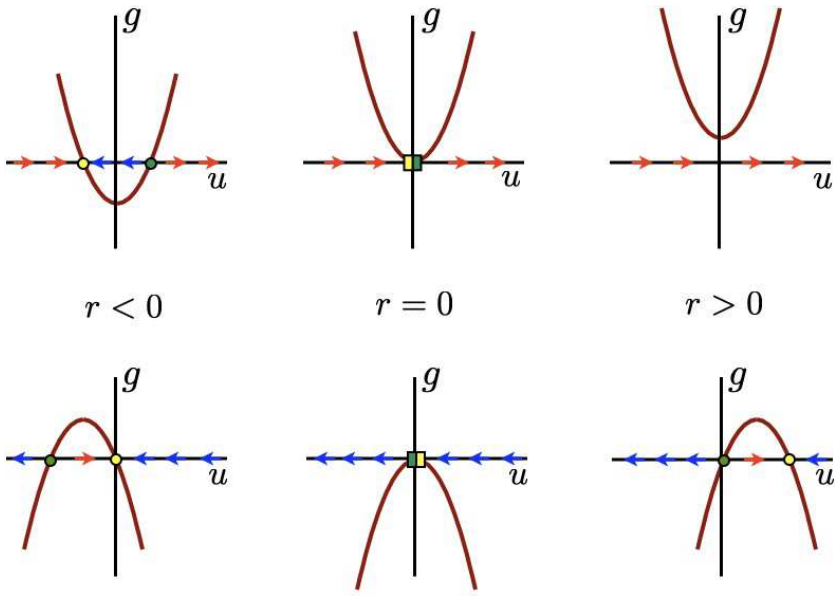


Figure 7.28: Flow diagrams for the saddle-node bifurcation $\dot{u} = r + u^2$ (top) and the transcritical bifurcation $\dot{u} = ru - u^2$ (bottom).

7.11.3 Transcritical bifurcation

Another situation which arises frequently is the *transcritical bifurcation*. Consider the equation $\dot{x} = g(x)$ in the vicinity of a fixed point x^*.

$$\frac{dx}{dt} = g'(x^*)\,(x - x^*) + \tfrac{1}{2}\,g''(x^*)(x - x^*)^2 + \ldots \quad . \tag{7.366}$$

We rescale $u \equiv \beta\,(x - x^*)$ with $\beta = -\frac{1}{2}\,g''(x^*)$ and define $r \equiv g'(x^*)$ as the control parameter, to obtain, to order u^2,

$$\frac{du}{dt} = ru - u^2 \quad . \tag{7.367}$$

Note that the sign of the u^2 term can be reversed relative to the others by sending $u \to -u$.

Consider a crude model of a laser threshold. Let n be the number of photons in the laser cavity, and N the number of excited atoms in the cavity. The dynamics of the laser are approximated by the equations

$$\begin{aligned} \dot{n} &= \gamma N n - k n \\ N &= N_0 - \alpha n \quad . \end{aligned} \tag{7.368}$$

Here γ is the gain coefficient and k the photon decay rate. N_0 is the pump strength, and α is a numerical factor. The first equation tells us that the number of photons in the cavity grows with a rate $\gamma N - k$, *i.e.* gain is proportional to the number of excited atoms, and the loss rate is a constant cavity-dependent quantity (typically through the ends, which are semi-transparent). The second equation says that the number of excited atoms is equal to the pump strength minus a term proportional to the number of photons (since the presence of a photon means an excited atom has decayed). Putting them together,

$$\dot{n} = (\gamma N_0 - k)\,n - \alpha\gamma n^2 \quad , \tag{7.369}$$

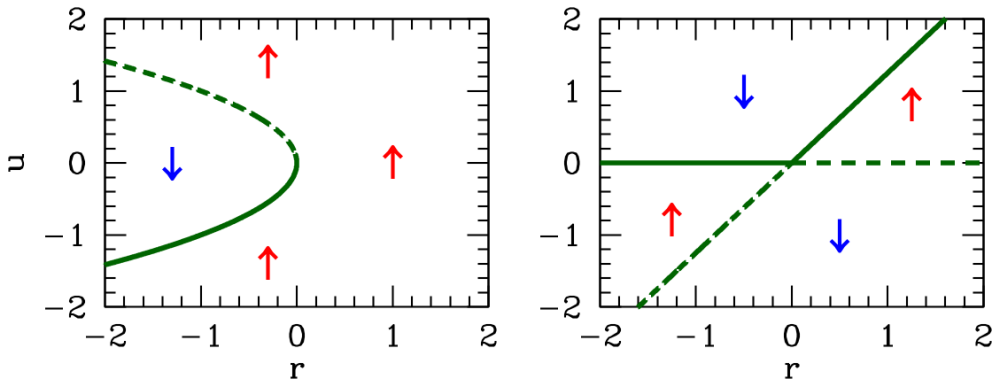


Figure 7.29: Extended phase space (r, u) flow diagrams for the saddle-node bifurcation $\dot{u} = r + u^2$ (left) and the transcritical bifurcation $\dot{u} = ru - u^2$ (right).

which exhibits a transcritical bifurcation at pump strength $N_0 = k/\gamma$. For $N_0 < k/\gamma$ the system acts as a lamp; for $N_0 > k/\gamma$ the system acts as a laser.

What happens in the transcritical bifurcation is an exchange of stability of the fixed points at $u^* = 0$ and $u^* = r$ as r passes through zero. This is depicted graphically in the bottom panel of Fig. 7.28.

7.11.4 Pitchfork bifurcation

The pitchfork bifurcation is commonly encountered in systems in which there is an overall parity symmetry ($u \to -u$). There are two classes of pitchfork: supercritical and subcritical. The normal form of the supercritical bifurcation is

$$\dot{u} = ru - u^3 \quad , \tag{7.370}$$

which has fixed points at $u^* = 0$ and $u^* = \pm\sqrt{r}$. Thus, the situation is as depicted in fig. 7.30 (top panel). For $r < 0$ there is a single stable fixed point at $u^* = 0$. For $r > 0$, $u^* = 0$ is unstable, and flanked by two stable fixed points at $u^* = \pm\sqrt{r}$.

If we send $u \to -u$, $r \to -r$, and $t \to -t$, we obtain the *subcritical pitchfork*, depicted in the bottom panel of fig. 7.30. The normal form of the subcritical pitchfork bifurcation is $\dot{u} = ru + u^3$. The fixed point structure in both supercritical and subcritical cases is shown in Fig. 7.31.

7.11.5 Imperfect bifurcation

The imperfect bifurcation occurs when a symmetry-breaking term is added to the pitchfork. The normal form contains two control parameters: $\dot{u} = h + ru - u^3$. The constant h explicitly breaks the $\mathbb{Z}_2$ parity symmetry $u \to -u$.

This equation arises from a crude model of magnetization dynamics. Let m be the magnetization density of a sample, and $f(m)$ the free energy density. Assuming m is small, we can expand $f(m)$ as

$$f(m) = \tfrac{1}{2}am^2 + \tfrac{1}{4}bm^4 - Hm + \ldots \quad , \tag{7.371}$$

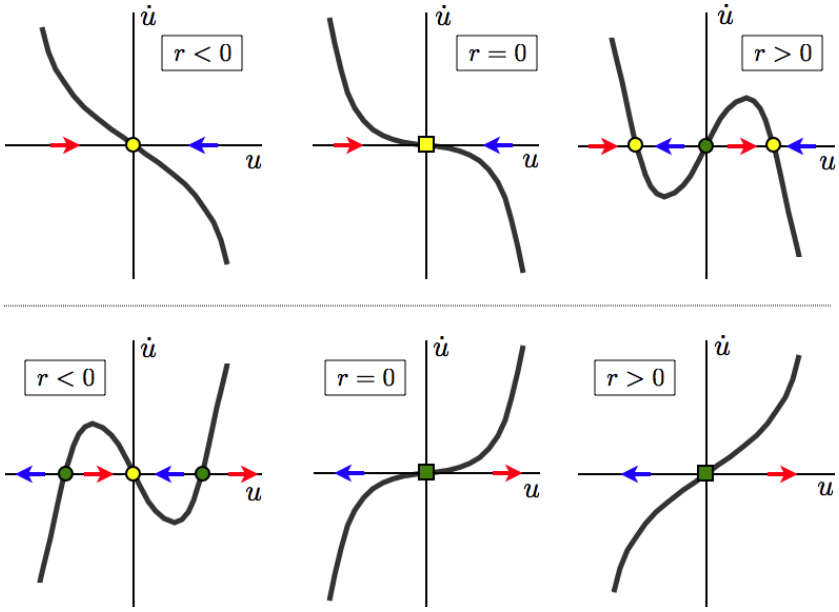


Figure 7.30: Top: supercritical pitchfork bifurcation $\dot{u} = ru - u^3$. Bottom: subcritical pitchfork bifurcation $\dot{u} = ru + u^3$.

where H is the external magnetic field, and a and b are temperature-dependent constants. This is called the *Landau expansion* of the free energy. We assume $b > 0$ in order that the minimum of $f(m)$ not lie at infinity. The dynamics of $m(t)$ are modeled by

$$\frac{dm}{dt} = -\Gamma \frac{\partial f}{\partial m} \quad , \tag{7.372}$$

with $\Gamma > 0$. Thus, the magnetization evolves toward a local minimum in the free energy. Note that the free energy is a decreasing function of time:

$$\frac{df}{dt} = \frac{\partial f}{\partial m}\frac{dm}{dt} = -\Gamma\left(\frac{\partial f}{\partial m}\right)^2 \quad . \tag{7.373}$$

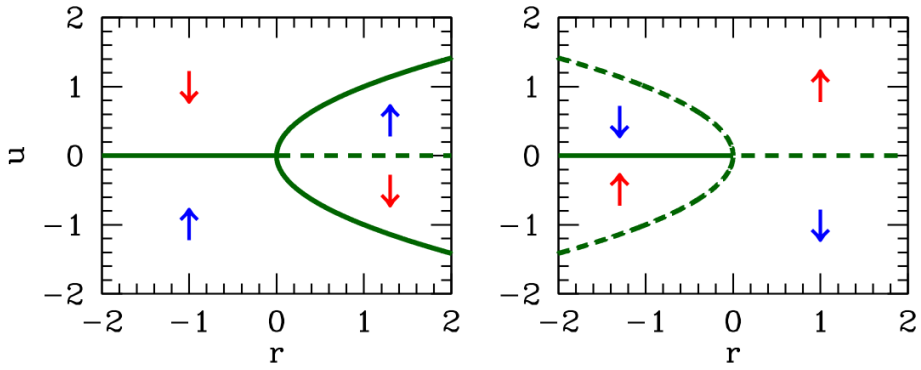


Figure 7.31: Extended phase space (r, u) flow diagrams for the pitchfork bifurcation. Left: supercritical pitchfork $\dot{u} = ru - u^3$. Right: subcritical pitchfork $\dot{u} = ru + u^3$.

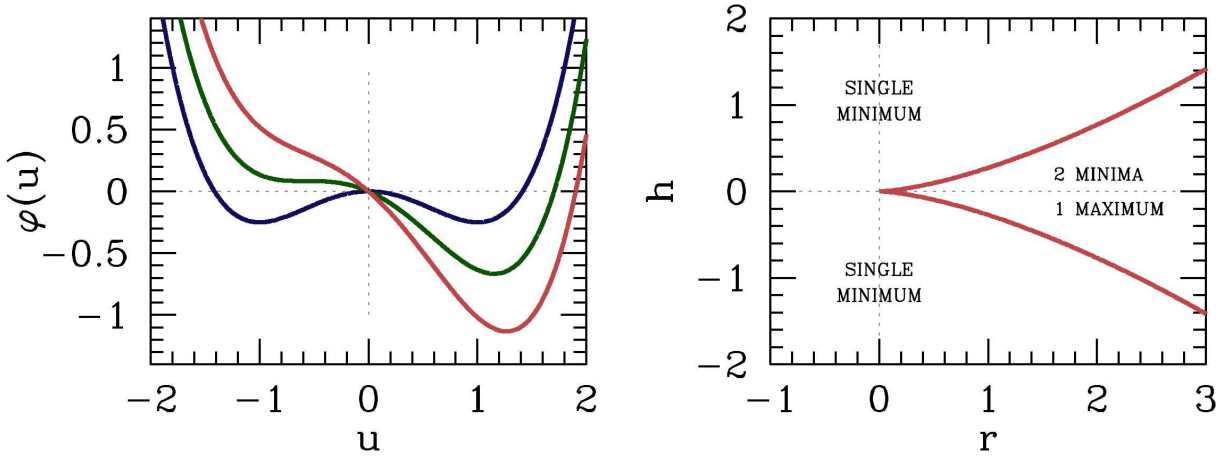


Figure 7.32: Left: scaled free energy $\varphi(u) = -\frac{1}{2}ru^2 + \frac{1}{4}u^4 - hu$, with $h = 0$ (blue), $h = h_{\rm c}$ (green), and $h = 2\,h_{\rm c}$ (red), where $h_{\rm c} = \frac{2}{3\sqrt{3}}\,r^{3/2}$. Right: phase diagram for the imperfect bifurcation $\dot u = -\varphi'(u) = h + ru - u^3$ in the (r, h) plane.

By rescaling $\tau \equiv \Gamma t$, $m \equiv b^{-1/2}u$, $h \equiv b^{1/2}H$, and defining $r \equiv -a$, we obtain the normal form of the bifurcation,

$$\dot u = h + ru - u^3 = -\frac{\partial\varphi}{\partial u} \quad , \tag{7.374}$$

where

$$\varphi(u) = -\tfrac{1}{2}ru^2 + \tfrac{1}{4}u^4 - hu \tag{7.375}$$

is a scaled version of the free energy. Fixed points satisfy the equation

$$u^3 - ru - h = 0 \quad , \tag{7.376}$$

and correspond to extrema in $\varphi(u)$. By the fundamental theorem of algebra, this cubic polynomial may be uniquely factorized over the complex plane. Since the coefficients are real, the complex conjugate $\bar u$ satisfies the same equation as u, hence there are two possibilities for the roots: either (i) all three roots are real, or (ii) one root is real and the other two are a complex conjugate pair. Clearly for $r < 0$ we are in situation (ii) since $u^3 - ru$ is then monotonically increasing for $u \in \mathbb{R}$, and therefore takes the value h precisely once for u real. For $r > 0$, there is a region $h \in \big[-h_{\rm c}(r), h_{\rm c}(r)\big]$ over which there are three real roots. To find $h_{\rm c}(r)$, we demand $\varphi''(u) = 0$ as well as $\varphi'(u) = 0$, which says that two roots have merged in a saddle-node bifurcation, forming an inflection point. Thus $\varphi''(u) = 3u^2 - r = 0$ yields $u = \pm(r/3)^{1/2}$, which requires $r > 0$, and using this to eliminate u from the equation $\varphi'(u) = 0$ yields the critical value of h as a function of r, *viz.* $h_{\rm c}(r) = \frac{2}{3\sqrt{3}}\,r^{3/2}\,\Theta(r)$.

Examples of the function $\varphi(u)$ for $r > 0$ are shown in the left panel of Fig. 7.32 for three different values of h. For $|h| < h_{\rm c}(r)$ there are three extrema satisfying $\varphi'(u^*) = 0$: $u_1^* < u_2^* < 0 < u_3^*$, assuming (without loss of generality) that $h > 0$. Clearly u_1^* is a local minimum, u_2^* a local maximum, and u_3^* the global minimum of the function $f(u)$. The 'phase diagram' for this system, plotted in the (r, h) control parameter space, is shown in the right panel of Fig. 7.32.

In Fig. 7.33 we plot the fixed points $u^*(r)$ for fixed h. A saddle-node bifurcation occurs at $r = r_{\rm c}(h) = \frac{3}{2^{2/3}}\,|h|^{2/3}$. For $h = 0$ this reduces to the supercritical pitchfork; for finite h the pitchfork is deformed and

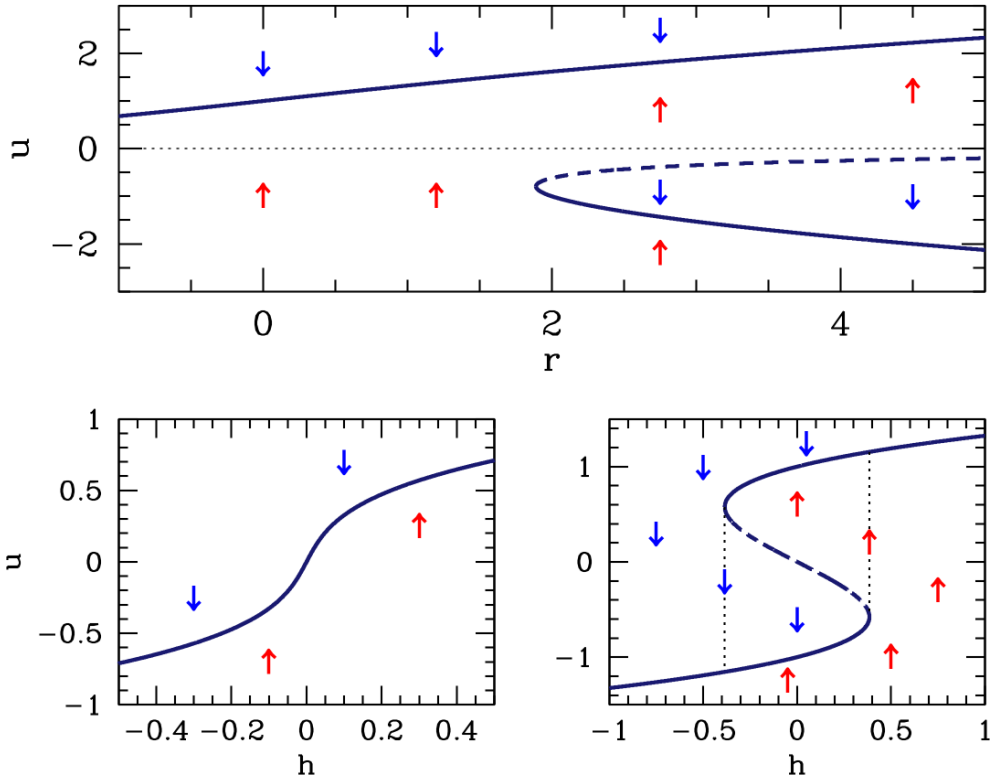


Figure 7.33: Top: extended phase space (r, u) flow diagram for $\dot{u} = h + ru - u^3$, the imperfect pitchfork bifurcation, at $h = 1$. This is in a sense a deformed supercritical pitchfork. The saddle-node bifurcation occurs at $r_{\rm c} = (3/2^{2/3})|h|^{2/3} = 1.8899$. Bottom: extended phase space (h, u) flow diagram for the imperfect pitchfork bifurcation $r = -0.2$ (left panel) and $r = 1$ (right panel). For $r < 0$ the behavior is completely reversible. For $r > 0$, a regime of irreversibility sets in between $-h_{\rm c}$ and $+h_{\rm c}$, where $h_{\rm c} = 2(r/3)^{3/2}$. The system then exhibits the phenomenon of hysteresis. The dotted vertical lines show the boundaries of the hysteresis loop.

even changed topologically. Finally, in Fig. 7.33 we show the behavior of $u^*(h)$ for fixed r. When $r < 0$ the curve retraces itself as h is ramped up and down, but for $r > 0$ the system exhibits the phenomenon of *hysteresis*, *i.e.* there is an irreversible aspect to the behavior. Fig. 7.33 shows a *hysteresis loop* when $r > 0$.

7.12 Appendix II: Equivalence of the Mean Field Descriptions

In both the variational density matrix and mean field Hamiltonian methods as applied to the Ising model, we obtained the same result $m = \tanh\big((m + h)/\theta\big)$. What is perhaps not obvious is whether these theories are in fact the same, *i.e.* if their respective free energies agree. Indeed, the two free energy functions,

$$f_{\rm A}(m, h, \theta) = -\tfrac{1}{2}\, m^2 - hm + \theta \left\{ \left(\frac{1+m}{2} \right) \log \left(\frac{1+m}{2} \right) + \left(\frac{1-m}{2} \right) \log \left(\frac{1-m}{2} \right) \right\} \tag{7.377}$$

and

$$f_{\rm B}(m,h,\theta) = +\tfrac{1}{2}\,m^2 - \theta\,\log\left(e^{+(m+h)/\theta} + e^{-(m+h)/\theta}\right) \quad , \tag{7.378}$$

where $f_{\rm A}$ is the variational density matrix result and $f_{\rm B}$ is the mean field Hamiltonian result, clearly are different functions of their arguments. However, it turns out that upon minimizing with respect to m in each case, the resulting free energies obey $f_{\rm A}(h,\theta) = f_{\rm B}(h,\theta)$. This agreement may seem surprising. The first method utilizes an approximate (variational) density matrix applied to the exact Hamiltonian $\hat{H}$. The second method approximates the Hamiltonian as $\hat{H}_{\rm MF}$, but otherwise treats it exactly. The two Landau expansions seem hopelessly different:

$$\begin{aligned} f_{\rm A}(m,h,\theta) &= -\theta\,\log 2 - hm + \tfrac{1}{2}\,(\theta-1)\,m^2 + \tfrac{\theta}{12}\,m^4 + \tfrac{\theta}{30}\,m^6 + \ldots \\ f_{\rm B}(m,h,\theta) &= -\theta\,\log 2 + \tfrac{1}{2}m^2 - \frac{(m+h)^2}{2\,\theta} + \frac{(m+h)^4}{12\,\theta^3} - \frac{(m+h)^6}{45\,\theta^5} + \ldots \quad . \end{aligned} \tag{7.379}$$

We shall now prove that these two methods, the variational density matrix and the mean field approach, are in fact equivalent, and yield the *same* free energy $f(\theta,h)$.

Let us generalize the Ising model and write

$$\hat{H} = -\sum_{i<j} J_{ij}\,\varepsilon(\sigma_i,\sigma_j) - \sum_i \Phi(\sigma_i) \quad . \tag{7.380}$$

Here, each 'spin' σ_i may take on any of K possible values, $\{s_1,\ldots,s_K\}$. For the $S=1$ Ising model, we would have $K=3$ possibilities, with $s_1=-1$, $s_2=0$, and $s_3=+1$. But the set $\{s_\alpha\}$, with $\alpha\in\{1,\ldots,K\}$, is completely arbitrary[50]. The 'local field' term $\Phi(\sigma)$ is also a completely arbitrary function. It may be linear, with $\Phi(\sigma) = H\sigma$, for example, but it could also contain terms quadratic in σ, or whatever one desires.

The symmetric, dimensionless interaction function $\varepsilon(\sigma,\sigma') = \varepsilon(\sigma',\sigma)$ is a real symmetric $K\times K$ matrix. According to the spectral decomposition theorem, any such matrix may be written in the form

$$\varepsilon(\sigma,\sigma') = \sum_{p=1}^{N_{\rm s}} A_p\,\lambda_p(\sigma)\,\lambda_p(\sigma') \quad , \tag{7.381}$$

where $\{A_p\}$ are the eigenvalues and $\big\{\lambda_p(\sigma)\big\}$ the eigenvectors. The number of terms $N_{\rm s}$ in this decomposition is such that $N_{\rm s}\le K$. This treatment can be generalized to account for continuous σ.

7.12.1 Variational density matrix

The most general single-site variational density matrix is written

$$\varrho(\sigma) = \sum_{\alpha=1}^{K} x_\alpha\,\delta_{\sigma,s_\alpha} \quad . \tag{7.382}$$

[50] It needn't be an equally spaced sequence, for example.

Thus, x_α is the probability for a given site to be in state α, with $\sigma = s_\alpha$. *The* $\{x_\alpha\}$ *are the* K *variational parameters, subject to the single normalization constraint,* $\sum_\alpha x_\alpha = 1$. We now have

$$\begin{aligned} f &= \frac{1}{N\hat{J}(0)}\Big\{ \mathsf{Tr}\,(\varrho\hat{H}) + k_{\rm B}T\ \mathsf{Tr}\,(\varrho\log\varrho)\Big\} \\ &= -\tfrac{1}{2}\sum_p\sum_{\alpha,\alpha'} A_p\,\lambda_p(s_\alpha)\,\lambda_p(s_{\alpha'})\,x_\alpha\,x_{\alpha'} - \sum_\alpha \varphi(s_\alpha)\,x_\alpha + \theta\sum_\alpha x_\alpha\log x_\alpha \quad , \end{aligned} \tag{7.383}$$

where $\varphi(\sigma) = \Phi(\sigma)/\hat{J}(0)$. We extremize in the usual way, introducing a Lagrange undetermined multiplier ζ to enforce the constraint. This means we extend the function $f\big(\{x_\alpha\}\big)$, writing

$$f^*(x_1,\ldots,x_K,\zeta) = f(x_1,\ldots,x_K) + \zeta\left(\sum_{\alpha=1}^K x_\alpha - 1\right) \quad , \tag{7.384}$$

and freely extremizing with respect to the $(K+1)$ parameters $\{x_1,\ldots,x_K,\zeta\}$. This yields K nonlinear equations,

$$0 = \frac{\partial f^*}{\partial x_\alpha} = -\sum_p\sum_{\alpha'} A_p\,\lambda_p(s_\alpha)\,\lambda_p(s_{\alpha'})\,x_{\alpha'} - \varphi(s_\alpha) + \theta\,\log x_\alpha + \zeta + \theta \quad , \tag{7.385}$$

for each α, and one linear equation, which is the normalization condition,

$$0 = \frac{\partial f^*}{\partial\zeta} = \sum_\alpha x_\alpha - 1 \quad . \tag{7.386}$$

We cannot solve these nonlinear equations analytically, but they may be recast, by exponentiating them, as

$$x_\alpha = \frac{1}{Z}\,\exp\left\{\frac{1}{\theta}\left[\sum_p\sum_{\alpha'} A_p\,\lambda_p(s_\alpha)\,\lambda_p(s_{\alpha'})\,x_{\alpha'} + \varphi(s_\alpha)\right]\right\} \quad , \tag{7.387}$$

with

$$Z = e^{(\zeta/\theta)+1} = \sum_\alpha \exp\left\{\frac{1}{\theta}\left[\sum_p\sum_{\alpha'} A_p\,\lambda_p(s_\alpha)\,\lambda_p(s_{\alpha'})\,x_{\alpha'} + \varphi(s_\alpha)\right]\right\} \quad . \tag{7.388}$$

From the logarithm of x_α, we may compute the entropy, and, finally, the free energy:

$$f(\theta) = \tfrac{1}{2}\sum_p\sum_{\alpha,\alpha'} A_p\,\lambda_p(s_\alpha)\,\lambda_p(s_{\alpha'})\,x_\alpha\,x_{\alpha'} - \theta\log Z \quad , \tag{7.389}$$

which is to be evaluated at the solution of 7.384, $\big\{x^*_\alpha(h,\theta)\big\}$.

7.12.2 Mean field approximation

We now derive a mean field approximation in the spirit of that used in the Ising model above. We write

$$\lambda_p(\sigma) = \big\langle\lambda_p(\sigma)\big\rangle + \delta\lambda_p(\sigma) \quad , \tag{7.390}$$

and abbreviate $\bar\lambda_p = \big\langle \lambda_p(\sigma) \big\rangle$, the thermodynamic average of $\lambda_p(\sigma)$ on any given site. We then have

$$\begin{aligned}\lambda_p(\sigma)\,\lambda_p(\sigma') &= \bar\lambda_p^2 + \bar\lambda_p\,\delta\lambda_p(\sigma) + \bar\lambda_p\,\delta\lambda_p(\sigma') + \delta\lambda_p(\sigma)\,\delta\lambda_p(\sigma') \\ &= -\bar\lambda_p^2 + \bar\lambda_p\,\big(\lambda_p(\sigma) + \lambda_p(\sigma')\big) + \delta\lambda_p(\sigma)\,\delta\lambda_p(\sigma') \quad .\end{aligned} \tag{7.391}$$

The product $\delta\lambda_p(\sigma)\,\delta\lambda_p(\sigma')$ is of second order in fluctuations, and we neglect it. This leads us to the mean field Hamiltonian,

$$\hat H_{\rm MF} = +\tfrac{1}{2} N \hat J(0) \sum_p A_p\,\bar\lambda_p^2 - \sum_{i=1}^N \left[\hat J(0) \sum_p A_p\,\bar\lambda_p\,\lambda_p(\sigma_i) + \Phi(\sigma_i) \right] \quad . \tag{7.392}$$

The free energy is then

$$f\big(\{\bar\lambda_p\},\theta\big) = \tfrac{1}{2}\sum_p A_p\,\bar\lambda_p^2 - \theta\,\log \sum_\alpha \exp\left\{ \frac{1}{\theta}\Big[\sum_p A_p\,\bar\lambda_p\,\lambda_p(s_\alpha) + \varphi(s_\alpha) \Big] \right\} \quad . \tag{7.393}$$

The variational parameters are the mean field values $\big\{\bar\lambda_p\big\}$.

The single site probabilities $\{x_\alpha\}$ are then

$$x_\alpha = \frac{1}{Z}\,\exp\left\{ \frac{1}{\theta}\left[\sum_p A_p\,\bar\lambda_p\,\lambda_p(s_\alpha) + \varphi(s_\alpha) \right] \right\} \quad , \tag{7.394}$$

with Z implied by the normalization $\sum_\alpha x_\alpha = 1$. These results reproduce exactly what we found in eqn. 7.384, since the mean field equation here, $\partial f/\partial\bar\lambda_p = 0$, yields

$$\bar\lambda_p = \sum_{\alpha=1}^K \lambda_p(s_\alpha)\,x_\alpha \quad . \tag{7.395}$$

The free energy is immediately found to be

$$f(\theta) = \tfrac{1}{2}\sum_p A_p\,\bar\lambda_p^2 - \theta\,\log Z \quad , \tag{7.396}$$

which again agrees with what we found using the variational density matrix.

Thus, whether one extremizes with respect to the set $\{x_1,\ldots,x_K,\zeta\}$, or with respect to the set $\{\bar\lambda_p\}$, the results are the same, in terms of all these parameters, as well as the free energy $f(\theta)$. Generically, both approaches may be termed 'mean field theory' since the variational density matrix corresponds to a mean field which acts on each site independently[51].

[51] The function $\Phi(\sigma)$ may involve one or more adjustable parameters which could correspond, for example, to an external magnetic field h. We suppress these parameters when we write the free energy as $f(\theta)$.

7.13 Appendix III: Additional Examples of Mean Field Theory

7.13.1 Blume-Capel model

The Blume-Capel model provides a simple and convenient way to model systems with vacancies. The simplest version of the model is written

$$\hat{H} = -\frac{1}{2}\sum_{i,j=1}^{N} J_{ij}\, S_i\, S_j + \Delta \sum_{i=1}^{N} S_i^2 \quad . \tag{7.397}$$

The spin variables S_i range over the values $\{-1\,,\,0\,,\,+1\}$, so this is an extension of the $S = 1$ Ising model. We explicitly separate out the diagonal terms, writing $J_{ii} \equiv 0$, and placing them in the second term on the RHS above. We say that site i is occupied if $S_i = \pm 1$ and vacant if $S_i = 0$, and we identify $-\Delta$ as the vacancy creation energy, which may be positive or negative, depending on whether vacancies are disfavored or favored in our system.

We make the mean field *Ansatz*, writing $S_i = m + \delta S_i$. This results in the mean field Hamiltonian,

$$\hat{H}_{\rm MF} = \tfrac{1}{2} N \hat{J}(0)\, m^2 - \hat{J}(0)\, m \sum_{i=1}^{N} S_i + \Delta \sum_{i=1}^{N} S_i^2 \quad . \tag{7.398}$$

Once again, we adimensionalize, writing $f \equiv F/N\hat{J}(0)$, $\theta = k_{\rm B}T/\hat{J}(0)$, and $\delta = \Delta/\hat{J}(0)$. We assume $\hat{J}(0) > 0$. The free energy per site is then

$$f(m,\theta,\delta) = \tfrac{1}{2}m^2 - \theta \log\Big(1 + 2e^{-\delta/\theta}\,\cosh(m/\theta)\Big) \quad . \tag{7.399}$$

Extremizing with respect to m, we obtain the mean field equation,

$$m = \frac{2\sinh(m/\theta)}{\exp(\delta/\theta) + 2\cosh(m/\theta)} \quad . \tag{7.400}$$

Note that $m = 0$ is always a solution. Finding the slope of the RHS at $m = 0$ and setting it to unity at $\theta = \theta^*$ yields

$$\theta^*(\delta) = \frac{2}{\exp(\delta/\theta^*) + 2} \quad . \tag{7.401}$$

This is an implicit equation for θ^* in terms of the vacancy energy δ. Equivalently, we can write

$$\delta^*(\theta) = \theta \log\left(\frac{2}{\theta} - 2\right) \quad . \tag{7.402}$$

Is $\theta^*(\delta)$ the critical temperature? We need to investigate further.

Let's expand the free energy in terms of the magnetization m. We find, to fourth order,

$$\begin{aligned} f = -\theta \log\big(1 + 2e^{-\delta/\theta}\big) + \frac{1}{2\theta}\left(\theta - \frac{2}{2+\exp(\delta/\theta)}\right)m^2 \\ + \frac{1}{12\,\big(2+\exp(\delta/\theta)\big)\theta^3}\left(\frac{6}{2+\exp(\delta/\theta)} - 1\right)m^4 + \ldots \quad . \end{aligned} \tag{7.403}$$

Note that setting the coefficient of the m^2 term to zero yields the equation for $\theta^*(\delta)$. However, upon further examination, we see that the coefficient of the m^4 term can *also* vanish. As we have seen, when the coefficients of the m^2 and the m^4 terms vanish concomitantly, we have a *tricritical point*[52]. Setting both coefficients to zero, we obtain

$$\theta_{\rm t} = \tfrac{1}{3} \quad , \quad \delta_{\rm t} = \tfrac{2}{3}\log 2 \quad . \tag{7.404}$$

At $\theta = 0$, it is easy to see we have a first order transition at $\delta = \frac{1}{2}$, simply by comparing the energies of the paramagnetic ($S_i = 0$) and ferromagnetic ($S_i = +1$ or $S_i = -1$) states. We have

$$\frac{E_{\rm MF}}{N\hat{J}(0)} = \begin{cases} 0 & \text{if } m = 0 \\ -\frac{1}{2} + \delta & \text{if } m = \pm 1 \end{cases} \quad . \tag{7.405}$$

These results are exact, and not only valid for the mean field theory. Mean field theory is approximate because it neglects fluctuations, but at zero temperature, there are no fluctuations to neglect!

How about the first order line in the phase diagram? To fix this, we seek the boundary between what are the analogs to regions D and E in fig. **??**. This requires that $\partial^2 f/\partial m^2 > 0$ for $m = 0$, which means $\delta > \delta^*(\theta)$. We then invoke the mean field equation eqn. 7.399 as well as the condition $f(m) = f(0)$. This latter condition is found to be

$$m^2 = 2\theta \log\left(\frac{1 + 2e^{-\delta/\theta}\cosh(m/\theta)}{1 + 2e^{-\delta/\theta}}\right) \quad . \tag{7.406}$$

The simultaneous solution of this equation and the mean field equation yield the equation of the first order portion of the critical line $\delta_{\rm c}(\theta)$, as well as the order parameter discontinuity $m^*(\theta)$ at the first order transition. As $\theta \to \theta_{\rm t}^-$, we have $\delta^*(\theta_{\rm t}^-) = \delta_{\rm t} = \frac{2}{3}\log 2$ and $m^*(\theta_{\rm t}^-) = 0$.

The phase diagram is shown in fig. 7.34. Note that for δ large and negative, vacancies are strongly disfavored, hence the only allowed states on each site have $S_i = \pm 1$, which is our old friend the two-state Ising model. Accordingly, the phase boundary there approaches the vertical line $\theta_{\rm c} = 1$, which is the mean field transition temperature for the two-state Ising model.

7.13.2 Ising antiferromagnet in an external field

Consider the following model:

$$\hat{H} = J\sum_{\langle ij\rangle} \sigma_i\,\sigma_j - H\sum_{i=1}^{N}\sigma_i \quad , \tag{7.407}$$

with $J > 0$ and $\sigma_i = \pm 1$. We've solved for the mean field phase diagram of the Ising ferromagnet; what happens if the interactions are antiferromagnetic?

It turns out that under certain circumstances, the ferromagnet and the antiferromagnet behave exactly the same in terms of their phase diagram, response functions, *etc.* This occurs when $H = 0$, and when

[52] We should really check that the coefficient of the sixth order term is positive, but that is left as an exercise to the eager student.

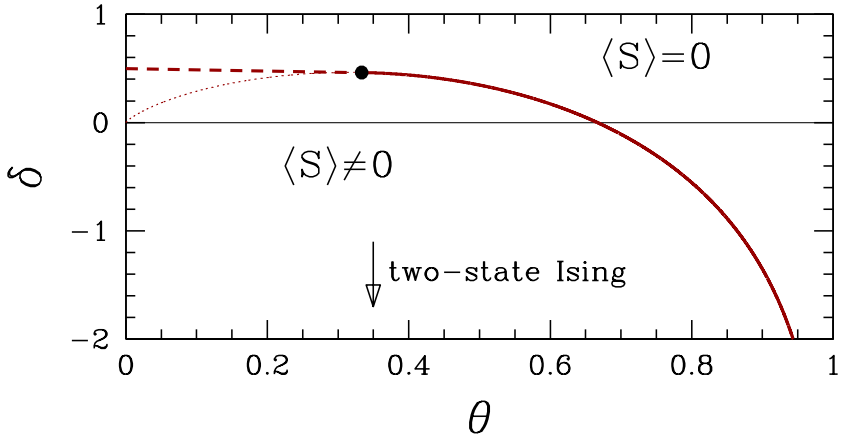


Figure 7.34: Mean field phase diagram for the Blume-Capel model. The black dot signifies a tricritical point, where the coefficients of m^2 and m^4 in the Landau free energy expansion both vanish. The dashed curve denotes a first order transition, and the solid curve a second order transition. The thin dotted line is the continuation of the $\delta^*(\theta)$ relation to zero temperature.

the interactions are between nearest neighbors on a *bipartite lattice*. A bipartite lattice is one which can be divided into two sublattices, which we call A and B, such that an A site has only B neighbors, and a B site has only A neighbors. The square, honeycomb, and body centered cubic (BCC) lattices are bipartite. The triangular and face centered cubic lattices are non-bipartite. Now if the lattice is bipartite and the interaction matrix J_{ij} is nonzero only when i and j are from different sublattices (they needn't be nearest neighbors only), then we can simply redefine the spin variables such that

$$\sigma'_j = \begin{cases} +\sigma_j & \text{if } j \in \mathrm{A} \\ -\sigma_j & \text{if } j \in \mathrm{B} \end{cases} \quad . \tag{7.408}$$

Then $\sigma'_i \sigma'_j = -\sigma_i \, \sigma_j$, and in terms of the new spin variables the exchange constant has reversed. The thermodynamic properties are invariant under such a redefinition of the spin variables.

We can see why this trick doesn't work in the presence of a magnetic field, because the field H would have to be reversed on the B sublattice. In other words, the thermodynamics of an Ising ferromagnet on a bipartite lattice in a uniform applied field is identical to that of the Ising antiferromagnet, with the same exchange constant (in magnitude), in the presence of a *staggered field* $H_{\mathrm{A}} = +H$ and $H_{\mathrm{B}} = -H$.

We treat this problem using the variational density matrix method, using two independent variational parameters m_{A} and m_{B} for the two sublattices:

$$\begin{aligned} \varrho_{\mathrm{A}}(\sigma) &= \frac{1+m_{\mathrm{A}}}{2}\,\delta_{\sigma,1} + \frac{1-m_{\mathrm{A}}}{2}\,\delta_{\sigma,-1} \\ \varrho_{\mathrm{B}}(\sigma) &= \frac{1+m_{\mathrm{B}}}{2}\,\delta_{\sigma,1} + \frac{1-m_{\mathrm{B}}}{2}\,\delta_{\sigma,-1} \quad . \end{aligned} \tag{7.409}$$

With the usual adimensionalization, $f = F/NzJ$, $\theta = k_{\mathrm{B}}T/zJ$, and $h = H/zJ$, we have the free energy

$$f(m_{\mathrm{A}}, m_{\mathrm{B}}) = \tfrac{1}{2} m_{\mathrm{A}} m_{\mathrm{B}} - \tfrac{1}{2}\,h\,(m_{\mathrm{A}} + m_{\mathrm{B}}) - \tfrac{1}{2}\,\theta\,s(m_{\mathrm{A}}) - \tfrac{1}{2}\,\theta\,s(m_{\mathrm{B}}) \quad , \tag{7.410}$$

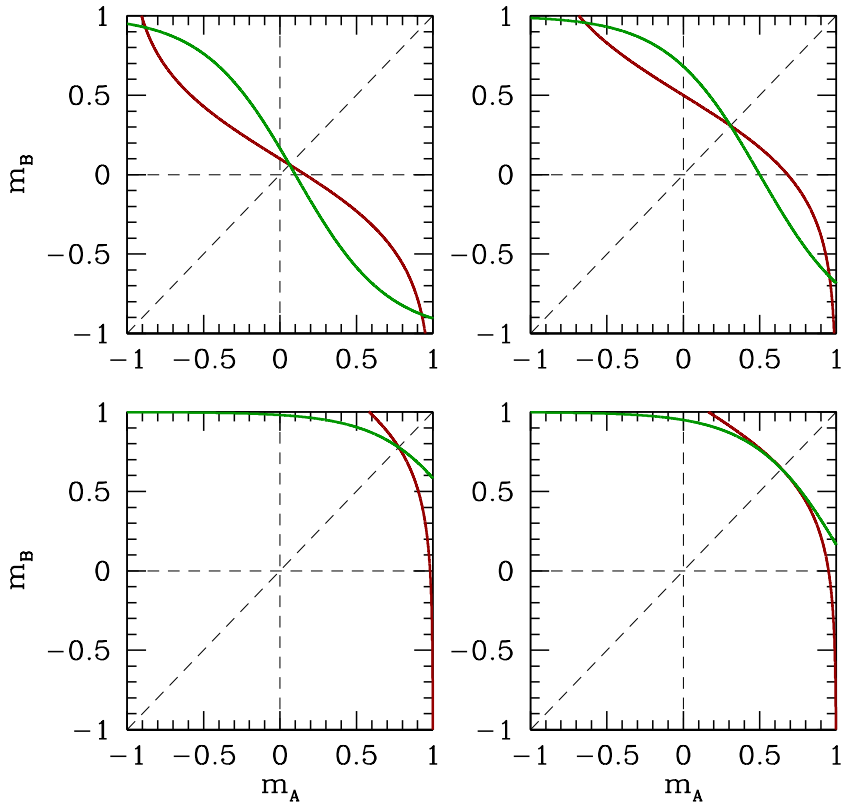


Figure 7.35: Graphical solution to the mean field equations for the Ising antiferromagnet in an external field, here for $\theta = 0.6$. Clockwise from upper left: (a) $h = 0.1$, (b) $h = 0.5$, (c) $h = 1.1$, (d) $h = 1.4$.

where the entropy function is

$$s(m) = -\left[\frac{1+m}{2}\,\log\!\left(\frac{1+m}{2}\right) + \frac{1-m}{2}\,\log\!\left(\frac{1-m}{2}\right)\right] \quad . \tag{7.411}$$

Note that

$$\frac{ds}{dm} = -\tfrac{1}{2}\,\log\!\left(\frac{1+m}{1-m}\right) \qquad , \qquad \frac{d^2s}{dm^2} = -\frac{1}{1-m^2} \quad . \tag{7.412}$$

Differentiating $f(m_{\rm A}, m_{\rm B})$ with respect to the variational parameters, we obtain two coupled mean field equations:

$$\begin{aligned} \frac{\partial f}{\partial m_{\rm A}} = 0 \quad &\Longrightarrow \quad m_{\rm B} = h - \frac{\theta}{2}\log\!\left(\frac{1+m_{\rm A}}{1-m_{\rm A}}\right) \\ \frac{\partial f}{\partial m_{\rm B}} = 0 \quad &\Longrightarrow \quad m_{\rm A} = h - \frac{\theta}{2}\log\!\left(\frac{1+m_{\rm B}}{1-m_{\rm B}}\right) \quad . \end{aligned} \tag{7.413}$$

Recognizing $\tanh^{-1}(x) = \frac{1}{2}\log\Big[(1+x)/(1-x)\Big]$, we may write these equations in an equivalent but

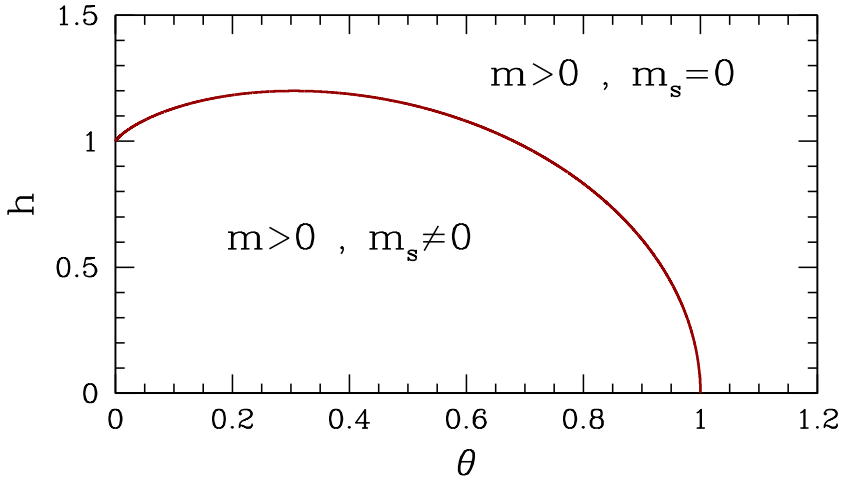


Figure 7.36: Mean field phase diagram for the Ising antiferromagnet in an external field. The phase diagram is symmetric under reflection in the $h = 0$ axis.

perhaps more suggestive form:

$$m_{\rm A} = \tanh\left(\frac{h - m_{\rm B}}{\theta}\right) \quad , \quad m_{\rm B} = \tanh\left(\frac{h - m_{\rm A}}{\theta}\right) \quad . \tag{7.414}$$

In other words, the A sublattice sites see an internal field $H_{\rm A,int} = -zJm_{\rm B}$ from their B neighbors, and the B sublattice sites see an internal field $H_{\rm B,int} = -zJm_{\rm A}$ from their A neighbors.

We can solve these equations graphically, as in fig. 7.35. Note that there is always a paramagnetic solution with $m_{\rm A} = m_{\rm B} = m$, where

$$m = h - \frac{\theta}{2}\log\left(\frac{1+m}{1-m}\right) \quad \Longleftrightarrow \quad m = \tanh\left(\frac{h-m}{\theta}\right) \quad . \tag{7.415}$$

However, we can see from the figure that there will be *three* solutions to the mean field equations provided that $\frac{\partial m_{\rm A}}{\partial m_{\rm B}} < -1$ at the point of the solution where $m_{\rm A} = m_{\rm B} = m$. This gives us two equations with which to eliminate $m_{\rm A}$ and $m_{\rm B}$, resulting in the curve

$$h^*(\theta) = m + \frac{\theta}{2}\log\left(\frac{1+m}{1-m}\right) \qquad \text{with} \;\; m = \sqrt{1-\theta} \quad . \tag{7.416}$$

Thus, for $\theta < 1$ and $|h| < h^*(\theta)$ there are three solutions to the mean field equations. It is *usually* the case that the broken symmetry solutions, which mean those for which $m_{\rm A} \neq m_{\rm B}$ in our case, are of lower energy than the symmetric solution(s). We show the curve $h^*(\theta)$ in fig. 7.36.

We can make additional progress by defining the average and staggered magnetizations m and $m_{\rm s}$,

$$m \equiv \tfrac{1}{2}(m_{\rm A} + m_{\rm B}) \quad , \quad m_{\rm s} \equiv \tfrac{1}{2}(m_{\rm A} - m_{\rm B}) \quad . \tag{7.417}$$

We expand the free energy in terms of $m_{\rm s}$:

$$\begin{aligned} f(m, m_{\rm s}) &= \tfrac{1}{2}m^2 - \tfrac{1}{2}m_{\rm s}^2 - h\,m - \tfrac{1}{2}\theta\, s(m + m_{\rm s}) - \tfrac{1}{2}\theta\, s(m - m_{\rm s}) \\ &= \tfrac{1}{2}m^2 - h\,m - \theta\, s(m) - \tfrac{1}{2}\Big(1 + \theta\, s''(m)\Big)\, m_{\rm s}^2 - \tfrac{1}{24}\theta\, s''''(m)\, m_{\rm s}^4 + \ldots \quad . \end{aligned} \tag{7.418}$$

The term quadratic in $m_{\rm s}$ vanishes when $\theta\, s''(m) = -1$, *i.e.* when $m = \sqrt{1-\theta}$. It is easy to obtain

$$\frac{d^3s}{dm^3} = -\frac{2m}{(1-m^2)^2} \qquad , \qquad \frac{d^4s}{dm^4} = -\frac{2\,(1+3m^2)}{(1-m^2)^3} \quad , \tag{7.419}$$

from which we learn that the coefficient of the quartic term, $-\frac{1}{24}\,\theta\, s''''(m)$, never vanishes. Therefore the transition remains second order down to $\theta = 0$, where it finally becomes first order.

We can confirm the $\theta \to 0$ limit directly. The competing states are the ferromagnet, with $m_{\rm A} = m_{\rm B} = \pm 1$, and the antiferromagnet, with $m_{\rm A} = -m_{\rm B} = \pm 1$. The free energies of these states are

$$f^{\rm FM} = \tfrac{1}{2} - |h| \qquad , \qquad f^{\rm AFM} = -\tfrac{1}{2} \quad . \tag{7.420}$$

There is a first order transition when $f^{\rm FM} = f^{\rm AFM}$, which yields $|h| = 1$.

7.13.3 Canted quantum antiferromagnet

Consider the following model for *quantum* $S = \frac{1}{2}$ spins:

$$\hat{H} = \sum_{\langle ij \rangle} \Big[-J\big(\sigma_i^x \sigma_j^x + \sigma_i^y \sigma_j^y\big) + \Delta\, \sigma_i^z \sigma_j^z \Big] + \tfrac{1}{4} K \sum_{\langle ijkl \rangle} \sigma_i^z \sigma_j^z \sigma_k^z \sigma_l^z \quad , \tag{7.421}$$

where $\boldsymbol{\sigma}_i$ is the vector of Pauli matrices on site i. The spins live on a square lattice. The second sum is over all square plaquettes. All the constants J, Δ, and K are positive.

Let's take a look at the Hamiltonian for a moment. The J term clearly wants the spins to align ferromagnetically in the (x, y) plane (in internal spin space). The Δ term prefers antiferromagnetic alignment along the $\hat{\boldsymbol{z}}$ axis. The K term discourages any kind of moment along $\hat{\boldsymbol{z}}$ and works against the Δ term. We'd like our mean field theory to capture the physics behind this competition.

Accordingly, we break up the square lattice into two interpenetrating $\sqrt{2} \times \sqrt{2}$ square sublattices (each rotated by 45° with respect to the original), in order to be able to describe an antiferromagnetic state. In addition, we include a parameter α which describes the *canting angle* that the spins on these sublattices make with respect to the $\hat{\boldsymbol{x}}$-axis. That is, we write

$$\begin{aligned} \varrho_{\rm A} &= \tfrac{1}{2} + \tfrac{1}{2} m \left(\sin\alpha\, \sigma^x + \cos\alpha\, \sigma^z \right) \\ \varrho_{\rm B} &= \tfrac{1}{2} + \tfrac{1}{2} m \left(\sin\alpha\, \sigma^x - \cos\alpha\, \sigma^z \right) \quad . \end{aligned} \tag{7.422}$$

Note that $\mathsf{Tr}\ \varrho_{\rm A} = \mathsf{Tr}\ \varrho_{\rm B} = 1$ so these density matrices are normalized. Note also that the mean direction for a spin on the A and B sublattices is given by

$$\boldsymbol{m}_{\rm A,B} = \mathsf{Tr}\,(\varrho_{\rm A,B}\, \boldsymbol{\sigma}) = \pm\, m \cos\alpha\, \hat{\boldsymbol{z}} + m \sin\alpha\, \hat{\boldsymbol{x}} \quad . \tag{7.423}$$

Thus, when $\alpha = 0$, the system is an antiferromagnet with its staggered moment lying along the $\hat{\boldsymbol{z}}$ axis. When $\alpha = \frac{1}{2}\pi$, the system is a ferromagnet with its moment lying along the $\hat{\boldsymbol{x}}$ axis.

Finally, the eigenvalues of $\varrho_{\rm A,B}$ are still $\lambda_\pm = \frac{1}{2}(1 \pm m)$, hence

$$\begin{aligned} s(m) &\equiv -\,\mathsf{Tr}\,(\varrho_{\rm A}\log\varrho_{\rm A}) = -\,\mathsf{Tr}\,(\varrho_{\rm B}\log\varrho_{\rm B}) \\ &= -\left[\frac{1+m}{2}\,\log\left(\frac{1+m}{2}\right) + \frac{1-m}{2}\,\log\left(\frac{1-m}{2}\right)\right] \quad . \end{aligned} \tag{7.424}$$

Note that we have taken $m_{\rm A} = m_{\rm B} = m$, unlike the case of the antiferromagnet in a uniform field. The reason is that there remains in our model a symmetry between A and B sublattices.

The free energy is now easily calculated:

$$\begin{aligned} F &= \mathsf{Tr}\,(\varrho\hat{H}) + k_{\rm B}T\,\mathsf{Tr}\,(\varrho\log\varrho) \\ &= -2N\Big(J\,\sin^2\alpha + \Delta\,\cos^2\alpha\Big)\,m^2 + \tfrac{1}{4}NKm^4\cos^4\alpha - Nk_{\rm B}T\,s(m) \end{aligned} \tag{7.425}$$

We can adimensionalize by defining $\delta \equiv \Delta/J$, $\kappa \equiv K/4J$, and $\theta \equiv k_{\rm B}T/4J$. Then the free energy per site is $f \equiv F/4NJ$ is

$$f(m,\alpha) = -\tfrac{1}{2}m^2 + \tfrac{1}{2}\big(1-\delta\big)\,m^2\cos^2\alpha + \tfrac{1}{4}\kappa\,m^4\cos^4\alpha - \theta\,s(m) \quad . \tag{7.426}$$

There are two variational parameters: m and α. We thus obtain two coupled mean field equations,

$$\begin{aligned} \frac{\partial f}{\partial m} &= 0 = -m + \big(1-\delta\big)\,m\,\cos^2\alpha + \kappa\,m^3\cos^4\alpha + \tfrac{1}{2}\theta\,\log\left(\frac{1+m}{1-m}\right) \\ \frac{\partial f}{\partial \alpha} &= 0 = -\Big(1-\delta+\kappa\,m^2\cos^2\alpha\Big)\,m^2\sin\alpha\,\cos\alpha \quad . \end{aligned} \tag{7.427}$$

Let's start with the second of the mean field equations. Assuming $m \neq 0$, it is clear from eqn. 7.425 that

$$\cos^2\alpha = \begin{cases} 0 & \text{if } \ \delta < 1 \\ (\delta-1)/\kappa m^2 & \text{if } \ 1 \le \delta \le 1+\kappa\,m^2 \\ 1 & \text{if } \ \delta \ge 1+\kappa\,m^2 \quad . \end{cases} \tag{7.428}$$

Suppose $\delta < 1$. Then we have $\cos\alpha = 0$ and the first mean field equation yields the familiar result

$$m = \tanh\big(m/\theta\big) \quad . \tag{7.429}$$

Along the θ axis, then, we have the usual ferromagnet-paramagnet transition at $\theta_{\rm c} = 1$.

For $1 < \delta < 1 + \kappa m^2$ we have canting with an angle

$$\alpha = \alpha^*(m) = \cos^{-1}\sqrt{\frac{\delta-1}{\kappa\,m^2}} \quad . \tag{7.430}$$

Substituting this into the first mean field equation, we once again obtain the relation $m = \tanh\big(m/\theta\big)$. However, eventually, as θ is increased, the magnetization will dip below the value $m_0 \equiv \sqrt{(\delta-1)/\kappa}$. This occurs at a dimensionless temperature

$$\theta_0 = \frac{m_0}{\tanh^{-1}(m_0)} < 1 \qquad , \qquad m_0 = \sqrt{\frac{\delta-1}{\kappa}} \quad . \tag{7.431}$$

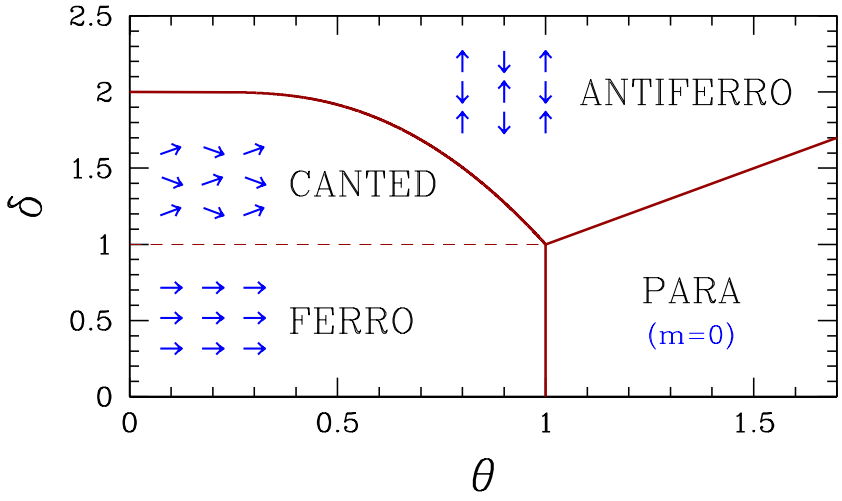


Figure 7.37: Mean field phase diagram for the model of eqn. 7.420 for the case $\kappa = 1$.

For $\theta > \theta_0$, we have $\delta > 1 + \kappa m^2$, and we must take $\cos^2\alpha = 1$. The first mean field equation then becomes

$$\delta m - \kappa m^3 = \frac{\theta}{2} \log\left(\frac{1+m}{1-m}\right) \quad , \tag{7.432}$$

or, equivalently, $m = \tanh\big((\delta m - \kappa m^3)/\theta\big)$. A simple graphical analysis shows that a nontrivial solution exists provided $\theta < \delta$. Since $\cos\alpha = \pm 1$, this solution describes an antiferromagnet, with $\boldsymbol{m}_{\rm A} = \pm m\hat{\boldsymbol{z}}$ and $\boldsymbol{m}_{\rm B} = \mp m\hat{\boldsymbol{z}}$. The resulting mean field phase diagram is then as depicted in fig. 7.37.

7.13.4 Coupled order parameters

Consider the Landau free energy

$$f(m,\phi) = \tfrac{1}{2}\,a_m\,m^2 + \tfrac{1}{4}\,b_m\,m^4 + \tfrac{1}{2}\,a_\phi\,\phi^2 + \tfrac{1}{4}\,b_\phi\,\phi^4 + \tfrac{1}{2}\Lambda\,m^2\,\phi^2 \quad . \tag{7.433}$$

We write

$$a_m \equiv \alpha_m\,\theta_m \qquad , \qquad a_\phi = \alpha_\phi\,\theta_\phi \quad , \tag{7.434}$$

where

$$\theta_m = \frac{T - T_{{\rm c},m}}{T_0} \qquad , \qquad \theta_\phi = \frac{T - T_{{\rm c},\phi}}{T_0} \quad , \tag{7.435}$$

where T_0 is some temperature scale. We assume without loss of generality that $T_{{\rm c},m} > T_{{\rm c},\phi}$. We begin by rescaling:

$$m \equiv \left(\frac{\alpha_m}{b_m}\right)^{1/2} \widetilde{m} \qquad , \qquad \phi \equiv \left(\frac{\alpha_\phi}{b_\phi}\right)^{1/2} \widetilde{\phi} \quad . \tag{7.436}$$

We then have

$$f = \varepsilon_0 \left\{ r\left(\tfrac{1}{2}\theta_m\,\widetilde{m}^2 + \tfrac{1}{4}\,\widetilde{m}^4\right) + r^{-1}\left(\tfrac{1}{2}\,\theta_\phi\,\widetilde{\phi}^2 + \tfrac{1}{4}\,\widetilde{\phi}^4\right) + \tfrac{1}{2}\,\lambda\,\widetilde{m}^2\widetilde{\phi}^2 \right\} \quad , \tag{7.437}$$

where

$$\varepsilon_0 = \frac{\alpha_m\,\alpha_\phi}{(b_m\,b_\phi)^{1/2}} \qquad , \qquad r = \frac{\alpha_m}{\alpha_\phi}\left(\frac{b_\phi}{b_m}\right)^{1/2} \qquad , \qquad \lambda = \frac{\Lambda}{(b_m\,b_\phi)^{1/2}} \quad . \tag{7.438}$$

It proves convenient to perform one last rescaling, writing

$$\tilde{m} \equiv r^{-1/4}\,\mathsf{m} \qquad , \qquad \tilde{\phi} \equiv r^{1/4}\,\varphi \quad . \tag{7.439}$$

Then

$$f = \varepsilon_0\left\{\tfrac{1}{2}q\,\theta_m\,\mathsf{m}^2 + \tfrac{1}{4}\,\mathsf{m}^4 + \tfrac{1}{2}q^{-1}\,\theta_\phi\,\varphi^2 + \tfrac{1}{4}\,\varphi^4 + \tfrac{1}{2}\,\lambda\,\mathsf{m}^2\,\varphi^2\right\} \quad , \tag{7.440}$$

where

$$q = \sqrt{r} = \left(\frac{\alpha_m}{\alpha_\phi}\right)^{1/2}\left(\frac{b_\phi}{b_m}\right)^{1/4} \quad . \tag{7.441}$$

Note that we may write

$$f(\mathsf{m},\varphi) = \frac{\varepsilon_0}{4}\begin{pmatrix}\mathsf{m}^2 & \varphi^2\end{pmatrix}\begin{pmatrix}1 & \lambda\\ \lambda & 1\end{pmatrix}\begin{pmatrix}\mathsf{m}^2\\ \varphi^2\end{pmatrix} + \frac{\varepsilon_0}{2}\begin{pmatrix}\mathsf{m}^2 & \varphi^2\end{pmatrix}\begin{pmatrix}q\,\theta_m\\ q^{-1}\,\theta_\phi\end{pmatrix} \quad . \tag{7.442}$$

The eigenvalues of the above 2×2 matrix are $1\pm\lambda$, with corresponding eigenvectors $\left(\begin{smallmatrix}1\\ \pm 1\end{smallmatrix}\right)$. Since $\varphi^2 > 0$, we are only interested in the first eigenvector $\left(\begin{smallmatrix}1\\ 1\end{smallmatrix}\right)$, corresponding to the eigenvalue $1+\lambda$. Clearly when $\lambda < -1$ the free energy is unbounded from below, which is unphysical.

We now set

$$\frac{\partial f}{\partial \mathsf{m}} = 0 \qquad , \qquad \frac{\partial f}{\partial \varphi} = 0 \quad , \tag{7.443}$$

and identify four possible phases:

- Phase I : $\mathsf{m} = 0$, $\varphi = 0$. The free energy is $f_{\rm I} = 0$.
- Phase II : $\mathsf{m} \neq 0$ with $\varphi = 0$. The free energy is

$$f = \frac{\varepsilon_0}{2}\left(q\,\theta_m\,\mathsf{m}^2 + \tfrac{1}{2}\,\mathsf{m}^4\right) \quad , \tag{7.444}$$

  hence we require $\theta_m < 0$ in this phase, in which case

$$\mathsf{m}_{\rm II} = \sqrt{-q\,\theta_m} \qquad , \qquad f_{\rm II} = -\frac{\varepsilon_0}{4}\,q^2\,\theta_m^2 \quad . \tag{7.445}$$

- Phase III : $m = 0$ with $\varphi \neq 0$. The free energy is

$$f = \frac{\varepsilon_0}{2}\left(q^{-1}\,\theta_\phi\,\varphi^2 + \tfrac{1}{2}\,\varphi^4\right) \quad , \tag{7.446}$$

  hence we require $\theta_\phi < 0$ in this phase, in which case

$$\varphi_{\rm III} = \sqrt{-q^{-1}\,\theta_\phi} \qquad , \qquad f_{\rm III} = -\frac{\varepsilon_0}{4}\,q^{-2}\,\theta_\phi^2 \quad . \tag{7.447}$$

- Phase IV : $\mathsf{m} \neq 0$ and $\varphi \neq 0$. Varying f yields

$$\begin{pmatrix} 1 & \lambda \\ \lambda & 1 \end{pmatrix} \begin{pmatrix} \mathsf{m}^2 \\ \varphi^2 \end{pmatrix} = - \begin{pmatrix} q\,\theta_m \\ q^{-1}\,\theta_\phi \end{pmatrix} \quad , \tag{7.448}$$

with solution

$$\begin{aligned} \mathsf{m}^2 &= \frac{q\,\theta_m - q^{-1}\,\theta_\phi\,\lambda}{\lambda^2 - 1} \\ \varphi^2 &= \frac{q^{-1}\,\theta_\phi - q\,\theta_m\,\lambda}{\lambda^2 - 1} \quad . \end{aligned} \tag{7.449}$$

Since m^2 and φ^2 must each be nonnegative, phase IV exists only over a yet-to-be-determined subset of the entire parameter space. The free energy is

$$f_{\rm IV} = \frac{q^2\,\theta_m^2 + q^{-2}\,\theta_\phi^2 - 2\lambda\,\theta_m\,\theta_\phi}{4(\lambda^2 - 1)} \quad . \tag{7.450}$$

We now define $\theta \equiv \theta_m$ and $\tau \equiv \theta_\phi - \theta_m = (T_{{\rm c},m} - T_{{\rm c},\phi})/T_0$. Note that $\tau > 0$. There are three possible temperature ranges to consider.

(1) $\theta_\phi > \theta_m > 0$. The only possible phases are I and IV. For phase IV, we must impose the conditions $m^2 > 0$ and $\phi^2 > 0$. If $\lambda^2 > 1$, then the numerators in eqns. 7.448 must each be positive:

$$\lambda < \frac{q^2\,\theta_m}{\theta_\phi} \quad , \quad \lambda < \frac{\theta_\phi}{q^2\,\theta_m} \quad \Rightarrow \quad \lambda < \min\left(\frac{q^2\,\theta_m}{\theta_\phi}\,,\,\frac{\theta_\phi}{q^2\theta_m}\right) \quad . \tag{7.451}$$

But since either $q^2\theta_m/\theta_\phi$ or its inverse must be less than or equal to unity, this requires $\lambda < -1$, which is unphysical.

If on the other hand we assume $\lambda^2 < 1$, the non-negativeness of m^2 and φ^2 requires

$$\lambda > \frac{q^2\,\theta_m}{\theta_\phi} \quad , \quad \lambda > \frac{\theta_\phi}{q^2\,\theta_m} \quad \Rightarrow \quad \lambda > \max\left(\frac{q^2\,\theta_m}{\theta_\phi}\,,\,\frac{\theta_\phi}{q^2\theta_m}\right) > 1 \quad . \tag{7.452}$$

Thus, $\lambda > 1$ and we have a contradiction.

Therefore, the only allowed phase for $\theta > 0$ is phase I.

(2) $\theta_\phi > 0 > \theta_m$. Now the possible phases are I, II, and IV. We can immediately rule out phase I because $f_{\rm II} < f_{\rm I}$. To compare phases II and IV, we compute

$$\Delta f = f_{\rm IV} - f_{\rm II} = \frac{(q\,\lambda\,\theta_m - q^{-1}\,\theta_\phi)^2\,\varepsilon_0}{4(\lambda^2 - 1)} \quad . \tag{7.453}$$

Thus, phase II has the lower energy if $\lambda^2 > 1$. For $\lambda^2 < 1$, phase IV has the lower energy, but the conditions $\mathsf{m}^2 > 0$ and $\varphi^2 > 0$ then entail

$$\frac{q^2\theta_m}{\theta_\phi} < \lambda < \frac{\theta_\phi}{q^2\theta_m} \quad \Rightarrow \quad q^2|\theta_m| > \theta_\phi > 0 \quad . \tag{7.454}$$

Thus, λ is restricted to the range

$$\lambda \in \left[-1\,,\, -\frac{\theta_\phi}{q^2|\theta_m|} \right] \quad . \tag{7.455}$$

With $\theta_m \equiv \theta < 0$ and $\theta_\phi \equiv \theta + \tau > 0$, the condition $q^2|\theta_m| > \theta_\phi$ is found to be

$$-\tau < \theta < -\frac{\tau}{q^2+1} \quad . \tag{7.456}$$

Thus, phase IV exists and has lower energy when

$$-\tau < \theta < -\frac{\tau}{r+1} \quad \text{and} \quad -1 < \lambda < \frac{\theta+\tau}{r\theta} \quad , \tag{7.457}$$

where $r = q^2$.

(3) $0 > \theta_\phi > \theta_m$. In this regime, any phase is possible, however once again phase I can be ruled out since phases II and III are of lower free energy. The condition that phase II have lower free energy than phase III is

$$f_{\rm II} - f_{\rm III} = \frac{\varepsilon_0}{4}\big(q^{-2}\theta_\phi^2 - q^2\theta_m^2\big) < 0 \quad , \tag{7.458}$$

i.e. $|\theta_\phi| < r|\theta_m|$, which means $r|\theta| > |\theta| - \tau$. If $r > 1$ this is true for all $\theta < 0$, while if $r < 1$ phase II is lower in energy only for $|\theta| < \tau/(1-r)$.

We next need to test whether phase IV has an even lower energy than the lower of phases II and III. We have

$$\begin{aligned} f_{\rm IV} - f_{\rm II} &= \frac{(q\,\lambda\,\theta_m - q^{-1}\,\theta_\phi)^2}{4(\lambda^2-1)} \\ f_{\rm IV} - f_{\rm III} &= \frac{(q\,\theta_m - q^{-1}\,\lambda\,\theta_\phi)^2}{4(\lambda^2-1)} \quad . \end{aligned} \tag{7.459}$$

In both cases, phase IV can only be the true thermodynamic phase if $\lambda^2 < 1$. We then require $\mathsf{m}^2 > 0$ and $\varphi^2 > 0$, which fixes

$$\lambda \in \left[-1\,,\, \min\!\left(\frac{q^2\,\theta_m}{\theta_\phi}\,,\, \frac{\theta_\phi}{q^2\theta_m} \right) \right] \quad . \tag{7.460}$$

The upper limit will be the first term inside the rounded brackets if $q^2|\theta_m| < |\theta_\phi|$, *i.e.* if $r|\theta| < |\theta| - \tau$. This is impossible if $r > 1$, hence the upper limit is given by the second term in the rounded brackets:

$$r > 1 \;:\; \lambda \in \left[-1\,,\, \frac{\theta+\tau}{r\,\theta} \right] \qquad \text{(condition for phase IV)} \quad . \tag{7.461}$$

If $r < 1$, then the upper limit will be $q^2\theta_m/\theta_\phi = r\theta/(\theta+\tau)$ if $|\theta| > \tau/(1-r)$, and will be $\theta_\phi/q^2\theta_m = (\theta+\tau)/r\theta$ if $|\theta| < \tau/(1-r)$.

$$\begin{aligned} r < 1 \quad , -\frac{\tau}{1-r} < \theta < -\tau \;:\; \lambda \in \left[-1\,,\, \frac{\theta+\tau}{r\theta} \right] \qquad \text{(phase IV)} \\ r < 1 \quad , \theta < -\frac{\tau}{1-r} \;:\; \lambda \in \left[-1\,,\, \frac{r\theta}{\theta+\tau} \right] \qquad \text{(phase IV)} \quad . \end{aligned} \tag{7.462}$$

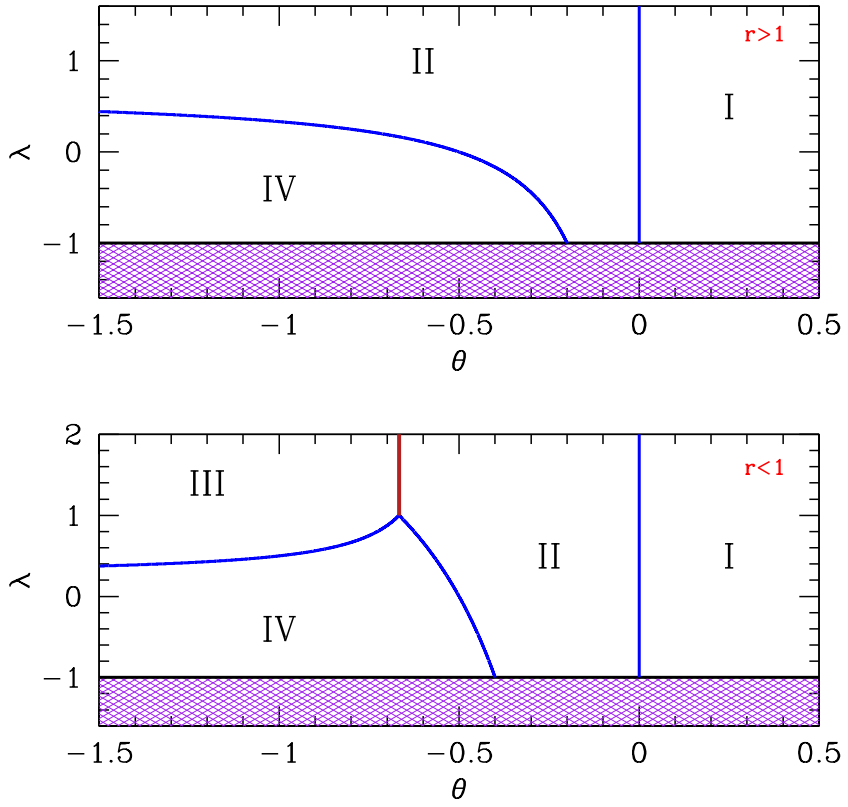


Figure 7.38: Phase diagram for $\tau = 0.5$, $r = 1.5$ (top) and $\tau = 0.5$, $r = 0.25$ (bottom). The hatched purple region is unphysical, with a free energy unbounded from below. The blue lines denote second order transitions. The thick red line separating phases II and III is a first order line.

Representative phase diagrams for the cases $r > 1$ and $r < 1$ are shown in fig. 7.38.

7.14 Appendix IV: Derivation of Ginzburg-Landau Free Energy

We can make some progress in systematically deriving the Ginzburg-Landau free energy. Consider the Ising model,

$$\frac{\hat{H}}{k_{\rm B}T} = -\tfrac{1}{2}\sum_{i,j=1}^{N} K_{ij}\,\sigma_i\,\sigma_j - \sum_{i=1}^{N} h_i\,\sigma_i + \tfrac{1}{2}\sum_{i=1}^{N} K_{ii} \quad , \tag{7.463}$$

where now $K_{ij} = J_{ij}/k_{\rm B}T$ and $h_i = H_i/k_{\rm B}T$ are the interaction energies and local magnetic fields in units of $k_{\rm B}T$. The last term on the RHS above cancels out any contribution from diagonal elements of K_{ij}. Our derivation makes use of a generalization of the Gaussian integral,

$$\int\limits_{-\infty}^{\infty} dx\; e^{-\frac{1}{2}ax^2 - bx} = \left(\frac{2\pi}{a}\right)^{1/2} e^{b^2/2a} \quad . \tag{7.464}$$

The generalization is

$$\int\limits_{-\infty}^{\infty} dx_1 \cdots \int\limits_{-\infty}^{\infty} dx_N \, e^{-\frac{1}{2}A_{ij}x_i x_j - b_i x_i} = \frac{(2\pi)^{N/2}}{\sqrt{\det A}} \, e^{\frac{1}{2}A^{-1}_{ij}\, b_i b_j} \quad , \tag{7.465}$$

where we use the Einstein convention of summing over repeated indices, and where we assume that the matrix A is positive definite (else the integral diverges). This allows us to write

$$\begin{aligned} Z &= e^{-\frac{1}{2}K_{ii}} \, \mathsf{Tr}\left[e^{\frac{1}{2}K_{ij}\sigma_i\,\sigma_j} \, e^{h_i\,\sigma_i} \right] \\ &= \det{}^{-1/2}(2\pi K)\, e^{-\frac{1}{2}K_{ii}} \int\limits_{-\infty}^{\infty} d\phi_1 \cdots \int\limits_{-\infty}^{\infty} d\phi_N \, e^{-\frac{1}{2}K^{-1}_{ij}\phi_i\phi_j} \; \mathsf{Tr}\, e^{(\phi_i + h_i)\sigma_i} \\ &= \det{}^{-1/2}(2\pi K)\, e^{-\frac{1}{2}K_{ii}} \int\limits_{-\infty}^{\infty} d\phi_1 \cdots \int\limits_{-\infty}^{\infty} d\phi_N \, e^{-\frac{1}{2}K^{-1}_{ij}\phi_i\phi_j} \, e^{\sum_{i=1}^N \log\left[2\cosh(\phi_i + h_i)\right]} \\ &\equiv \int\limits_{-\infty}^{\infty} d\phi_1 \cdots \int\limits_{-\infty}^{\infty} d\phi_N \, e^{-\Phi(\phi_1\,,\,\ldots\,,\,\phi_N)} \quad , \end{aligned} \tag{7.466}$$

where

$$\Phi = \tfrac{1}{2} \sum_{i,j=1}^{N} K^{-1}_{ij}\, \phi_i\, \phi_j - \sum_{i=1}^{N} \log\cosh(\phi_i + h_i) + \tfrac{1}{2}\log\det(2\pi K) + \tfrac{1}{2}\,\mathsf{Tr}\; K - N\log 2 \quad . \tag{7.467}$$

We assume the model is defined on a Bravais lattice, in which case we can write $\phi_i = \phi_{\boldsymbol{R}_i}$. We can then define the Fourier transforms,

$$\phi_{\boldsymbol{R}} = \frac{1}{\sqrt{N}} \sum_{\boldsymbol{q}} \hat{\phi}_{\boldsymbol{q}}\, e^{i\boldsymbol{q}\cdot\boldsymbol{R}} \qquad , \qquad \hat{\phi}_{\boldsymbol{q}} = \frac{1}{\sqrt{N}} \sum_{\boldsymbol{R}} \phi_{\boldsymbol{R}}\, e^{-i\boldsymbol{q}\cdot\boldsymbol{R}} \tag{7.468}$$

and

$$\hat{K}(\boldsymbol{q}) = \sum_{\boldsymbol{R}} K(\boldsymbol{R})\, e^{-i\boldsymbol{q}\cdot\boldsymbol{R}} \quad . \tag{7.469}$$

A few remarks about the lattice structure and periodic boundary conditions are in order. For a Bravais lattice, we can write each direct lattice vector $\boldsymbol{R}$ as a sum over d basis vectors with integer coefficients, *viz.* $\boldsymbol{R} = \sum_{\mu=1}^{d} n_\mu\, \boldsymbol{a}_\mu$, where d is the dimension of space. The reciprocal lattice vectors $\boldsymbol{b}_\mu$ have dimensions inverse to those of $\boldsymbol{R}$ and satisfy $\boldsymbol{a}_\mu \cdot \boldsymbol{b}_\nu = 2\pi\,\delta_{\mu\nu}$. The set $\{\boldsymbol{b}_\mu\}$ is complete, hence any wavevector $\boldsymbol{q}$ may be expressed as

$$\boldsymbol{q} = \frac{1}{2\pi} \sum_{\mu=1}^{d} \theta_\mu\, \boldsymbol{b}_\mu \quad . \tag{7.470}$$

We can impose periodic boundary conditions on a system of size $L_1 \times L_2 \times \cdots \times L_d$ by requiring

$$\phi_{\boldsymbol{R} + \sum_{\mu=1}^{d} l_\mu L_\mu \boldsymbol{a}_\mu} = \phi_{\boldsymbol{R}} \quad . \tag{7.471}$$

This leads to the *quantization* of the wavevectors, which must then satisfy

$$e^{iL_\mu \boldsymbol{q}\cdot\boldsymbol{a}_\mu} = e^{iL_\mu\theta_\mu} = 1 \quad , \tag{7.472}$$

and therefore $\theta_\mu = 2\pi m_\mu/L_\mu$, where m_μ is an integer. There are then $L_1 L_2 \cdots L_d = N$ independent values of $\boldsymbol{q}$, which can be taken to be those corresponding to $m_\mu \in \{1, \ldots, L_\mu\}$.

Let's now expand the function $\Phi(\boldsymbol{\phi})$ in powers of the ϕ_i, and to first order in the external fields h_i. We obtain

$$\Phi = \tfrac{1}{2}\sum_{\boldsymbol{q}} \Big(\hat{K}^{-1}(\boldsymbol{q}) - 1\Big)\,|\hat{\phi}_{\boldsymbol{q}}|^2 + \tfrac{1}{12}\sum_{\boldsymbol{R}} \phi_{\boldsymbol{R}}^4 - \sum_{\boldsymbol{R}} h_{\boldsymbol{R}}\,\phi_{\boldsymbol{R}} + \mathcal{O}\big(\phi^6, h\phi^3, h^2\big) \tag{7.473}$$
$$+ \tfrac{1}{2}\,\mathsf{Tr}\; K + \tfrac{1}{2}\,\mathsf{Tr}\,\log(2\pi K) - N\log 2 \quad .$$

On a d-dimensional lattice, for a model with nearest neighbor interactions K_1 only, we have $\hat{K}(\boldsymbol{q}) = K_1 \sum_{\boldsymbol{\delta}} e^{i\boldsymbol{q}\cdot\boldsymbol{\delta}}$, where $\boldsymbol{\delta}$ is a nearest neighbor separation vector. These are the eigenvalues of the matrix K_{ij}. We note that K_{ij} is then not positive definite, since there are negative eigenvalues[53]. To fix this, we can add a term K_0 everywhere along the diagonal. We then have

$$\hat{K}(\boldsymbol{q}) = K_0 + K_1 \sum_{\boldsymbol{\delta}} \cos(\boldsymbol{q}\cdot\boldsymbol{\delta}) \quad . \tag{7.474}$$

Here we have used the inversion symmetry of the Bravais lattice to eliminate the imaginary term. The eigenvalues are all positive so long as $K_0 > zK_1$, where z is the lattice coordination number. We can therefore write $\hat{K}(\boldsymbol{q}) = \hat{K}(0) - \alpha\,\boldsymbol{q}^2$ for small $\boldsymbol{q}$, with $\alpha > 0$. Thus, we can write

$$\hat{K}^{-1}(\boldsymbol{q}) - 1 = a + \kappa\,\boldsymbol{q}^2 + \ldots \quad . \tag{7.475}$$

To lowest order in $\boldsymbol{q}$ the RHS is isotropic if the lattice has cubic symmetry, but anisotropy will enter in higher order terms. We'll assume isotropy at this level. This is not necessary but it makes the discussion somewhat less involved. We can now write down our Ginzburg-Landau free energy density:

$$\mathcal{F} = \tfrac{1}{2}a\,\phi^2 + \tfrac{1}{2}\kappa\,|\boldsymbol{\nabla}\phi|^2 + \tfrac{1}{12}\,\phi^4 - h\,\phi \quad , \tag{7.476}$$

valid to lowest nontrivial order in derivatives, and to fourth order in ϕ.

One might wonder what we have gained over the inhomogeneous variational density matrix treatment, where we found

$$F = -\tfrac{1}{2}\sum_{\boldsymbol{q}} \hat{J}(\boldsymbol{q})\,|\hat{m}(\boldsymbol{q})|^2 - \sum_{\boldsymbol{q}} \hat{H}(-\boldsymbol{q})\,\hat{m}(\boldsymbol{q})$$
$$+ k_{\rm B}T \sum_{i=1}^{N} \left\{ \left(\frac{1+m_i}{2}\right)\log\left(\frac{1+m_i}{2}\right) + \left(\frac{1-m_i}{2}\right)\log\left(\frac{1-m_i}{2}\right)\right\} \quad . \tag{7.477}$$

Surely we could expand $\hat{J}(\boldsymbol{q}) = \hat{J}(0) - \frac{1}{2}a\boldsymbol{q}^2 + \ldots$ and obtain a similar expression for $\mathcal{F}$. However, such a derivation using the variational density matrix is only approximate. The method outlined in this section is in principle exact.

[53] To evoke a negative eigenvalue on a d-dimensional cubic lattice, set $q_\mu = \pi/a$ for all μ. The eigenvalue is then $-2dK_1$.

Let's return to our complete expression for Φ:

$$\Phi(\boldsymbol{\phi}) = \Phi_0(\boldsymbol{\phi}) + \sum_{\boldsymbol{R}} v(\phi_{\boldsymbol{R}}) \quad , \tag{7.478}$$

where

$$\Phi_0(\boldsymbol{\phi}) = \tfrac{1}{2}\sum_{\boldsymbol{q}} G^{-1}(\boldsymbol{q})\,\big|\hat{\phi}(\boldsymbol{q})\big|^2 + \tfrac{1}{2}\,\mathsf{Tr}\left(\frac{1}{1+G^{-1}}\right) + \tfrac{1}{2}\,\mathsf{Tr}\,\log\left(\frac{2\pi}{1+G^{-1}}\right) - N\log 2 \quad . \tag{7.479}$$

Here we have defined

$$v(\phi) = \tfrac{1}{2}\phi^2 - \log\cosh\phi = \tfrac{1}{12}\,\phi^4 - \tfrac{1}{45}\,\phi^6 + \tfrac{17}{2520}\,\phi^8 + \ldots \tag{7.480}$$

and

$$G(\boldsymbol{q}) = \frac{\hat{K}(\boldsymbol{q})}{1-\hat{K}(\boldsymbol{q})} \quad . \tag{7.481}$$

We now want to compute

$$Z = \int D\boldsymbol{\phi}\; e^{-\Phi_0(\boldsymbol{\phi})}\; e^{-\sum_{\boldsymbol{R}} v(\phi_{\boldsymbol{R}})} \tag{7.482}$$

where $D\boldsymbol{\phi} \equiv d\phi_1\, d\phi_2 \cdots d\phi_N$. We expand the second exponential factor in a Taylor series, allowing us to write

$$Z = Z_0\left\{1 - \sum_{\boldsymbol{R}}\big\langle v(\phi_{\boldsymbol{R}})\big\rangle + \tfrac{1}{2}\sum_{\boldsymbol{R}}\sum_{\boldsymbol{R}'}\big\langle v(\phi_{\boldsymbol{R}})\,v(\phi_{\boldsymbol{R}'})\big\rangle + \ldots\right\} \quad , \tag{7.483}$$

where

$$\begin{aligned} Z_0 &= \int D\boldsymbol{\phi}\; e^{-\Phi_0(\boldsymbol{\phi})} \\ \log Z_0 &= \tfrac{1}{2}\,\mathsf{Tr}\left[\log(1+G) - \frac{G}{1+G}\right] + N\log 2 \end{aligned} \tag{7.484}$$

and

$$\big\langle F(\boldsymbol{\phi})\big\rangle = \frac{\int D\boldsymbol{\phi}\; F\; e^{-\Phi_0}}{\int D\boldsymbol{\phi}\; e^{-\Phi_0}} \quad . \tag{7.485}$$

To evaluate the various terms in the expansion of eqn. 7.482, we invoke Wick's theorem, which says

$$\begin{aligned} \big\langle x_{i_1}\, x_{i_2}\cdots x_{i_{2L}}\big\rangle &= \int\limits_{-\infty}^{\infty} dx_1 \cdots \int\limits_{-\infty}^{\infty} dx_N\; e^{-\frac{1}{2}\mathcal{G}^{-1}_{ij}x_i x_j}\; x_{i_1}\, x_{i_2}\cdots x_{i_{2L}} \Bigg/ \int\limits_{-\infty}^{\infty} dx_1 \cdots \int\limits_{-\infty}^{\infty} dx_N\; e^{-\frac{1}{2}\mathcal{G}^{-1}_{ij}x_i x_j} \\ &= \sum_{\substack{\text{all distinct}\\ \text{pairings}}} \mathcal{G}_{j_1 j_2}\mathcal{G}_{j_3 j_4}\cdots\mathcal{G}_{j_{2L-1}j_{2L}} \quad , \end{aligned} \tag{7.486}$$

where the sets $\{j_1,\ldots,j_{2L}\}$ are all permutations of the set $\{i_1,\ldots,i_{2L}\}$. In particular, $\big\langle x_i^4\big\rangle = 3\big(\mathcal{G}_{ii}\big)^2$, so

$$\big\langle \phi_{\boldsymbol{R}}^4\big\rangle = 3\left(\frac{1}{N}\sum_{\boldsymbol{q}} G(\boldsymbol{q})\right)^2 \quad . \tag{7.487}$$

Thus, if we write $v(\phi) \approx \frac{1}{12}\,\phi^4$ and retain only the quartic term in $v(\phi)$, we obtain

$$\begin{aligned}\frac{F}{k_{\rm B}T} = -\log Z &= \tfrac{1}{2}\,\mathsf{Tr}\left[\frac{G}{1+G} - \log(1+G)\right] + \frac{1}{4N}\big(\,\mathsf{Tr}\;G\big)^2 - N\log 2 \\ &= -N\log 2 + \frac{1}{4N}\big(\mathsf{Tr}\;G\big)^2 - \frac{1}{4}\,\mathsf{Tr}\,\big(G^2\big) + \mathcal{O}\big(G^3\big) \quad .\end{aligned} \tag{7.488}$$

Note that if we set K_{ij} to be diagonal, then $\hat{K}(\boldsymbol{q})$ and $G(\boldsymbol{q})$ are constant functions of $\boldsymbol{q}$. The $\mathcal{O}\big(G^2\big)$ term then vanishes, which is required since the free energy cannot depend on the diagonal elements of K_{ij}.